



Kent Academic Repository

Li, Zhiyuan (2016) *Analysis of factors that modulate the toxicity of the yeast prion protein Rnq1*. Doctor of Philosophy (PhD) thesis, University of Kent,.

Downloaded from

<https://kar.kent.ac.uk/55116/> The University of Kent's Academic Repository KAR

The version of record is available from

This document version

UNSPECIFIED

DOI for this version

Licence for this version

UNSPECIFIED

Additional information

Versions of research works

Versions of Record

If this version is the version of record, it is the same as the published version available on the publisher's web site. Cite as the published version.

Author Accepted Manuscripts

If this document is identified as the Author Accepted Manuscript it is the version after peer review but before type setting, copy editing or publisher branding. Cite as Surname, Initial. (Year) 'Title of article'. To be published in *Title of Journal*, Volume and issue numbers [peer-reviewed accepted version]. Available at: DOI or URL (Accessed: date).

Enquiries

If you have questions about this document contact ResearchSupport@kent.ac.uk. Please include the URL of the record in KAR. If you believe that your, or a third party's rights have been compromised through this document please see our [Take Down policy](https://www.kent.ac.uk/guides/kar-the-kent-academic-repository#policies) (available from <https://www.kent.ac.uk/guides/kar-the-kent-academic-repository#policies>).

**Analysis of factors that modulate
the toxicity of the yeast prion
protein Rnq1**

by

Zhiyuan Li



A thesis submitted to the University of Kent for the degree of PhD in
Biochemistry in the School of Biosciences April 2016

Declaration

No part of this thesis has been submitted in support of any other application for a degree or qualification of the University of Kent or any other University or Institute of learning.

Zhiyuan Li

April 2016

This thesis is composed of seven chapters. I declare that I performed all the experimental work presented here.

*This thesis is dedicated to the memory of
my grandparents*

Jian Li (1920-2009)

Zhijian Jing (1934-2009)

Meilan Qi (1932-2015)

Acknowledgments

Firstly, I would like to thank Prof. Mick Tuite for his patience, motivation and support but also for the guidance which helped me to widen my research from various perspectives throughout my PhD. Besides my supervisor, I would like to thank my thesis committee: Dr. Ian Blomfield and Prof. Flaviano Giorgini, for their insightful comments and encouragement. My sincere thank also goes to Dr. Gary Robinson who provided me an opportunity to upgrade to this PhD programme.

I would also like to thank Gemma, Jintana, Ilectra, Brian, Wes, Ricardo and all other current and past members of Kent Fungal Group for fun working atmosphere and entertaining conversations. For financially supporting me and my PhD studies, I would like to thank my family, School of Biosciences and Pfizer Ltd.

I would also like to thank the good friends that put up with me during these years, especially Eleanna, Hong and Xiaotu. Last but not least, for their encouragement and unconditional support, I would like to thank my family in Beijing, with a special thank you to my parents, Jie Jing and Weidong Li for everything.

Abstract

Prions are infectious proteins that form transmissible, self-propagating amyloids that convert protein from its normal state into the prion state. The accumulation of amyloid is the causative agent of several neurodegenerative diseases, for instance, Huntington's disease, which is caused by a polyglutamine expansion in the huntingtin (Htt) protein. In this study, a yeast-based Huntington's disease model was created to investigate the mechanism of amyloid toxicity and how nuclear genes modulate this toxicity. The model amyloid used was Rnq1, a transferable epigenetic modifier which is able to form a prion known as [PIN+]. [PIN+] is known to enhance the formation of polyglutamine aggregates in yeast. In this study, a series of cellular assays were employed to determine the mechanism of Rnq1-mediated cytotoxicity and compared with polyglutamine-rich-protein-mediated cytotoxicity dependent upon the [PIN+] prion. In [PIN+] cells *RNQ1* overexpression leads to a significant increase in the production of reactive oxygen species (ROS). Furthermore, overexpression of *RNQ1* resulted in a nuclear migration defect in [PIN+] cells. Upf1 (**Up**-frameshift protein 1), a highly conserved protein that plays an important role in nonsense-mediated mRNA decay, was found to modify amyloid toxicity. In a *upf1Δ* deletion strain, both Rnq1 and polyglutamine-rich-protein-mediated cytotoxicity were suppressed in a [PIN+] background. To further study the novel role of Upf1 in amyloid toxicity, a combination of cell biological and genetic approaches were being employed.

Table of Contents

Chapter 1 Introduction

1.1 Common structure of amyloid and amyloid fibril formation	2
1.2 Overview of prions.....	4
1.2.1 Definition of a prion protein.....	4
1.2.2 The properties of a prion protein.....	4
1.2.3 Discovery of prions in mammals	5
1.2.4 Discovery of prions in fungi.....	6
1.2.5 Genetic criteria used to identify a prion.....	6
1.3 Prion propagation mechanism	9
1.3.1 Role of cellular factors in prion propagation.....	10
1.3.2 Role of chaperones in prion propagation.....	11
1.4 Sup35 and the [PSI⁺] prion.....	12
1.4.1 Variants of the [PSI ⁺] prion	12
1.4.2 Sequence features that define a prion-forming domain	14
1.5 Rnq1 and [PIN⁺] prions.....	16
1.5.1 [PIN ⁺] prion and [PIN ⁺] variants.....	16
1.5.2 [PIN ⁺] as a toxic amyloid model	17
1.6 Polyglutamine (polyQ) tract induced toxicity	18
1.6.1 Huntington's disease	18
1.6.2 Polyglutamine (polyQ) tract induced toxicity	21
1.7 Genetic modifiers affect Rnq1 and Polyglutamine (polyQ) mediated toxicity.....	21
1.7.1 Bna4	21
1.7.2 UPF proteins.....	22
1.8 Project aims	24

Chapter 2 Materials and Methods

2.1 Chemicals and reagents	27
2.2 Growth media	27
2.2.1 Yeast media for the culture of <i>Saccharomyces cerevisiae</i>	28
2.2.2 Growth media for culturing <i>Escherichia coli</i>	28
2.3 Strains	29
2.3.1 <i>Saccharomyces cerevisiae</i> strains	29
2.3.2 <i>Escherichia coli</i> strains	30
2.4 Plasmids	30
2.5 Oligonucleotide primers	31
2.6 DNA methods	31
2.6.1 Purification of plasmid DNA from <i>Escherichia coli</i>	31
2.6.2 Agarose gel electrophoresis	32
2.6.3 Restriction enzyme digestion	32
2.6.4 Determination of DNA concentration	33
2.6.5 QuikChange Lightning Site-Directed Mutagenesis	33
2.6.6 DNA sequencing	33
2.7 Recombinant DNA methods	34
2.7.1 Preparation of competent <i>E. coli</i> cells	34
2.7.2 Transformation of plasmid DNA into <i>Escherichia coli</i>	35
2.7.3 Transformation of plasmid DNA into <i>Saccharomyces cerevisiae</i>	35
2.8 Growth conditions and analysis	36
2.8.1 Determination of cell density	36
2.8.2 Cell induction by galactose	36
2.8.3 Growth analysis by microplate reader	37
2.8.4 Calculation of doubling time	37
2.9 Biological assays	37
2.9.1 [<i>PIN</i> ⁺] <i>de novo</i> conversion assay	37
2.9.2 Toxicity assay	38
2.9.3 Reactive Oxygen Species (ROS) detection using Fluorescence Activated Cell Sorting (FACS)	39
2.10 Protein methods	40

2.10.1 Preparation of cell extract for quantitative western blot analysis.....	40
2.10.2 Separation of proteins by SDS-polyacrylamide gel electrophoresis (SDS-PAGE).....	40
2.10.3 Coomassie brilliant blue staining and destaining	41
2.10.4 Western blotting.....	41
2.10.5 Chemiluminescence detection	42
2.11 Fluorescence microscopy methods	43
2.11.1 GFP microscopy	43
2.11.2 DAPI staining.....	43
2.12 Electron microscopy methods.....	44

Chapter 3 *De novo* formation of [PSI⁺] prion detected by different [PIN⁺] variants

3.1 Introduction	46
3.2 [PIN ⁺] variants show different frequencies of <i>de novo</i> formation of [PSI ⁺]	48
3.3 The spectrum of [PSI ⁺] variants that arises <i>de novo</i> is influenced by the [PIN ⁺] variants	49
3.4 Quantitative analysis of the <i>de novo</i> formation of strong [PSI ⁺] and weak [PSI ⁺] in strains carrying different [PIN ⁺] variants	52
3.5 Levels of the Rnq1 protein in different [PIN ⁺] variants	53
3.6 Discussion	55

Chapter 4 [PIN⁺]-dependent toxicity mediated by the Rnq1 protein

4.1 Introduction	58
4.2 Rnq1 overexpression is toxic in different [PIN ⁺] variants but not in a [pin ⁻] background.....	59
4.3 Rnq1 overexpression causes a growth defect in [PIN ⁺] cells.....	64
4.4 Rnq1-GFP forms fluorescent aggregates in [PIN ⁺] cells.....	67

4.5 Rnq1 overexpression causes a nuclear migration defect.....	71
4.6 Rnq1 overexpression causes mitochondrial dysfunction in a [<i>PIN</i> ⁺]-dependent manner	77
4.7 Discussion	87

Chapter 5 [*PIN*⁺]-dependent toxicity mediated by the polyglutamine (polyQ) expansion proteins

5.1 Introduction	90
5.2 Overexpression of a polyQ expansion protein HttQ103 is toxic in different [<i>PIN</i> ⁺] variants but not in a [<i>pin</i> ⁻] background	91
5.3 Overexpression of Q103 causes a growth defect in [<i>PIN</i> ⁺] cells.....	95
5.4 Q103-GFP forms fluorescent aggregates in [<i>PIN</i> ⁺] cells	98
5.5 Overexpression of Q103 does not lead to a nuclear migration defect	101
5.6 Overexpression of Q103 does not lead to mitochondrial dysfunction in a [<i>PIN</i> ⁺] background	106
5.7 Discussion	112

Chapter 6 The role of modifier genes in both Rnq1- and polyQ- induced toxicity

6.1 Introduction	115
6.2 Rnq1 and polyQ overexpression-mediated cytotoxicity is suppressed in <i>upf1</i> Δ and <i>upf2</i> Δ [<i>PIN</i> ⁺] strains but not in <i>upf3</i> Δ [<i>PIN</i> ⁺] strain	116
6.3 [<i>PIN</i> ⁺]-dependent growth defect caused by Rnq1 and polyQ103 overexpression is suppressed in <i>upf1</i> Δ and <i>upf2</i> Δ strains but not in <i>upf3</i> Δ strain	122
6.4 Expression of the wild type <i>UPF1</i> gene in the <i>upf1</i> Δ strain restores both Rnq1- and polyQ103-induced toxicity.....	126
6.5 Expression of the Upf1 protein in the <i>upf1</i> Δ strain shows the growth defects caused by Rnq1- and polyQ103 overexpression-mediated toxicity.....	131

6.6 Rnq1 overexpression does not cause a nuclear migration defect in the <i>upf1</i> Δ and <i>upf2</i> Δ strains	135
6.7 Construction of <i>UPF1</i> mutations	138
6.8 Expression of <i>upf1</i> mutant genes in the <i>upf1</i> Δ strain partially suppress Rnq1 and polyQ overexpression-induced toxicity in [<i>PIN</i> ⁺] cells.....	140
6.9 Expression of the mutant Upf1 protein in the <i>upf1</i> Δ strain shows the general growth defects.....	145
6.10 Rnq1 and polyQ103 overexpression-mediated cytotoxicity is suppressed in a <i>bna4</i> Δ [<i>PIN</i> ⁺] strain.....	149
6.12 Rnq1 and polyQ103 overexpression does not cause a nuclear migration defect in the <i>bna4</i> Δ strain	153
6.13 Discussion	156

Chapter 7 General Discussion

7.1 Overview of the project	159
7.2 Is the mechanism of amyloid toxicity the same for Rnq1 and polyQ103?.....	162
7.3 Is mitochondrial deficiency a consequence of amyloid toxicity in yeast?.....	163
7.4 Is nuclear migration defect a feature of amyloid toxicity?.....	163
7.5 Why dose Upf1 and Upf2 proteins suppress amyloid toxicity?.....	164
7.6 Why does <i>bna4</i> Δ suppress amyloid toxicity?	165

References.....	167
-----------------	-----

Chapter 1

Introduction

1.1 Common structure of amyloid and amyloid fibril formation

Over the past four decades, deposition of amyloid leading to systemic amyloidosis in the body was thought to be the major causative agents in a number of fatal neurodegenerative diseases such as Alzheimer's disease, Parkinson's disease, Huntington disease and Creutzfeldt-Jakob disease (Roth et al., 1966). Recent evidence indicates that soluble amyloid oligomers which are also known as prefibrillar oligomers may be the toxic protein species in amyloid pathogenesis, rather than the mature amyloid fibrils, for example, amyloid plaques which are insoluble and highly organised by the repeating β -sheets structure (Hardy et al., 2002, Lesne et al., 2006).

The term amyloid arises from the combination of amylo (starch) and oid (like) representing the mistaken origin of identification of the substance as starch that was based on inaccurate staining techniques. Amyloids were first discovered by Astbury (Astbury et al., 1935). Amyloids are insoluble misfolded fibrillar proteins which are able to polymerize to form a cross- β structure either *in vivo* or *in vitro* (Nilsson, 2004). The most characteristic feature of amyloid is the cross- β structure which can be visualised by particular dyes such as Congo red and thioflavin. The cross- β structure enhances the stability of amyloid fibrils, the tendency to form polymerized structures and their self-seeding property (Nelson et al., 2005).

Aggregation of misfolded proteins can form different protein assemblies like oligomers, amorphous aggregates, amyloid fibrils and plaques. Different types of misfolded proteins can give rise to prefibrillar oligomers acting as soluble intermediate aggregates in the amyloid fibril formation pathway. These protein particles are able to form either amorphous aggregates or amyloidogenic nuclei by conformational change (Figure 1.1). An amyloidogenic nucleus can initiate the formation of amyloid fibrils which are insoluble and have a highly organised structure (Goldsbury et al., 2000).

That amyloid polymerization is amino acid sequence-dependent implies that mutations in the sequence may reduce or block amyloid self-assembly. Amyloid polymerization can be achieved by two types of intermolecular forces, hydrogen bonding or hydrophobic interactions depending on two distinct amyloid-forming polypeptide sequences (Pawar et al., 2005). A sequence enriched in glutamine can enhance the cross- β structure by forming hydrogen bonds. In this case, glutamine content is thought to correlate with toxicity. For instance, in Huntington disease, the longer the polyglutamine sequence is, the earlier the age of onset (Morley et al., 2002). Despite polyglutamine sequences, a non-repeated sequence can also illuminate the cross- β structure by means of hydrophobic interactions (Pawar et al., 2005).

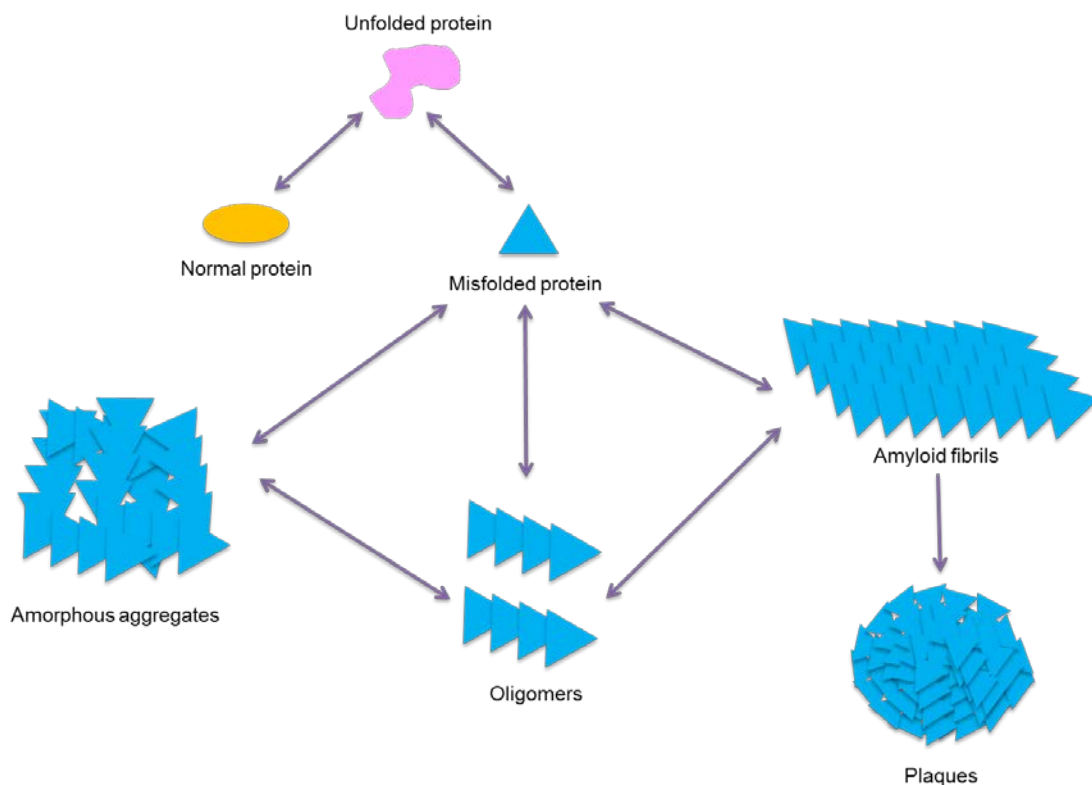


Figure 1.1 Aggregation of misfolded protein can generate amyloid fibrils and plaques and amorphous aggregates (Treusch et al., 2009).

1.2 Overview of prions

1.2.1 Definition of a prion protein

In 1982, Stanley Prusiner proposed the word 'prion' derived from 'proteinaceous' and 'infectious' to describe an unusual amyloid protein which can transmit genetic information by means of unique mechanisms other than changes in the underlying DNA sequence (Prusiner, 1982). Prions are infectious agents that are believed to cause a number of neurodegenerative diseases in humans, for example, Creutzfeldt-Jacob Disease (CJD) (Prusiner, 1998). One of the most unusual characteristics of the prion diseases is that it can be transmitted in the absence of DNA or RNA according to Prusiner's 'protein-only' hypothesis. Prions are also found in fungi such as *Saccharomyces cerevisiae* (Wickner, 1994) and *Podospora anserina* (Coustou et al., 1997).

1.2.2 The properties of a prion protein

All prion proteins in mammals or fungi can exist in one of two states: a native non-prion form ($[prion]$) or a heritable prion form ($[PRION^+]$). The prion-free indicates that the protein has normal cellular activity and is in its soluble form, while the prion form is not able to maintain its normal function and aggregates into amyloid deposits. The conformational change between a natural protein and its prion state may lead to different effects on the protein's function and eventually impact on the host cell phenotype. In fungi prions can also serve as novel regulators of the cellular phenotype of the host cell (Tuite and Serio, 2010). The second difference between the two states is that the $[prion]$ form is sensitive to protease treatment whereas the $[PRION^+]$ form is protease resistant. Prions of the same protein can have distinct conformational isoforms which is known as variants. Different variants lead to the same disease, but different disease characteristics (Aguzzi et al., 2007). For example, the

causative agent of transmissible spongiform encephalopathies (TSEs), PrP^{Sc}, can form distinct aggregates which cause disease with distinct characteristics, such as incubation period, pattern of PrP^{Sc} distribution, and regional severity of histopathological changes in the brain (Poggiolini et al., 2013). In addition, all prions are amyloids, but most amyloids are not prions; i.e. most disease-associated amyloids are not infectious and cannot be transmitted between individuals (Wickner et al, 2000).

1.2.3 Discovery of prions in mammals

The first of prion diseases to be described was scrapie, a disease of sheep recognized for over 250 years. The symptoms of the disease are hyperexcitability, itching, and ataxia that eventually leads to paralysis and death (Gordon, 1946). In mammals, it was discovered that an infectious agent named as PrP (prion protein), which may occur both in infectious and non-infectious forms, was involved in causing a class of fatal neurodegenerative diseases, the Transmissible Spongiform Encephalopathies (TSE). PrP is a cellular protein whose function is still unknown. PrP^{Sc} refers to the infectious [*PRION*⁺] form of PrP while PrP^C represents the normal [*prion*] form of the protein. PrP^C is a soluble glycoprotein which is found anchored to the extracellular membrane of several cell types whereas PrP^{Sc}, the prion form of PrP^C is insoluble, partially resistant to proteolysis, and forms amorphous and amyloid-like aggregates which lead to its abnormal accumulation in tissues resulting in severe cellular damages (Prusiner, 1998). PrP^{Sc} is capable of converting PrP^C proteins into its infectious state by triggering a change in the conformation of PrP^C (Figure 1.2). The assembly of prions into amyloids is a self-perpetuating process that displays a typical nucleation-elongation reaction. The pre-existing PrP^{Sc} acts as a seed to catalyse amyloid polymerization leading to the disease (Caughey et al., 2009).

The PrP amino acid sequence of its N-terminus is highly conserved in mammals (Goldfarb et al., 1991). The PrP^{Sc} protein has a structure with a high

proportion of β -sheets which usually binds to Congo red (CR) and thioflavin-T (Th-T) dyes whereas PrP^c is highly flexible consisting of an unstructured N-terminal tail and a globular C-terminal region rich in α -helices (Riek et al., 1996) i.e. there is a distinct difference in their conformation (Pan et al., 1993). Moreover, it was established that PrP^{Sc} was responsible for the formation of amyloid fibers and neurodegeneration. Amyloid fibrils are also rich in β -sheet structures and are protease-resistant and have been linked to a number of different human neurodegenerative diseases (Prusiner, 1998).

1.2.4 Discovery of prions in fungi

Yeast prions were identified with genetic studies in *Saccharomyces cerevisiae*. During the last five decades, only [PSI⁺] (Cox, 1965) and [URE3] (Lacroute, 1971) have been described but whose molecular basis was poorly understood. The initial discovery of [PSI⁺] was made by Brain Cox (Cox, 1965) in a strain auxotrophic for adenine due to a nonsense mutation. The *ade2-1* mutation, a premature UAA terminator, resulted in the accumulation of a red pigment derived from the Ade2 substrate. When the [PSI⁺] was present, the read-through of the premature UAA stop codon in the *ade2-1* gene was efficient enough to allow cell growth without adenine. [Het-s] is the only prion discovered in a filamentous fungus, *Podospora anserine*, and was the first prion protein whose bacterial inclusion bodies were shown to display amyloid-like properties. (Table 1.1). Recent studies revealed that there are more than 20 newly discovered prions in *S. cerevisiae* (Alberti et al., 2009).

1.2.5 Genetic criteria used to identify a prion

Wickner has proposed three genetic criteria to identify a fungal prion (Wickner, 1994) and most prions in fungi satisfy all three criteria, whereas nucleic acid-based determinants do not.

Table 1.1 Prions and its corresponding protein and prion-associated effects on host cells

Prion Form	Normal Protein	Species	Cellular function	Prion phenotypes	References
PrP ^{Sc}	PrP ^C	mammals	Unknown	Neurodegeneration and death	(Prusiner, 1998)
[<i>URE3</i>]	Ure2	<i>Saccharomyces cerevisiae</i>	Transcription regulation	Poor in nitrogen metabolism and inactive Ure2 formation	(Lacroute,1971) (Wickner,1994)
[<i>PSI</i> ⁺]	Sup35	<i>Saccharomyces cerevisiae</i>	Translation termination	Nonsense suppression, defect in translation termination	(Cox,1965) (Wickner,1994)
[<i>PIN</i> ⁺]/ [<i>RNQ</i> ⁺]	Rnq1	<i>Saccharomyces cerevisiae</i>	Unknown	Facilitating <i>de novo</i> conversion of [<i>PSI</i> ⁺] and [<i>URE3</i>]	(Sondheimer et al., 2000) (Derkatch et al., 2001)
[<i>SWI</i> ⁺]	Swi1	<i>Saccharomyces cerevisiae</i>	Subunit of the SWI-SNF chromatin remodelling complex	Repression of transcription	(Derkatch et al., 2001) (Du et al., 2008)
[<i>OCT</i> ⁺]	Cyc8	<i>Saccharomyces cerevisiae</i>	Transcriptional co-repressor	Derepression of transcription	(Patel et al., 2009)
[<i>MOT</i> ⁺]	Mot3	<i>Saccharomyces cerevisiae</i>	Transcriptional co-repressor	Derepression of transcription	(Alberti et al., 2009)
[<i>ISP</i> ⁺]	Sfp1	<i>Saccharomyces cerevisiae</i>	Transcriptional activator	Transcriptional accuracy	(Volkov et al., 2002) (Rogoza et al., 2010)
[Het-s]	HET-s	<i>Podospora anserina</i>	Unknown	Vegetative incompatibility and cell death	(Coustou et al., 1997)

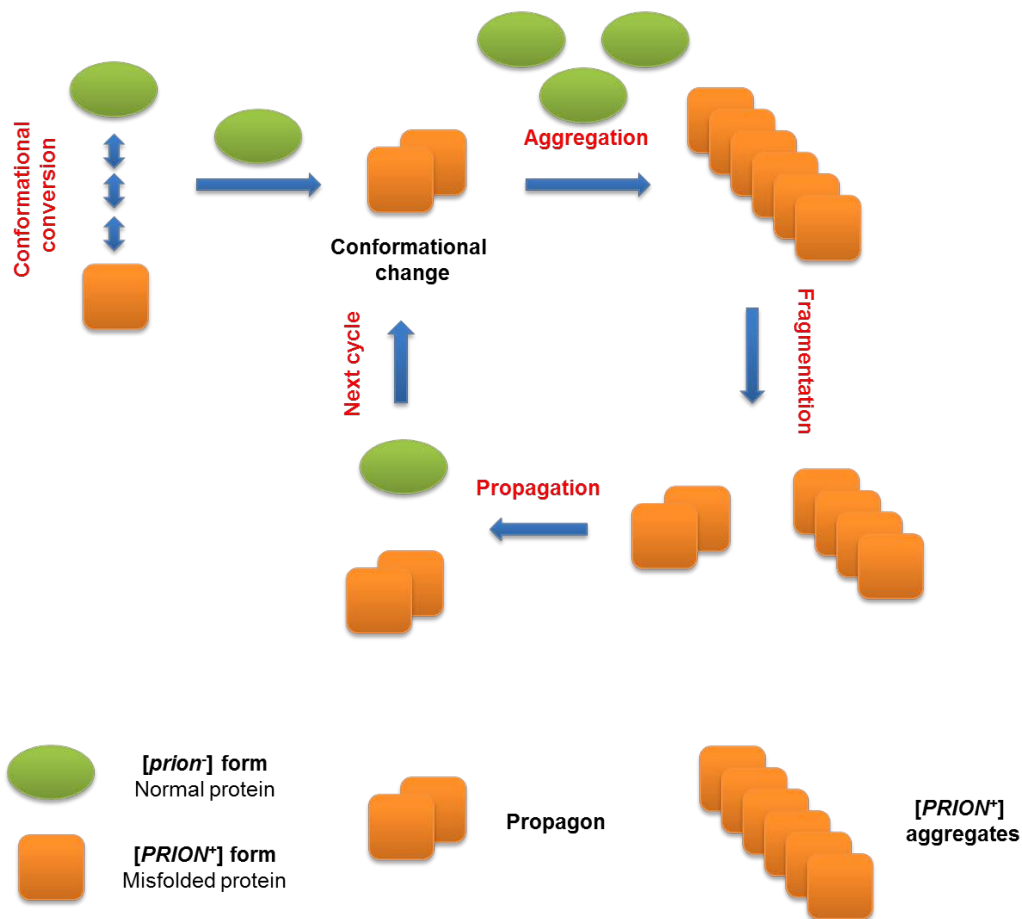


Figure 1.2 The overview of prion formation and propagation

Proteins in their [PRION*] state are capable of converting [prion-] (i.e. normal protein) into the [PRION*] form. [PRION*] molecules can rearrange and generate insoluble amyloid deposits by polymerisation. Propagons derived from the process of fragmentation are able to facilitate the conversion of [prion] into the [PRION*] state.

Firstly, the process of converting the normal protein ([prion]) to its abnormal form ([PRION*]) should be reversible which means if the infectious form of the protein can be eliminated from a cell, it can also reappear by spontaneous conversion no matter what treatment was used for eliminating the underlying non-chromosomal element from the cell. The reversible curability can be achieved by growing cells in the presence of 3-5 mM guanidine hydrochloride (Tuite et al., 1981). In addition, maintenance of the [PRION*] form requires the presence of molecular chaperones and expression of its corresponding prion protein.

Secondly, overproduction of the protein can induce the *de novo* appearance of the [PRION⁺] form indicating that the higher the concentration of the cellular protein is, the higher the efficiency of generating the prion *de novo*.

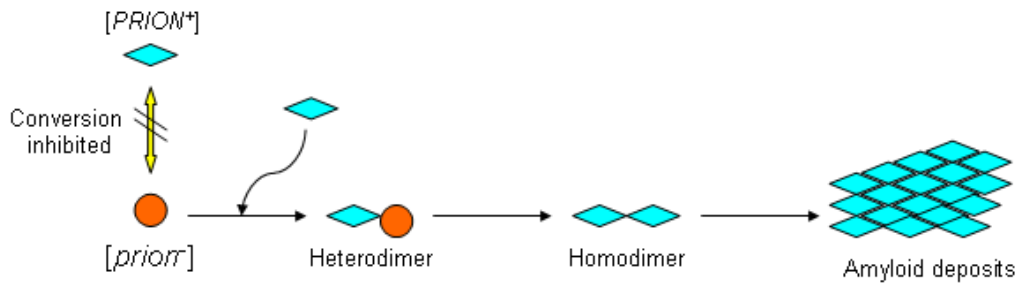
Thirdly, the phenotype of [PRION⁺] cells is similar to the phenotype of cells expressing a corresponding mutated and non-functional version of the protein. In addition, prions should show non-Mendelian inheritance i.e. the transmission of prions at meiosis is in a non-Mendelian manner.

1.3 Prion propagation mechanism

A well-characterised property of prions is that the [PRION⁺] form can propagate by the mechanism of binding and converting protein molecules existing in its normal [*prion*⁻] state, to the abnormal [PRION⁺] form. Two hypotheses have been proposed to explain the self-propagation of prions. One of the possible mechanisms of prion propagation in fungi is the “template-directed refolding” model (Figure 1.3A) that proposes that a prion protein in its [PRION⁺] form acts as a template to convert the normal soluble protein ([*prion*⁻]) to its infectious state. The “template” was thought to be a polymer of prion protein molecules and this resulted in the assembly of the amyloid fibrils via “conformational conversion” (Griffith, 1967; Prusiner, 1991). In addition, the spontaneous conversion between the normal soluble form ([*prion*⁻]) and the prion conformer ([PRION⁺]) of a prion protein is thought to be prevented by a high activation energy barrier (Cohen and Prusiner 1998).

Another hypothesis for prion self-propagation is the “seeded polymerisation” model (Figure 1.3B) that suggests that the formation of the infectious seed is the key component of the whole process. The infectious seeds are generated by accumulation of several monomeric prion conformers and consequently drive the polymerization of other prion conformers to form amyloid deposits. New seeds are generated by fragmentation of the amyloid aggregates and the seed is recruited for continued prion propagation. This fragmentation could be enzyme-mediated or by physical process.

A. “Template-directed refolding” model



B. “Seeded polymerisation” model

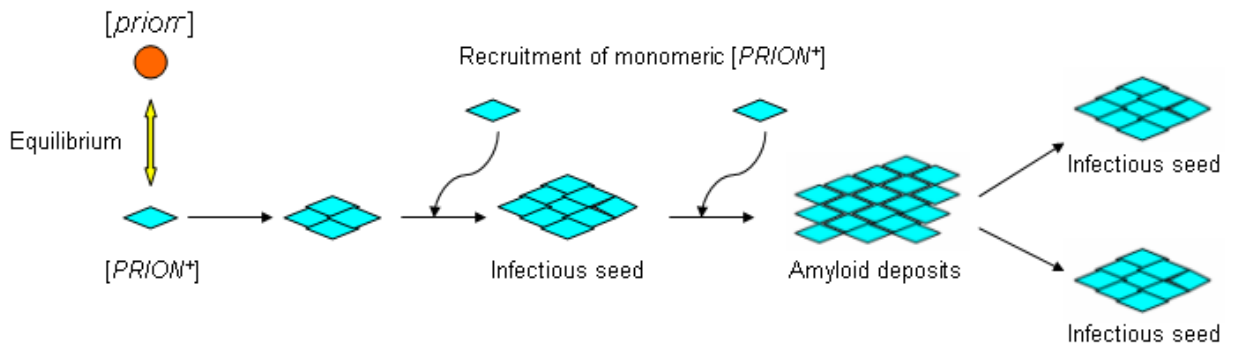


Figure 1.3 Two proposed models for de novo conversion and prion propagation. (A). The “template-directed refolding” model in which a prion conformer serves as a template for the conversion of a prion protein from its normal soluble form ($[prion]$) to its prion form ($[PRION^*]$). (B). The “seeded polymerisation” model suggests that there is an equilibrium between the ($[prion]$) form and ($[PRION^*]$) form of the prion protein since the monomer of ($[PRION^*]$) is unstable and can easily switch the equilibrium towards ($[prion]$). An oligomer of ($[PRION^*]$) can generate an infectious seed, or propagon, which is capable of recruiting further monomeric ($[PRION^*]$) to form amyloid aggregates. Fragmentation of the amyloid deposits can generate several infectious seeds for further conversion and prion propagation.

1.3.1 Role of cellular factors in prion propagation

Fungal prions are not able to propagate without an input from cellular factors. In particular prion-specific chaperones play a very important role in prion propagation. Chaperones are able to prevent proteins from aggregating and to disaggregate proteins that have misfolded. For instance, the molecular chaperone Hsp104, is involved in the propagation and maintenance of the $[PSI^+]$ prion (Chernoff et al., 1995). Hsp104 is an ATPase that is capable of

binding to the aggregated proteins and re-solubilizing the protein aggregates in the presence of ATP (Glover et al, 1998). Yeast cells cannot propagate the [*PRION⁺*] form of a protein if the Hsp104 ATPase activity is inhibited (Chernoff et al., 1995). Moreover, Hsp104 seems to form a chaperone complex with members of the Hsp40 and Hsp70 protein families to allow the propagation of prions to proceed successfully (Glover et al, 1998; Jones and Masison, 2003). For example, Hsp104 and GroEL play an important role in the regulation of PrP conformation. It was suggested that the conversion of PrP^C to PrP^{Sc} is a two-step process by kinetic analysis. PrP^C was firstly converted to a pelletable state in the presence of GroEL and PrP^{Sc} via recruitment of intermediate PrP and then converted to PrP^{Sc} once the PrP pelletable state was established (DeBurman et al., 1997). In mammals, RNA molecules are thought to act as cellular co-factors for PrP^{Sc} to convert PrP^C proteins into its infectious state, but there is no evidence for this in yeast (Deleault et al., 2003).

1.3.2 Role of chaperones in prion propagation

Previous studies established that Hsp104 cannot fully perform its function as a disaggregase without joining at least two other chaperones, Ydj1 belonging to the Hsp40 family and Ssa1 a member of the Hsp70 family. There is an interaction between Ydj1 and Hsp104 while Ssa1 interacts with Ydj1 (Glover et al, 1998, Cyr et al, 1992). Following the discovery that Hsp104 is not capable of restoring the activity of a denatured protein alone, it emerged that Ssa1 functions to help Hsp104 to refold the protein aggregates and this also facilitates the process of prion propagation (Allen et al., 2005). Ssa1 and Ydj1 were thought to stabilize and fold the protein at a first step followed by Hsp104 that further promote the folding of the protein (Glover et al, 1998). Moreover, Ssa1 plays a key role in the prion curing process of [*PSI⁺*]; for example, it was reported that increased levels of Ssa1 reduce [*PSI⁺*] elimination by Hsp104 overexpression indicated that there is an antagonistic effect of Ssa1 on Hsp104 when both Ssa1 and Hsp104 are overexpressed. In addition,

overexpression of Ssa1 can eliminate [*URE3*], whereas overexpression of Ssa1 has no effect on [*PSI⁺*] propagation (Schwimmer and Masison, 2002).

1.4 Sup35 and the [*PSI⁺*] prion

1.4.1 Variants of the [*PSI⁺*] prion

[*PSI⁺*], as one of the best studied yeast prions, is the prion form of the Sup35 protein. Sup35 is a translation termination factor that is responsible for recognising a termination codon and cleaving the completed peptide from peptidyl tRNA (Stansfield et al., 1995). The read-through of stop codons is increased when Sup35 is present in the [*PSI⁺*] form suggests that its translation termination activity is attenuated.

The [*PSI⁺*] prion can exist as one of a number of different variants which were first identified by their differential effects on nonsense suppression. In [*PSI⁺*] cells, the Sup35 protein forms aggregates resulting in the read-through of the *ade1-14* nonsense mutation. The *ade 1-14* mutation is a mutation in a gene that encodes an enzyme required for adenine synthesis. This mutation results in adenine auxotrophy i.e. the yeast strain cannot survive unless adenine is provided in the growth medium. The *ade1-14* mutation gives red yeast colonies that are adenine deficient if the [*PSI⁺*] prion is not present. This is because the defect in adenine biosynthesis causes the accumulation of a pathway intermediate that develops into a red pigment. On the other hand, white yeast colonies are formed due to the read-through of the *ade1-14* nonsense (UGA) mutation. Strong [*PSI⁺*] variants generate white colonies on adenine deficient media since they show a high efficiency of *ade1-14* nonsense suppression whereas the weak [*PSI⁺*] variants generate pink colonies because of their lower efficiency of *ade1-14* nonsense suppression (Zhou et al., 1999). The *ade 1-14* mutation displays a clearly visible phenotype.

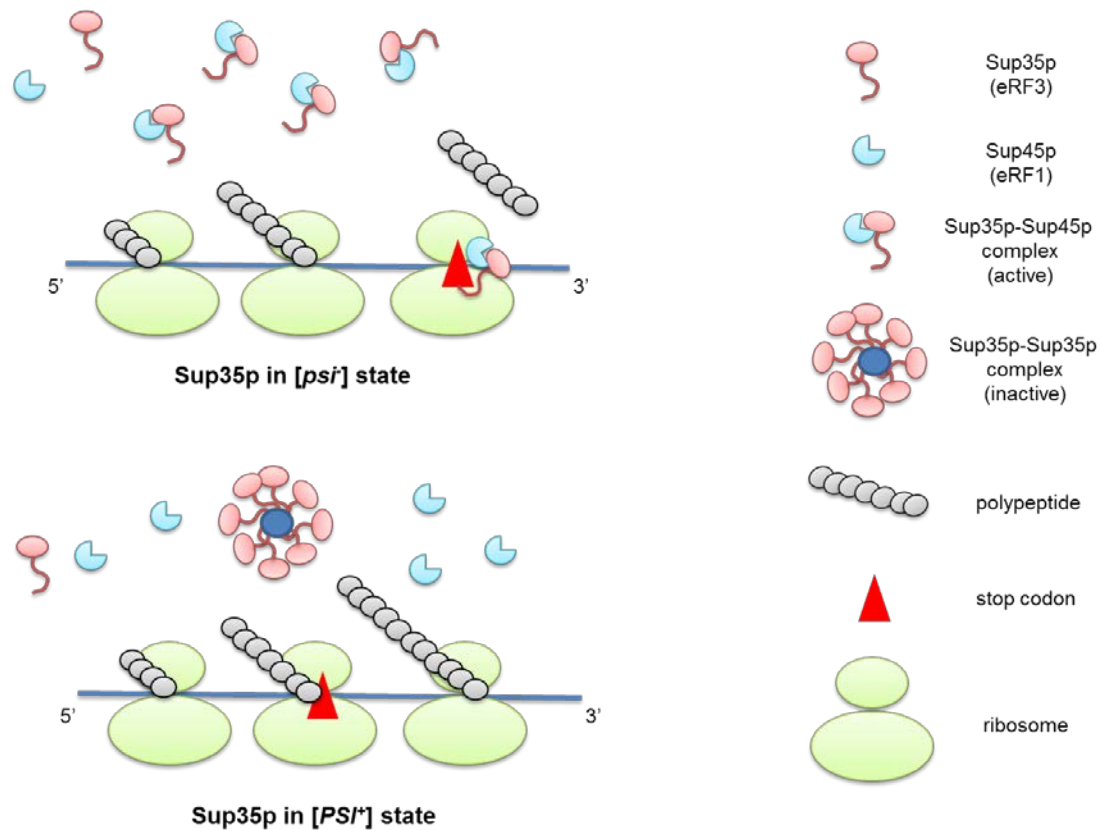


Figure 1.4 The Sup35 protein leads to read-through of mRNA stop-codons in [*PSI*⁺] cells. The Sup35 (eRF3) binds to Sup45 (eRF1) to form an active complex in [*psi*⁺] strains. mRNA translation is terminated and the polypeptide is released since the Sup35p-Sup45p complex recognise the stop codon on mRNA. By contrast, Sup35 is insoluble in its [*PSI*⁺] state resulting in read-through of mRNA stop codons and an increased polypeptide synthesis.

Sup35 consists of three domains: the N-terminal domain, the middle M-domain and the C-terminal domain. The N-terminal domain is rich in glutamine (Q) and asparagine (N) and is primarily responsible for prion formation and aggregation (Derkatch et al., 1996). The M-domain is involved in prion maintenance but not critical for prion formation (Liu et al., 2002). The C-terminal domain plays an important role in translation termination and therefore is essential for growth (Ter-Avanesyan et al., 1993). Moreover, recent studies have revealed that the C-terminal domain is not only essential for cell viability but also prion propagation (Kabani et al., 2011).

[*PSI*⁺] cells can be cured of the prion form of Sup35 after guanidine hydrochloride (GuHCl) treatment or deletion of the *HSP104* gene (Tuite et al,

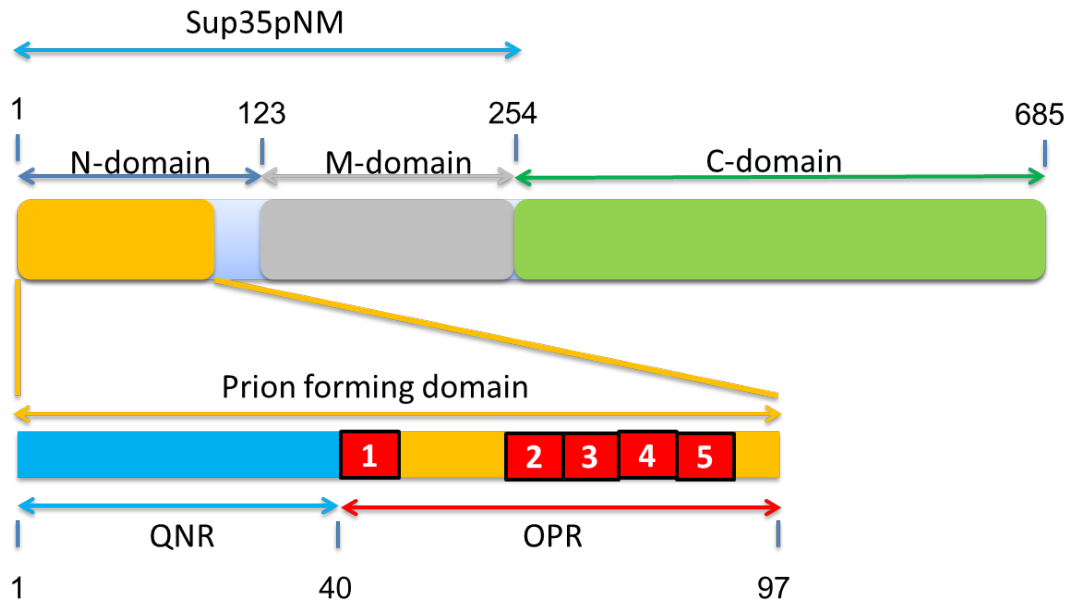
1981; Chernoff et al., 1995). [*PSI*⁺] cells are found to be resistant to a variety of physical and chemical stresses and also more resistant to heat and ethanol stresses in certain strains (Eaglestone et al., 1999; True et al., 2000). Overexpression of the prion forming domain of Sup35 causes the *de novo* formation of [*PSI*⁺] which can be significantly increased by the presence of the [*PIN*⁺] prion (Derkatch et al., 1997).

1.4.2 Sequence features that define a prion-forming domain

Studies of the structure and amino acid sequences of the various yeast prion proteins have suggested that the prion-forming domain (PrD) has two diagnostic features. One is conformational flexibility of the region and the other feature is that this region is particularly rich in glutamine and asparagine residues (Scheibel and Lindquist, 2001; Nazabal et al., 2003; Alberti et al., 2009).

The prion-forming domain of Sup35 is located in its N terminus (Figure 1.5) and contains two distinct elements: a QN-rich region (QNR) and a region containing a series of oligopeptide repeats (OPR). The QNR element is composed of 40 residues that are rich in uncharged polar amino acids namely glutamine and asparagine. The amino acids between residues 8-26 are crucial for prion propagation (DePace et al. 1998). Unlike other cellular proteins which are rich in aliphatic residues, the QNR element of the prion protein has a low number of aliphatic amino acids such as glycine, leucine and valine. The QN-rich region (QNR) by acting as an “amyloid core”, plays a key role in prion propagation. This was demonstrated by showing that if one of the uncharged polar residues, glutamine or asparagine, is replaced by the polar residues, for instance, aspartic acid in the QNR region, this can result in a decrease in joining the pre-existing prion aggregates or preventing further aggregation of Sup35 molecules (DePace et al., 1998).

(a) Structure of Sup35 protein



(b) Sequence of QNR region

1 **MSDSNQGNQNNQNYQQYSQNGNQQQGNNRYQGYQAYNAQAQ** 40

(c) Sequence of OPR region

41 **PAGGYQNYQGYSGYQQGGYQQYNPDAGYQQQYNPQGGYQQYNPQGGYQQQFNQGG** 97

Figure 1.5 Domain architecture of Sup35 protein. (a)The Sup35p protein contains three domains, a N-terminal domain (amino acid 1-123), a middle domain (amino acid 123-254) and the C-terminal domain (amino acid 254-685). The prion forming domain (amino acid 1-97) of Sup35 consists of two elements: the glutamine (Q) and asparagine (N) rich (QNR) region (amino acid 1-40) which initiates the process of protein aggregation, and the oligopeptide repeats (OPR) region (amino acid 41-97) containing five a-repeats (labelled 1-5) that are responsible for prion propagation. Different colours represent different regions of amino acid sequence of Sup35p. **(b)** The sequence of QNR region (amino acids 1-40). **(c)** The sequence of OPR region (amino acids 41-97).

Another element of the prion-forming domain is the oligopeptide region (OPR) which contains 57 residues that is able to form highly stable amyloid aggregates. In this region, a heptapeptide sequence GGYQQYN is thought to

generate a hydrophobic environment of the protein thus increasing the amyloidogenic potential of the prion protein (Balbirnie et al., 2001; Perutz et al., 2002).

1.5 Rnq1 and $[PIN^+]$ prions

1.5.1 $[PIN^+]$ prion and $[PIN^+]$ variants

The $[PIN^+]$ prion was first discovered from studies on the *de novo* formation of the $[PSI^+]$ prion (Derkatch et al., 1997). It was reported that $[PSI^+]$ strains could generate two types of $[psi^-]$ clones when cured by guanidine hydrochloride. In one type of $[psi^-]$ population, $[PSI^+]$ could be generated by Sup35 over-expression, while in the other $[psi^-]$ population it could not. Due to the difference between these two distinct $[psi^-]$ populations, the derivatives that could be induced to $[PSI^+]$ were designated $[PIN^+]$ for $[PSI^+]$ inducibility whereas the derivatives which maintained the $[psi^-]$ phenotype were designated as $[pin^-]$ (Derkatch et al., 1997). Subsequently, it was demonstrated that the $[PIN^+]$ prion is capable of increasing the *de novo* formation of not only the $[PSI^+]$ prion, but also the $[URE3]$ prion (Bradley et al., 2002). However, the $[PIN^+]$ prion is not required for the continued propagation of the $[PSI^+]$ prion (Derkatch et al., 2000).

$[PIN^+]$ is usually the prion form of the Rnq1 protein which is so named because the Rnq1 protein is rich in glutamine and asparagine residues (Derkatch et al., 2001; Osherovich et al., 2001). The Rnq1 protein consists of two domains: an N-terminal domain and a QN-rich C-terminal domain which constitutes the prion-forming domain (PrD) of Rnq1. The function of Rnq1 protein still remains unknown (Sondheimer and Lindquist, 2000). Recent studies have revealed that $[SWI^+]$ is capable of facilitating the *de novo* formation of $[PIN^+]$ (Du et al., 2014).

As the $[PSI^+]$ prion, the $[PIN^+]$ prion can take up differential heritable variants. Such $[PIN^+]$ variants differ in several ways, their efficiency of promoting the *de novo* appearance of $[PSI^+]$ and $[URE3]$ prions, the level of soluble and aggregated Rnq1 protein and the fluorescence pattern of Rnq1-GFP in the cytosol. Five variants of $[PIN^+]$ were originally identified and named as $[pin]$, low $[PIN^+]$, medium $[PIN^+]$, high $[PIN^+]$ and very high $[PIN^+]$ according to their distinct efficiency of $[PSI^+]$ induction (Bradley et al., 2002). Genetic studies have confirmed that distinct Rnq1 conformers define the different $[PIN^+]$ variants because the *RNQ1* gene sequence in these variants is identical (G. L. Staniforth, personal communication). A recent study has revealed that $[PIN^+]$ variants differ mainly in their cross-seeding abilities, but not in their seed (propagon) numbers or in other features in promoting $[PSI^+]$ conversion (Sharma and Liebman., 2013).

1.5.2 $[PIN^+]$ as a toxic amyloid model

Studies focusing on fatal neurodegenerative diseases such as Alzheimers disease have revealed that amyloids are key pathogenic components of these diseases. However, whether amyloids cause toxicity and the associated neurodegeneration remains unknown. Moreover, whether amyloid *per se* is cytotoxic or protective is still unclear. To help elucidate the mechanism of amyloid toxicity, several yeast models have been developed to investigate the relationship between aggregation of amyloid and the toxicity of its corresponding amyloid protein aggregates. The three major models are based on α -synuclein, polyQ and Rnq1.

S. cerevisiae has been used as a model to elucidate the mechanism of toxicity associated with Huntington disease. Huntington disease is caused by the accumulation of expanded polyglutamine (polyQ) huntingtin protein molecules encoded by the *huntingtin* gene with CAG repeat expansions (Gutkunst et al., 1999). Huntingtin molecules with expanded polyQ are more prone to aggregate into intracellular inclusion bodies and this leads to cell toxicity

(Scherzinger et al., 1997; Bates et al., 1998). Overexpression of the yeast prion protein Rnq1 can also lead to the formation of inclusion bodies similar to those observed in huntingtin with a polyQ expansion. Moreover, Rnq1 in its [*PIN*⁺] prion form is crucial for polyQ aggregation and consequently results in cell death (Meriin et al., 2002).

The yeast model provides a useful approach to investigate polyQ-induced toxicity not least because there is a direct link between aggregation of the expanded polyQ domain and its cytotoxicity. In addition, Hsp104, one of the most important molecular chaperones in prion propagation (see Section 1.3), can affect polyglutamine toxicity either directly via modulation of polyglutamine aggregates, or indirectly through modulation of prions that interact with polyglutamine aggregation (Gokhale et al., 2005). Moreover, defects in Hsp104 function can lead to inhibition of seeding of polyQ aggregates (Meriin et al., 2002).

[*PIN*⁺] can interact with other amyloidogenic proteins and facilitate their conversion into their amyloid conformation. It was reported that overexpression of Rnq1 is toxic when endogenous Rnq1 is pre-existing in the [*PIN*⁺] state (Douglas et al., 2008). This toxicity can be suppressed via interactions between a molecular chaperone namely Sis1 (Sondheimer et al., 2001). Moreover, overproduction of Rnq1 is ineffective at enhancing prion conversions (Derkatch et al., 2001).

1.6 Polyglutamine (polyQ) tract induced toxicity

1.6.1 Huntington's disease

Huntington's disease (HD) was first described as an autosomal dominant disease by George Huntington in 1872 (Huntington, 1872). HD is a fatal neurodegenerative disorder which is diagnosed by the selective loss of

medium spiny neurons in the striatum of HD patients. The most characteristic symptoms of HD include uncontrollable movement, neuropsychiatric abnormalities and cognitive dysfunction (Van Duijn, 2007).

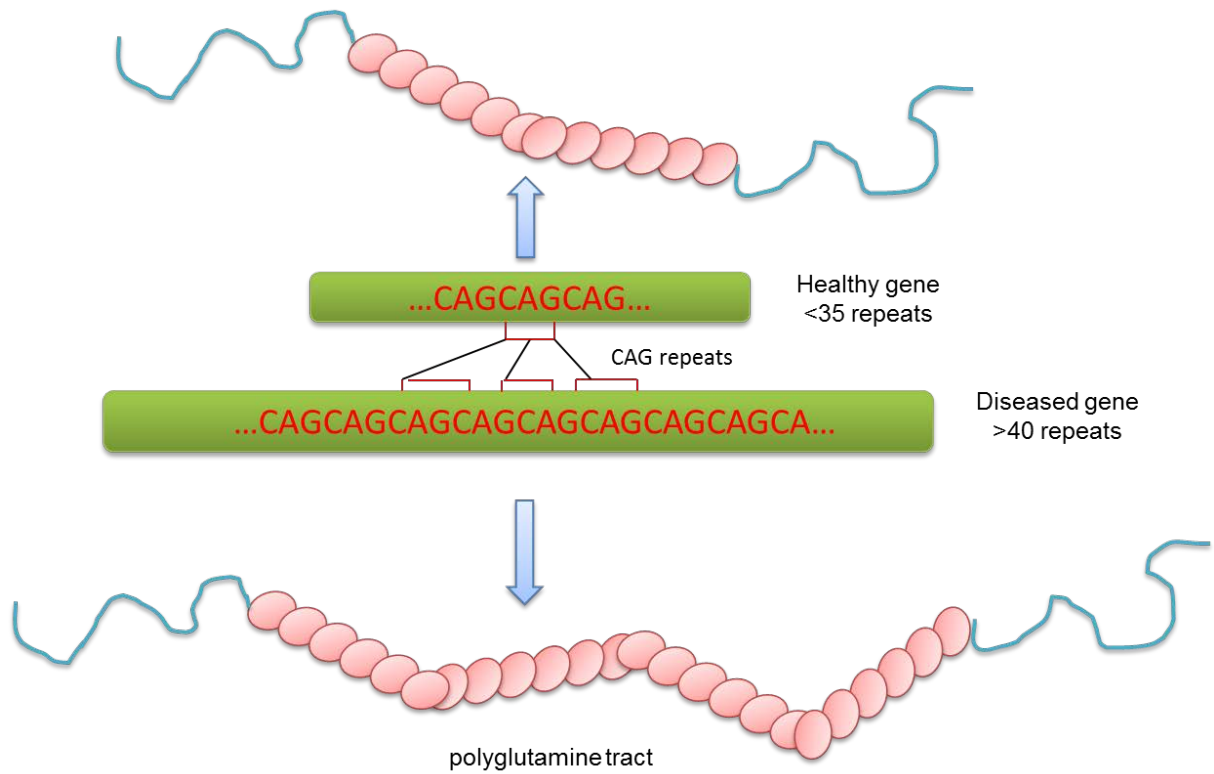


Figure 1.6 Huntington disease is caused by an expansion of the number of copies of the Gln CAG codon. If the elongated CAG repeat is translated, it generates a protein with an expanded glutamine stretch. The number of CAG repeats is typically less than 35 in normal individuals, but is 40 or more in patients with the disease.

Table 1.2. Classification of HD depending on the number of CAG repeats

Number of CAG repeats (n)	Classification	Disease status	Risk to offspring
n<35	Normal	Normal	None
35<n<40	Incomplete penetrant	May or may not be affected	50%
n>40	Fully penetrant	Diseased	50%

Genetically, HD is defined a 'trinucleotide repeat disorder' which is caused by an expansion in the number of a repeated trinucleotide (CAG) in the Huntingtin (*HTT*) gene. The *HTT* gene (also known as the *IT-15* gene) is located on the short arm of chromosome 4 (Walker, 2007). The CAG trinucleotide repeat encodes a polyglutamine (polyQ) tract in the huntingtin (*htt*) protein which varies in length between normal and diseased populations. Huntingtin is expressed in all human and mammalian cells, with the highest concentrations in the brain and testes (DiFiglia et al., 1995). Individuals with 35 or less CAG repeats in the *HTT* gene are able to produce normal *htt* proteins while the diseased population with a sequence of 35 or more CAG repeats results in the production of abnormal *htt* proteins with a propensity to aggregate (Table 1.2, Figure 1.6) (Walker, 2007). Moreover, individuals with a large number of CAG repeats, usually of 60 or more CAG units, are diagnosed as juvenile HD (Nance, 2001). The longer the polyQ expansion, the more severe the disease and the earlier its onset.

A huntingtin exon I fragment is found in huntingtin aggregates within neurons of HD patients and is sufficient to produce neurodegeneration in mouse models (Mende-Mueller et al., 2001). Similarly, Huntingtin exon I fragment with polyQ regions of different lengths were developed in many yeast models, which recapitulates the molecular basis of polyQ length-dependent toxicity (Krobitsch and Lindquist., 2000; Meriin et al., 2002). The huntingtin constructs of different yeast strains tested are related but differ in the nature of sequences flanking the polyQ region. Only Meriin's model has been found to be toxic (Meriin et al., 2002). It was reported that the commonly used FLAG-epitope (DYKDDDK) at the amino terminus of huntingtin exon I can unmask the toxicity of an otherwise benign polyQ protein, whereas the endogenous carboxyl-terminal polyproline region of huntingtin exon I can convert toxic proteins into nontoxic ones. This finding suggests that specific amino acid sequences flanking the polyQ region of huntingtin exon I greatly influence polyQ length-dependent toxicity (Duennwald et al., 2006).

1.6.2 Polyglutamine (polyQ) tract induced toxicity

In eukaryotes, a number of repetitive nucleotide triplets, CAG or CAA, vary in length resulting in the production of a chain of glutamine (Q) units referred to a polyglutamine (polyQ) tract. A subdomain of neurodegenerative disorders known as polyglutamine (polyQ) disorders is caused by such an expansion of a trinucleotide (CAG) repeat. The polyQ expansion was found associated with Spinal and Bulbar Muscular Atrophy (SMBA) in 1991 suggesting polyQ expansion plays an important role in a number of neurodegenerative disorders in addition to HD. Subsequently, another seven genes with polyQ expansions were found to be the causative agents of specific neurodegenerative diseases including that was known before 1991, DentatoRubral and Pallidoluysian Atrophy (DRPLA) and six types of Spino-Cerebellar Ataxias (SCA-1, SCA-2, SCA-3, SCA-6, SCA-7 and SCA-17).

PolyQ disorders have some features in common, such as that to be genetically inherited neurodegenerative disorders, toxic mutant proteins and a family of late onset and progress disorders. Apart from these common features, polyQ tract expansions lead to selective neuronal dysfunction and degeneration with specific populations of neurons resulting in different neurodegenerative diseases.

1.7 Genetic modifiers affect Rnq1 and Polyglutamine (polyQ) mediated toxicity

1.7.1 Bna4

The *BNA4* gene encodes the yeast orthologue of the mammalian enzyme, kynurenine 3-monooxygenase (KMO), which is involved in the mitochondrial kynurenine pathway. Tryptophan is metabolised mainly through the kynurenine pathway. The key compound of the kynurenine pathway is

kynurenine (KYN) which can undergo two distinct pathways. The metabolite of one pathway is kynurenic acid (KYNA) while the metabolites of the other pathway are 3-hydroxykynurenine (3-OH-KYN) and quinolinic acid (QUIN) which are the precursors of NAD (Figure 1.7).

KYNA is as an endogenous excitatory amino acid receptor blocker that links the nicotinic–cholinergic system and the KYN pathway in the brain (Hilmas et al., 2001). Increased levels of QUIN have been implicated in the pathophysiology of HD (Giorgini, 2008). An elevated level of 3-OH-KYN has been found in cells expressing a toxic mutant htt fragment (Giorgini et al., 2005; Giorgini et al., 2008). and these three tryptophan metabolites (KYNA, 3-OH-KYN and QUIN) are known as “neuroactive KYNs”. Imbalance of the kynurenine pathway metabolism is a key factor of pathogenesis in HD. The KMO protein has been identified as a drug target for HD that can be genetically or pharmacologically inhibited resulting in a reduced level of 3-OH-KYN and QUIN and therefore reducing disease-relevant phenotypes (Tauber et al., 2011).

Moreover, previous studies had revealed that *BNA4* deletion was able to suppress polyglutamine-rich-protein-mediated (Htt 103Q) cytotoxicity in a [*PIN*⁺] background (Giorgini et al., 2005).

1.7.2 UPF proteins

Upf proteins, Upf1, Upf2 and Upf3, are three key factors in the nonsense-mediated mRNA decay (NMD) pathway. NMD is an evolutionary conserved cellular pathway that results in degradation of aberrant mRNA transcripts that carry premature termination codons (PTCs) and therefore prevents synthesis of harmful C-terminally truncated proteins. In Upf1, Upf2 or Upf3 mutants, mRNA transcripts containing premature termination codons (PTCs) are stabilised.

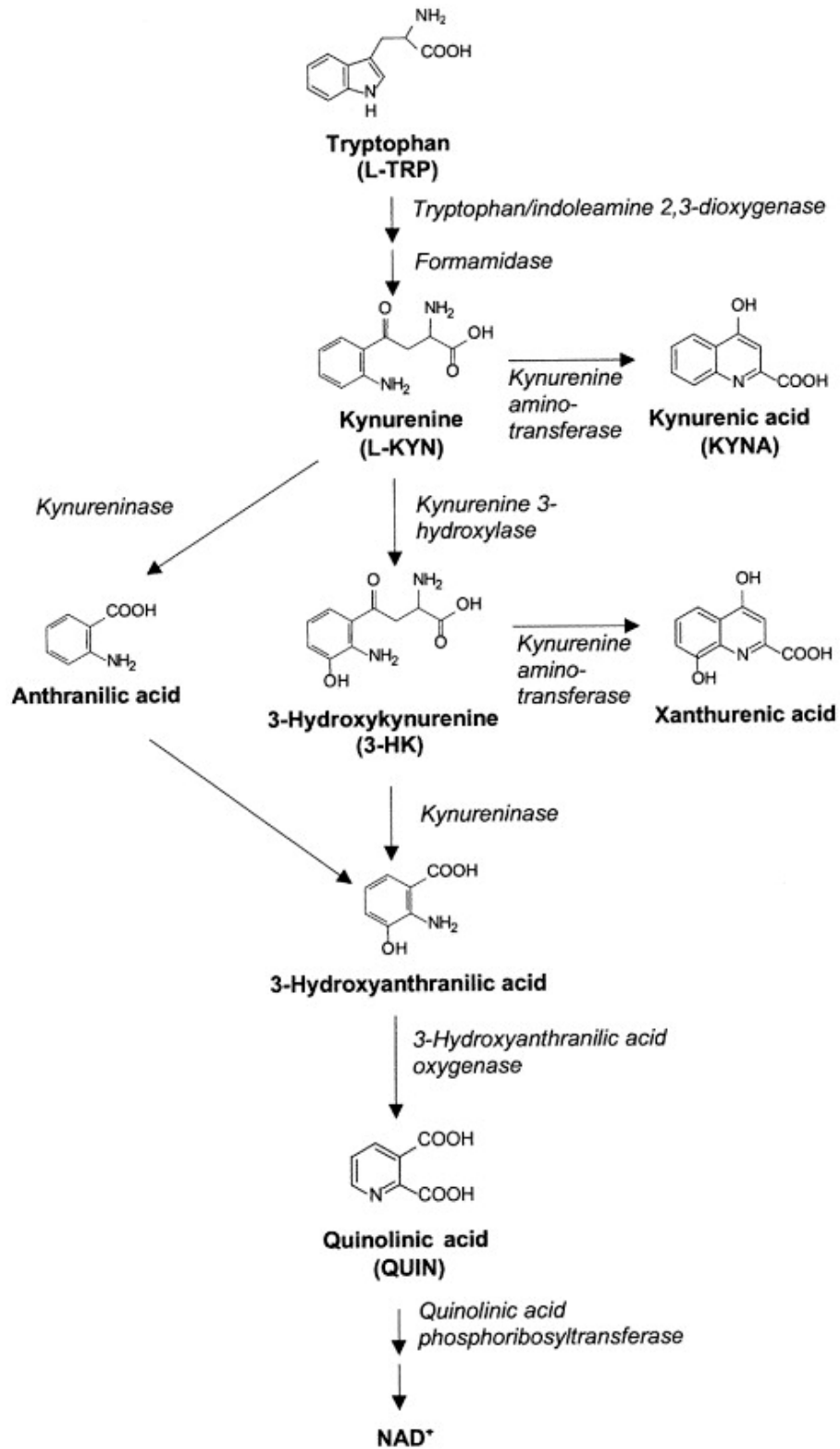


Figure 1.7 The kynurenine pathway (Obtained from Sas et al., 2007).

The Upf1 protein (also known as Nam7 in yeast) is an ATP-dependent RNA helicase distributed in the cytoplasm (He and Jacobson, 1995). The Upf2 protein (also known as Nmd2 in yeast) localises to the cytoplasm where it can interact with both the Upf1 and Upf3 protein (He et al., 1997). The Upf3 protein also localises to the nucleus and is rich in basic amino acid residues while the Upf2 protein is rich in acidic amino acid residues (Shirley et al., 1997).

The Upf proteins act as a complex since deletions of single or multiple *UPF* genes lead to equivalent stabilization of aberrant mRNA transcripts. Recent studies have revealed that the Upf1 protein not only binds to the NMD substrates but a number of transcripts which are not involved in the NMD pathway (Zund et al., 2013).

The two polypeptide release factors, eRF1 (Sup45) and eRF3 (Sup35), can interact with Upf proteins in yeast. Both eRF1 and eRF3 interact with Upf1 while only eRF3 interacts with Upf2 and Upf3. Since *UPF* gene deletions promote nonsense suppression, the Upf proteins not only play a crucial role in NMD but also translation termination (Wang et al., 2001).

1.8 Project aims

The accumulation of amyloids is the key pathogenic component of several neurodegenerative diseases including Huntington's disease, which is caused by a polyglutamine expansion in the huntingtin (Htt) protein. However, the molecular basis of amyloid toxicity is poorly understood. To reveal the molecular basis of pathogenesis of amyloid diseases, [*PIN*⁺] was chosen as a yeast-based toxic amyloid model system to determine the mechanism of toxicity and to identify how cellular factors can modulate this toxicity. In this study, a series of cellular and biochemical assays were employed to determine the mechanism of Rnq1-mediated cytotoxicity and compared with

polyglutamine-rich-protein-mediated cytotoxicity, both of which are dependent upon the presence of the [*PIN*⁺] prion.

The overall aim of my project was to establish the mechanism of Rnq1 overexpression-induced toxicity and compare the results with the expression of polyglutamine protein-mediated toxicity in yeast strains carrying different conformational variants of prion form of Rnq1.

The three specific aims were:

1. To analyse Rnq1-induced cytotoxicity in different [*PIN*⁺] variants when Rnq1 is overexpressed. The focus was to be on cell morphology, defects in cell growth, defects in nuclear migration and level of reactive oxygen species (ROS).
2. To compare the toxicity of polyglutamine-rich-proteins and Rnq1 overexpression in the different [*PIN*⁺] conformational variants
3. To further study the mechanism of Rnq1 toxicity by using a combination of cell biological and genetic approaches in several strains carrying gene deletions that reduced toxicity. The deletion strain *bna4*Δ was previously identified as suppressing polyglutamine-rich-protein-mediated cytotoxicity in the [*PIN*⁺] background. Upf1, a highly conserved protein that plays an important role in nonsense-mediated mRNA decay, was also found to modify amyloid toxicity.

Chapter 2

Materials and Methods

Chapter 2

2.1 Chemicals and reagents

Risk assessments including COSHH were carried out for all procedures involving use of hazardous chemicals or equipment and suitable control measures were employed. All work involving genetically modified organisms and pathogens were performed in an ACDP category two laboratory.

Table 2.1. Chemicals and reagents used in this study

Materials	Content	Source
Chemicals and reagents	Ethanol, Ethylenediaminetetraacetic acid, Guanidine hydrochloride, Polyethylene glycol, Tris-acetate-EDTA, Tetramethylethylenediamine, Tris(hydroxymethyl)aminomethane, Lithium acetate	Sigma Aldrich, Fisher scientific
Restriction enzymes	<i>Xho</i> I, <i>Hind</i> III	Promega, Roche, New England Biolabs
Reaction kits	QuikChange Lightning Site-Directed Mutagenesis Kit, QIAprep Spin Miniprep Kit (50)	Bio-Rad, QIAGEN, Invitrogen, Agilent Technologies
Media and amino acid drop-outs	Complete Supplement Mixture (CSM) single drop-outs: CSM, -ade; CSM, -ura; CSM, -leu; Complete Supplement Mixture (CSM) double drop-outs: CSM, -leu, ura	Difco, Formedium

2.2 Growth media

All components of the various growth media were weighted to two decimal places using a Sartorius MC1 LC620D balance (Sartorius). All components for liquid media were dissolved in ultrapure water produced by Direct-Q® 3 Ultrapure Water System (Merck Millipore) and autoclaved at 126°C with an 11 min cycle using a Prestige Medical benchtop autoclave. The autoclave was used to eliminate the risk of contamination from bacteria and other organisms. For solid media, granulated agar was added for solidification at a final concentration of 2% (w/v) prior to autoclaving. Solid media were prepared by pouring 20-25 ml molten media into one Petri dish.

Chapter 2

2.2.1 Yeast media for the culture of *Saccharomyces cerevisiae*

Table 2.2. Yeast growth media used in this study

Media	Recipe
YEPD (Yeast extract, peptone, dextrose) complete medium	2 % (w/v) glucose, 1 % (w/v) yeast extract, 2 % (w/v) bactopeptone
¼ YEPD (Yeast extract, peptone, dextrose) complete medium	2 % (w/v) glucose, 0.25 % (w/v) yeast extract, 2 % (w/v) bactopeptone
SC (Synthetic complete) 2% glucose drop-out medium	2 % (w/v) glucose, 0.67 % Yeast Nitrogen Base (without amino acids, with ammonium sulphate), the appropriate concentration of yeast synthetic complete drop-out media supplement
SC (Synthetic complete) 2% raffinose drop-out medium	2 % (w/v) Raffinose, the appropriate concentration of yeast synthetic complete drop-out media supplement
SC (Synthetic complete) 2% galactose and 1 % raffinose drop-out medium	2 % (w/v) Galactose, 1 % Raffinose, the appropriate concentration of yeast synthetic complete drop-out media supplement
SC (Synthetic complete) 2% galactose drop-out medium	2 % (w/v) galactose, 0.67 % Yeast Nitrogen Base (without amino acids, with ammonium sulphate), the appropriate concentration of yeast synthetic complete drop-out media supplement

2.2.2 Growth media for culturing *Escherichia coli*

Table 2.3. Bacterial growth media used in this study

Media	Recipe
LB (Luria Bertani) medium	1% (w/v) tryptone, 0.5% (w/v) yeast extract, 1% (w/v) sodium chloride
NZY ⁺ Broth	1% (w/v) NZ amine (casein hydrolysate), 0.5% (w/v) yeast extract, 0.5% (w/v) sodium chloride, adjust to pH 7.5 using sodium hydroxide and then autoclave Add the following filter-sterilized supplements prior to use: 1.25% (w/v) 1 M magnesium chloride, 1.25% (w/v) 1 M magnesium sulfate, 1% (w/v) 2 M glucose

Ampicillin was used to select for *E.coli* cells transformed with plasmids containing the AmpR gene. Filter-sterilized ampicillin was added to the LB medium at a final concentration of 100 µg/ml from a 100 mg/ml stock solution after autoclaving and cooling to 50°C.

Chapter 2

2.3 Strains

All *Saccharomyces cerevisiae* strains (Table 2.4) were grown in 50 ml Falcon tubes or 250 ml conical flasks containing appropriate media at 30°C incubator with shaking at 200rpm or on solid media in 30°C incubator. All strains were kept as glycerol stocks and stored at -80°C freezer.

2.3.1 *Saccharomyces cerevisiae* strains

Table 2.4. *Saccharomyces cerevisiae* strains used in this study

Strain	Notes	Genotype	References
74D-694	[<i>pin</i> ⁻]	<i>MATa ade1-14(UGA) trp1-289(UAG) ura3-52 his3-Δ200 leu2-3, 112</i>	Chernoff et al. 1993
74D-694	Low [<i>PIN</i> ⁺]	<i>MATa ade1-14(UGA) trp1-289(UAG) ura3-52 his3-Δ200 leu2-3, 112</i>	Chernoff et al. 1993
74D-694	Medium [<i>PIN</i> ⁺]	<i>MATa ade1-14(UGA) trp1-289(UAG) ura3-52 his3-Δ200 leu2-3, 112</i>	Chernoff et al. 1993
74D-694	High [<i>PIN</i> ⁺]	<i>MATa ade1-14(UGA) trp1-289(UAG) ura3-52 his3-Δ200 leu2-3, 112</i>	Chernoff et al. 1993
74D-694	Very high [<i>PIN</i> ⁺]	<i>MATa ade1-14(UGA) trp1-289(UAG) ura3-52 his3-Δ200 leu2-3, 112</i>	Chernoff et al. 1993
BY4741	[<i>pin</i> ⁻]	<i>MATa his3Δ1 leu2Δ0 met15Δ0 ura3Δ0</i>	Zhiyuan Li
BY4741	[<i>PIN</i> ⁺]	<i>MATa his3Δ1 leu2Δ0 met15Δ0 ura3Δ0</i>	Research Genetics, Huntsville, AL
BY4741	<i>RNQ1</i> deleted	<i>MATa his3Δ1 leu2Δ0 met15Δ0 ura3Δ0</i>	G. L. Staniforth
BY4741	<i>BNA4</i> deleted	<i>MATa his3Δ1 leu2Δ0 met15Δ0 ura3Δ0</i>	G. L. Staniforth
BY4741	<i>UPF1</i> deleted	<i>MATa his3Δ1 leu2Δ0 met15Δ0 ura3Δ0</i>	G. L. Staniforth
BY4741	<i>UPF2</i> deleted	<i>MATa his3Δ1 leu2Δ0 met15Δ0 ura3Δ0</i>	G. L. Staniforth
BY4741	<i>UPF3</i> deleted	<i>MATa his3Δ1 leu2Δ0 met15Δ0 ura3Δ0</i>	G. L. Staniforth

Chapter 2

2.3.2 Escherichia coli strains

All *Escherichia coli* strains (Table 2.5) were grown in 1.5 ml Eppendorf tubes, 50 ml Falcon tubes or 250 ml conical flasks containing appropriate media at 37°C incubator with shaking at 200 rpm or on solid media in 37°C incubator. All strains were kept as glycerol stocks and stored at -80°C freezer.

Table 2.5. *Escherichia coli* strains used in this study

Strain	Genotype	Source
TOP10	F- <i>mcrA</i> Δ(<i>mrr-hsdRMS-mcrBC</i>) Φ80 <i>lacZ</i> Δ <i>M15</i> Δ <i>lacX74</i> <i>recA1</i> <i>araD139</i> Δ(<i>ara leu</i>) 7697 <i>galU</i> <i>galK</i> <i>rpsL</i> (StrR) <i>endA1</i> <i>nupG</i>	
XL10-Gold Ultracompetent cells	Tet ^r Δ(<i>mcrA</i>)183 Δ(<i>mcrCB-hsdSMR- mrr</i>)173 <i>endA1</i> <i>supE44</i> <i>thi-1</i> <i>recA1</i> <i>gyrA96</i> <i>relA1</i> <i>lac</i> Hte [F' <i>proAB</i> <i>lacI</i> ^q <i>ZDM15</i> Tn10 (Tet ^r) Amy Cam ^r]	QuikChange Lightning Site- Directed Mutagenesis Kit

2.4 Plasmids

Table 2.6. Plasmid used in this study

Plasmid	Characteristic	Insert
pYES2	<i>GAL1</i> P, <i>URA3</i> , 2μ, Amp ^R	none
pYES2	<i>GAL1</i> P, <i>URA3</i> , 2μ, Amp ^R	<i>RNQ1</i>
pYES2	<i>GAL1</i> P, <i>URA3</i> , 2μ, Amp ^R	polyQ25
pYES2	<i>GAL1</i> P, <i>URA3</i> , 2μ, Amp ^R	polyQ103
pYES2	<i>GAL1</i> P, <i>URA3</i> , 2μ, Amp ^R	<i>RNQ1</i> deletion
pYES2	<i>GAL1</i> P, <i>URA3</i> , 2μ, Amp ^R	<i>BNA4</i> deletion
pYES2	<i>GAL1</i> P, <i>URA3</i> , 2μ, Amp ^R	<i>UPF1</i> deletion
pYES2	<i>GAL1</i> P, <i>URA3</i> , 2μ, Amp ^R	<i>UPF2</i> deletion
pYES2	<i>GAL1</i> P, <i>URA3</i> , 2μ, Amp ^R	<i>UPF3</i> deletion
P6442	<i>CUP1</i> P, <i>URA3</i> , <i>CEN6/ARS</i> , Ampr + <i>SUP35</i> NM ORF	none
pAG426	<i>GAL1</i> P, <i>URA3</i> , 2μ, <i>RNQ1</i> ORF, N-terminal <i>GFP</i> tag	<i>RNQ1-GFP</i>
pAG415		<i>UPF1</i>

GAL1P: promoter of the *GAL1* gene; *CUP1*: promoter of the *CUP1* gene; *URA3*: selective markers, uracil biosynthesis gene from *Saccharomyces cerevisiae*

Chapter 2

2.5 Oligonucleotide primers

All oligonucleotide primers were synthesised by Eurofins MWG Operon. The primers were diluted at a final concentration of 100 pmol/μl in an appropriate amount of sterilised ultrapure water produced by Direct-Q® 3 Ultrapure Water System (Merck Millipore) and stored at -20°C.

Table 2.7. Oligonucleotide primers used for Site-directed mutagenesis

Primer's name	Sequence (5'-3')	Target gene
His94Arg_F	CGGTACAAGCAGCTCCCGCATTGTTAATCACTTAGT	<i>UPF1</i>
His94Arg_R	ACTAAGTGATTAACAATGCGGGAGCTGCTTGTACCG	<i>UPF1</i>
Lys436Ala_F	GGCCCACCAGGCACTGGTGCAACAGTTACTTCAGCAAC	<i>UPF1</i>
Lys436Ala_R	GTTGCTGAAGTAACTGTTGCACCAGTGCCTGGTGGGCC	<i>UPF1</i>

Table 2.8. Oligonucleotide primers used for verification of Site-directed mutagenesis

Primer's name	Sequence (5'-3')	Target gene
UPF1_His94_F	CAATTCATGTGCGTATTG	<i>UPF1</i>
UPF1_His94_R	CACGTTCTTACGTCCAC	<i>UPF1</i>
UPF1_K436A_F	GATGTCCCATTACCT	<i>UPF1</i>
UPF1_K436A_R	AACCCAAGTCACGTA	<i>UPF1</i>

2.6 DNA methods

2.6.1 Purification of plasmid DNA from *Escherichia coli*

QIAprep Spin Miniprep Kit (50) (QIAGEN, Cat. no. 27104) was used to purify all plasmid DNA. The procedure was carried out as detailed in the manufacturer's protocol in the QIAprep® Miniprep Handbook [pp22-23].

Chapter 2

2.6.2 Agarose gel electrophoresis

0.5 g of agarose was added into a 250 ml conical flask containing 49 ml of deionised water and 1 ml of 50 × TAE buffer (40 mM tris, 1 mM EDTA, 20 mM acetic acid, pH 8.5). The mixture was placed in a microwave oven for 1 min at full power until the agarose was completely dissolved in the buffer. The boiled agarose solution was allowed to cool down for 10 min. Then 5 µl of SYBR-Safe DNA stain (Invitrogen, S33102) was added to the solution. The gel solution was slowly poured into a gel tray with the appropriate comb in place. 20-30 min was allowed for the gel to solidify at room temperature. 500 ml of 1 × TAE buffer was poured in an electrophoresis tank. 2 µl of 6x blue/orange loading buffer (Promega) was added to 10 µl of each DNA sample before loading onto the gel. The agarose gel was run at 100 volts for 30-40 mins. The DNA fragments were visualised using either a UV transilluminator with safety glasses or using FLA-5100 imaging system (FujiFilm).

2.6.3 Restriction enzyme digestion

Plasmid DNA was digested by restriction endonucleases in buffers provided by the enzyme manufactures (Promega, Roche or New England Biolabs). The restriction digest reagent mixture was made of restriction endonucleases (1 µl each), appropriate buffer (2 µl), Bovine Serum Albumin (2 µl at a final concentration of 2 µg/µl), plasmid DNA (1.5 µl at a final concentration of 1-1.5 µg/µl) and sterile ultrapure water to a final volume of 20 µl. For double digestions, an appropriate buffer was chosen by web-based restriction enzyme assistant software provided by the manufacturer's website (e.g. <https://www.neb.com/tools-and-resources/interactive-tools/double-digest-finder>). The reaction mixture was incubated at 37°C for 3 hours. The result of digestion reaction was visualised by agarose gel electrophoresis (Section 2.7.2).

2.6.4 Determination of DNA concentration

DNA concentration was obtained by adding 1 μ l of DNA to 99 μ l of distilled H₂O (dH₂O). DNA samples were mixed by pipetting in a 1.5 ml Eppendorf and transferred to a single sealed cuvette (10 x2 x 36 mm). The DNA sample was loaded in the centre of the measuring area and steps were taken to ensure that there were no air bubbles. A blank of dH₂O was used as a reference. DNA concentration was measured at 230, 260 and 280 nm using a BioPhotometer plus (Eppendorf) at a path-length of 1 cm. RNA and protein contaminations were determined by a comparison of the 260 nm absorbance divided by the 280 nm absorbance, while organic compounds or chaotropic salts contaminations were determined by the absorbance at 260 nm divided by the absorbance at 230 nm. These values are used to verify the purity of DNA samples. Typically, DNA samples in good-quality have an A_{260}/A_{280} ratio of 1.7- 2.0 and an A_{260}/A_{230} ratio greater than 1.5 (Promega).

2.6.5 QuikChange Lightning Site-Directed Mutagenesis

Mutations in the *UPF1* gene were created using a QuickChange Lightning Site-Directed Mutagenesis kit (Agilent technologies, Cat. no. 210518). Mutagenic primer design was carried out using the QuickChange Primer Design Program at www.agilent.com/genomics/qcpd. The oligonucleotides used are listed in Table 1.7. Mutant strand synthesis reaction, restriction enzyme digestion and transformation of XL10-Gold ultracompetent cells were performed according to the instruction manual (pp 7-11)

2.6.6 DNA sequencing

All DNA sequencing in this project was performed by Source BioScience (1 Orchard Place, Nottingham Business Park, Nottingham, NG8 6PX) using Sanger sequencing technique. Purified plasmid DNA sample was diluted at a

Chapter 2

final concentration of 100 ng/μl with a total volume of 10 μl. Associated primers of each plasmid DNA sample were diluted with sterile ultrapure water at a final concentration of 60-70 ng/μl with a total volume of 10 μl for each reaction. An online order for DNA sequencing was submitted via the website <http://www.lifesciences.sourcebioscience.com/> and both purified plasmid DNA samples and their corresponding primers were sent directly to Source Bioscience. The results of DNA sequencing were received by e-mail and analysed using Multiple Sequence Alignment (<http://www.ebi.ac.uk/Tools/msa/clustalw2/>) and Blast translate (<http://blast.ncbi.nlm.nih.gov/Blast.cgi>).

2.7 Recombinant DNA methods

2.7.1 Preparation of competent *E. coli* cells

A single colony was picked from an LB plate and transferred into 10 ml of LB broth in a 50 ml Falcon tube. The bacterial culture was placed in a 37°C incubator with shaking at 220 rpm and grown for 12-16 hrs. 32 μl of saturated overnight culture was transferred into 112 ml of LB broth in a 250 ml of conical flask and incubated at 37°C with shaking at 220 rpm until OD₆₀₀ of 0.5 was reached (usually 4 hours). 15 ml of glycerol was heated in a microwave then placed in a 37°C water bath. Then 15 ml of sterilized warm glycerol was slowly added into the bacterial culture when OD₆₀₀ was approximately reaching 0.5. The culture was placed on ice for 10 mins then transferred into a pre-chilled 500 ml centrifuge tube. Cultures were centrifuged at 4000 rpm for 10 mins at 4°C. The supernatant was carefully discarded by pouring and pipetting while the cell pellet was re-suspended in an equal volume of ice-cold 0.1M MgCl₂ with 15% (v/v) sterile glycerol pipetting up and down to gently mix. Cells were centrifuged at 3800 rpm for 8 mins at 4°C. The supernatant was removed then cells were resuspended in 25 ml of ice-cold T-salts (0.075 M CaCl₂, 0.006 M MgCl₂, 15 % (v/v) glycerol) and transferred to a pre-chilled 50

Chapter 2

ml Falcon tube. Cells were incubated on ice for 20 mins with occasional mixing by flicking the bottom of the falcon tube gently. After 20 mins, cells were centrifuged at 3600 rpm for 6 mins at 4°C. Finally, the cell pellet was resuspended in 5 ml of ice-cold T-salts then transferred into fifty pre-chilled 1.5 ml Eppendorf tubes as 100 µl aliquots. Aliquoted cells were stored immediately at -80°C freezer until required.

2.7.2 Transformation of plasmid DNA into *Escherichia coli*

An aliquot of competent cells was thawed on ice and mixed by flicking the tube gently when it had thawed. 2 µl (200-300 ng/µl) of plasmid was added to 50 µl of competent cells in 1.5 ml Eppendorf tube and was placed on ice for 30 mins. The Eppendorf tube with the cells was put in a 42°C water bath for 45 seconds then the tube placed on ice immediately for 2 mins. The cells were then re-suspended in 800 µl of LB broth and incubated at 37°C with shaking (180 rpm) for one hour. 120 µl of the transformation mixture was plated out onto appropriate agar plates containing the appropriate antibiotics according to the selective marker on the plasmid. The plates were then placed upside down in the 37°C incubator overnight.

2.7.3 Transformation of plasmid DNA into *Saccharomyces cerevisiae*

Yeast cells were harvested by centrifugation at 13000 rpm for 20 seconds at room temperature from 2 ml of overnight yeast culture. The supernatant was discarded and the cell pellet was resuspended in 82.5 µl of transformation solution which was composed of 36 µl of 1 M lithium acetate, 10 µl of freshly denatured single-stranded carrier DNA (salmon sperm DNA, 10 mg/ml), 2.5 µl of β- mercaptoethanol and 34 µl of sterile deionised H₂O. Then 240 µl of polyethylene glycol (PEG)-3350 (50 % w/v) and 3 µl (200-300 ng/µl) of plasmid DNA were added to the transformation mixture. Cells were completely resuspended by vortexing at full speed for 1 min. The

Chapter 2

transformation mixture was then incubated at 30°C incubator for 30 mins followed by heat shock of 42°C for a further 30 mins. Cells were harvested by centrifugation at 2000 rpm for 5 mins. The supernatant was discarded and the cell pellet resuspended in 150 µl of sterile ultrapure water. Cells were plated onto appropriate agar plates that allowed for selection of transformed cell (e.g. SC-ura plate for plasmid carrying the *URA3* marker). The plates were then placed upside down in the 30°C incubator for 3-4 days.

2.8 Growth conditions and analysis

2.8.1 Determination of cell density

Cell density was obtained by measuring either diluted or undiluted cell culture up to 1 ml of corresponding medium into a plastic cuvette. The cell sample was mixed by vortexing. A blank of growth medium (i.e. no cells) was used as a reference. Cell density was measured at 600 nm using BioPhotometer plus (Eppendorf) at a path-length of 1 cm.

2.8.2 Cell induction by galactose

Yeast cells were grown overnight in 5 ml of SC (Synthetic complete) 2% glucose drop-out medium (Table 2.2) at 30°C incubator with shaking at 200 rpm. Cells were collected by centrifugation at 3000 rpm for 5 mins at room temperature. The supernatant was discarded and cells were washed in sterile water three times in order to remove all the glucose containing medium. 5 ml of SC (Synthetic complete) 2% galactose drop-out medium (Table 2.2) was added for induction. Cells were incubated at 30°C incubator with shaking at 200 rpm for 8 hours. Galactose was used to induce the expression of certain

Chapter 2

genes under the control of the plasmid with *GAL1* promoter (e.g. pYES2-based constructs).

2.8.3 Growth analysis by microplate reader

A single colony of the required yeast strain was inoculated into a 50ml Falcon tube containing 5 ml of appropriate liquid medium as a starter culture. This culture was grown overnight at 30°C with shaking at 200 rpm. Cells were then diluted to an OD₆₀₀ of 0.1 with a final volume of 1ml in a 24-well sterile plate (Greiner). Growth curves were generated by a Fluostar Omega microplate reader according to the reading of OD₆₀₀ hour by hour (usually use 24 or 36 hours as a period).

2.8.4 Calculation of doubling time

Doubling time is the amount of time it takes for a given quantity to double in size or value at a constant growth rate. The doubling time of each strain used in this study was determined with the following calculation: time in minutes was plotted against OD600 values using MS Excel, an exponential trend-line was applied to the graph along with the trend-line equation, the natural logarithm of 2 was divided by the equation x value to give the doubling time in minutes.

2.9 Biological assays

2.9.1 [*PIN*⁺] *de novo* conversion assay

One [*pin*⁻] and four [*PIN*⁺] variants ([*PIN*⁺]Low, [*PIN*⁺]Medium, [*PIN*⁺]High and [*PIN*⁺]Very high of the 74D-694 yeast strain were transformed with plasmid

Chapter 2

p6442 as described in Section 2.4. The plasmid p6442 contains a region of expressing Sup35pNM-GFP fusion protein under the *CUP1* promoter. A small portion of a single transformed colony of each variant was inoculated into 50 ml of selective medium according to the selective marker on the plasmid in a 250 ml conical flask for overnight growth at 30°C incubator with shaking at 200 rpm. The cell number of 1 ml of the overnight culture was calculated by a haemocytometer. Cells were diluted in sterile water to a final volume of 100 µl which contains approximately 300 cells. Then 100 µl of diluted cells were plated onto appropriate agar plate. The plates were placed upside down in the 30°C incubator for three days. After three days, a single colony was randomly selected from each plate containing different [*PIN*] variants and re-suspended each colony into a 250 ml conical flask containing 50 ml of appropriate selective medium with CuSO₄ at a final concentration of 25µM. The flask was placed into 30°C incubator with shaking (200 rpm) for 24 hours. 5 µl of each variant was spotted onto three distinct fresh synthetic complete drop-out selection media (1/4 YPD complete medium, SC-ade medium, 1/4 YPD + 3mM GdnHCl medium). The plates were dried at room temperature until the culture was totally absorbed by the agar. The plates were placed upside down in a 30°C incubator for 3-4 days until colonies were grown to an appropriate size. The plates were scanned under a black background for good contrast.

2.9.2 Toxicity assay

Expression of the relevant GAL1 promoter-regulated gene was induced by galactose as described in section 2.9.2. Cell samples were diluted to an OD₆₀₀ of 0.5 into 1 ml of 2% galactose synthetic complete selective repressing medium in 1.5 ml Eppendorf. 200 µl of the diluted sample was transferred into the first well as the most concentrated culture. 120 µl of 2% galactose synthetic complete selective repressing medium was loaded to well 2, 3, 4 and 5 by a multi-channel pipette. Then 30 µl of the most concentrated culture was transferred from well 1 into well 2 containing 120 µl of 2% galactose

Chapter 2

synthetic complete selective repressing medium. This represents a 1:5 dilution from the concentrated culture. Five consecutive dilutions were carried out by transferring 30 μ l of concentrated culture to the following well with 120 μ l of 2% galactose synthetic complete selective repressing medium. The cumulative dilutions of the sample from the most concentrated culture to the least concentrated culture were 1, 1:5, 1:25, 1:125, 1:625 respectively. Cell suspensions were mixed thoroughly by pipetting the 30 μ l of the culture up and down at least 10 times for each dilution step. 4 μ l of each dilution was spotted onto three different fresh synthetic complete drop-out selection plates [$\frac{1}{4}$ YEPD complete medium, SC (Synthetic complete) drop-out medium, SC (Synthetic complete) 2 % galactose drop-out medium]. The plates were dried at room temperature until the culture was totally absorbed by the agar. The plates were placed upside down in a 30°C incubator for 3-4 days until colonies were grown to an appropriate size. The plates were scanned under a black background for good contrast.

2.9.3 Reactive Oxygen Species (ROS) detection using Fluorescence Activated Cell Sorting (FACS)

Cells were induced by galactose induction as described in section 2.9.2. Samples were diluted with 1 \times PBS to an OD₆₀₀ of 0.5 at a final volume of 1 ml. 2 μ l of dihydroethidium (DHE) dye was added to each sample to a final concentration of 10 μ M DHE. DHE was used for detecting the production of superoxide radicals. Dihydroethidium is fluorescent blue while it turns to fluorescent red in its oxidised form (hydroxyethidium) as generated by superoxide radicals. Cells were incubated with DHE for 10 mins before Reactive Oxygen Species (ROS) detection by a BD FACSCalibur flow cytometer. The results were analysed by BD CellQuest Pro Software.

2.10 Protein methods

2.10.1 Preparation of cell extract for quantitative western blot analysis

Cell extract preparation was carried out based on the protocol published by von der Haar (2007). A yeast culture was grown in 250 ml of conical flask containing appropriate medium until an OD₆₀₀ of approximately 0.6- 0.8. Eight OD₆₀₀ units of the cell culture in exponential phase of growth were harvested by centrifugation at 3000 rpm for 5 min at room temperature. The medium was discarded and the cell pellet was washed once with sterile ultrapure water. Then the cell pellet was resuspended in 200 µl of quantitative lysis buffer (0.1 M NaOH, 0.05 M EDTA, 2% SDS, 2% β-mercaptoethanol). The cell suspension was incubated for 10 min at 90°C followed by the addition of 5 µl of 4 M acetic acid in order to neutralise NaOH of the lysis buffer and vortexing for 30 secs to mix. Then the suspension was incubated at 90°C for a further 10 mins. Samples were allowed to cool and 50 µl of loading buffer (0.25 M Tris-HCl pH6.8, 50% glycerol, 0.05% bromophenol blue) was added to 200 µl of cells extracts.

2.10.2 Separation of proteins by SDS-polyacrylamide gel electrophoresis (SDS-PAGE)

SDS-PAGE gels were prepared with a resolving gel (0.375 M Tris, pH 8.8, 0.1% SDS, 10% acrylamide, 0.15% ammonium persulphate, 0.07% TEMED) and a upper stacking gel (0.25 mM Tris, pH 6.8, 0.1% SDS, 0.23% ammonium persulphate, 0.07% TEMED) using a 1 mm cassette (Invitrogen). The resolving gel mixture was mixed by swirling and immediately loaded into the 1 mm cassette with a pipette filled to approximately 4/5 of the cassette. 100% ethanol was added on the top of the resolving gel. Once the resolving gel was solidified, ethanol was poured off and the cassette was rinsed with ultrapure water. The cassette was dried using paper towels but avoiding

Chapter 2

touching the resolving gel. The stacking gel solution was then mixed and pipetted onto the top of the resolving gel. A comb with an appropriate size was placed into the stacking gel and then removed once the stacking gel was set. The SDS-PAGE gel was run at 150 V for 90 mins with SDS running buffer (0.025 M Tris base, 0.188 M Glycine, 0.15% (w/v) SDS) of a X- Cell Surelock gel tank (Invitrogen) using either a PS304 (GibcoBRL) or 200/2.0 (Bio-Rad) electrophoresis power supply.

2.10.3 Coomassie brilliant blue staining and destaining

The SDS-PAGE gel was immersed in Coomassie brilliant blue stain (40 % (v/v) Methanol, 20 % (v/v) Glacial acetic acid, 0.1 % (w/v) Coomassie brilliant blue R250) and incubated for 30 mins on an orbital shaker at room temperature. The Coomassie brilliant blue stain was then discarded and replaced by destain solution (10 % (v/v) Methanol, 10 % (v/v) Acetic acid). The gel was destained against two or three changes of the destain solution at room temperature on an orbital shaker until protein bands were clearly visualised.

2.10.4 Western blotting

A piece of Hybond ECL nitrocellulose blotting membrane (GE healthcare) was cut to fit the size of the SDS-PAGE gel (7× 8 cm for Invitrogen pre-cast gels). The membrane and the SDS-PAGE gel were transferred to a box containing Transfer buffer (20% Methanol, 0.037% SDS, 48 mM Tris base and 38.6 mM Glycine) and incubated on a shaker for 15 mins. Two pieces of thick blotting paper (Biorad) were cut to the same size as the membrane and soaked in the box containing transfer buffer. One piece of the blotting paper was placed in the middle of the blotting apparatus and air bubbles were removed using a roller with little pressure. The membrane, SDS-PAGE gel and the other piece of the blotting paper (from bottom to top) were placed exactly on the top of the first piece of blotting paper. Remaining air bubbles were removed again with

Chapter 2

the roller over the top of the sandwich. The electrophoretic transfer was carried out using a trans-blot SD semi-dry transfer cell (Bio-Rad) at 10V for 45 mins.

2.10.5 Chemiluminescence detection

The transferred membrane was removed from the blotting apparatus and incubated in PBS-M buffer (5% (w/v) milk powder (Marvel), 1 × PBS) for at least 10 mins at room temperature with shaking. Primary antibody was diluted to an appropriate concentration in 10- 15 ml of PBS-M buffer and incubated at 4 °C overnight with shaking. The following day, the membrane was washed briefly with 20 ml of fresh PBS-M buffer and incubated with the secondary antibody solution for 1- 2 hrs at room temperature with shaking. The secondary antibody solution was prepared in 10- 15 ml of PBS-M buffer to an appropriate concentration. After incubation with the secondary antibody, the membrane was washed three times in PBS for 5 mins each with shaking. In the dark room, a 1:1 mixture of the following two solutions: ECL solution 1 (2.5 mM Luminol, 396 µM Coumaric acid, 0.1 M Tris-HCl, pH 8.5) and ECL solution 2 (0.0192% Hydrogen peroxide, 0.1 M Tris-HCl, pH 8.5) was freshly made and incubated with the membrane for 1- 2 mins. The ECL solution 1 and ECL solution 2 were protected from light with aluminium and mixed only before using. The membrane and one piece of Amersham hyperfilm ECL (GE Healthcare) were placed in the cassette for a few sec and developed using a Xograph compact 4× imaging system.

2.11 Fluorescence microscopy methods

2.11.1 GFP microscopy

Log phase cells ($OD_{600} \sim 0.6$ to 1) were harvested by centrifugation at 13,000 rpm for 1 min. The supernatant was discarded and the pellet washed once in sterile water. Cells were re-suspended in an appropriate amount of sterile water. 3-5 μ l of sample was pipetted on a glass slide covered with the coverslip. One drop of oil was dripped onto the coverslip for protecting lens. Cells were visualised by a green excitation filter on an Olympus 1X81 fluorescent microscope with Hamamatsu Photonics Orca AG cooled CCD camera. Images were captured analysed by Olympus Cell^R software.

2.11.2 DAPI staining

1 ml of log-phase cells ($OD_{600} \sim 0.6$ to 1) were harvested by centrifugation at 13,000 rpm for 1 min. The supernatant was discarded, the pellet was fixed in 70% ethanol for 10 mins and then the cells were washed once in sterile water. Cells were re-suspended in appropriate amount of sterile water (typically 30 μ l) and 4',6-diamidino-2-phenylindole (DAPI) as a fluorescent stain which binds to A-T rich regions in both nuclear and mitochondrial DNA was added at a final concentration of 1 μ g/ml. 3-5 μ l of sample was spotted on a glass slide covered with the coverslip. One drop of oil was dripped onto the coverslip in order to protect the lens. Cells were visualised by a blue excitation filter on an Olympus 1X81 fluorescent microscope with Hamamatsu Photonics Orca AG cooled CCD camera. Images were captured analysed by Olympus Cell^R software.

2.12 Electron microscopy methods

Yeast cells were grown and induced by galactose as described in Section 2.8.2. An equivalent of 10 OD₆₀₀ units of log phase cells was harvested by centrifugation at 3000 rpm for 5 min at 4°C at two time points (t=0 and t=6). Two volumes of 2 × fixative (5% glutaraldehyde in PBS) were then added to each culture, thoroughly mixed and harvested by centrifugation at 3000 rpm for 5 min at 4°C. The supernatant was discarded and the cell pellet was resuspended in one volume of 1× fixative (2.5% glutaraldehyde in PBS) and kept as cell suspension at 4°C overnight. On the following day, cells were pelleted by centrifugation at 3000 rpm for 5 min at 4°C. All further steps involving osmium tetroxide fixation, dehydration, embedding, thin section and positive staining were performed by Ian Brown a Microscopy Suite Facility Manager of the University of Kent. Images were acquired on a JEOL JEM-1230 transmission electron microscope (80 kV; Jeol) with a Gatan Orius SC1000 CCD camera (Gatan, Pleasanton) and Gatan DigitalMicrograph software (Gatan).

Chapter 3

***De novo* formation of [PSI⁺] prion detected
by different [PIN⁺] variants**

3.1 Introduction

The *de novo* formation of the $[PSI^+]$ prion occurs either spontaneously or can be induced by the overexpression of Sup35NM domain or full-length Sup35 (Chernoff *et al.*, 1993; Derkatch *et al.*, 1996). The spontaneous *de novo* conversion of Sup35 into $[PSI^+]$ arises at a very low rate, approximately 5×10^{-7} (Lund *et al.*, 1981; Lancaster *et al.*, 2010). The spontaneous and induced *de novo* formation of $[PSI^+]$ is facilitated by other prions. Evidence suggests that the presence of $[PIN^+]$ (Derkatch *et al.*, 1997), $[URE3]$ (Derkatch *et al.*, 2001), $[SWI^+]$ (Du *et al.*, 2014) and aggregating variants of huntingtin (Derkatch *et al.*, 2004) can enhance the *de novo* appearance of the $[PSI^+]$ prion.

Similar to the mammalian prion, PrP^{Sc}, which has different variants generating distinct symptoms of transmissible spongiform encephalopathies (Bruce., 1993), $[PSI^+]$ can exist in the form of different types of aggregates known as variants. These variants have an unaltered genotype but show different strengths of the $[PSI^+]$ -associated nonsense suppression phenotype (Derkatch *et al.*, 1996; Derkatch *et al.*, 1997; Zhou *et al.*, 2001). There are mainly two types of $[PSI^+]$ variants: strong $[PSI^+]$ and weak $[PSI^+]$ variants. The strong $[PSI^+]$ *ade1-14* variant forms white Ade⁺ colonies while the weak $[PSI^+]$ variant forms red/pink colonies on rich medium and poor growth on adenine deficient medium. This is because *ade1-14* nonsense suppression is more efficient in a strong $[PSI^+]$ variant than a weak $[PSI^+]$ variant. In addition, the activity of molecular chaperones has been found to affect prion variants. For example, Hsp70 activity is affected by either over- or under-expression of *SSE1* that results in a specific $[PSI^+]$ variant when induced (Fan *et al.*, 2007). Evidence suggests that Sse1 acts as a nucleotide exchange factor for Hsp70 members, in this case, Ssa1 and Ssb1 (Dragovic *et al.*, 2006). Sse1 promotes the *de novo* formation of $[PSI^+]$ mainly based on Ssa1 function. It was established that overexpression of Sse1 can more efficiently stimulate the function of Ssa1 indicating that Sse1 interacts preferentially with Ssa1. Interaction between Sse1 and Ssa1 plays a key role in establishing the full spectrum of $[PSI^+]$ (Fan *et al.*, 2007). Moreover, the $[PSI^+]$ variants can be

Chapter 3

eliminated by either overexpression of Hsp104 or growth in the presence of millimolar concentrations of guanidine hydrochloride (GdnHCl) (Tuite *et al.*, 1981). GdnHCl treatment results in the inhibition of the replication of the $[PSI^+]$ seeds thus impeding $[PSI^+]$ propagation. The Hsp104 chaperone is crucial for the propagation of the $[PSI^+]$ prion and the ATPase activity of Hsp104 can be inhibited by GdnHCl at low concentration thus blocking $[PSI^+]$ propagation (Eaglestone *et al.*, 2000; Ferreira *et al.*, 2001).

For the various $[PSI^+]$ variants, the efficiency of translation termination corresponds to the level of soluble Sup35, whereas the phenotype of $[PIN^+]$ variants do not correspond to levels of soluble Rnq1 (Bradley *et al.*, 2002). The nomenclature of $[PIN^+]$ variants is based on the relative strength of the *de novo* formation of $[PSI^+]$ seen in strains carrying the $[PIN^+]$ variants. Using *de novo* $[PSI^+]$ formation by Sup35 overexpression, five different $[PIN]$ variants were identified according to the frequency of the *de novo* formation of $[PSI^+]$. The variants were identified as $[pin^-]$, low $[PIN^+]$, medium $[PIN^+]$, high $[PIN^+]$ and very high $[PIN^+]$ (Derkatch *et al.*, 1997).

Each $[PIN^+]$ variant has a distinct phenotype that differs in the efficiency of $[PSI^+]$ induction (Bradley *et al.*, 2002), the morphology of Rnq1-GFP aggregates (Bradley *et al.*, 2003), the stability of Rnq1 aggregates (Bradley *et al.*, 2002; Liebman *et al.*, 2006), and the degree of variant dominance (Bradley *et al.*, 2002). These distinct phenotypes make $[PIN^+]$ a potent candidate to further investigate the property of prion variants not least because the Rnq1 protein has no known function other than the gain of function seen in *de novo* prion formation. In this chapter, $[pin^-]$ and four different $[PIN^+]$ variants were used to study the *de novo* formation of $[PSI^+]$ prion.

3.2 [*PIN*⁺] variants show different frequencies of *de novo* formation of [*PSI*⁺]

The best characterised phenotype associated with the [*PIN*⁺] prion is the enhancement of the *de novo* formation of [*PSI*⁺]. A nonsense suppression assay (Section 2.9.1) was initially used to confirm whether the different [*PIN*⁺] variants had the expected differences in frequency of *de novo* appearance of [*PSI*⁺]. In brief, the *de novo* formation of [*PSI*⁺] was achieved by overexpressing a Sup35NM-GFP fusion protein under the control of a *CUP1* promoter and monitoring the appearance of [*PSI*⁺] colonies following induction with 25µM of CuSO₄.

A [*pin*⁻] derivative and four different [*PIN*⁺] variants of 74D-694 were each transformed with the p6442 plasmid which is a copper-driven expression vector. Cells of each variant were grown in 2% glucose-ade medium with CuSO₄ at a final concentration of 25 µM for 24 hours at 30°C. 5 µl of cells were then spotted on to SC-ade + 1% YEPD plates, ¼ YEPD plate and ¼ YEPD plates supplemented with 3 mM GdnHCl. The appearance of colonies and colony colour were compared. Only [*PSI*⁺] strains could grow on the SC-ade + 1% YEPD plates since the nonsense mutant *ade1-14* was suppressed resulting in synthesis of adenine. The [*psi*⁻] strain is not able to synthesize adenine due to production of a truncated Ade1 protein in the adenine synthesis pathway and hence the Ade⁻ phenotype (Chernoff *et al.*, 1995). The ¼ YEPD plates supplemented with 3 mM GdnHCl served as an additional control. If the white or pink colonies on the ¼ YEPD plates reverted to red colonies on GdnHCl supplemented plates, this confirms that this strain is [*PSI*⁺]. Cells growth on the selective medium (SC-ade + 1% YEPD plate) is indicative of positive complementation. The ¼ YEPD plate as a non-selective medium which contains adenine is used as a control. The ¼ YEPD plate supplemented with 3 mM GdnHCl is used as another control for assessing the phenotype of colony colour.

Chapter 3

The highest efficiency of $[PSI^+]$ *de novo* formation was found in very high $[PIN^+]$ variant while the $[pin]$ strain showed only two Ade^+ colonies that might be due to the spontaneous *de novo* formation of $[PSI^+]$ (Figure 3.1).

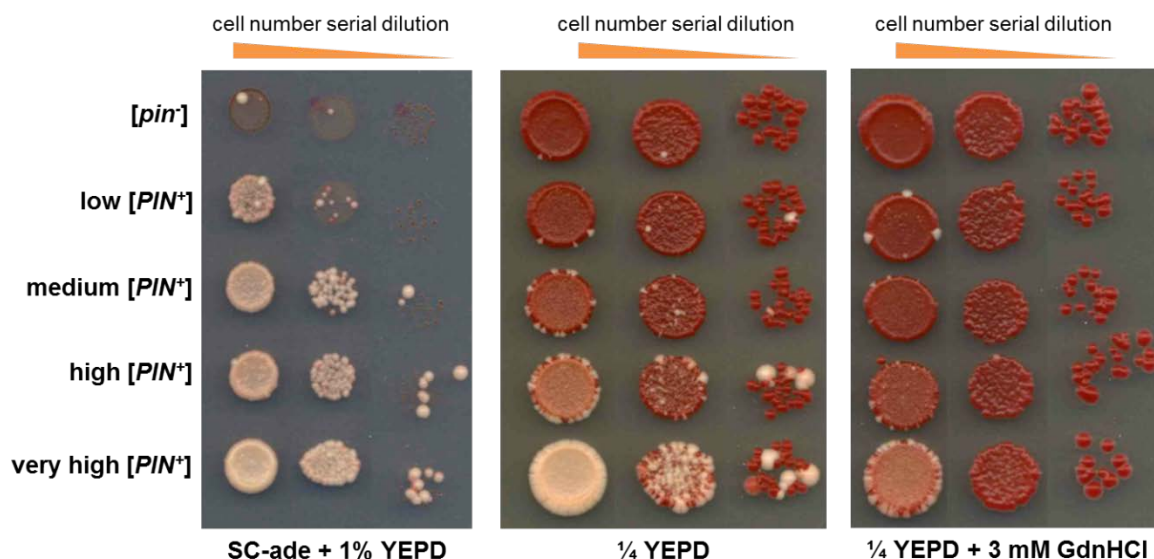


Figure 3.1 The efficiency of *de novo* formation of $[PSI^+]$ differs in different $[PIN^+]$ variants of the strain 74D-694. The highest efficiency of $[PSI^+]$ *de novo* formation was observed in very high $[PIN^+]$ variant.

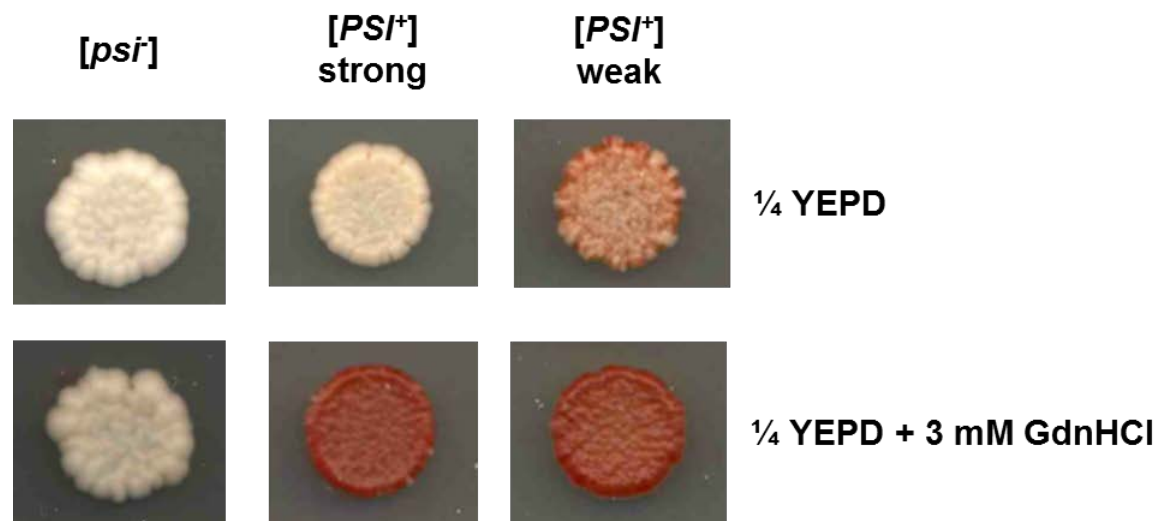
3.3 The spectrum of $[PSI^+]$ variants that arises *de novo* is influenced by the $[PIN^+]$ variants

As described in Section 3.2, the $[PIN^+]$ *de novo* conversion assay showed that the efficiency of *de novo* appearance of $[PSI^+]$ differed in different $[PIN^+]$ variants. To further test whether different $[PIN^+]$ variants gave rise to different types of $[PSI^+]$ variants, 40 colonies of each $[PIN^+]$ variant were randomly selected and spotted onto three different solid media. SC-ade + 1% YEPD plates showed the *de novo* appearance of the $[PSI^+]$ prion. Strong $[PSI^+]$ variants form white colonies while weak $[PSI^+]$ give rise to pink colonies (Figure 3.2 a). $1/4$ YEPD plates were used as a spotting control for monitoring general growth defects that might not be associated with the *de novo* appearance of the $[PSI^+]$ prion. $1/4$ YEPD + 3mMGdnHCl plates served as an additional control for confirming whether the *de novo* formed colony is a $[PSI^+]$. The phenotype of $[PSI^+]$ can be eliminated by GdnHCl and converted into $[psi^-]$

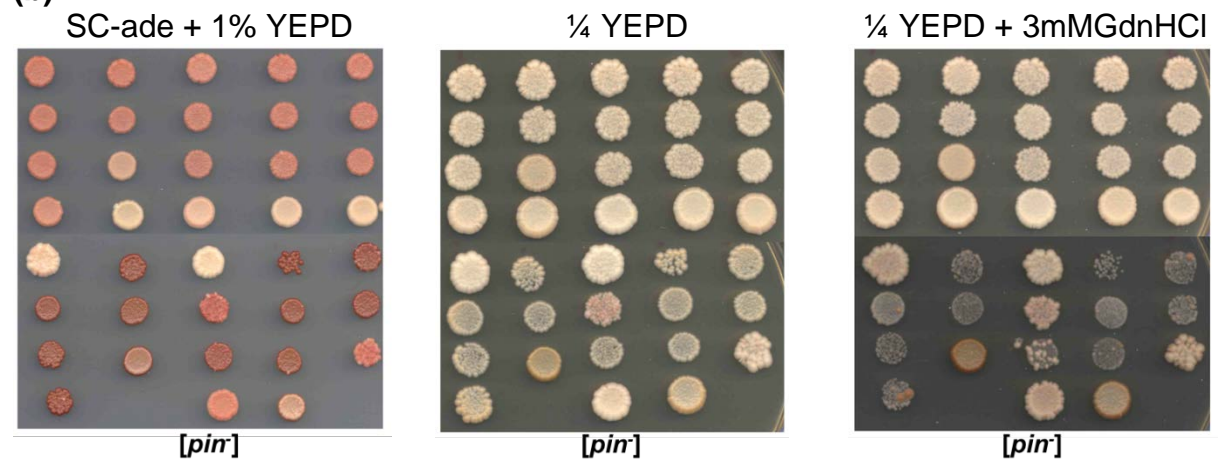
Chapter 3

which forms red colonies (Tuite *et al.*, 1981). If a colony remains white or pink on GdnHCl supplemented plates, it can be concluded that the candidate cell has a nuclear suppressor mutation (Lund *et al.*, 1981; Lancaster *et al.*, 2010). The results revealed different $[PIN^+]$ variants are capable of generating both strong $[PSI^+]$ and weak $[PSI^+]$ variants while $[pin^-]$ cannot form $[PSI^+]$ (Figure 3.2 b).

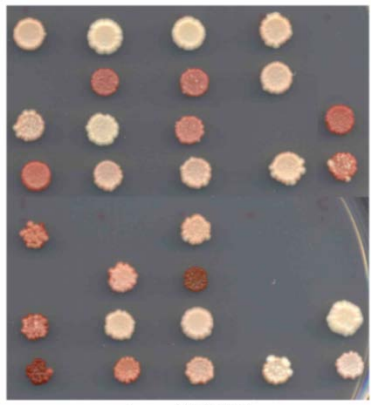
(a)



(b)



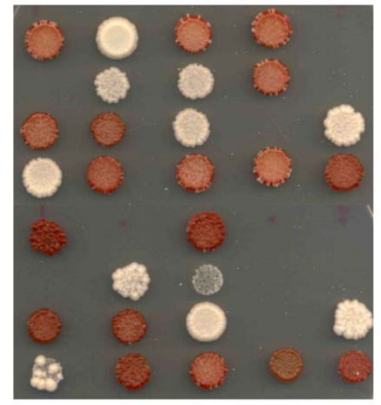
Chapter 3



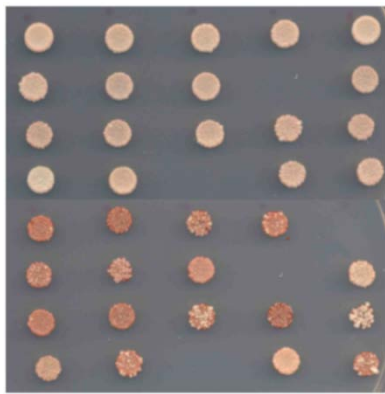
low [*PIN*⁺]



low [*PIN*⁺]



low [*PIN*⁺]



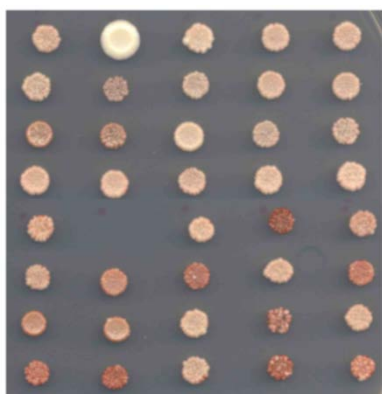
medium [*PIN*⁺]



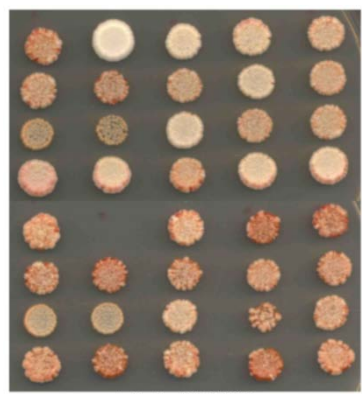
medium [*PIN*⁺]



medium [*PIN*⁺]



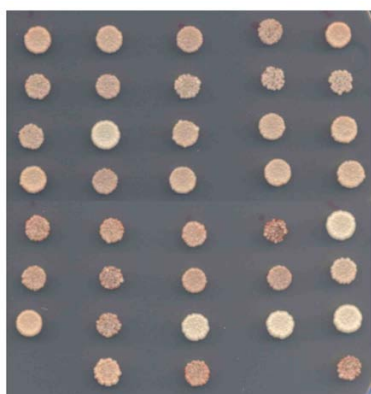
high [*PIN*⁺]



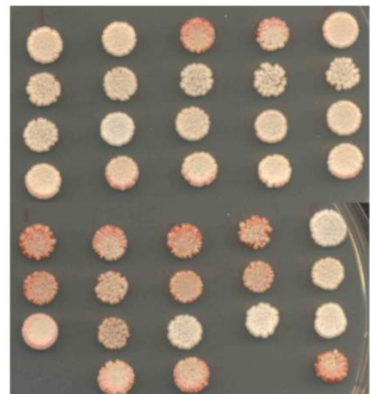
high [*PIN*⁺]



high [*PIN*⁺]



very high [*PIN*⁺]



very high [*PIN*⁺]



very high [*PIN*⁺]

Figure 3.2 *[PIN⁺]* variants can generate both strong *[PSI⁺]* and weak *[PSI⁺]*. (a) Illustration of *[psi⁻]*, strong *[PSI⁺]* and weak *[PSI⁺]* phenotype. (b) Different *[PIN⁺]* variants show different efficiency on the *de novo* formation of strong *[PSI⁺]* and weak *[PSI⁺]*.

3.4 Quantitative analysis of the *de novo* formation of strong *[PSI⁺]* and weak *[PSI⁺]* in strains carrying different *[PIN⁺]* variants

Since the different *[PIN⁺]* variants gave rise to both strong *[PSI⁺]* and weak *[PSI⁺]*, it was next of interest to determine the effects of different *[PIN⁺]* variants on the efficiency of *de novo* formation of strong *[PSI⁺]* and weak *[PSI⁺]*. 40 *[PSI⁺]* colonies were selected for each strain. The total number of Ade⁺ colonies was counted from the adenine drop-out medium, YEPD supplemented (SC-Ade + 1% YEPD) medium as a baseline. The number of non-*[PSI⁺]* colonies was obtained by a comparison of the corresponding colonies on the SC-Ade + 1% YEPD medium and ¼ YEPD medium supplemented with 3 mM GdnHCl. If the corresponding colony was red on the medium containing 3mM GdnHCl, it could be confirmed as a *[PSI⁺]*. White colonies on the SC-Ade + 1% YEPD plates were counted as strong *[PSI⁺]* variant while pink colonies were recorded as weak *[PSI⁺]* variant (Table 3.1).

As expected, the *[pin]* strain cannot generate any *[PSI⁺]* variant. All four *[PIN⁺]* variants can generate different *[PSI⁺]*. The low *[PIN⁺]* variant shows the highest frequency of nuclear mutation. The low and medium *[PIN⁺]* variants preferentially gave rise to weak *[PSI⁺]* variant. Interestingly, the high *[PIN⁺]* variant shows the highest frequency of strong *[PSI⁺]* formation while the very high *[PIN⁺]* variant shows the highest frequency of weak *[PSI⁺]* formation. This suggests that different *[PIN⁺]* variants may underlie different pathways on the *de novo* formation of *[PSI⁺]* variants.

Chapter 3

Table 3.1 Quantitative analysis of the *de novo* formation of strong [*PSI⁺*] and weak [*PSI⁺*] depending on different [*PIN⁺*] variants.

[<i>PIN⁺</i>] variant	No. Ade ⁺ colonies analysed	Classes of Ade ⁺ [†]		
		No. weak* [<i>PSI⁺</i>] variants	No. strong* [<i>PSI⁺</i>] variants	Nuclear Ade ⁺ mutation
[<i>pin</i>]	38	0	0	38 (100%)
[<i>PIN⁺</i>]LOW	29	10 (34%)	7 (24%)	12 (41%)
[<i>PIN⁺</i>]MED	35	19 (54%)	16 (46%)	0
[<i>PIN⁺</i>]HIGH	39	27 (69%)	7(18%)	5 (13%)
[<i>PIN⁺</i>]VERY H.	38	13 (34%)	24 (63%)	1 (3%)

These data indicate that [*pin*] cannot form [*PSI⁺*]. [*PIN⁺*]LOW shows the lowest frequency of [*PSI⁺*] formation. All four [*PIN⁺*] variants can generate different [*PSI⁺*] i.e strong [*PSI⁺*], weak [*PSI⁺*].

[*PSI⁺*] were defined by the loss of the Ade phenotype when grown on a medium containing 3mM GdnHCl;

* % of total in bracket

3.5 Levels of the Rnq1 protein in different [*PIN⁺*] variants

As described in Section 3.2, the efficiency of [*PSI⁺*] *de novo* formation was different in the four [*PIN⁺*] variants. It was important to further investigate whether the levels of the Rnq1 protein have an impact on the efficiency of [*PSI⁺*] *de novo* formation. This was tested by western blot (Section 2.10.4). Since the testing protein Rnq1 and the loading control protein PGK have similar molecular weights (43kDa and 47kDa respectively), the two proteins were loaded on two separate gels and detected with either anti-Rnq1 or anti-PGK antibody (Figure 3.3).

The first attempt of the western blot was to load both Rnq1 and PGK on the 10% gel. However, the bands of Rnq1 and PGK were stacked up due to their similar molecular weight. The second attempt was to use 12% gel aiming at separating the bands of Rnq1 and PGK proteins. However, this failed to show the band clearly. Then 15% gel was used to further separate the two proteins but this did not work either (data not shown). Finally, the testing protein Rnq1

Chapter 3

and the loading control protein PGK were loaded on separate 10% gels and put into one picture by 'paint' software as shown in Figure 3.3.

The result showed that the high and very high [*PIN*⁺] variants contain more Rnq1 than the low and medium [*PIN*⁺] variants, as compared to the loading control which was used to confirm that the Rnq1 protein had been evenly loaded. However, no Rnq1 was seen in the [*pin*⁻] variant, which might be due to soluble Rnq1 being unstable (G. L. Staniforth, personal communication). The low and medium [*PIN*⁺] variants may be slightly susceptible to degradation while the high and very high [*PIN*⁺] variants are much more robust. This result was consistent with the [*PIN*⁺] *de novo* conversion assay i.e. higher efficiency of [*PSI*⁺] *de novo* formation was found in the high and very high [*PIN*⁺] variants, while lower efficiency of [*PSI*⁺] *de novo* formation was found in the low and medium [*PIN*⁺] variants. This result suggests that the levels of Rnq1 may have an impact on the *de novo* formation of [*PSI*⁺].

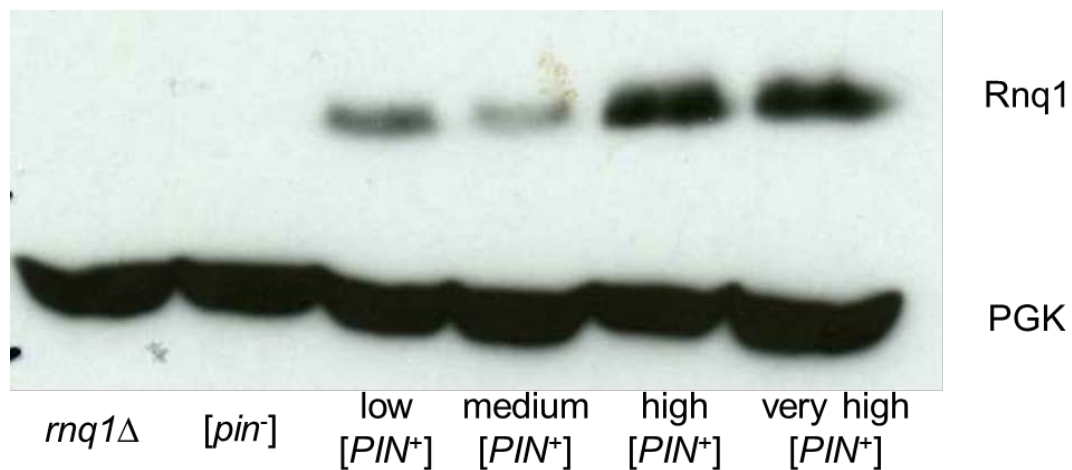


Figure 3.3 Western blot analysis showed the levels of Rnq1 differed in [*PIN*⁺] variants.

3.6 Discussion

The [*PIN*⁺] *de novo* conversion assay confirmed that [*pin*] cannot form [*PSI*⁺] *de novo* while four [*PIN*⁺] variants (low [*PIN*⁺], medium [*PIN*⁺], high [*PIN*⁺] and very high [*PIN*⁺]) gave rise to two different types of [*PSI*⁺] variant: weak [*PSI*⁺] and strong [*PSI*⁺]. This same result i.e. that different [*PIN*⁺] variants can generate different [*PSI*⁺] variants, was very recently published by Sharma and Liebman (2013). The very high [*PIN*⁺] variant showed the highest efficiency on the *de novo* formation of [*PSI*⁺] whereas the low [*PIN*⁺] variant showed the lowest frequency of the *de novo* appearance of [*PSI*⁺]. There was also a difference between the percentage of *de novo* formed weak [*PSI*⁺] and strong [*PSI*⁺] variants depending on the type of different [*PIN*⁺] variant.

As far as we know, determination of [*PSI*⁺] variants is based on the level of soluble cellular Sup35 in the strain i.e. the weak [*PSI*⁺] variant has more soluble Sup35 protein than the strong [*PSI*⁺]. The [*PIN*⁺] variant was first distinguished by the efficiency of the *de novo* formation of [*PSI*⁺] when Sup35 was overexpressed. Like [*PSI*⁺] variants, the [*PIN*⁺] variant has different amount of soluble Rnq1 protein, but this does not influence the efficiency of the different [*PSI*⁺] formation. Thus it is interesting to investigate what is the possible factor that regulates the *de novo* formation of different [*PSI*⁺] variants depending on different [*PIN*⁺] variants.

One possible reason is that each [*PIN*⁺] variant with its distinct steric structure can act as a prion seed during the formation of [*PSI*⁺] variants. The distinct conformation of different [*PIN*⁺] variants may be able to facilitate the formation of [*PSI*⁺] variants at different rate thereby preferentially producing a particular variant of [*PSI*⁺]. Moreover, it was established that the binding of Sup35 to different [*PIN*⁺] variants happens with the same efficiency while the conversion of Sup35 to the particular aggregated form is the key step during the process (Sharma and Liebman., 2013).

Chapter 3

Since the strong [PSI^+] variant has more prion seeds than the weak [PSI^+] variant (Derdowski et al., 2010), another possible reason for different [PIN^+] variants generating different [PSI^+] variant is that the [PIN^+] variant may affect the formation of the [PSI^+] seed.

Chapter 4

**[*PIN*⁺]-dependent toxicity mediated by the
Rnq1 protein**

4.1 Introduction

Elevated protein levels, for example, overexpression of Rnq1, can have an impact on protein homeostasis which in turn can lead to amyloid formation. As far as we know, the appearance of amyloid deposits is associated with a number of protein misfolding diseases. However, the specific correlation between the pathogenicity of neurodegenerative diseases and amyloid formation still remains poorly understood. In general, almost any misfolded protein is able to generate some level of toxicity or cause cellular dysfunctions (Stefani and Dobson, 2003).

In the yeast *Saccharomyces cerevisiae*, the Rnq1 protein can exist in its soluble state as a monomer or an aggregated infectious state known as the $[PIN^+]$ prion. The only known biological function of Rnq1 is that it enhances the conversion of other prion proteins from their normal states to their prion states when itself is in the prion form, i.e. $[PIN^+]$ (Derkatch *et al.*, 2001 and Osherovich *et al.*, 2001). Since the cellular function of Rnq1 is poorly understood, little information is known about how it might differentially impact on the cell in its normal ($[pin^-]$) and prion ($[PIN^+]$) states.

A previous study revealed that overexpression of Rnq1 is toxic to cells if the endogenous Rnq1 protein is in its prion form ($[PIN^+]$), whereas it is not toxic to cells when the endogenous Rnq1 is in its soluble form i.e. $[pin^-]$ (Douglas *et al.*, 2008). This $[PIN^+]$ -dependent toxicity of Rnq1 can be suppressed by overexpression of Sis1, a molecular chaperone from the Hsp40 family (Douglas *et al.*, 2008). In addition, eight other genes had been found that when overexpressed suppress Rnq1 toxicity: *GPG1*, *HRR25*, *MSA1*, *NVJ1*, *SPC29*, *THI2* and *YNL208w*. In $[PIN^+]$ cells, Rnq1 overexpression triggers a spindle checkpoint leading to a cell cycle arrest in mitosis as duplication of spindle pole body is affected by the overexpression of Rnq1 (Treusch and Lindquist, 2012). Evidence suggests that there is an accumulation of large-budded cells when Rnq1 is overexpressed in a $[PIN^+]$ background. This indicates a cell cycle arrest (Hardwick, 1998; Nyberg *et al.*, 2002). Moreover,

replicated DNA content was found in these cells that had not undergone mitosis. Thus the cell cycle arrest can be triggered by the spindle checkpoint or DNA damage checkpoint (Treusch and Lindquist, 2012).

In this chapter, a combination of cell biological and genetic approaches such as comparative toxicity assays, growth assays, determination of the levels reactive oxygen species (ROS) and microscopy were used to further investigate the impact of Rnq1 overexpression in [*PIN*⁺] cells in order to better understand the mechanism of Rnq1 overexpression-induced cytotoxicity in different [*PIN*⁺] variants.

4.2 Rnq1 overexpression is toxic in different [*PIN*⁺] variants but not in a [*pin*⁻] background

Since Rnq1 overexpression is known to be toxic in [*PIN*⁺] cells, but not in [*pin*⁻] cells (Douglas *et al.*, 2008), it was of interest to further examine the toxicity phenotype in different [*PIN*⁺] variants when Rnq1 was overexpressed. As discussed in *Chapter 3*, different [*PIN*⁺] variants show different frequencies of *de novo* formation of [*PSI*⁺] and the hypothesis to be tested was that different [*PIN*⁺] variants would also give rise to different degree of toxicity when Rnq1 was overexpressed, linking the two processes i.e. *de novo* formation of prions and amyloid-associated toxicity, at least mechanistically.

In order to test this hypothesis, the galactose-inducible promoter *GAL1* was used to overexpress the *RNQ1* gene in the *S. cerevisiae* strain 74D-694. A [*pin*⁻] derivative and four different [*PIN*⁺] derivatives of 74D-694 i.e. low [*PIN*⁺], medium [*PIN*⁺], high [*PIN*⁺] and very high [*PIN*⁺] (Derkatch *et al.*, 1997) were each transformed with either the pYES2 (control) or the pYES2-*RNQ1* plasmids. Strains harbouring pYES2 or pYES2-*RNQ1* were grown overnight in a synthetic dropout medium (SC-ura) containing 2% glucose. The overnight cultures were washed three times in order to remove all glucose-containing medium before adding the inducing medium i.e. synthetic dropout medium

Chapter 4

(SC-ura) containing 2% galactose. Cells were incubated for 8 hours in this inducing medium and then Rnq1 overexpression induced cytotoxicity was determined by spotting 5-fold serial dilutions of the cells of each yeast sample (i.e. 74D-694 based four different $[PIN^+]$ strains and $[pin^-]$ strain) onto the surface of different agar plates. Glucose-ura agar plates were used as controls since there would be no elevation of Rnq1 levels in cells grown on this medium. $\frac{1}{4}$ YEPD agar plates served as an additional control to monitor general growth defects that may not be associated with the overexpression of Rnq1 proteins. 2% Galactose-ura agar plates were used to evaluate the growth defects of $[PIN^+]$ cells overexpressing Rnq1 using the protocol illustrated in Figure 4.1.

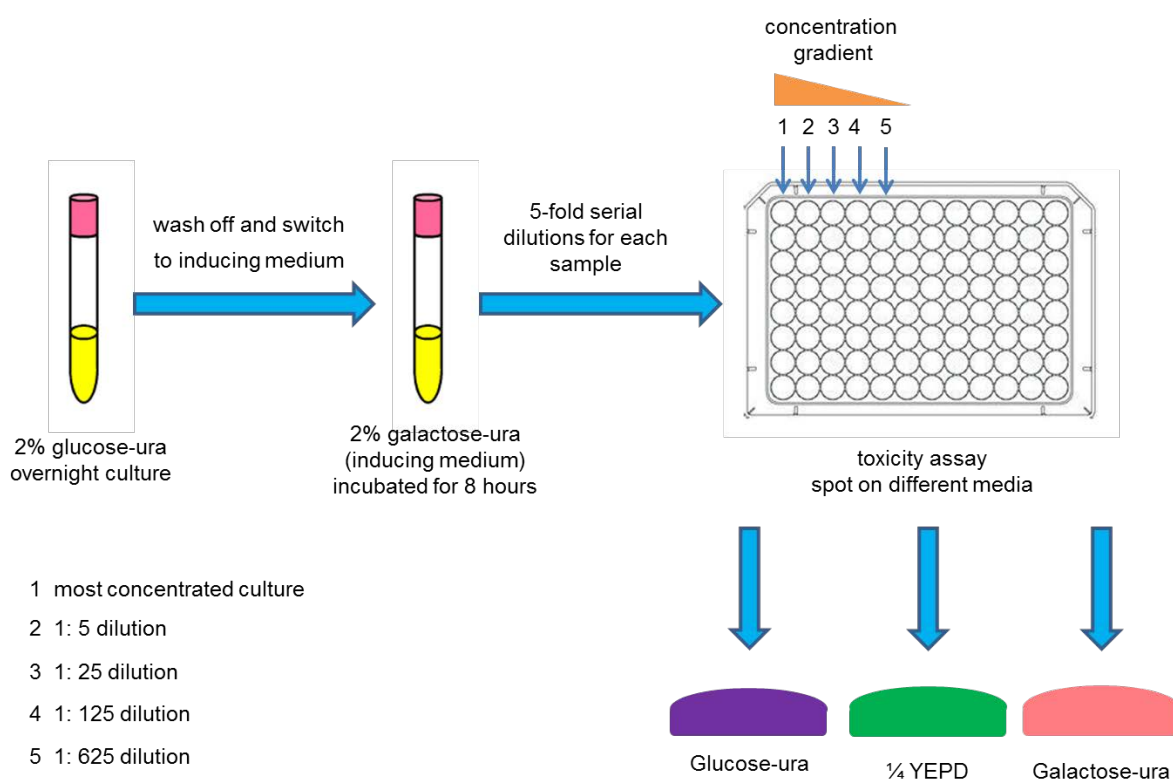
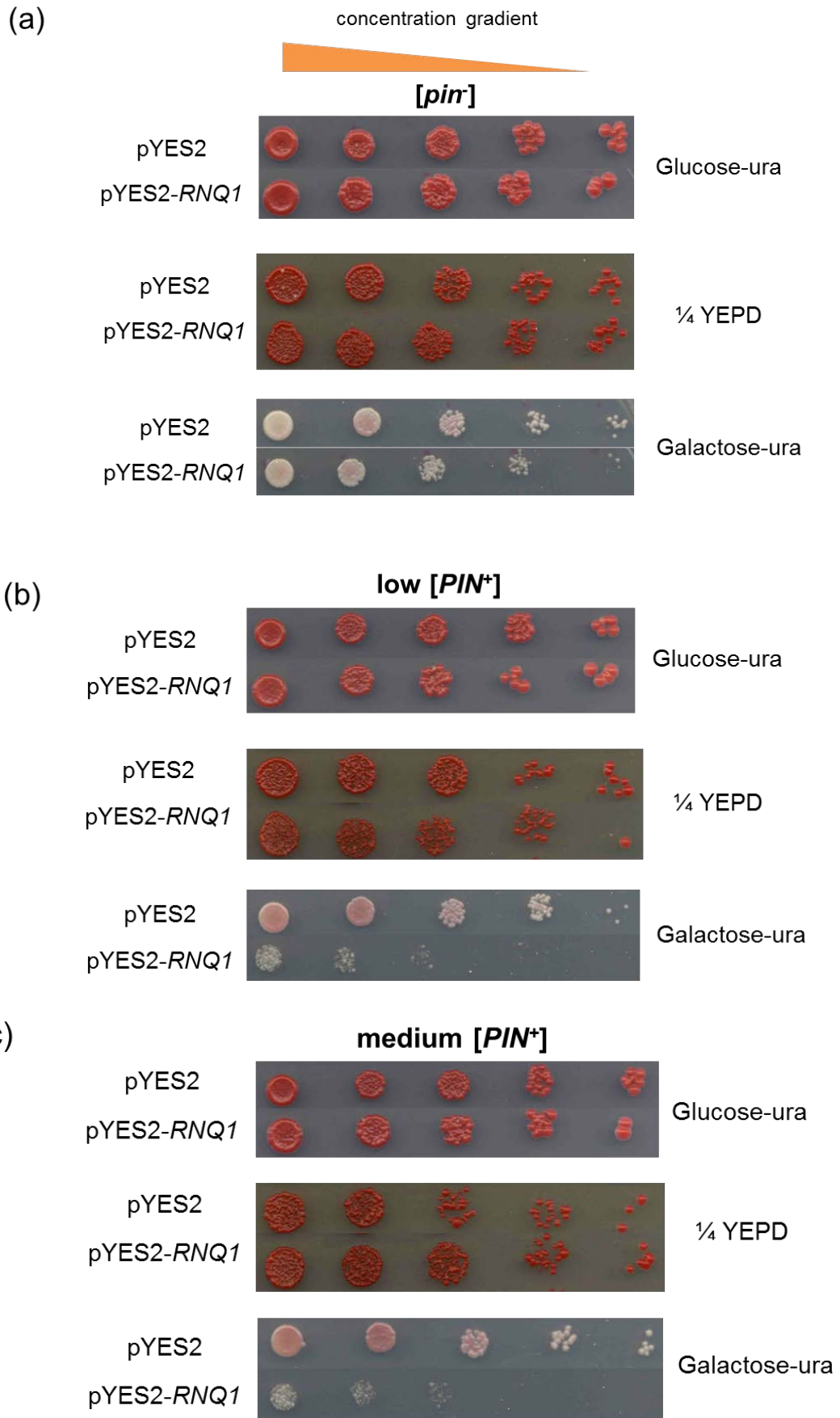


Figure 4.1 Illustration of Rnq1-induced toxicity assay. General overview of the toxicity assays performed in this study.

As previously reported (Douglas *et al.*, 2008), Rnq1 overexpression was not toxic in a $[pin^-]$ background whereas it was toxic in all four different $[PIN^+]$ variants. Moreover, the degree of toxicity also differed between the different $[PIN^+]$ variants. For example, overexpression of Rnq1 was less toxic in low and medium $[PIN^+]$ strains compared with the high and very high $[PIN^+]$

Chapter 4



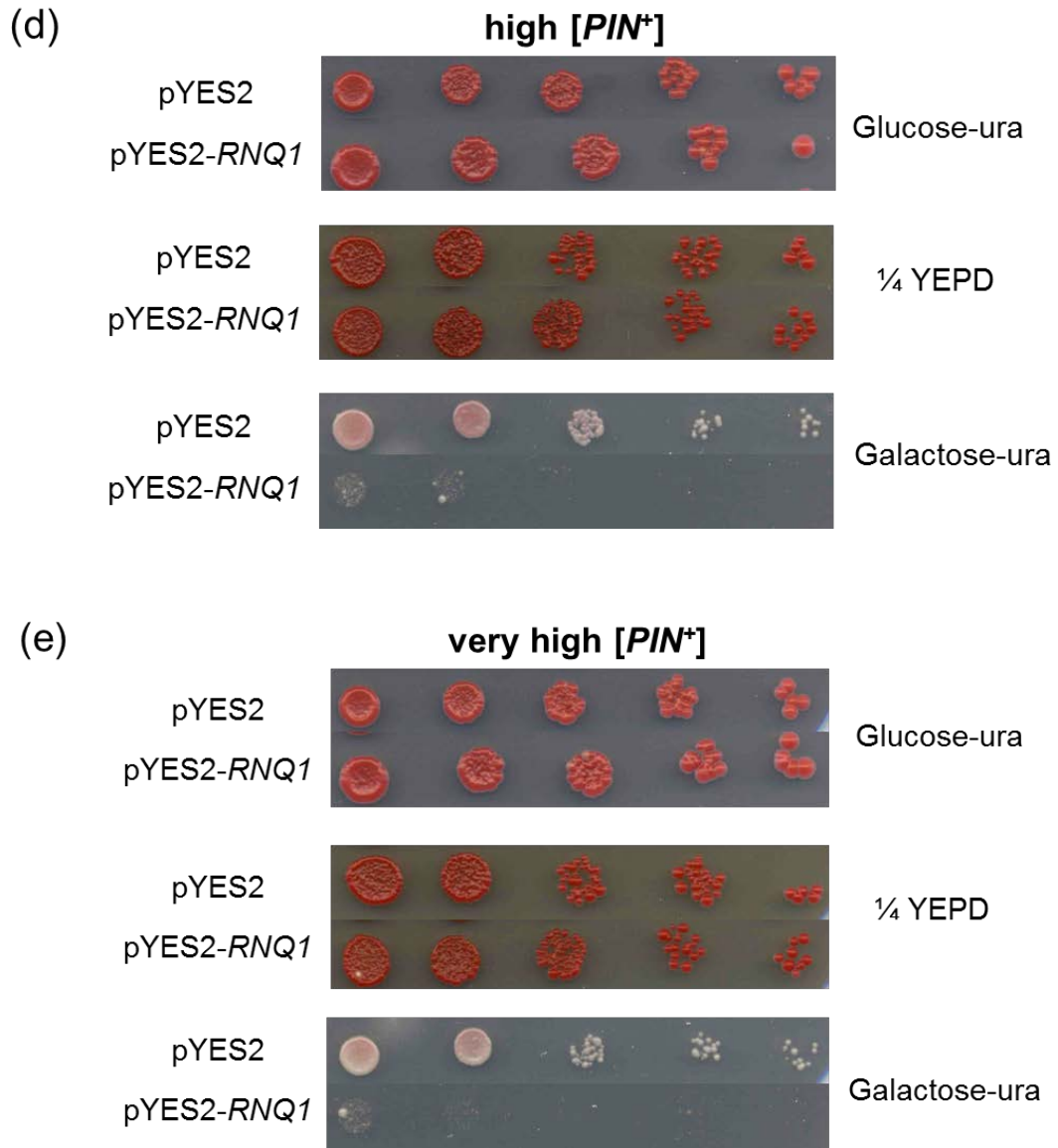


Figure 4.2 Overexpression of Rnq1 results in different degrees of cytotoxicity in different [*PIN*⁺] variants of 74D-694 cells. (a) Rnq1 overexpression was not toxic in [*pin*⁻] variant. (b) (c) (d) (e) Rnq1 overexpression was toxic in all four [*PIN*⁺] variants as indicated. pYES2 is the control plasmid while pYES2-*RNQ1* is the pYES2 vector carrying the *RNQ1* gene. Three biological replicates were performed for each strain and one representative is shown for each.

strains (Figure 4.2). This result was also supported by the findings reported in Chapter 3, namely that different [*PIN*⁺] variants showed different frequencies of *de novo* formation of [*PSI*⁺] i.e. the low [*PIN*⁺] variant showed the lowest frequency of the *de novo* formation of [*PSI*⁺] while very high [*PIN*⁺] variant showed the highest frequency of the *de novo* formation of [*PSI*⁺]. These findings suggest that the mechanism that underlies *de novo* prion formation

Chapter 4

may be similar to that leads to cytotoxicity. Therefore, increased frequency of the *de novo* formation of $[PSI^+]$ by different $[PIN^+]$ variants correlates to increased cytotoxicity when Rnq1 was overexpressed.

Rnq1 overexpression-induced cytotoxicity was also determined in another *Saccharomyces cerevisiae* strain BY4741. The BY4741 strain is $[PIN^+]$ (G.L.Staniforth, personal communication) but has a very different genetic origin to 74D-694 and hence was used to control for any non-specified effects of genetic background on amyloid-induced toxicity. In addition, BY4741 is a haploid derivative of strain S288C while 74D-694 is a Russian strain of unknown origin (M. F. Tuite, personal communication). The generation of a $[pin^-]$ derivative of BY4741 was achieved by sequential passage of cells on YEPD plates containing 3 mM guanidine hydrochloride (GdnHCl) as this eliminates $[PIN^+]$ (Sondheimer and Lindquist 2000). Toxicity assays showed that Rnq1 overexpression was toxic in $[PIN^+]$ cells but not $[pin^-]$ cells of BY4741 (Figure 4.3). Thus, the same outcome of Rnq1 overexpression-induced cytotoxicity was seen in yeast strain BY4741 indicating that there was no impact on the toxicity phenotype from non-specified genetic background effects.

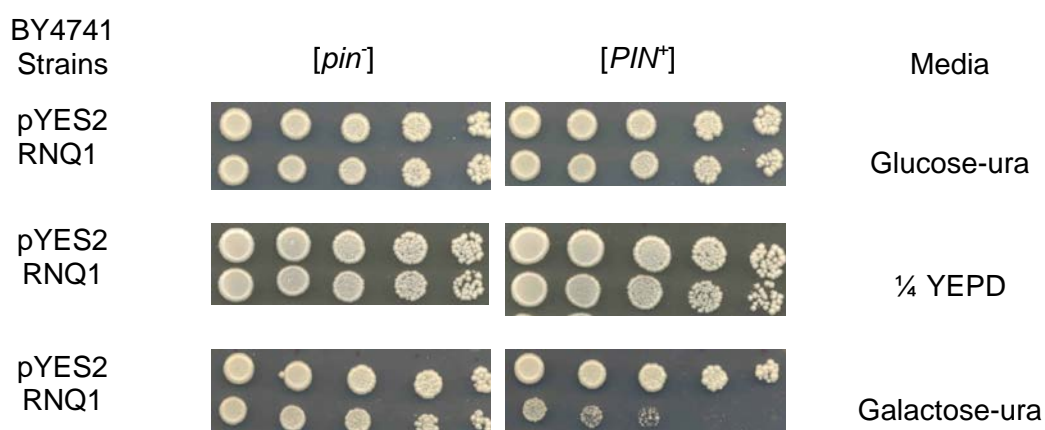


Figure 4.3 Overexpression of Rnq1 also resulted in $[PIN^+]$ -dependent cytotoxicity in BY4741 cells. Rnq1 overexpression was not toxic in $[pin^-]$ but toxic in $[PIN^+]$ strains. pYES2 is the control plasmid while RNQ1 is the pYES2 vector with *RNQ1* insert. Three biological replicates were performed for each strain and one representative is shown for each

4.3 Rnq1 overexpression causes a growth defect in [*PIN*⁺] cells

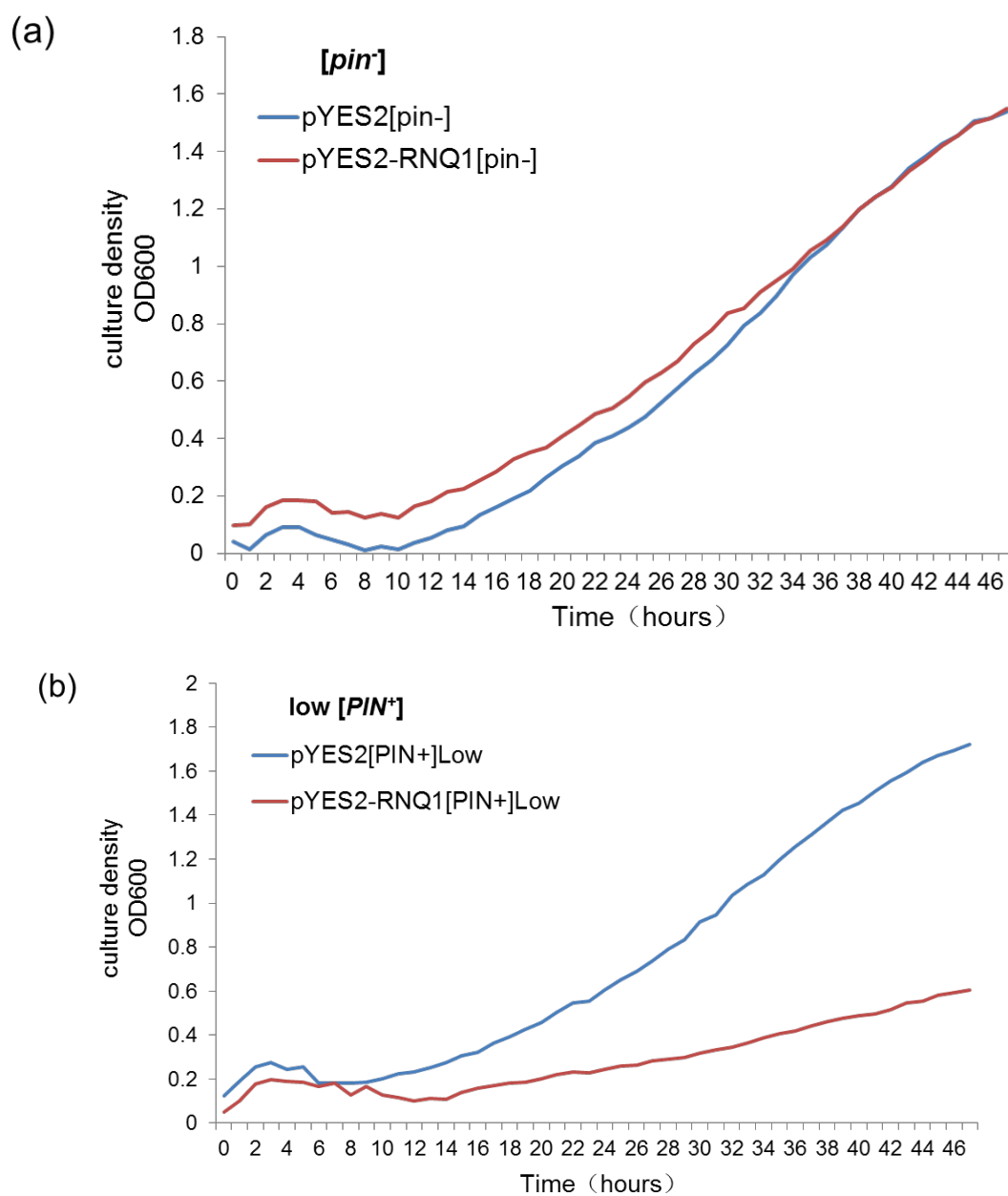
In order to confirm the results obtained from toxicity assays, growth assays were carried out to quantify the impact of Rnq1 overexpression on the growth rate of both [*pin*⁻] and [*PIN*⁺] 74D-694 strains. Cells were grown under the same conditions as the toxicity assays (see Section 2.8.3) and after washing off all the glucose-containing medium, cells were grown in the selective, inducing medium i.e. SD 2% galactose for 48 hours at 30°C. Readings of OD₆₀₀ were recorded every hour using a Fluostar Omega microplate reader. The results of growth analysis confirm that Rnq1 overexpression does not cause a growth defect in [*pin*⁻] cells but does lead to growth defects in all four [*PIN*⁺] strains (Figure 4.4). The doubling time of the [*pin*⁻] strain expressing the pYES2 plasmid or Rnq1 was similar. In the low and medium [*PIN*⁺] strains overexpressing Rnq1, the doubling time was about 25 hours compared to 20 hours in the corresponding [*PIN*⁺] strains expressing the pYES2 plasmid. While in the high and very high [*PIN*⁺] strains overexpressing Rnq1, the doubling time was increased to approximately 33 hours (Table 4.1). The longer doubling time confirmed that Rnq1 overexpression was more toxic in the high and very high [*PIN*⁺] strains compared with the low and medium [*PIN*⁺] strains.

Table 4.1 Doubling time in exponential growth and cell density measured by the optical density of 600nm at the 36 hour time point for each strain of 74D-694 and BY4741

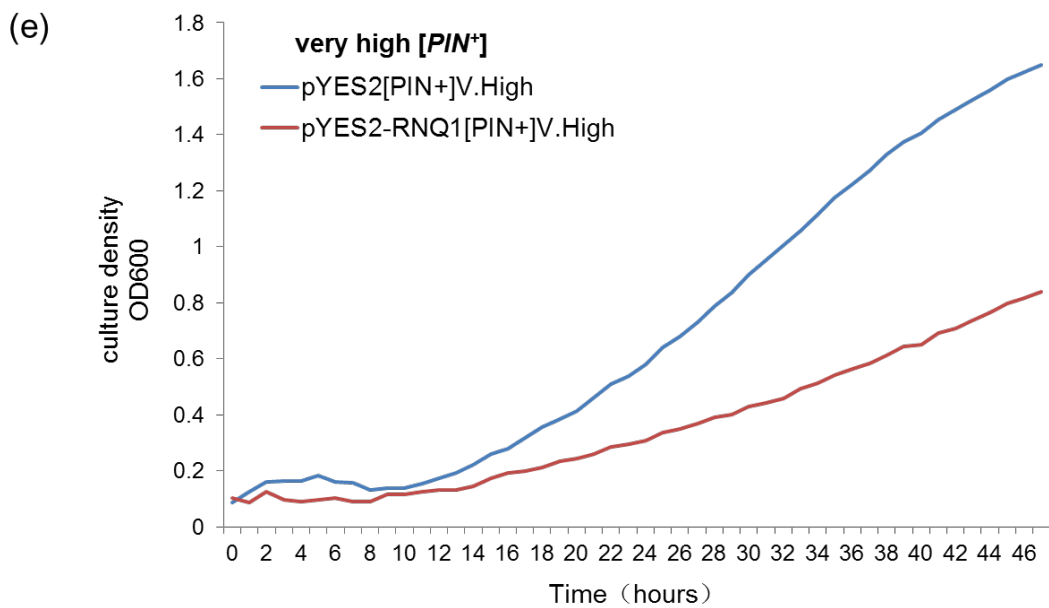
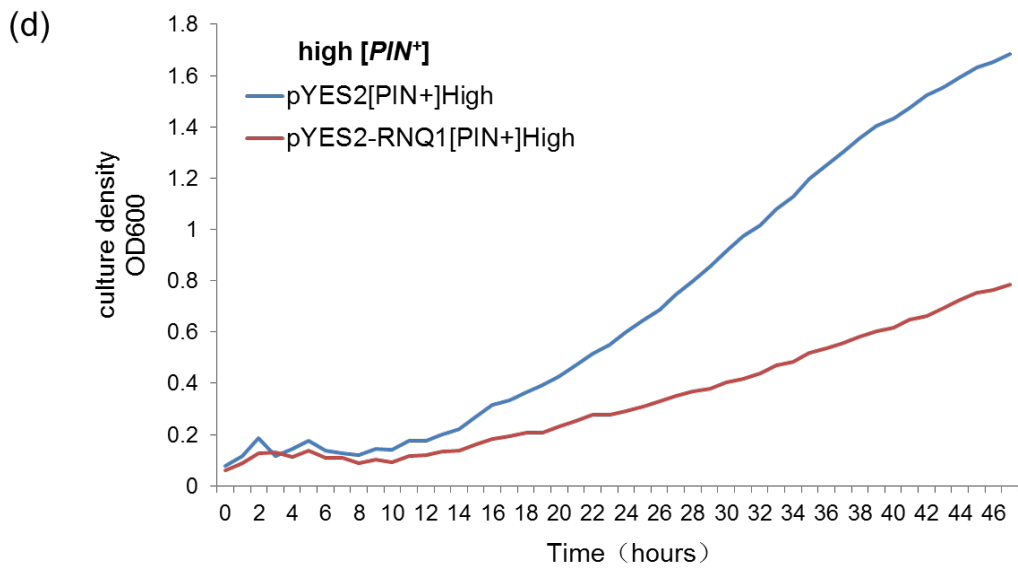
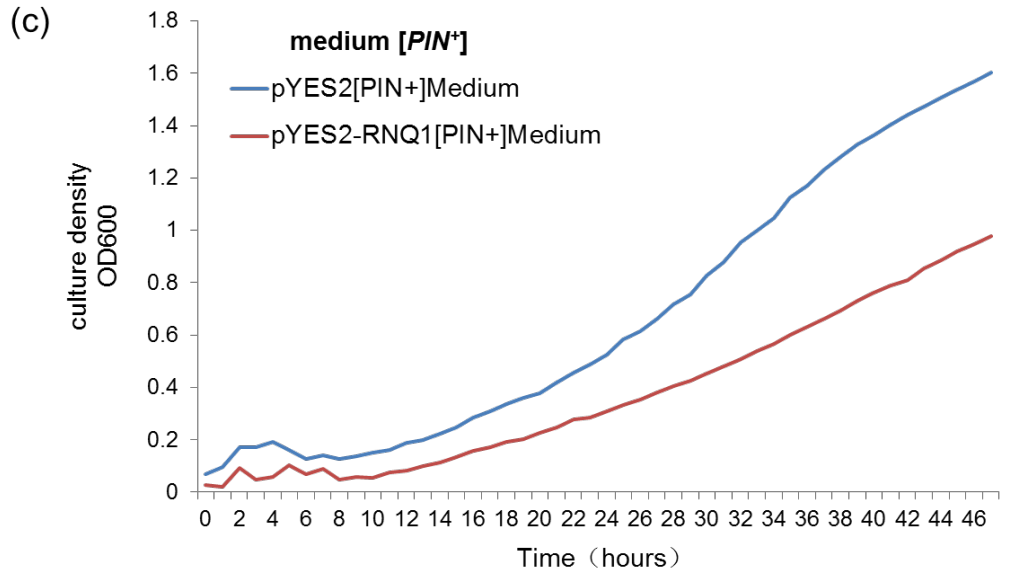
Strain	Plasmid	Doubling time (hr)	OD600 t = 36 h
74D-694[<i>pin</i> ⁻]	pYES2	18.82	1.07
74D-694[<i>pin</i> ⁻]	pYES2- <i>RNQ1</i>	20.16	1.09
74D-694[<i>PIN</i> ⁺]low	pYES2	20.75	1.25
74D-694[<i>PIN</i> ⁺]low	pYES2- <i>RNQ1</i>	25.96	0.41
74D-694[<i>PIN</i> ⁺]medium	pYES2	20.29	1.17
74D-694[<i>PIN</i> ⁺]medium	pYES2- <i>RNQ1</i>	24.81	0.63
74D-694[<i>PIN</i> ⁺]high	pYES2	19.71	1.25
74D-694[<i>PIN</i> ⁺]high	pYES2- <i>RNQ1</i>	33.63	0.53
74D-694[<i>PIN</i> ⁺]v. high	pYES2	18.5	1.22
74D-694[<i>PIN</i> ⁺]v. high	pYES2- <i>RNQ1</i>	32.71	0.56
BY4741[<i>PIN</i> ⁺]	pYES2	3.87	2.08
BY4741[<i>PIN</i> ⁺]	pYES2- <i>RNQ1</i>	20.01	1.13

Chapter 4

Similarly, the growth assays were also performed in the $[PIN^+]$ strains of BY4741. A growth defect was seen in the $[PIN^+]$ strain overexpressing Rnq1 with a doubling time of 20 hours compared to about 4 hours in the control $[PIN^+]$ strain expressing the empty pYES2 plasmid (Table 4.1) The result confirmed that Rnq1 overexpression was toxic in a $[PIN^+]$ background of BY4741 (Figure 4.4).



Chapter 4



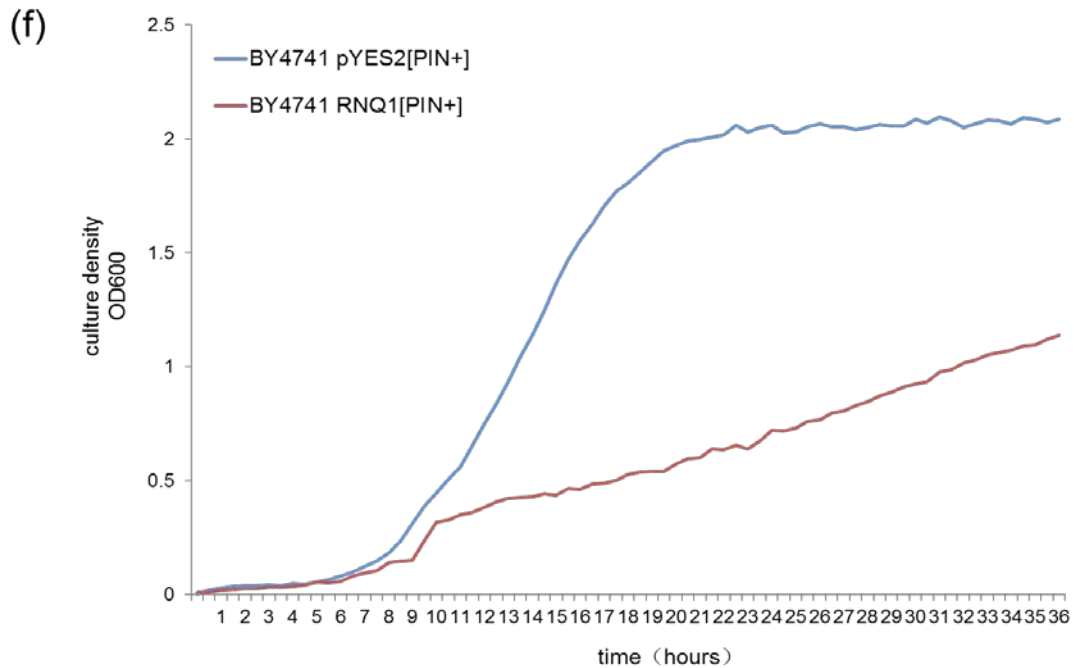


Figure 4.4 Overexpression of Rnq1 leads to growth defects in different $[PIN^+]$ variants of 74D-694 cells. Cell density as measured by optical density of 600nm was determined in the inducing medium i.e. SD 2% galactose-ura for 48 hours at 30°C. **(a)** Rnq1 overexpression did not cause a growth defect in $[pin^-]$ cells. **(b) - (e)** Rnq1 overexpression resulted in growth defects in the $[PIN^+]$ variants of 74D-694. **(f)** Rnq1 overexpression resulted in growth defects in the BY4741 $[PIN^+]$ strain. pYES2 is the control plasmid while pYES2-RNQ1 is the pYES2 vector with *RNQ1* insert. Three biological replicates were performed for each strain and average is plotted in the above.

4.4 Rnq1-GFP forms fluorescent aggregates in $[PIN^+]$ cells

In order to examine the $[PIN^+]$ status of the 74D-694 strains used in this study, the $[pin^-]$ derivative and four different $[PIN^+]$ derivatives of this strain were each transformed with the plasmid pAG426 that encodes a Rnq1-GFP fusion (C-terminal GFP tag) under the galactose-inducible *GAL1* promoter. The localization of Rnq1-GFP in 74D-694 $[pin^-]$ and $[PIN^+]$ cells was monitored by fluorescence microscopy (Figure 4.5).

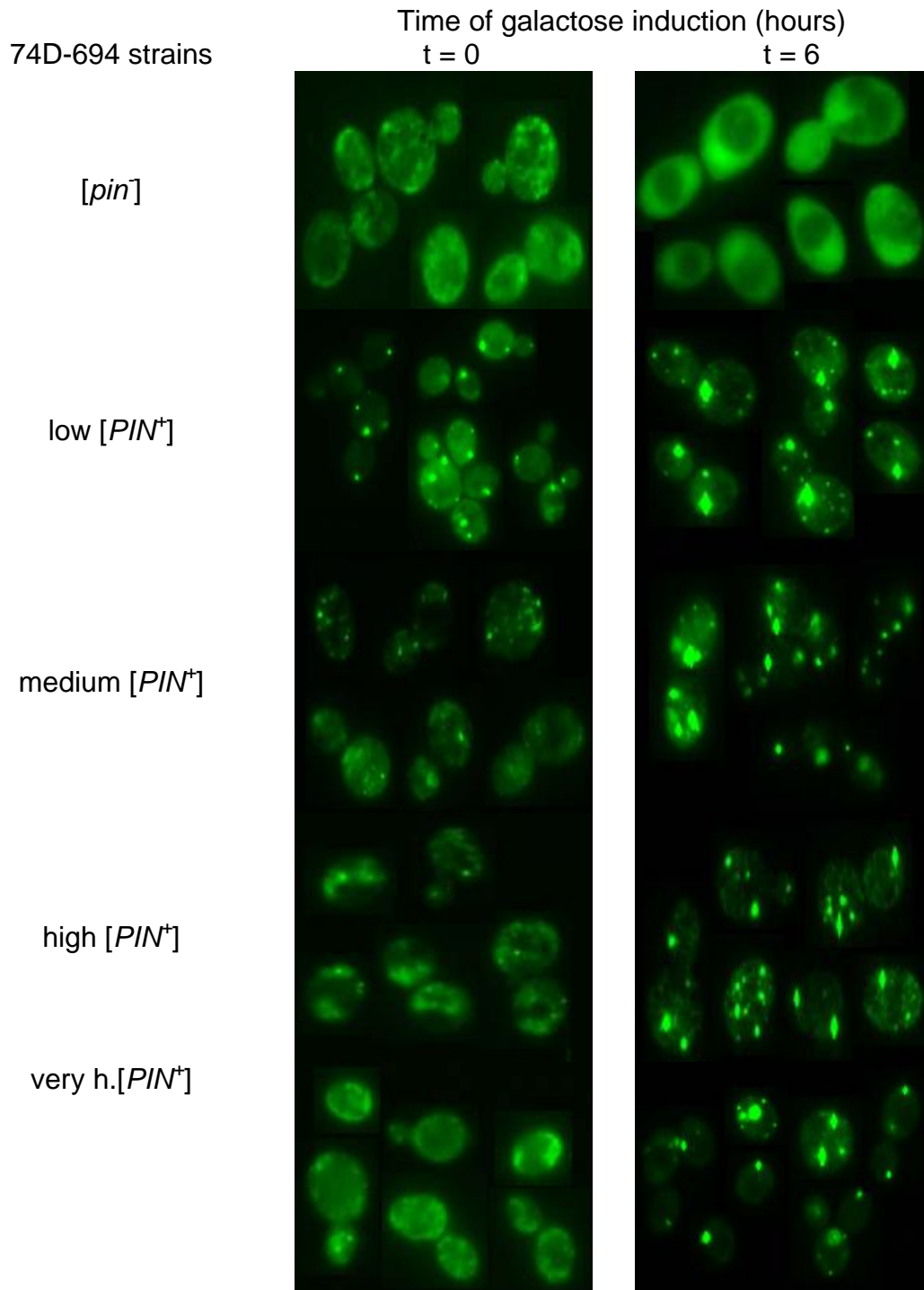


Figure 4.5 Fluorescence of the Rnq1-GFP fusion protein in 74D-694-based [*pin*] and [*PIN*⁺] cells. A uniform fluorescence was observed in [*pin*] cells while [*PIN*⁺] cells with four different [*PIN*⁺] variants showed the appearance of aggregates of the fusion protein after 6 hours induction. Cells were grown in the inducing medium i.e. SD 2% galactose-ura for at 30°C. Samples were collected at time point 0 and 6 and visualised by a green excitation filter on an Olympus 1X81 fluorescent microscope with Hamamatsu Photonics Orca AG cooled CCD camera. Images were captured analysed by Olympus Cell^R software.

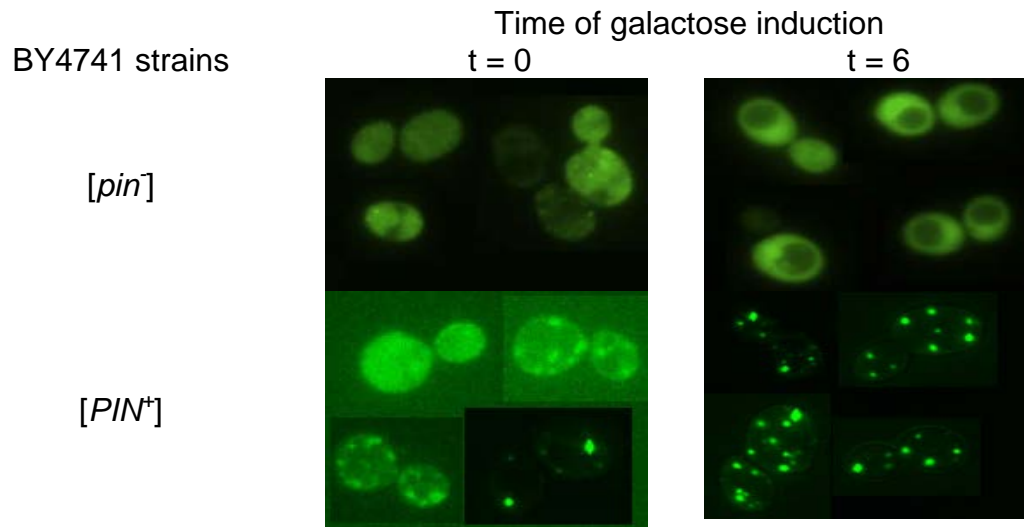


Figure 4.6 Fluorescence of the Rnq1-GFP fusion protein was observed in BY4741-based *[pin]* and *[PIN⁺]* cells. A uniform fluorescence was observed in *[pin]* cells. The Rnq1-GFP fusion protein was detected within fluorescent foci in *[PIN⁺]* cells after 6 hours induction. NB: Each contains a number of images taken from different fields of viewing.

In *[pin]* cells, Rnq1-GFP showed diffuse fluorescence after 6 hours induction (t = 6) whereas in *[PIN⁺]* cells, this fusion protein was observed within fluorescent foci after 6 hours induction (t = 6). Moreover, the fluorescence pattern of different *[PIN⁺]* variants differed. The low *[PIN⁺]*, medium *[PIN⁺]* and very high *[PIN⁺]* variants formed single fluorescence aggregates in 80% of cells whereas high *[PIN⁺]* variant showed multiple fluorescent foci in 80% of cells (Table 4.2). This result was consistent with previous findings published by Liebman *et al.*, (2006).

Unexpectedly, several small single or multiple fluorescent foci were observed before induction of expression of the Rnq1-GFP fusion by the addition of galactose i.e. t = 0. This may be caused by elevated expression of Rnq1 in glucose medium since *GAL1* is a leaky promoter (G.L.Staniforth, personal communication)

Chapter 4

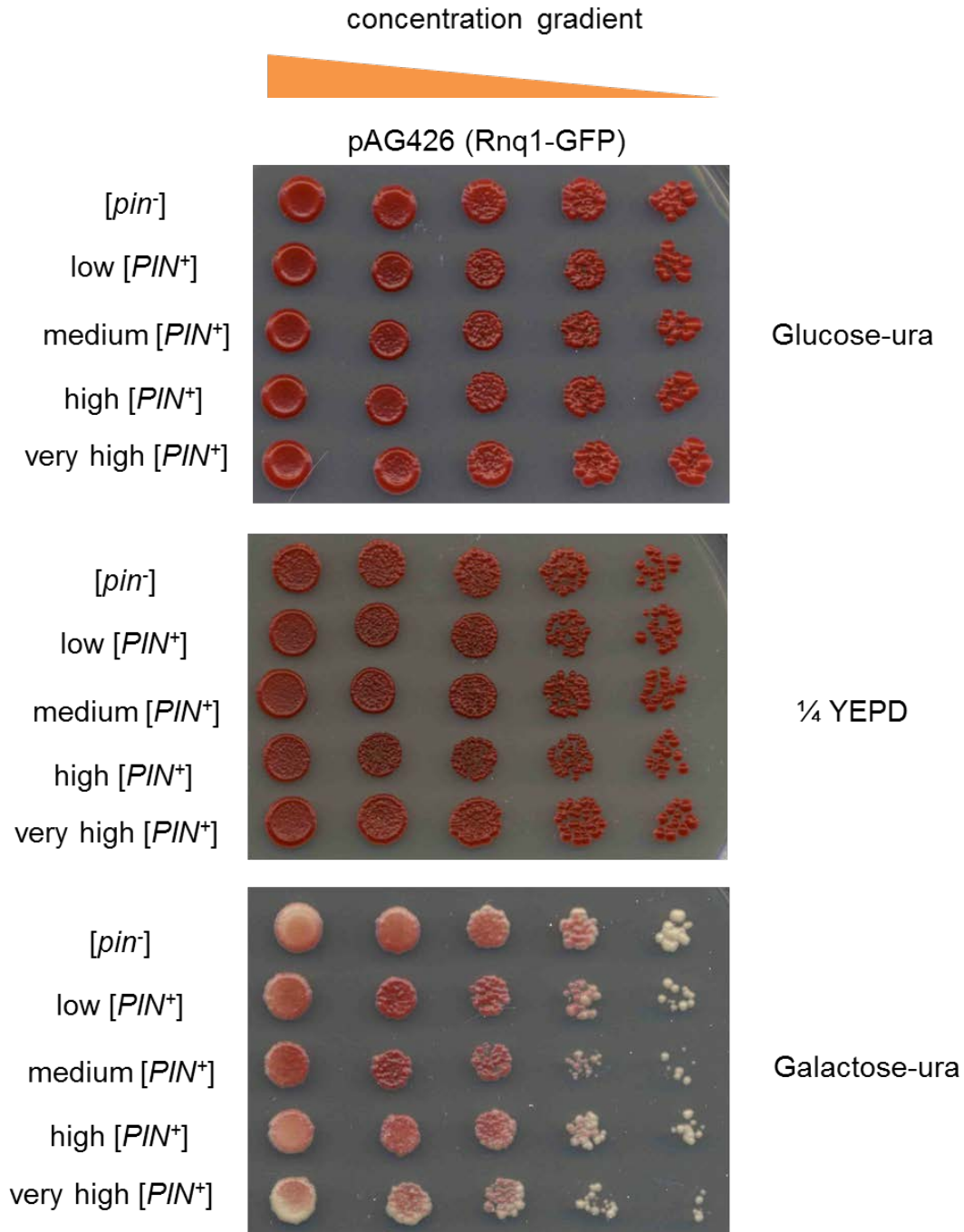


Figure 4.7 Overexpression of Rnq1-GFP fusion protein was not toxic in 74D-694 based [*pin*⁻] and [*PIN*⁺] strains. Cells were grown under the same conditions as toxicity assays of pYES2 and pYES2-RNQ1 strains (See section 4.2).

Because the type of [*PIN*⁺] variant in the BY4741 strain had not previously been established (G.L.Staniforth, personal communication), the BY4741 [*pin*⁻] and [*PIN*⁺] strains were transformed with the pAG426 plasmid expressing a galactose-inducible Rnq1-GFP and the localization of Rnq1-GFP evaluated by fluorescence microscopy. In [*pin*⁻] cells, the Rnq1-GFP fusion showed a

Chapter 4

diffuse fluorescence pattern as expected while in [*PIN*⁺] cells it formed multiple fluorescent aggregates indicating the [*PIN*⁺] variant in the yeast strain BY4741 is most likely a 'high' [*PIN*⁺] variant (Figure 4.6).

As shown in Section 4.2, Rnq1 overexpression in a [*PIN*⁺] strain leads to cytotoxicity and so it was important to establish whether the overexpressed Rnq1-GFP fusion protein was also toxic. Consequently, overexpression of Rnq1-GFP was examined in plasmid AG426-RNQ1 transformants of [*pin*⁻] and four different [*PIN*⁺] derivatives of 74D-694. Interestingly, overexpression of Rnq1-GFP was neither toxic in [*pin*⁻] nor in any of the four [*PIN*⁺] derivatives (Figure 4.7). This loss of cytotoxicity may be due to the structural change of Rnq1-GFP aggregates (C-terminal GFP tag) as a consequence of the 26.9kDa GFP sequence added to the C terminus of Rnq1 (43kDa).

Table 4.2 Quantitative analysis of the fluorescent aggregates formed in different [*PIN*⁺] variants at the 0 and 6 hour time points for each strain of 74D-694 and BY4741

[<i>PIN</i> ⁺] variant	No. cells analysed	No. cells with aggregates T=0	No. cells with aggregates T=6
74D-694 [<i>pin</i> ⁻]	98	3 (3%)	2 (2%)
74D-694 [<i>PIN</i> ⁺]LOW	95	10 (11%)	77 (80%) single
74D-694 [<i>PIN</i> ⁺]MED	95	13 (14%)	79 (83%) single
74D-694 [<i>PIN</i> ⁺]HIGH	97	7 (7%)	81 (84%) multiple
74D-694 [<i>PIN</i> ⁺]VERY H.	93	4 (4%)	76 (82%) single
BY4747 [<i>pin</i> ⁻]	95	3 (3%)	4 (4%)
BY4741 [<i>PIN</i> ⁺]	100	9 (9%)	81 (81%) multiple

4.5 Rnq1 overexpression causes a nuclear migration defect

Since growth defects were found in [*PIN*⁺] cells when Rnq1 was overexpressed, further investigation into the factors that cause the observed growth defects was undertaken. Log phase 74D-694 cells were observed following staining with 4',6-diamidino-2-phenylindole (DAPI) which is widely used to visualise nuclear DNA or mitochondrial DNA (Chazotte., 2011). The [*pin*⁻] and four [*PIN*⁺] variants were again transformed with pYES2 (control)

Chapter 4

and pYES2-RNQ1 plasmids and overexpression of the *RNQ1* gene induced by galactose. The nuclear DNA was visualized by fluorescence microscopy under ultraviolet light using DAPI to stain the DNA (Figure 4.8). Likewise the BY4741 strains were transformed with the pYES2-based plasmids and the galactose-inducible promoter *GAL1* used to overexpress the Rnq1 protein.

Overexpression of Rnq1 in BY4741 strain resulted in the localisation of nuclear DNA to the bud-neck 6 hours post induction of Rnq1 overexpression in this [*PIN*⁺] variant. This nuclear migration defect was not observed in the BY4741 [*pin*] derivative (Figure 4.8). Such a nuclear migration defect would be expected to lead to a cell cycle blockage, as was subsequently reported by Treusch and Lindquist (2012). Rnq1 overexpression causes the Spc42 to be localised to the unduplicated spindle pole body (SPB) thus resulting in cell cycle arrest (Treusch and Lindquist, 2002).

In 74D-694 [*pin*] cells, the localization of nuclear DNA was similar with both pYES2 (control) and pYES2-*RNQ1* strains before ($t = 0$) and after 6 hours induction ($t = 6$). This was observed in all four [*PIN*⁺] variants and thus no defect in nuclear migration was detected in the 74D-694 strains (Figure 4.9).

These findings suggest that while the effect of different genetic backgrounds on Rnq1-induced cytotoxicity was negligible, there was an effect on nuclear division that was dependent on genetic background. Importantly, this would further suggest that the observed nuclear migration defect was not the cause of Rnq1-induced cytotoxicity.

Chapter 4

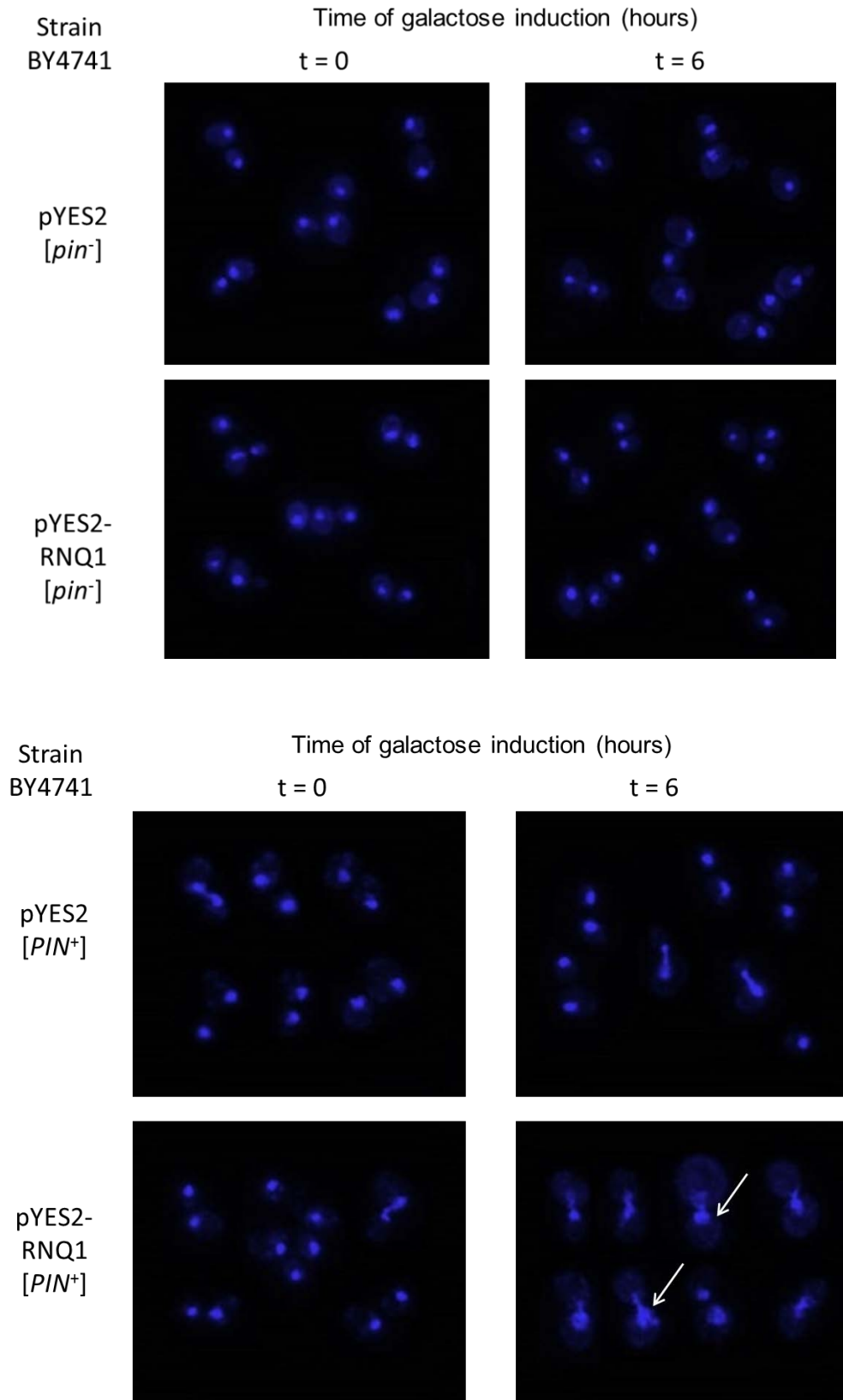
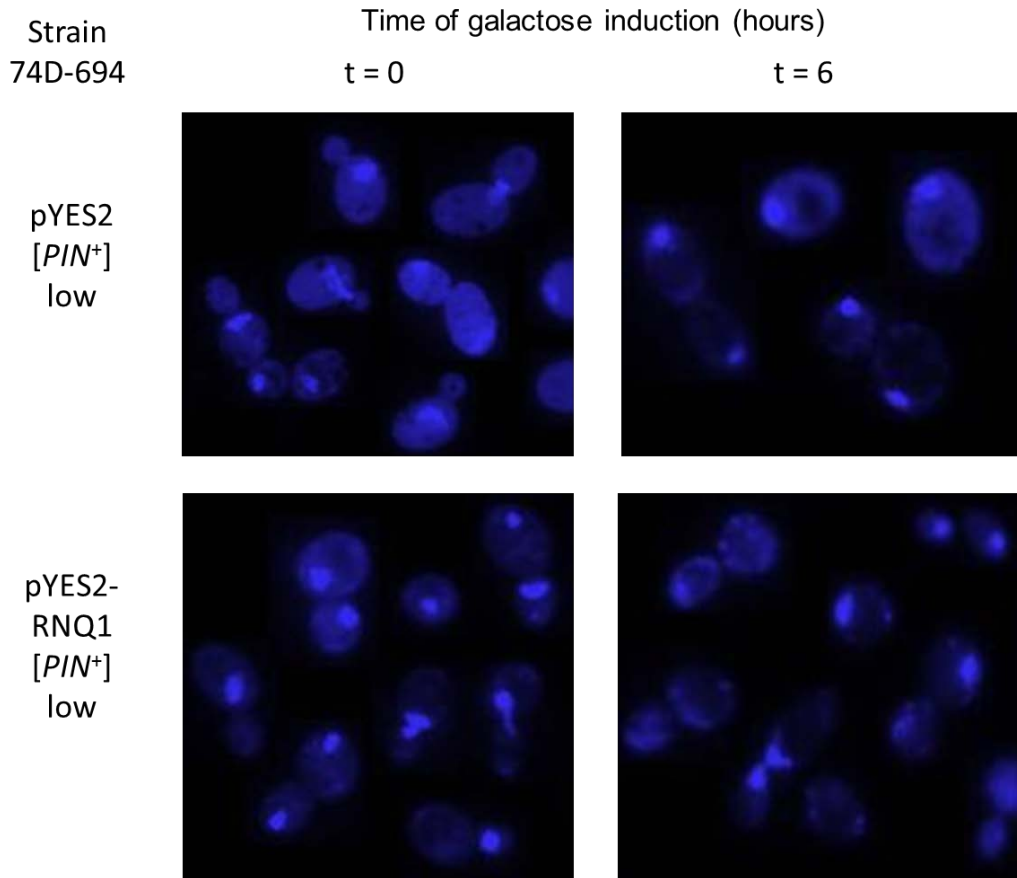
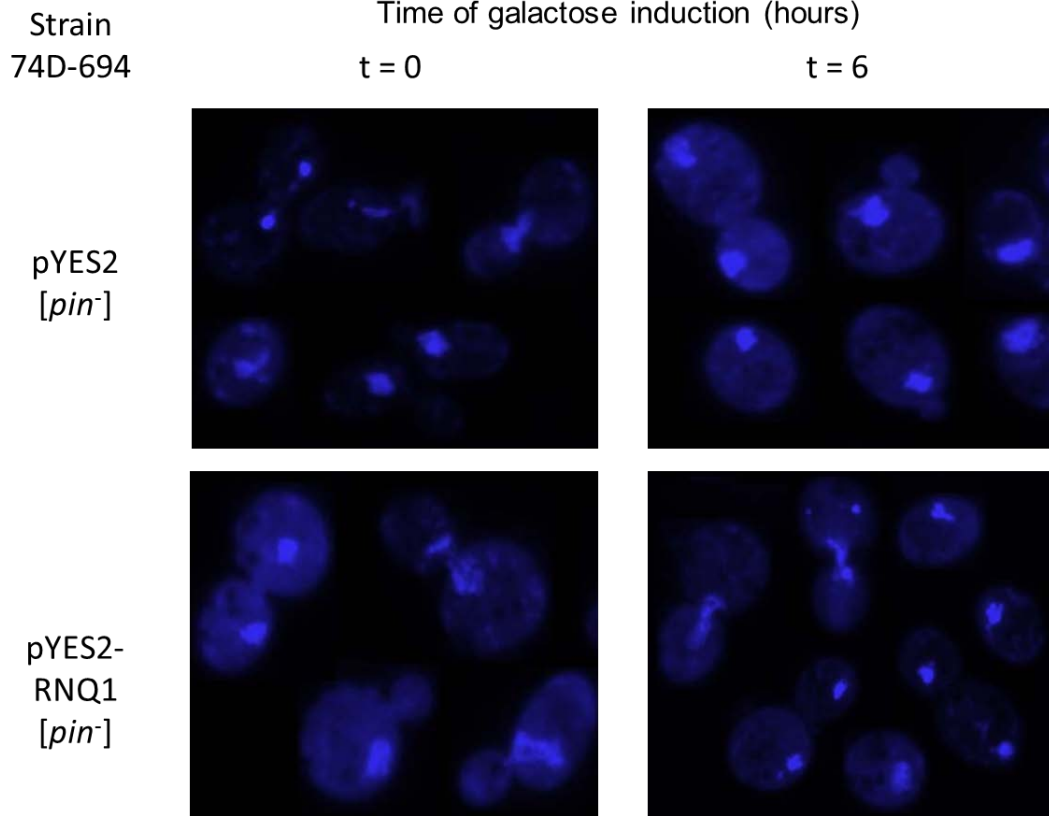
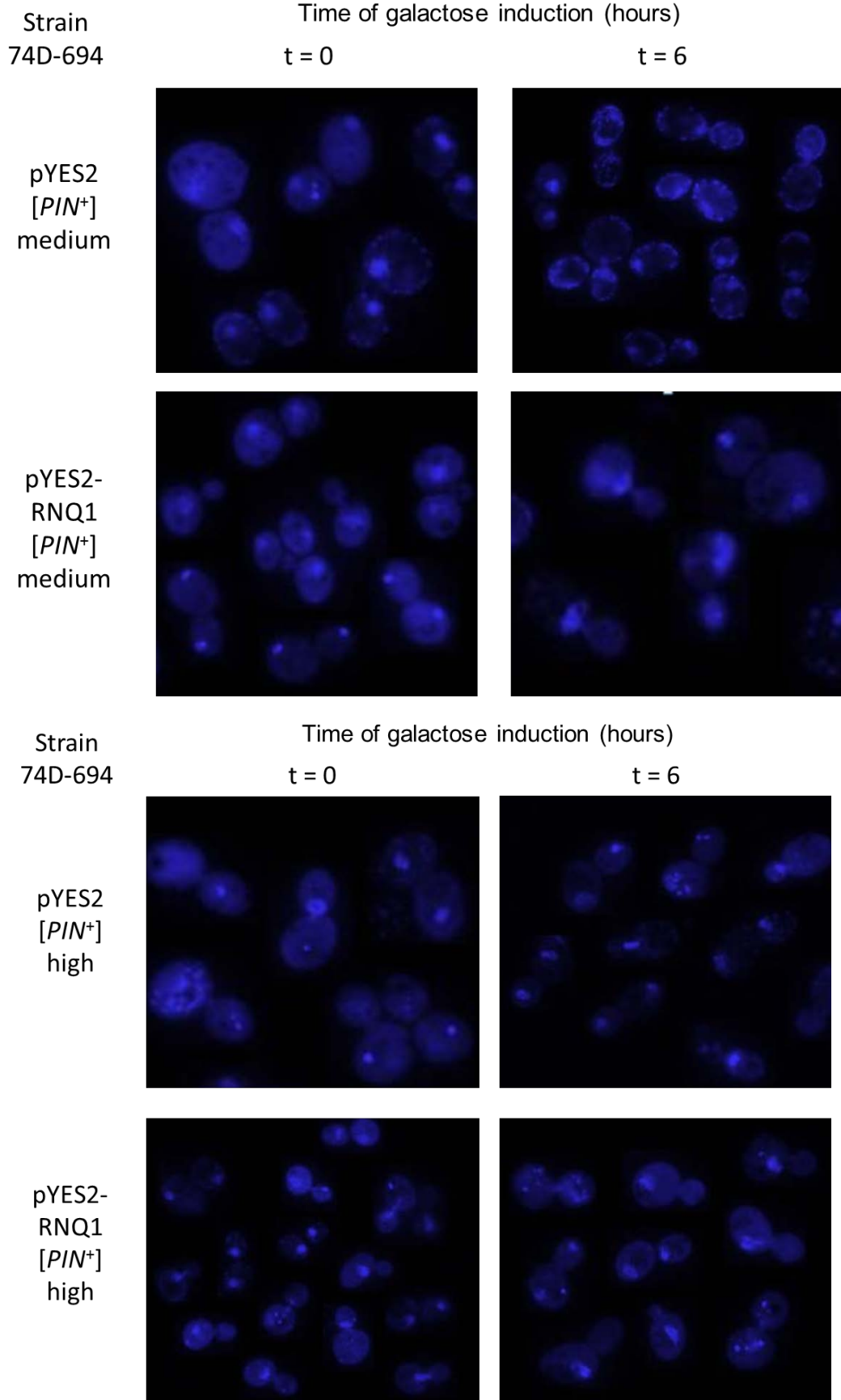


Figure 4.8 Overexpression of Rnq1 results in a nuclear migration defect in BY4741[*PIN*⁺] cells. Rnq1 overexpression leads to nuclear DNA localised to the bud-neck after 6 hours induction in pYES2-*RNQ1*[*PIN*⁺] strain whereas this was not observed in a [*pin*⁻] background. By contrast, the nuclear migration defects were not detected in pYES2[*PIN*⁺] and pYES2[*pin*⁻] (control) strains.

Chapter 4



Chapter 4



Chapter 4

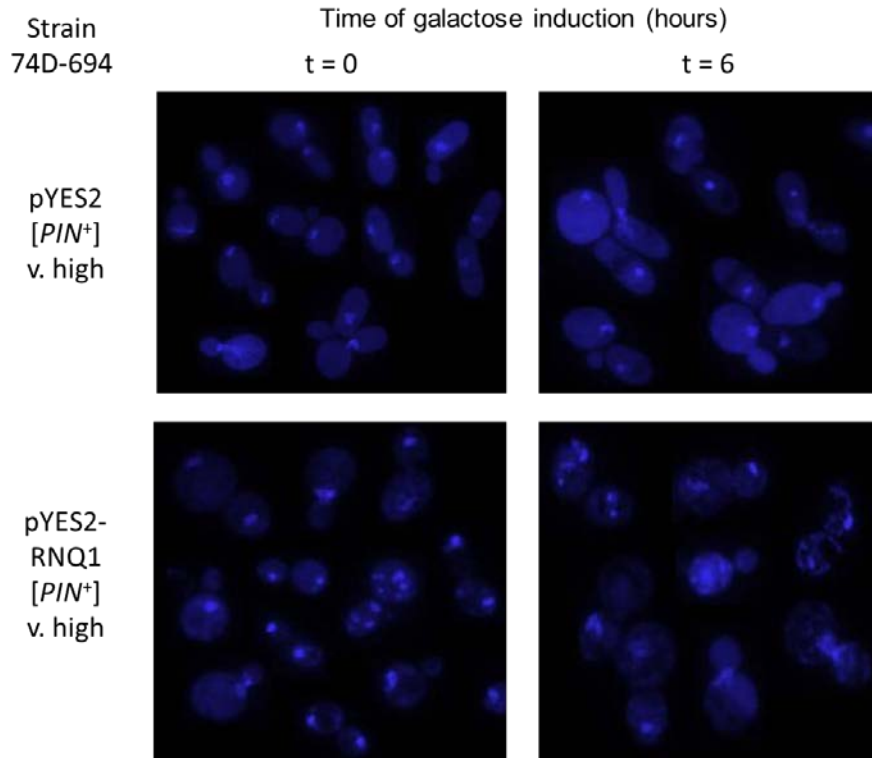


Figure 4.9 Overexpression of Rnq1 does not lead to a nuclear migration defect in any of the 74D-694 [PIN⁺] variants. Rnq1 overexpression does not cause nuclear DNA localised to the bud-neck after 6 hours induction in all four [PIN⁺] variants. No the nuclear migration defects were detected in pYES2 control strains. Cells were visualised by a blue excitation filter on an Olympus 1X81 fluorescent microscope with Hamamatsu Photonics Orca AG cooled CCD camera. Images were captured analysed by Olympus CellR software.

Table 4.3 Quantitative analysis of the nuclear migration defect in different [PIN⁺] variants at the 0 and 6 hour time points for each strain of 74D-694 and BY4741

[PIN ⁺] variant	No. cells analysed	No. cells with nuclear migration defect	No. cells without nuclear migration defect	No. cells with nuclear migration defect	No. cells without nuclear migration defect
		T=0	T=0	T=6	T=6
74D pY-[pin]	100	0	100	0	100
74D pY-[PIN ⁺]LOW	100	0	100	2	98
74D pY-[PIN ⁺]MED	100	1	99	2	98
74D pY-[PIN ⁺]HIGH	100	1	99	3	97
74D pY-[PIN ⁺]VERY H.	100	2	98	2	98
74D pY-RNQ1[pin]	100	0	100	0	100
74D pY-RNQ1[PIN ⁺]LOW	100	1	99	2	98
74D pY-RNQ1[PIN ⁺]MED	100	0	100	1	99
74D pY-RNQ1[PIN ⁺]HIGH	100	3	97	2	98
74D pY-RNQ1[PIN ⁺]VERY H.	100	2	98	5	95
BY pY-[pin]	100	3	97	2	98
BY pY-RNQ1[PIN ⁺]	100	1	99	75	25

4.6 Rnq1 overexpression causes mitochondrial dysfunction in a [*PIN*⁺]-dependent manner

Since the Rnq1-induced toxic phenotype was observed in different [*PIN*⁺] variants, it was interesting to further investigate whether Rnq1 overexpression leads to defects in mitochondria. Mitochondrial dysfunction can be detected by assaying the level of reactive oxygen species (ROS) in cells as mitochondria are believed to be the major intracellular source of ROS and ROS production is inherent in mitochondrial oxidative metabolism (DAutreaux and Toledano, 2007).

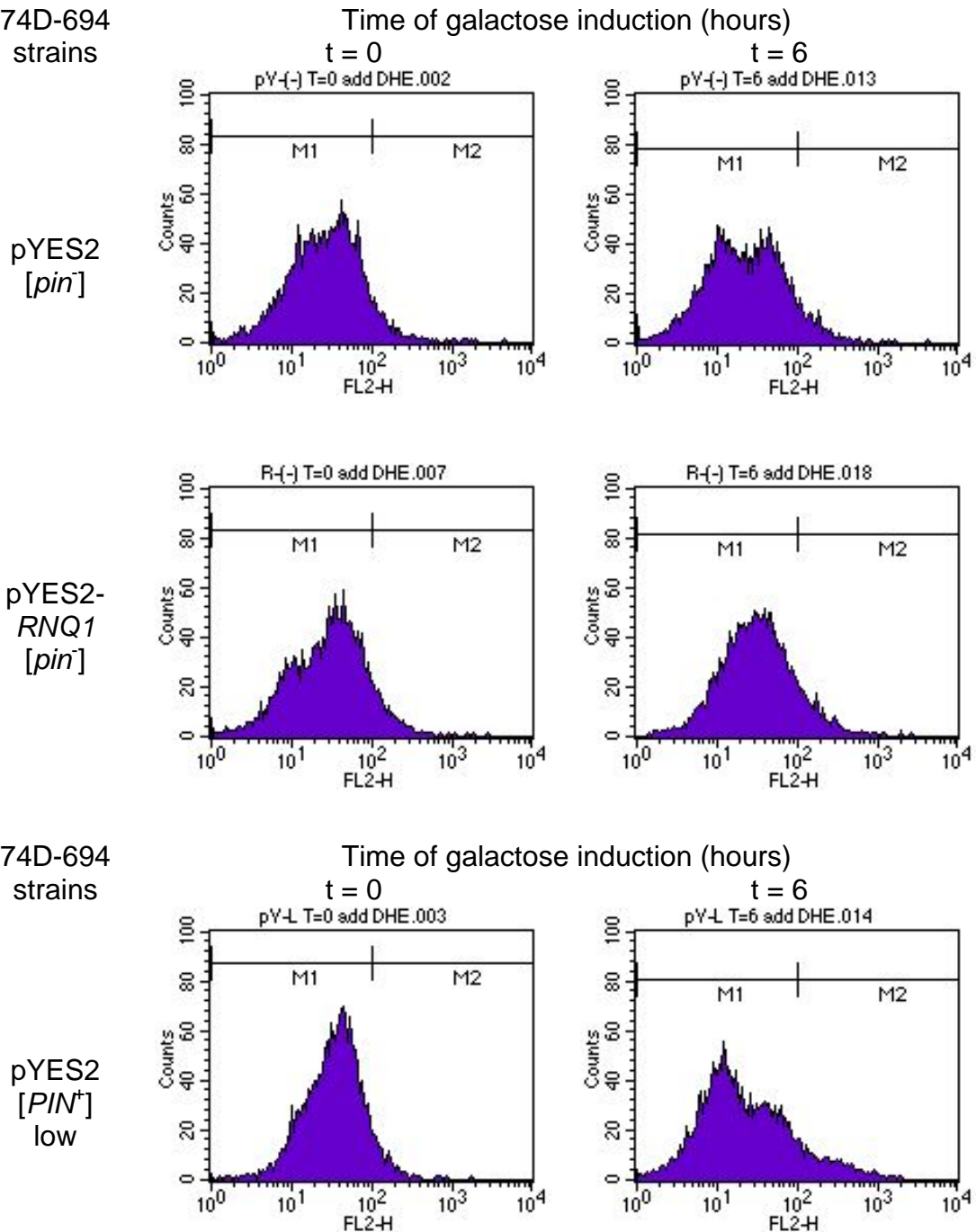
The ROS assay used to evaluate mitochondrial dysfunction has been designed to measure the level of superoxide in cells with ROS production being estimated by following the oxidation of dihydroethidium (DHE). DHE is perhaps the most specific and least problematic dye as it detects essentially superoxide radicals, is retained well by cells, and may even tolerate mild fixation. Therefore, in order to explore whether Rnq1 overexpression leads to mitochondrial dysfunction, ROS assays (see *Section 2.9.3*) were performed on 74D-694-based [*pin*⁻] and the four [*PIN*⁺] variants before and after induction of overexpression of Rnq1. The level of superoxide in each strains was detected and quantified using a BD FACSCalibur flow cytometer and the results were analysed using BD CellQuest Pro Software. These data are shown in Figure 4.10.

In the 74D-694 strains engineered to overexpress the *RNQ1* gene, the level of superoxide was about five times higher after six hours induction than un-induced cells. For example, the value of M2 (M2 indicates the amount of cells with mitochondrial defects) is 7.84 in un-induced very high [*PIN*⁺] cells while it is increased to 33.90 after six hours induction. The M2 value after induction divided by the M2 value before induction is 4.3 meaning that the amount of superoxide was about five times higher after six hours induction than un-induced very high [*PIN*⁺] cells (This calculation was used in every strain in this experiment.). However, in the control strain (pYES2), it was only elevated one

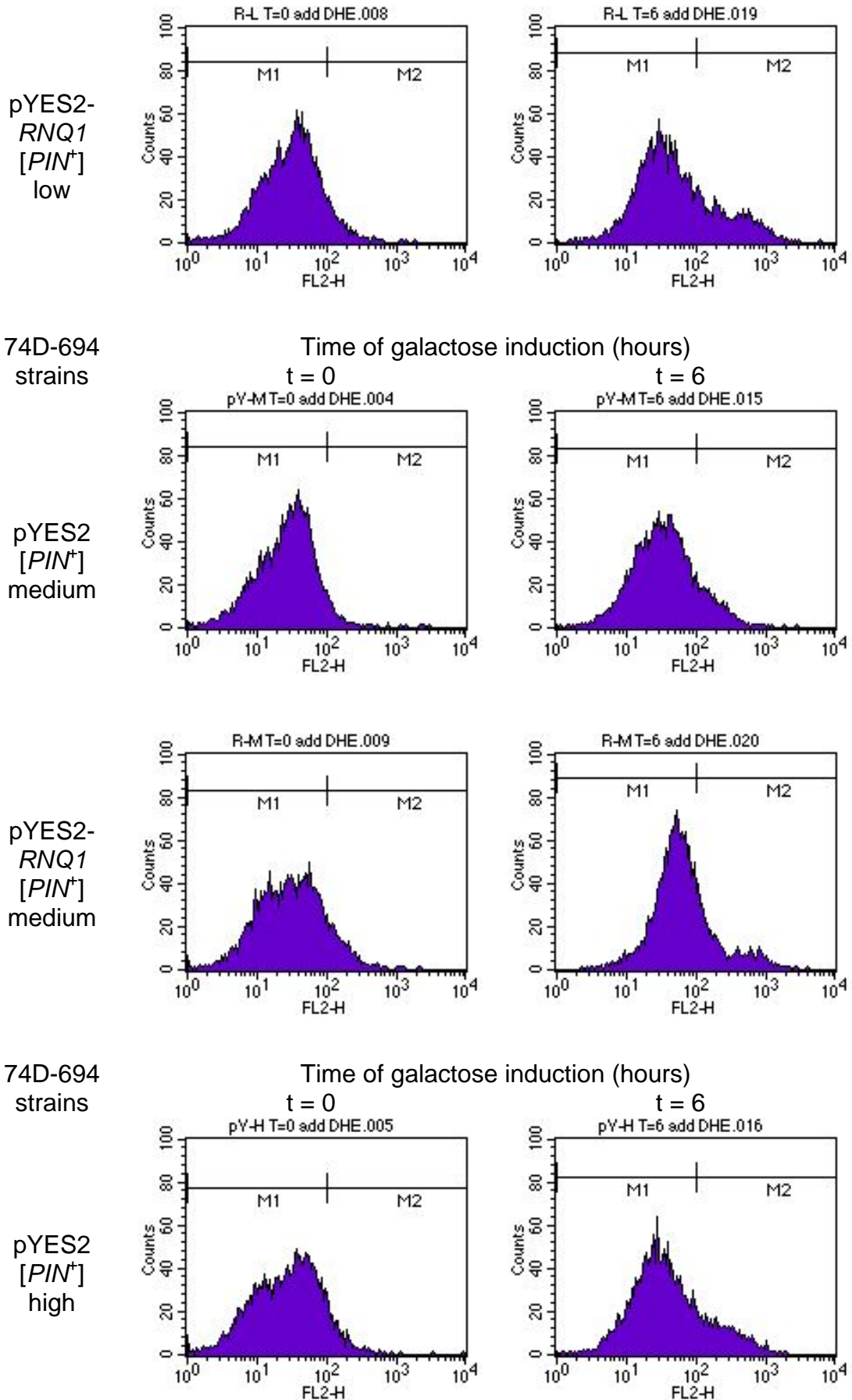
Chapter 4

to two-fold over in induced cells suggesting that Rnq1 overexpression causes a degree of mitochondrial dysfunction in the presence of $[PIN^+]$ (Figure 4.11).

74D-694
strains



Chapter 4



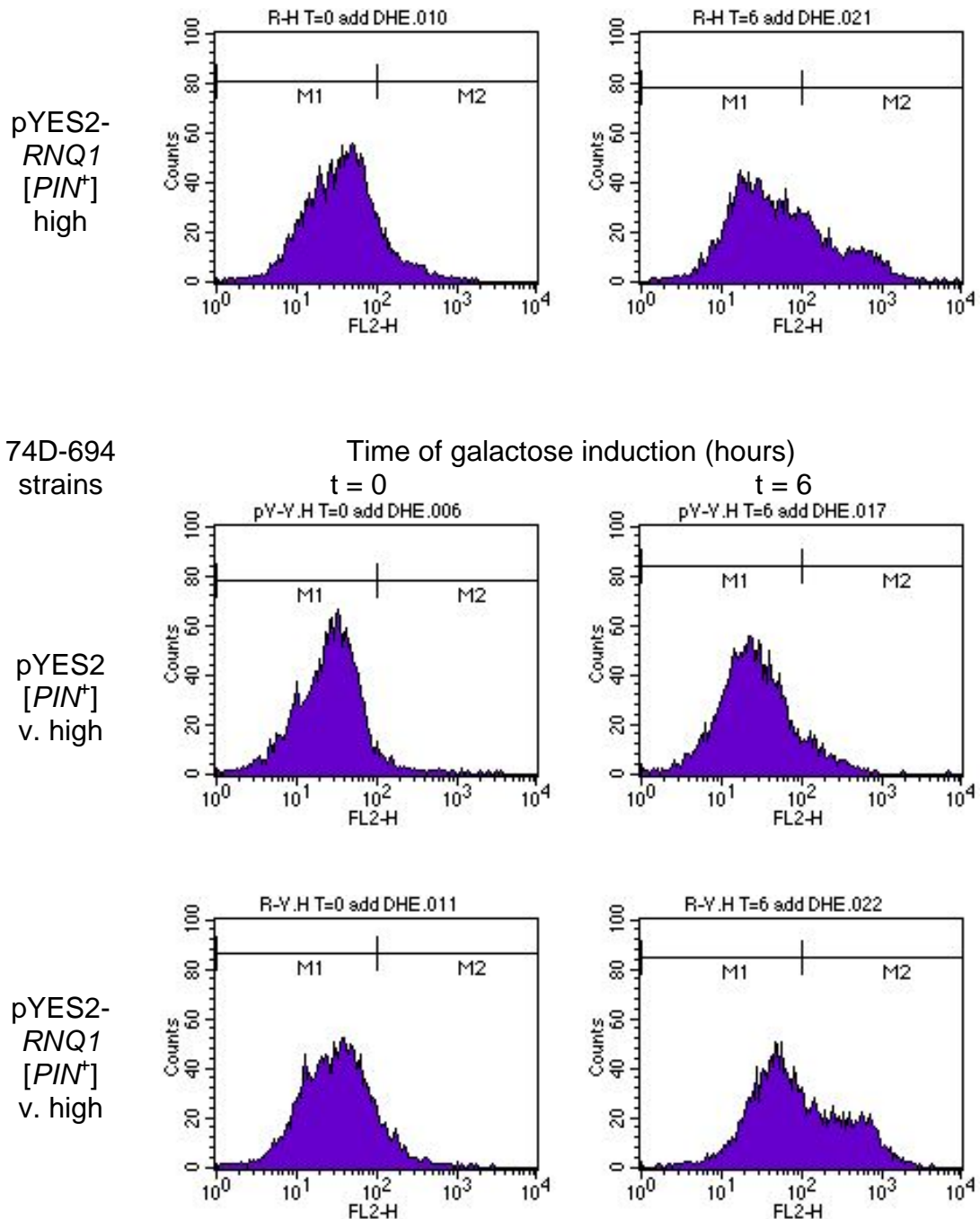
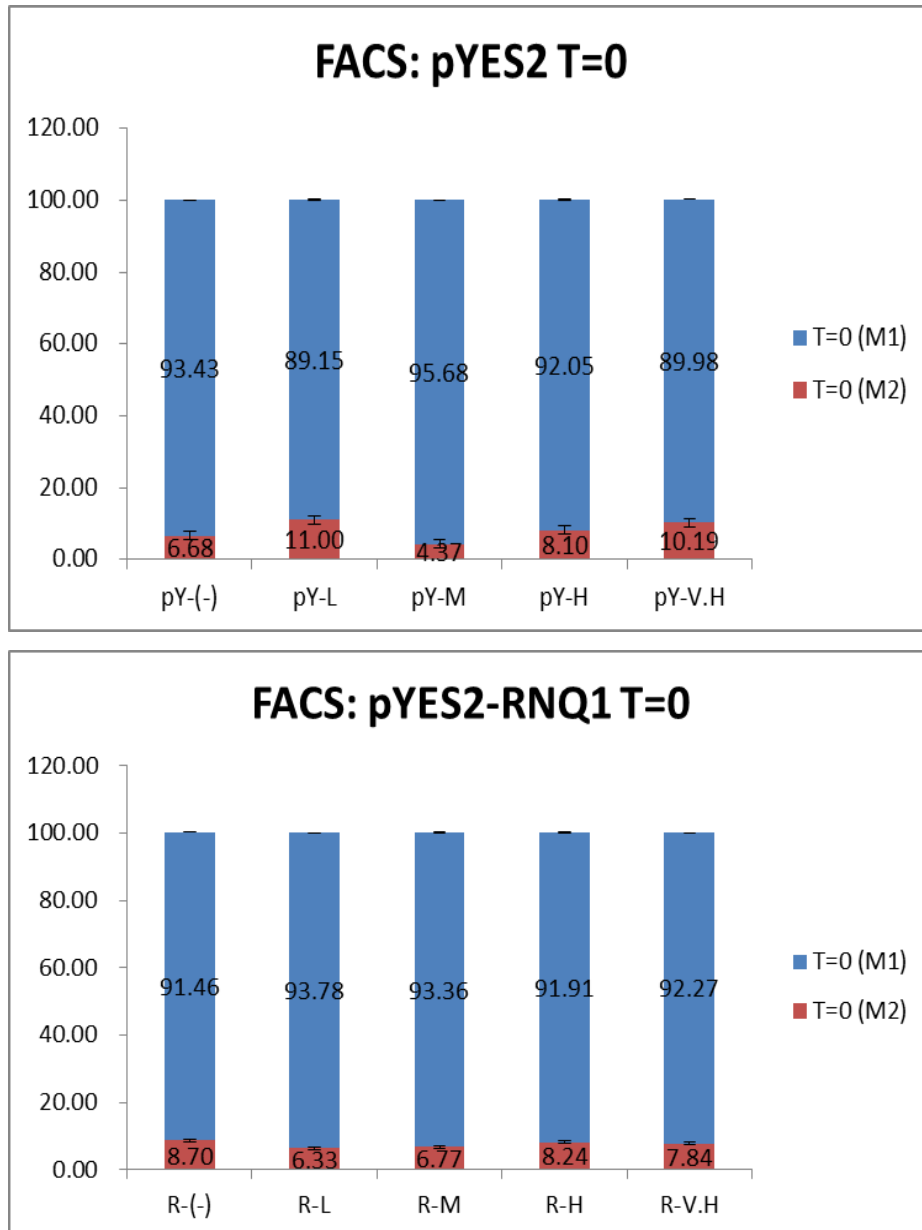


Figure 4.10 The level of superoxide generated by overexpression of *Rnq1* as determined by flow cytometry. Marker (M1) represents the control peak which is used to establish the baseline fluorescence intensity. The peak shift to the right, which is the region labelled M2 indicates the amount of cells with mitochondrial defects.

In the [*PIN*⁺] BY4741 strain overexpressing the *RNQ1* gene, a 20-fold increase in the level of superoxide was detected after six hours induction

Chapter 4

compared with the control strain (pYES2). In un-induced cells overexpressing Rnq1, the level of superoxide was very close to the strain expressing the empty plasmid pYES2 (Figure 4.12). Thus, the same result of Rnq1 overexpression leading to mitochondrial dysfunction in [*PIN*⁺] cells was confirmed in BY4741 strains.



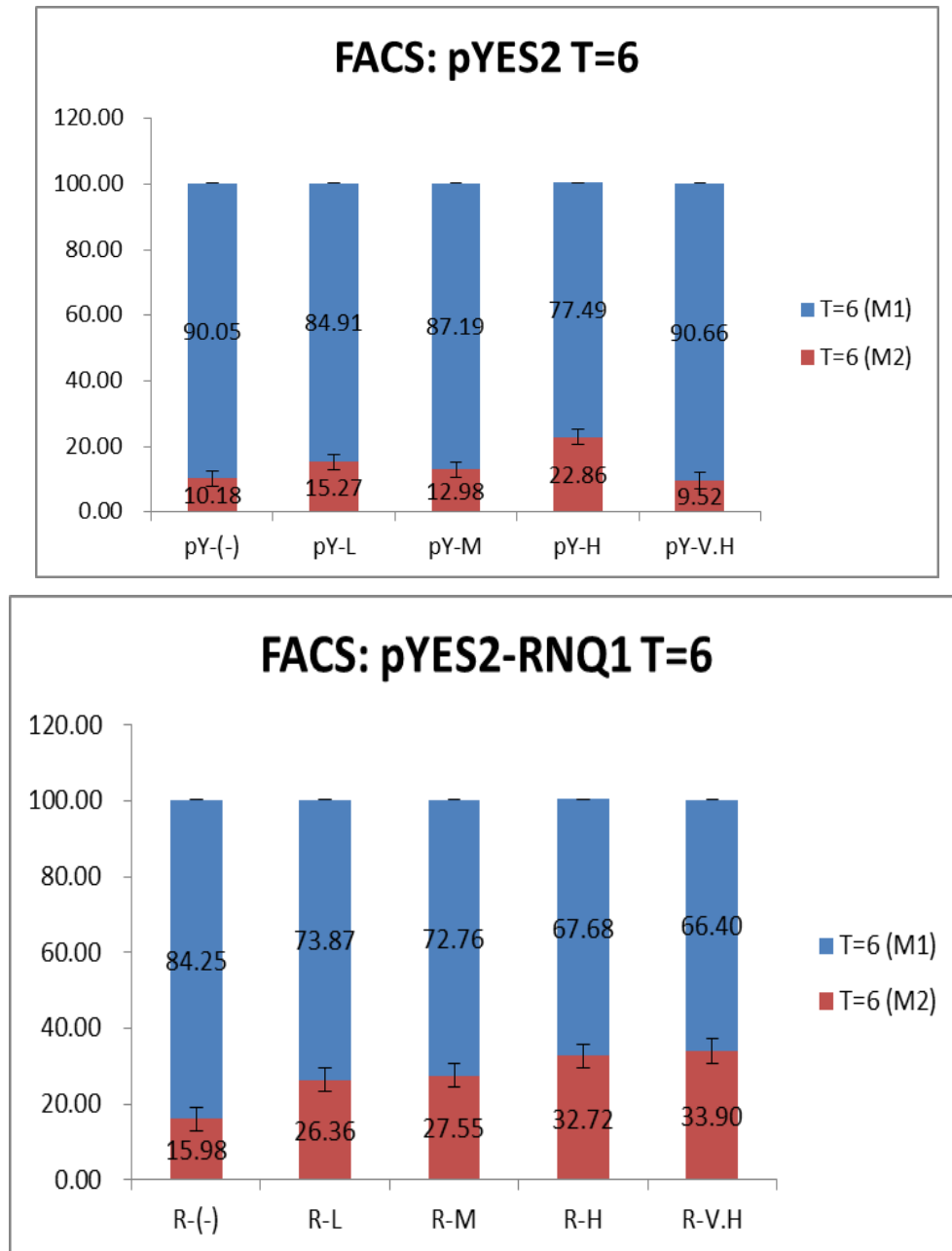


Figure 4.11 Quantitative analysis of ROS production in different [*PIN*⁺] variants of 74D-694 strains engineered to overexpress Rnq1. The red bars indicate the proportion of cells accumulating high levels of the fluorescence probe (DHE).

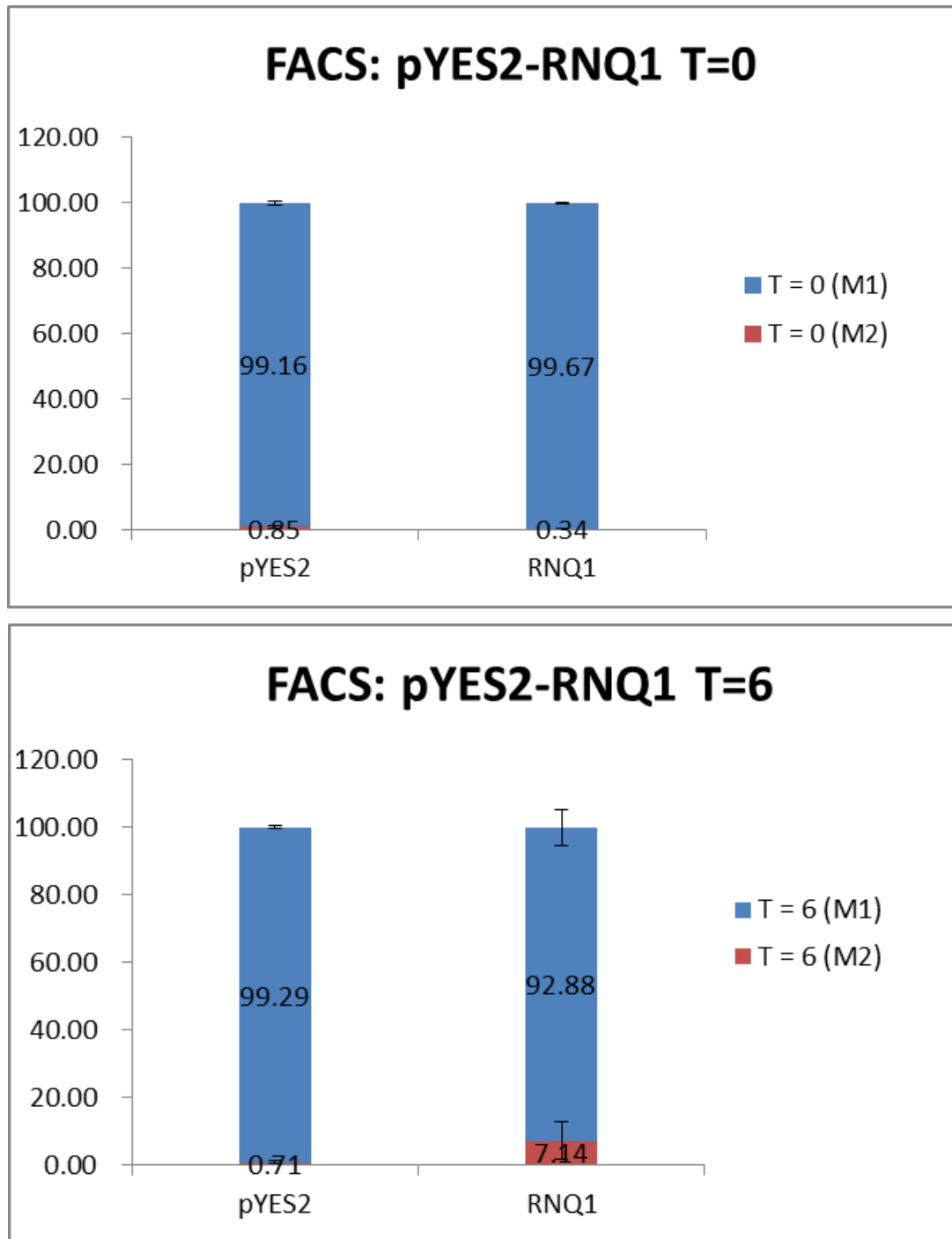
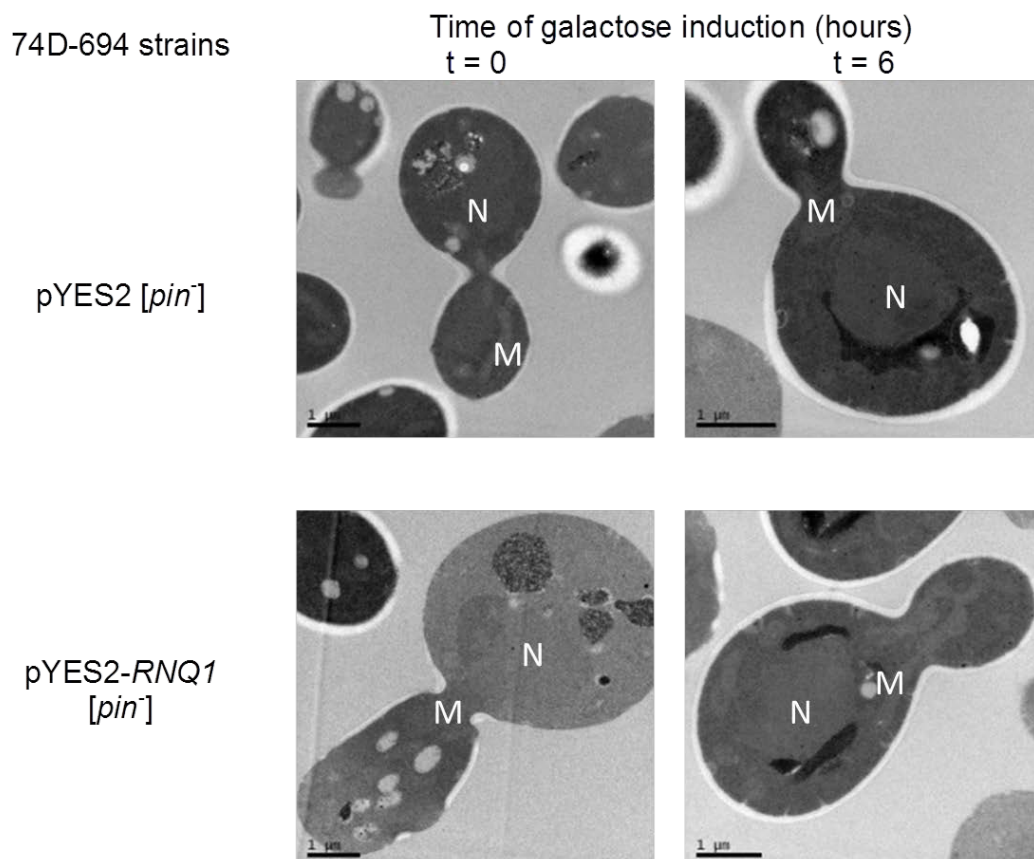


Figure 4.12 Quantitative analysis of ROS production of [*PIN*⁺] variant of BY4741 strains engineered to overexpress Rnq1. The red bars indicate the proportion of cells accumulating high levels of the fluorescence probe (DHE).

Chapter 4

To further evaluate whether Rnq1 overexpression led to an ultrastructural defect in mitochondria that in turn resulted in the higher levels of ROS seen in 74D-694-based [*pin*⁻] and four [*PIN*⁺] variants, transmission electron microscopy (TEM) of sectioned log phased cells was undertaken before and after 6 hours induction. The images obtained showed the structure of mitochondria was changed after six hours induction in four [*PIN*⁺] variants but not [*pin*⁻] (Figure 4.13). These changes were largely an elongation of the mitochondria and how they were stacked in the daughter cells i.e. there are several elongated mitochondria stacked at the bud neck as well as in the daughter cells. The abnormal morphologies of mitochondria confirm that Rnq1 overexpression-induced elevated ROS levels could be due to mitochondrial dysfunction in [*PIN*⁺] cells.



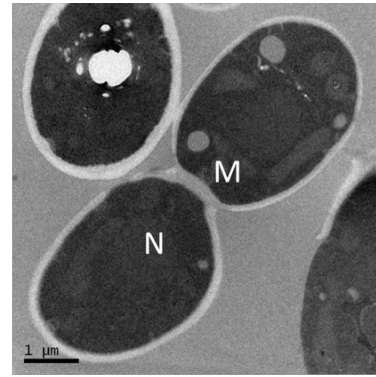
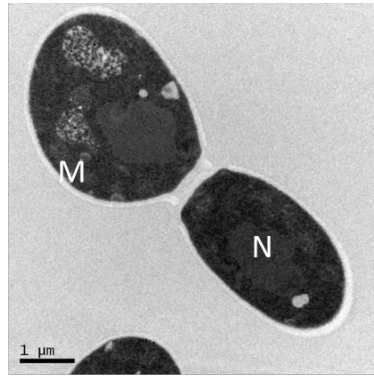
Chapter 4

Time of galactose induction (hours)

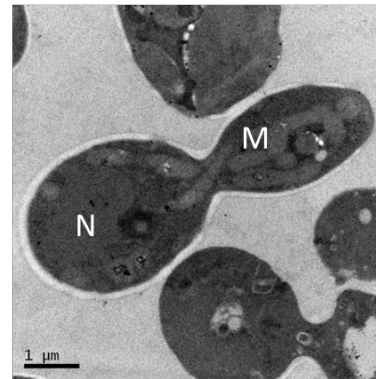
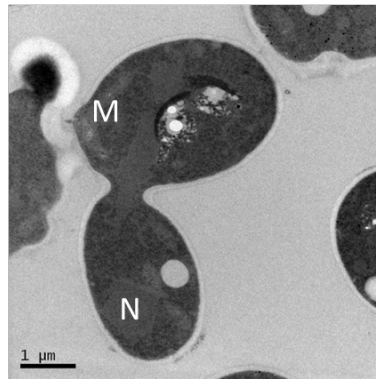
t = 0

t = 6

pYES2
[PIN⁺]
low



pYES2-
RNQ1
[PIN⁺]
low

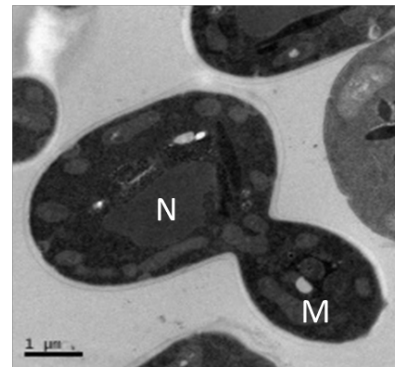
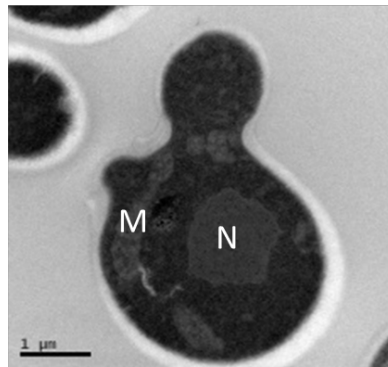


Time of galactose induction (hours)

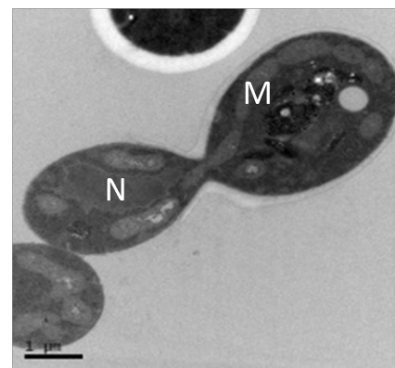
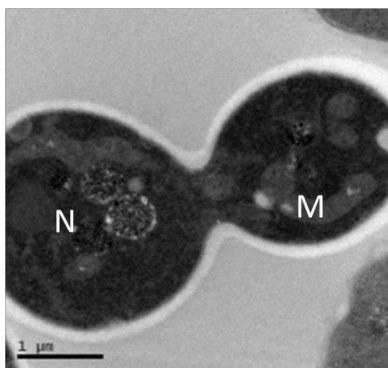
t = 0

t = 6

pYES2
[PIN⁺]
medium



pYES2-
RNQ1
[PIN⁺]
medium



Chapter 4

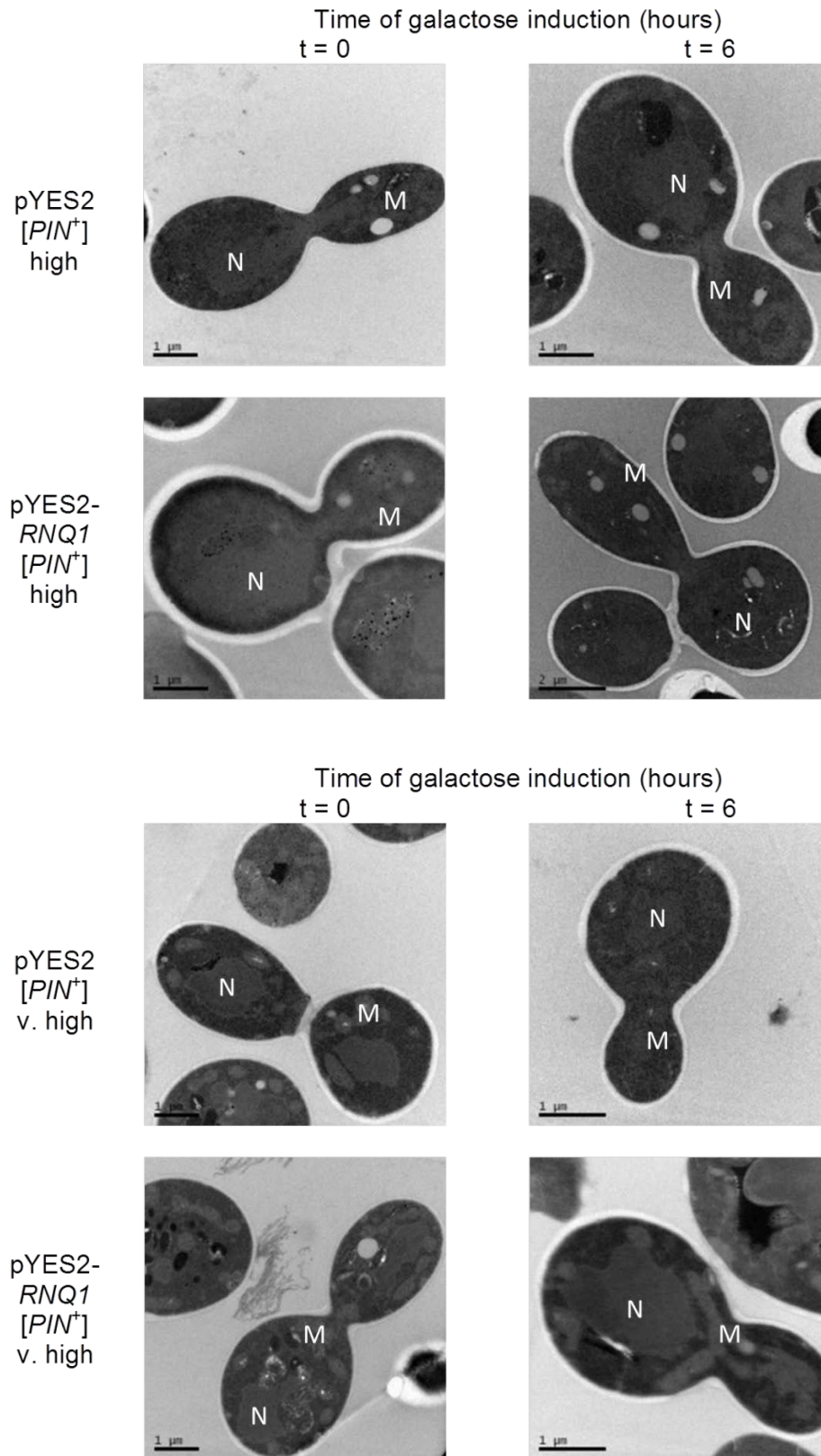


Figure 4.13 Cell ultrastructure of the 74D-694-based [PIN] variants. Cells were induced in galactose medium at 30°C for 6 hours. The structure of mitochondria was changed after 6 hours induction in low [PIN⁺], medium [PIN⁺], high [PIN⁺] and very high [PIN⁺] variants.

4.7 Discussion

As the results shown previously, Rnq1 overexpression is toxic in [*PIN*⁺] variants and leads to mitochondrial dysfunction in [*PIN*⁺] cells. However, the same phenotype was not found in [*pin*⁻] cells. Moreover, these findings were confirmed in different a genetic background i.e. the 74D-694 and BY4741 strains. This suggests that the mitochondrial dysfunction is associated with Rnq1 overexpression in a [*PIN*⁺] background but not due to the loss of the cellular function of Rnq1 when it switches into a presumably non-functional amyloid form. Although a number of studies were carried out to explore the defects in mitochondrial function, the exact mechanism of mitochondrial dysfunction is still unclear. One possible explanation could be that Rnq1, as an intrinsically disordered protein, randomly interacts with other proteins resulting in disturbance in the cellular protein network, for example, actin cytoskeleton (Vavouri et al., 2009). Changes in actin cytoskeleton may cause alterations in mitochondrial morphology and dysfunction.

However, the nuclear migration defect was only found in the BY4741 [*PIN*⁺] strains while the Rnq1 overexpression-induced cytotoxicity was observed in both BY4741 and 74D-694 strains in a [*PIN*⁺] background. This suggests that the toxic phenotype induced by Rnq1 overexpression does not dependent on the nuclear migration defect. Although Rnq1 overexpression mediated cytotoxicity is not caused by the nuclear migration defect, it is still interesting to explore why overexpression of Rnq1 results in nuclear migration defect in BY4741 [*PIN*⁺] background. It was established that Spc42, a highly phosphorylated coiled-coil protein at the core of the spindle pore body (SPB) (Bullitt et al., 1997), is specifically sequestered by Rnq1 overexpression resulting in a defect in the duplication of SPB. SPB plays a very important role in many essential mitotic processes, such as nuclear migration, spindle formation and chromosome movement (Byers and Goetsch, 1975). It has been found that Spc42 is localised to two foci i.e. duplicated SPB in budded cells in [*pin*⁻] background, while Spc42 is localised to a single focus i.e. unduplicated SPB in [*PIN*⁺] background. Moreover, an elevated level of Spc42

Chapter 4

can reduce the cytotoxicity caused by Rnq1 overexpression as the effect of Rnq1-mediated sequestration is overcome by an increased amount of Spc42 (Lindquist et al., 2012).

Chapter 5

[*PIN*⁺]-dependent toxicity mediated by the polyglutamine (polyQ) expansion proteins

5.1 Introduction

Proteins containing polyglutamine (polyQ) expansions lead to nine neurodegenerative diseases as the misfolded proteins have an impact on proper cellular function and result in cytotoxicity. Despite distinct polyQ expansion proteins being associated with different polyQ disorders, an expansion of a trinucleotide repeat CAG encoding a polyQ tract is the pathogenic agent of all of these polyQ disorders. Although there is intense research underlying the pathogenicity of these diseases, the mechanism of polyQ disorders at least at a molecular level, still remains unclear.

During the past ten years, several models were developed to investigate polyQ cytotoxicity such as the invertebrate *Caenorhabditis elegans* models, *Drosophila* models and yeast *Saccharomyces cerevisiae* models. For example, polyQ-YFP fusion protein was found to be toxic in *C. elegans* body wall muscle cells suggesting that polyQ tract is linked to the associated toxicity (Morley *et al.*, 2002). The cytotoxicity of polyQ tract had been demonstrated in *Drosophila* model in 2005 (McLeod *et al.*, 2005). The first yeast model was developed by Meriin in 2002 who established a direct link between the aggregation of polyQ tract and its cytotoxicity (Meriin *et al.*, 2002). Moreover, a yeast model was used to determine the pathologies of polyQ disorders influenced by the intramolecular and intermolecular factors associated with polyQ expansion proteins (Lindquist *et al.*, 2006). Recent studies revealed that interaction between Sup35 and polyQ tract via its prion domain plays an important role in polyQ toxicity when [*PSI⁺*] is present (Gong *et al.*, 2012).

Huntington disease is one of the nine fatal neurodegenerative polyQ disorders which is caused by a polyQ expansion in the huntingtin (Htt) protein resulting in protein aggregation (Ross and Tabrizi, 2011). A previous study had revealed that overexpression of polyQ leads to cytotoxicity in a [*PIN⁺*] background (Meriin *et al.*, 2002). Since the Rnq1 protein is rich in polyglutamine and Rnq1 overexpression is also only toxic in a [*PIN⁺*]

dependent manner (Douglas *et al.*, 2008), it was interesting to compare polyQ expansion protein mediated cytotoxicity with Rnq1 mediated cytotoxicity in different [*PIN*⁺] variants.

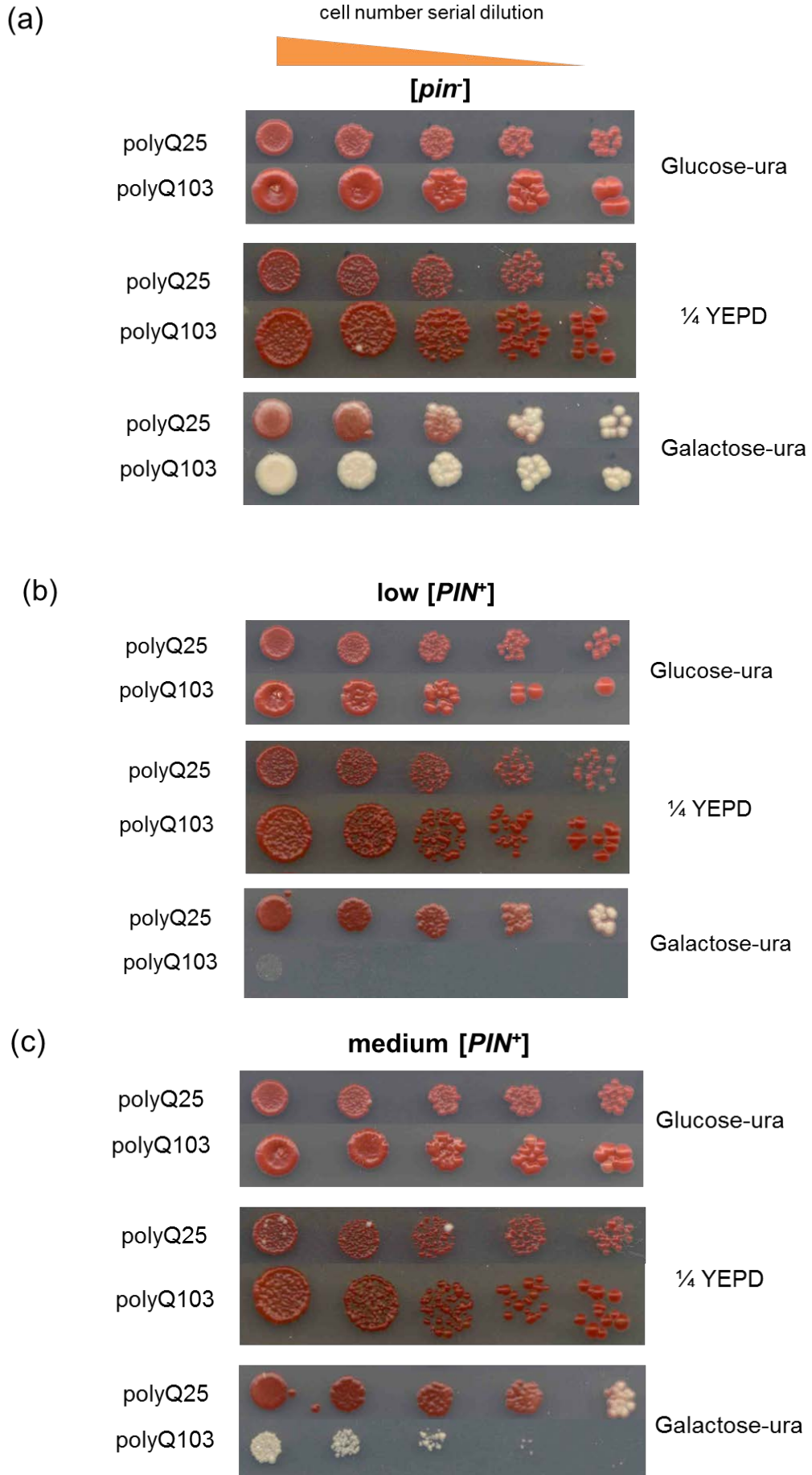
In this chapter, a yeast-based Huntington disease model was used to investigate the mechanism of polyQ toxicity. Similarly, a series of cellular assays were employed to determine the mechanism of polyQ expansion protein-mediated cytotoxicity dependent upon the [*PIN*⁺] prion.

5.2 Overexpression of a polyQ expansion protein HttQ103 is toxic in different [*PIN*⁺] variants but not in a [*pin*⁻] background

In order to examine the toxic phenotype in different [*PIN*⁺] variants when a polyQ expansion protein was overexpressed, the two plasmid pYES2-Q25 (control) and pYES2-Q103 obtained from Y. Chernoff (Meriin *et al.*, 2002) were separately transformed into a [*pin*⁻] derivative and four different [*PIN*⁺] derivatives of yeast strain 74D-694 (Derkatch *et al.*, 1997). As described in Chapter 4 (Section 4.2), cells were grown under the same conditions as strains harbouring pYES2 or pYES2-*RNQ1*. Q25 and Q103 were inserted into the pYES2 plasmid by Y. Chernoff (Meriin *et al.*, 2002) placing expression of the Q25 and Q103 proteins under the control of a galactose inducible promoter *GAL1*. Strains expressing Q25 and Q103 were serially diluted and spotted onto different agar plates to assess growth (Figure 5.1).

As previously reported (Meriin *et al.*, 2002), Overexpression of Q103 was not toxic in a [*pin*⁻] strain whereas it was toxic in all four different [*PIN*⁺] variants. By contrast, overexpression of Q25 was neither toxic in [*pin*⁻] nor [*PIN*⁺] background. Interestingly, the low [*PIN*⁺] variant showed the highest degree of cytotoxicity when Q103 was overexpressed. This is different from the Rnq1-mediated cytotoxicity reported in Chapter 4 where overexpression of Rnq1 was less toxic in the low [*PIN*⁺] variant compared with the high and very high [*PIN*⁺] strains.

Chapter 5



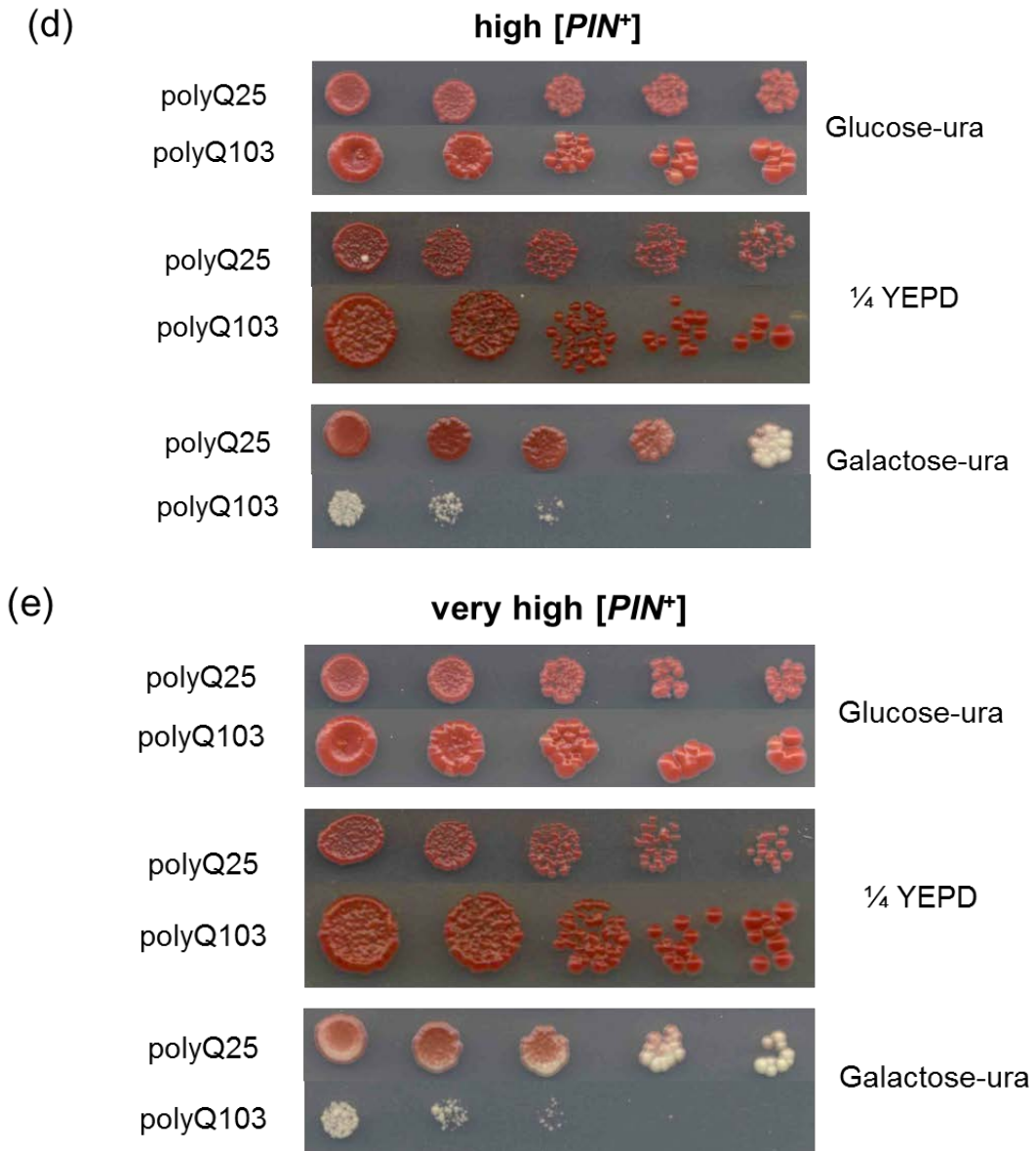


Figure 5.1 Overexpression of Q103 results in different degrees of cytotoxicity in different [*PIN*⁺] variants of 74D-694 cells. Cells were grown in the inducing medium i.e. SD 2% galactose-ura for 8 hours at 30°C with shaking and diluted and spotted onto different agar plates. **(a)** Q103 overexpression was not toxic in [*pin*⁻] variant. **(b) (c) (d) (e)** Q103 overexpression was toxic in all four [*PIN*⁺] strains. polyQ25 presents the pYES2 plasmid with Q25 insert (control) while polyQ103 presents the pYES2 vector with Q103 insert. Three biological replicates were performed for each strain and one representative is shown for each.

Chapter 5

Since Rnq1 overexpression-induced cytotoxicity was examined in two different yeast strains 74D-694 and BY4741, overexpression of Q103 mediated cytotoxicity was also determined in the [*PIN*⁺] strain of BY4741. The result of these assays showed that overexpression of Q103 was also toxic in these [*PIN*⁺] cells but not in a [*pin*] derivative. Overexpression of Q25 was not toxic in either [*PIN*⁺] and [*pin*] cells (Figure 5.2). Thus, the same result of Q103 overexpression mediated cytotoxicity was confirmed in the yeast strain BY4741 indicating that the different genetic backgrounds had no impact on the toxic phenotype.

Overexpression of both Rnq1 and Q103 result in cytotoxicity in a [*PIN*⁺]-dependent manner while Rnq1 and Q103 mediated cytotoxicity in different [*PIN*⁺] variants differed i.e. the very high [*PIN*⁺] variant showed the highest degree of cytotoxicity when Rnq1 was overexpressed while the low [*PIN*⁺] variant showed the highest degree of cytotoxicity when Q103 was overexpressed. This suggests that Rnq1 and polyQ mediated cytotoxicity in different [*PIN*⁺] variants may undertake different mechanisms. One possible reason is that the low [*PIN*⁺] variant, as a prion seed, is more efficient in the aggregation of polyQ103 than Rnq1, depending on its steric conformation.

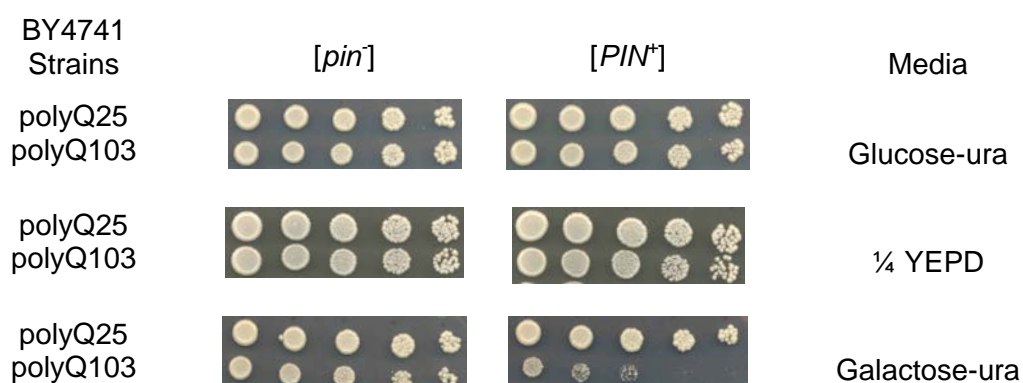
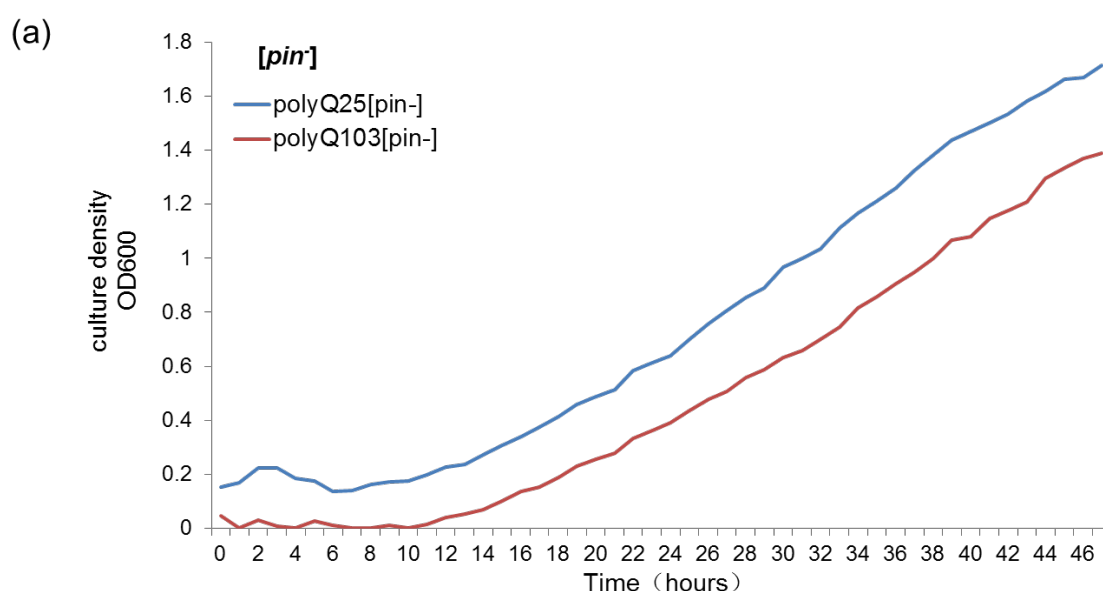


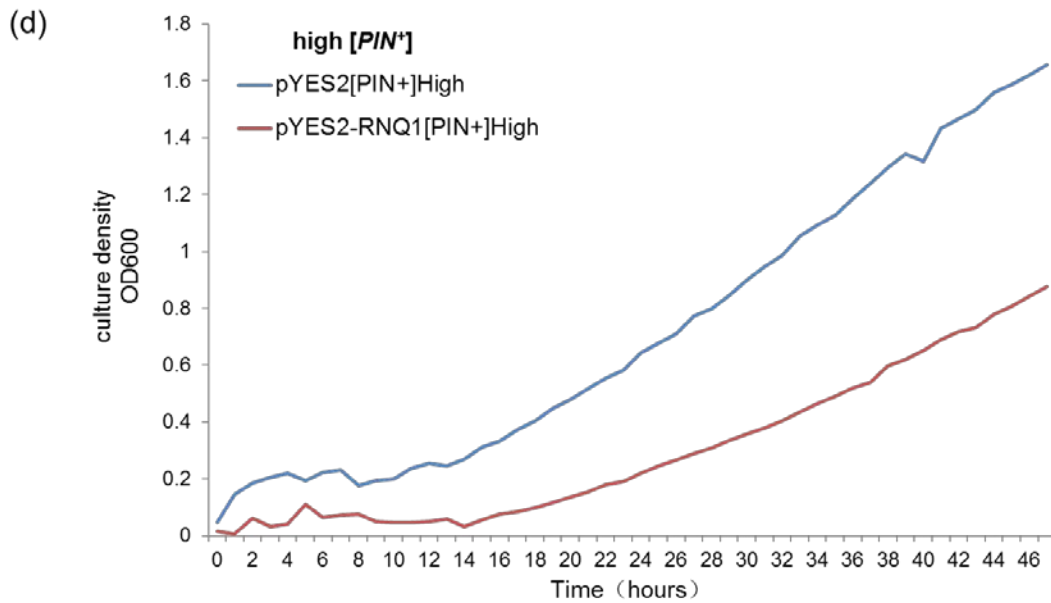
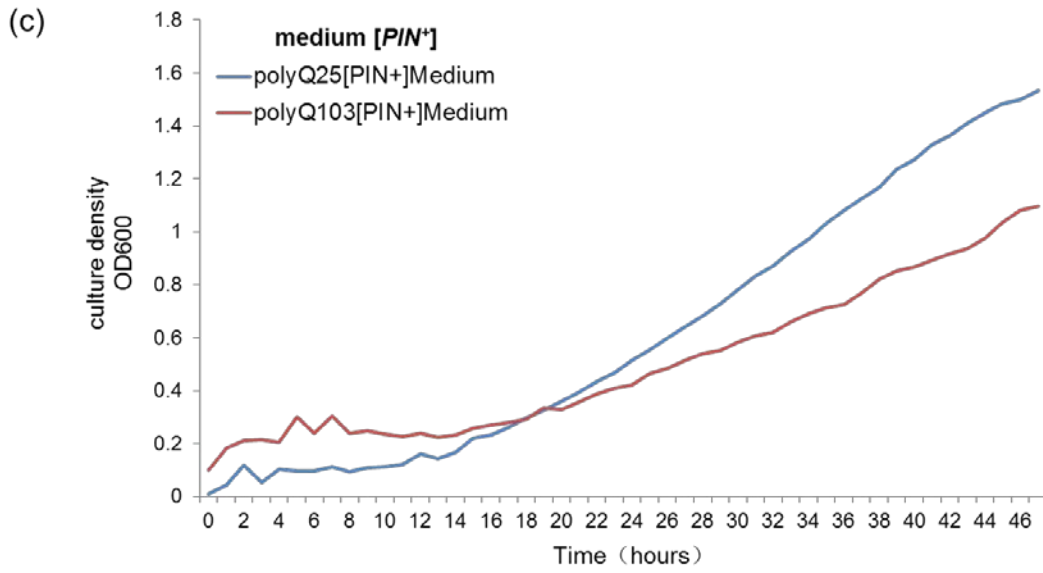
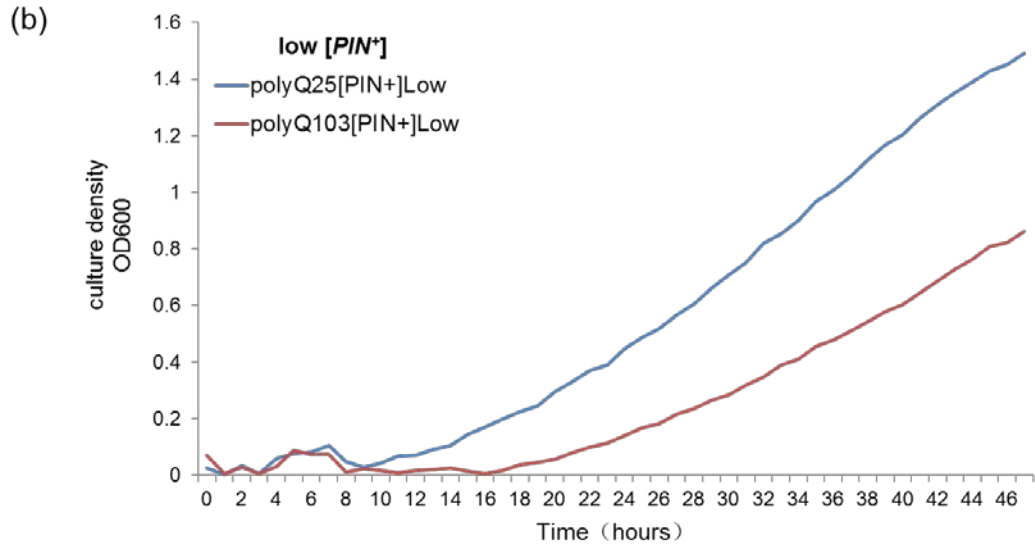
Figure 5.2 Overexpression of Q103 results in [*PIN*⁺]-dependent cytotoxicity in BY4741 cells. Q103 overexpression was not toxic in [*pin*] but toxic in [*PIN*⁺] strains. polyQ25 presents the pYES2 plasmid with Q25 insert (control) while polyQ103 presents the pYES2 vector with Q103 insert.

5.3 Overexpression of Q103 causes a growth defect in [*PIN*⁺] cells

In order to confirm the results obtained from toxicity assays, growth assays were performed to quantify the impact of overexpression of Q103 on the growth rate of both [*pin*⁻] and [*PIN*⁺] 74D-694 strains. Cells were grown under the same conditions as strains overexpressing the Rnq1 protein (See section 4.3). After washing off all the glucose-containing medium, cells were grown in the selective, inducing medium i.e. SD 2% galactose for 48 hours at 30°C. Readings of OD₆₀₀ were recorded every hour using a Fluostar Omega microplate reader. The results of growth analysis confirm that overexpression of Q103 does not cause a growth defect in [*pin*⁻] cells but confirms a growth defect in all four [*PIN*⁺] strains. Overexpression of Q25 did not lead to a growth defect in the [*PIN*⁺] strains or the [*pin*⁻] derivative (Figure 5.3). The doubling time of the four different [*PIN*⁺] strains overexpressing Q103 is much higher than the corresponding [*PIN*⁺] strains overexpressing Q25. The [*pin*⁻] derivative of 74D-694 overexpressing Q25 or Q103 showed similar doubling time (Table 5.1). The same finding was observed in strains overexpressing the Rnq1 protein (Section 4.3 Figure 4.4).



Chapter 5



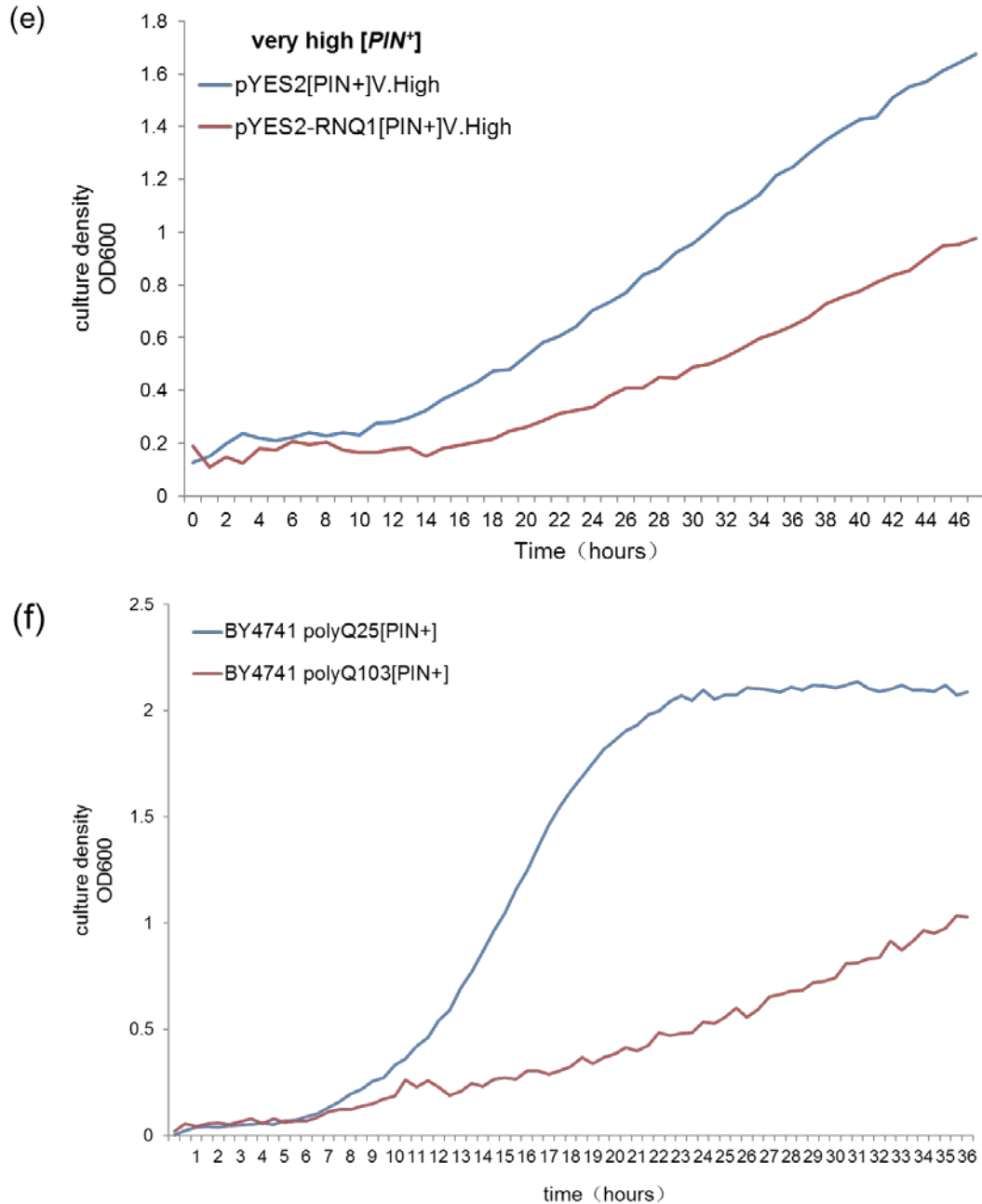


Figure 5.3 Q103 overexpression leads to growth defects in different $[PIN^+]$ variants of 74D-694 cells compared to a $[pin^-]$ derivative. Cell density was determined in the inducing medium i.e. SD 2% galactose-ura for 47 hours at 30°C. **(a)** Overexpression of Q103 did not cause a growth defect in $[pin^-]$ cells. **(b) (c) (d) (e)** Overexpression of Q103 resulted in growth defects in $[PIN^+]$ strains. **(f)** polyQ103 overexpression resulted in growth defects in the BY4741 $[PIN^+]$ strain. polyQ25 presents the pYES2 plasmid with Q25 insert (control) while polyQ103 presents the pYES2 vector with Q103 insert. Three biological replicates were performed for each strain and average is plotted in the above.

Table 5.1 Doubling time in exponential growth and cell density measured by the optical density of 600nm at the 36 hour time point for each strain of 74D-694 and BY4741

Strain	Plasmid	Doubling time (hour)	OD600 t = 47 hour
74D-694[<i>pin</i> ⁻]	pYES2-Q25	15.94	1.25
74D-694[<i>pin</i> ⁻]	pYES2-Q103	16.35	0.90
74D-694[<i>PIN</i> ⁺]low	pYES2-Q25	14.54	1.00
74D-694[<i>PIN</i> ⁺]low	pYES2-Q103	19.09	0.47
74D-694[<i>PIN</i> ⁺]medium	pYES2-Q25	16.14	1.08
74D-694[<i>PIN</i> ⁺]medium	pYES2-Q103	25.29	0.72
74D-694[<i>PIN</i> ⁺]high	pYES2-Q25	17.49	1.18
74D-694[<i>PIN</i> ⁺]high	pYES2-Q103	22.35	0.51
74D-694[<i>PIN</i> ⁺]v. high	pYES2-Q25	18.47	1.24
74D-694[<i>PIN</i> ⁺]v. high	pYES2-Q103	25.85	0.64
BY4741[<i>PIN</i> ⁺]	pYES2-Q25	4.13	2.08
BY4741[<i>PIN</i> ⁺]	pYES2-Q103	16.27	1.02

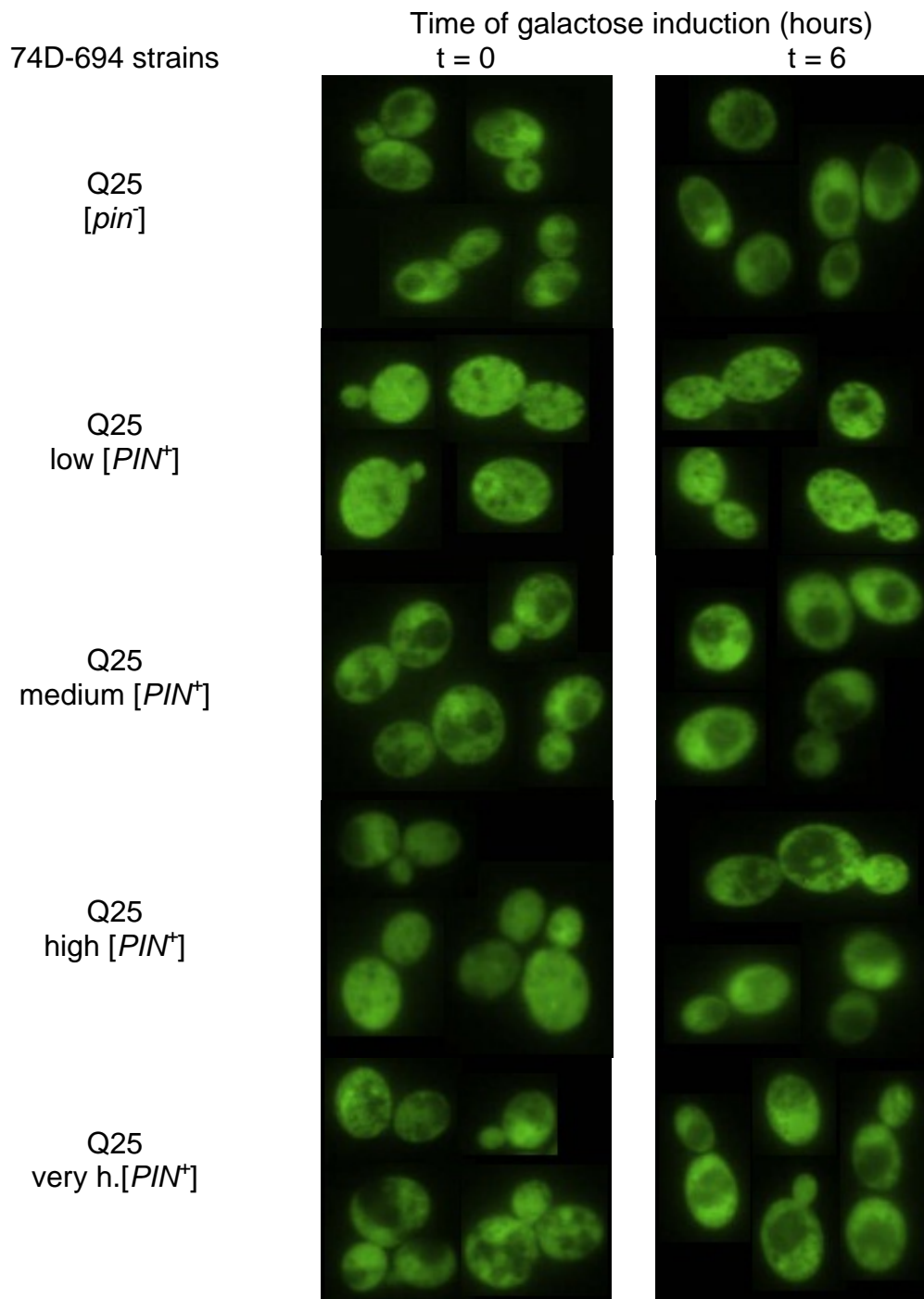
5.4 Q103-GFP forms fluorescent aggregates in [*PIN*⁺] cells

As Rnq1-GFP forms fluorescent aggregates in [*PIN*⁺] cells and it is known to modulate HTT aggregates, it was interesting to further investigate whether overexpression of Q103 is able to form fluorescent aggregates in different [*PIN*⁺] variants. Q25 and Q103 were fused in frame with a GFP tag at C-terminus while a FLAG tag was present at the N-terminus of each construct (Meriin *et al.*, 2002). The localization of Q25-GFP and Q103-GFP in 74D-694 [*pin*⁻] and [*PIN*⁺] cells was monitored by fluorescence microscopy (Figure 5.4).

In both [*pin*⁻] and [*PIN*⁺] cells, Q25-GFP showed diffuse fluorescence after 6 hours induction (t = 6) as expected. By contrast, in [*PIN*⁺] cells expressing Q103-GFP, the fusion protein was observed within fluorescent foci after 6 hours induction (t = 6). However, several small single or multiple fluorescent foci were observed before induction of galactose (t = 0). This may be caused by low levels of expression of Q103 in the repressing glucose medium since *GAL1* is a leaky promoter (G. L. Staniforth and M. F. Tuite personal communication).

Chapter 5

As discussed in Chapter 4, the fluorescence pattern of different $[PIN^+]$ variants are differed when Rnq1 was overexpressed i.e. the high $[PIN^+]$ variant showed multiple fluorescent foci while the low $[PIN^+]$, medium $[PIN^+]$ and very high $[PIN^+]$ variants formed single fluorescence aggregates. However, all four different $[PIN^+]$ variants formed multiple Q103-GFP foci in 80% of cells in Q103 strains.



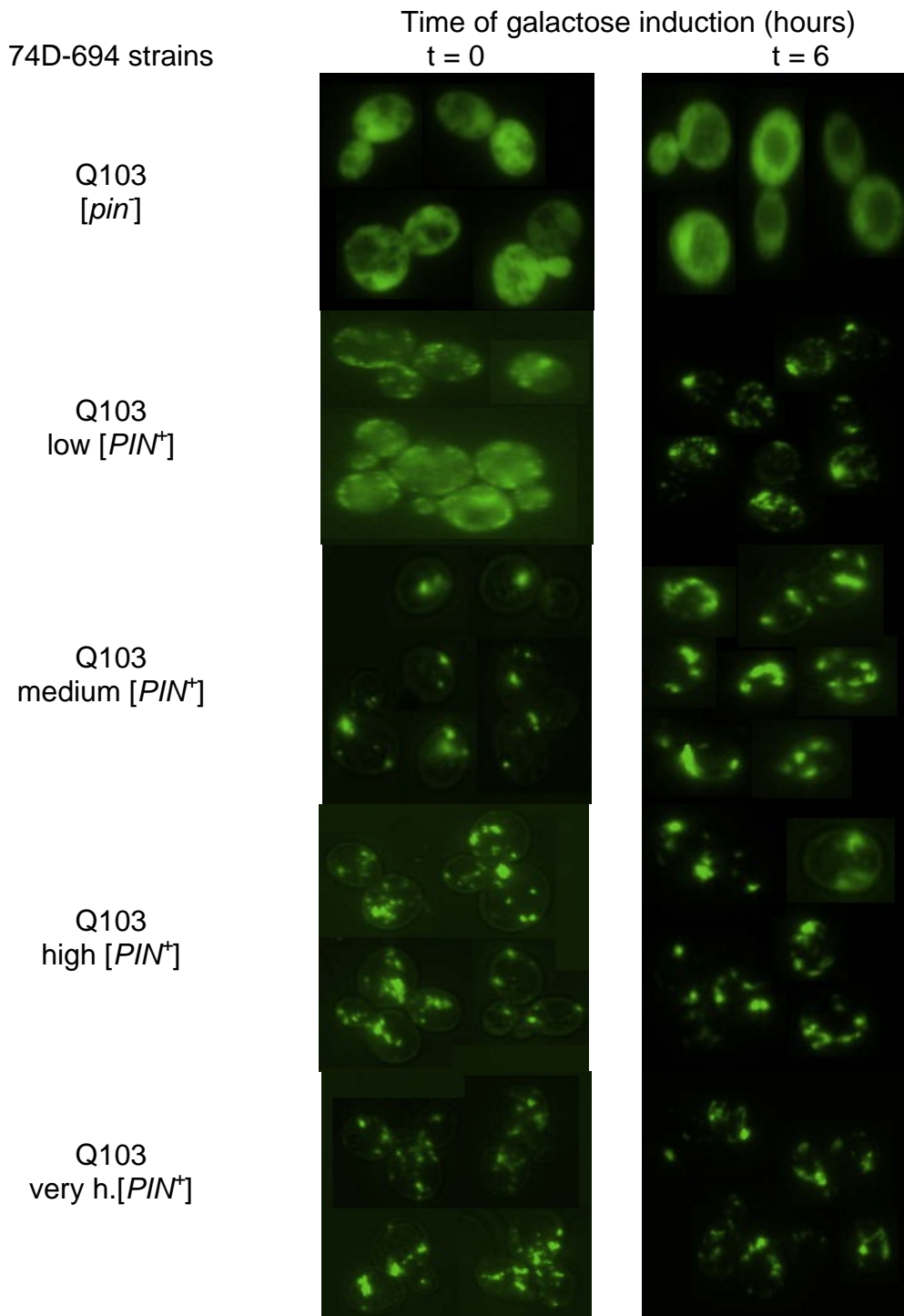


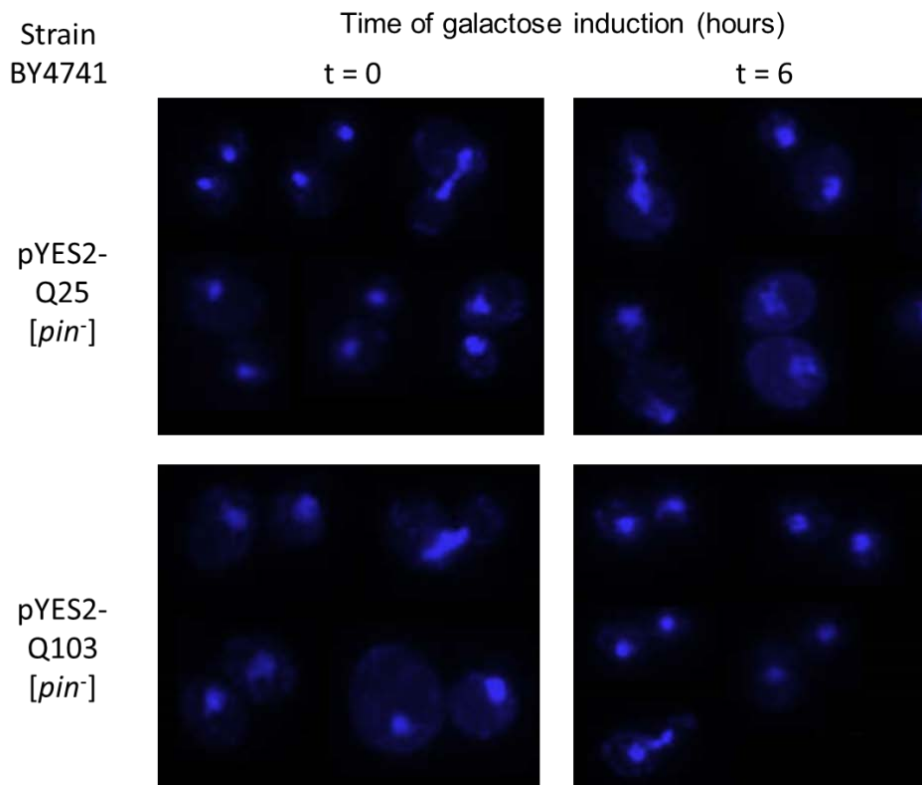
Figure 5.4 Fluorescence of the Q103-GFP fusion protein was observed in 74D-694-based [*pin*] and [*PIN*⁺] cells. A uniform fluorescence was observed in [*pin*] cells while [*PIN*⁺] cells with four different [*PIN*⁺] variants in the appearance of aggregates of the fusion protein after 6 hours induction. Cells were grown in the inducing medium i.e. SD 2% galactose-ura for at 30°C. Samples were collected at time point 0 and 6 and visualised by a green excitation filter on an Olympus 1X81 fluorescent microscope with Hamamatsu Photonics Orca AG cooled CCD camera. Images were captured analysed by Olympus Cell^R software.

Chapter 5

5.5 Overexpression of Q103 does not lead to a nuclear migration defect

As described in Chapter 4 (Section 4.5), Rnq1 overexpression causes a nuclear migration defect in $[PIN^+]$ cells of strain BY4741. Thus, whether overexpression of Q103 leads to a nuclear migration defect was observed in parallel by fluorescence microscope with 4',6-diamidino-2-phenylindole (DAPI) staining. Q25 and Q103 fused with a GFP tag at the C-terminus (Meriin *et al.*, 2002) were each transformed with $[pin^-]$ and $[PIN^+]$ cells of strain BY4741 and the $[pin^-]$ derivative and four different $[PIN^+]$ variants of 74D-694. The constructs were induced under the control of a *GAL1* promoter i.e. overexpression of Q103 was induced by galactose.

The fluorescence images showed that overexpression of Q103 does not have any impact on the localisation of nuclear DNA in either $[pin^-]$ or $[PIN^+]$ cells of strain BY4741 6 hours post induction by Q103 overexpression. As expected, the $[pin^-]$ or $[PIN^+]$ cells expressing Q25 (control) also do not exhibit any aberrant localisation of nuclear DNA (Figure 5.5). This suggested that Q103 overexpression does not cause a nuclear migration defect in BY4741 strains.



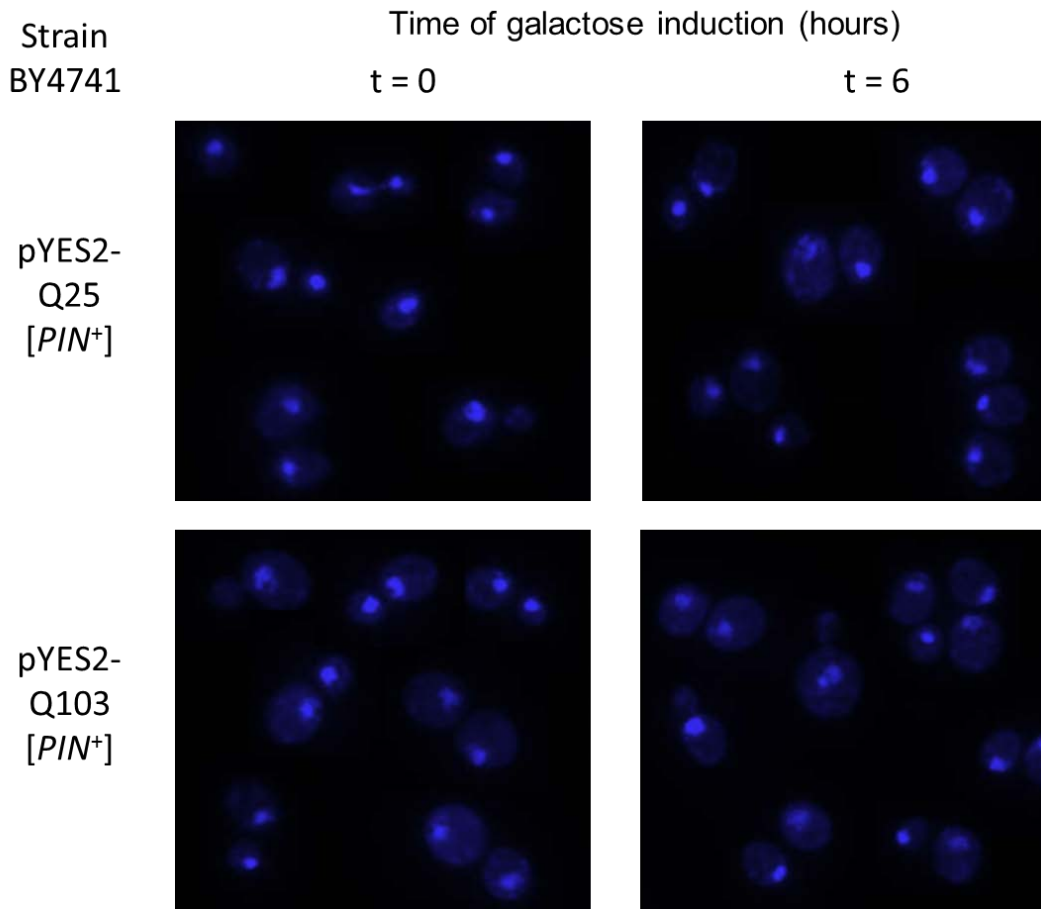
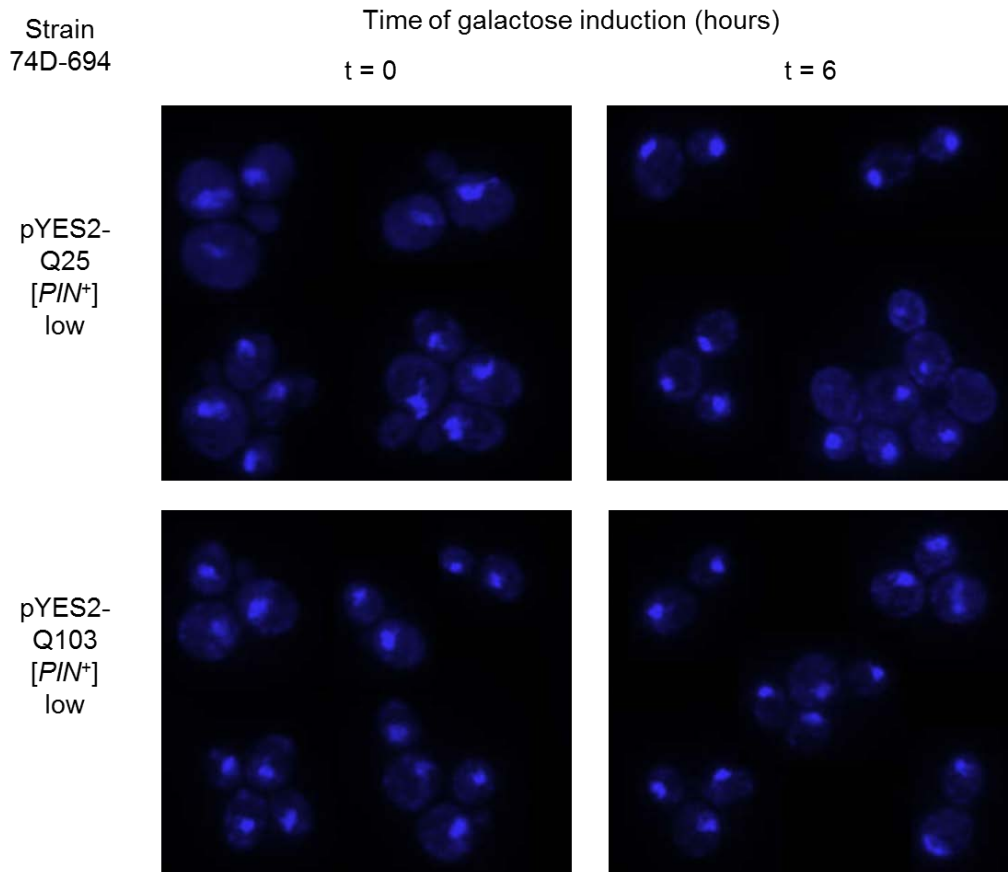
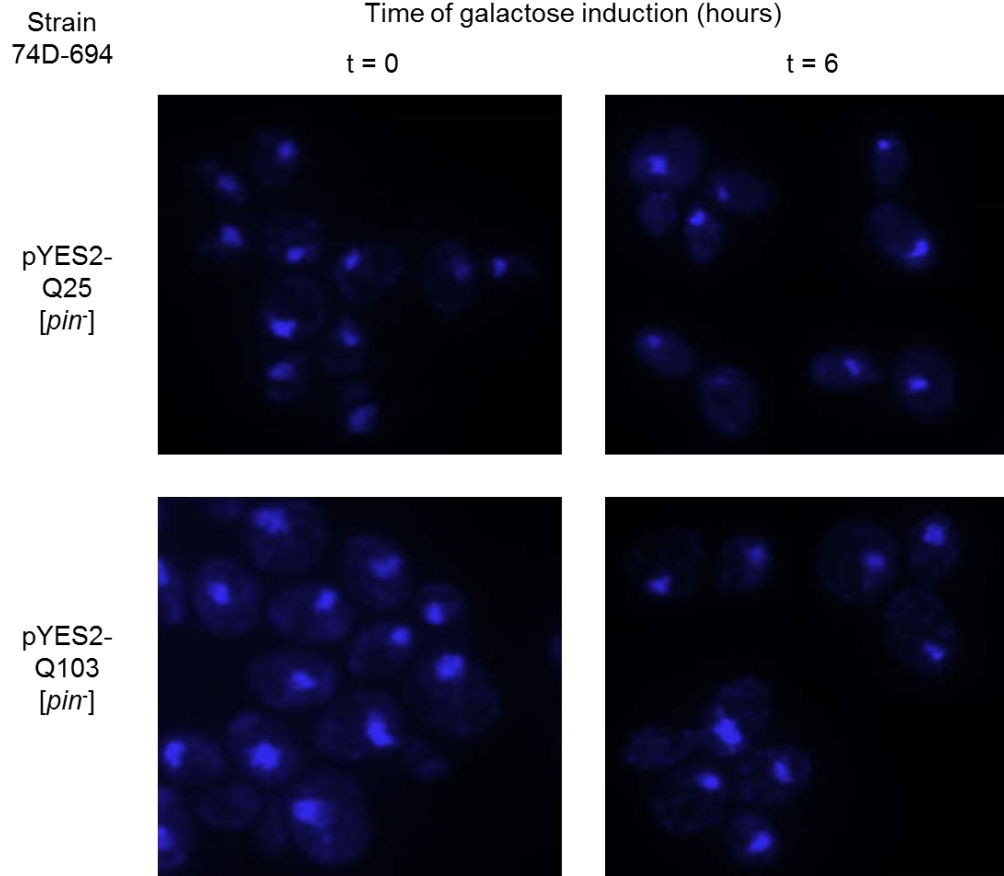
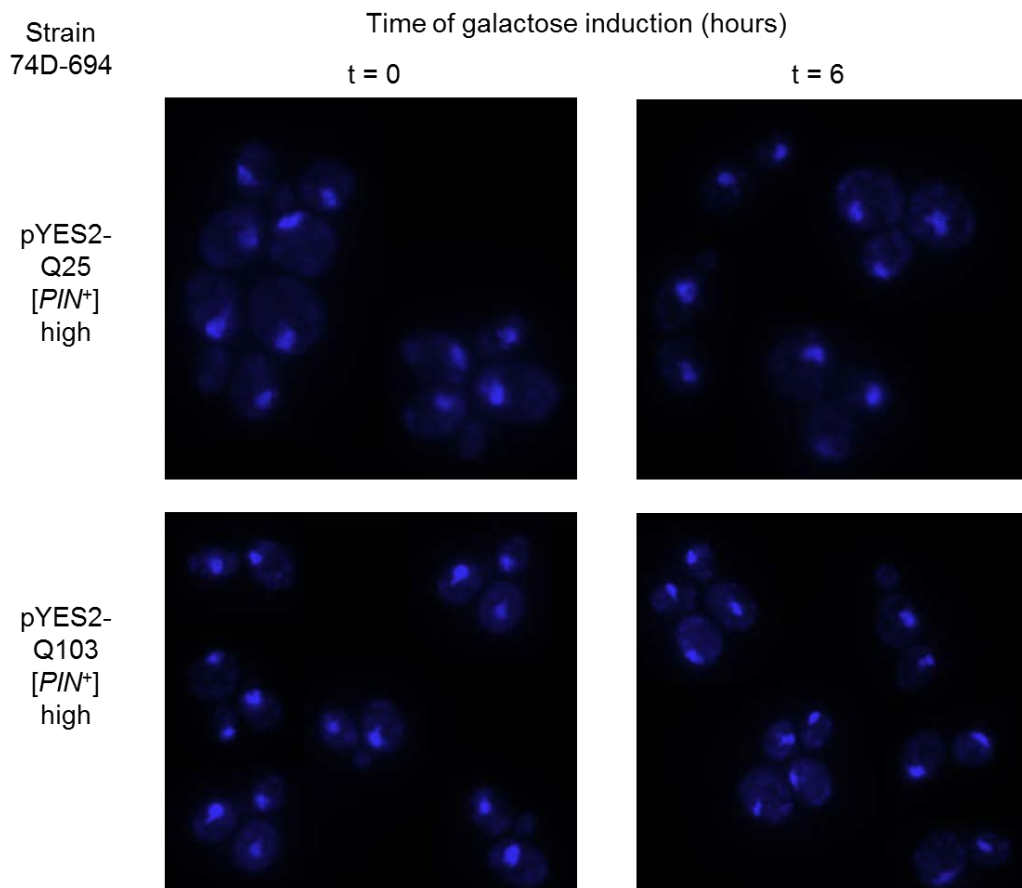
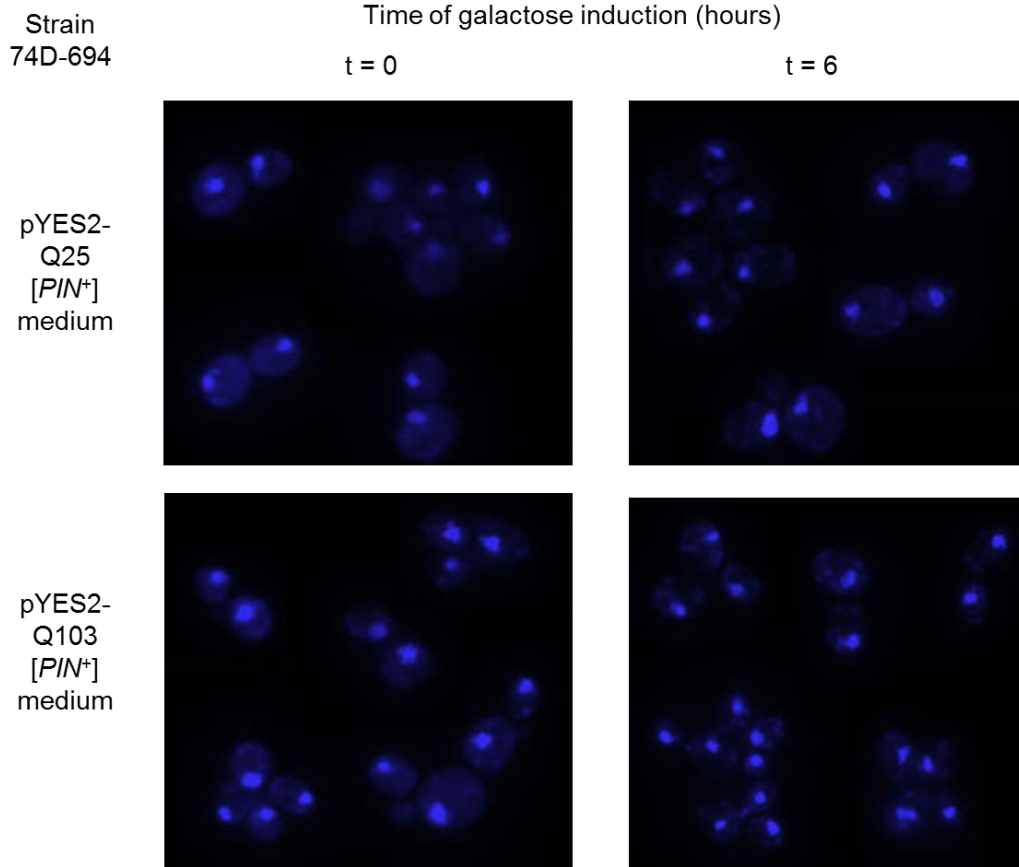


Figure 5.5 Overexpression of Q103 does not cause a nuclear migration defect in BY4741[PIN⁺] cells. Cells overexpressing Q103 showed normal localisation of nuclear DNA Rnq1 after 6 hours induction in both [*pin*⁻] and [*PIN*⁺] background. Cells were visualised by a blue excitation filter on an Olympus 1X81 fluorescent microscope with Hamamatsu Photonics Orca AG cooled CCD camera. Images were captured analysed by Olympus CellR software.

Chapter 5



Chapter 5



Chapter 5

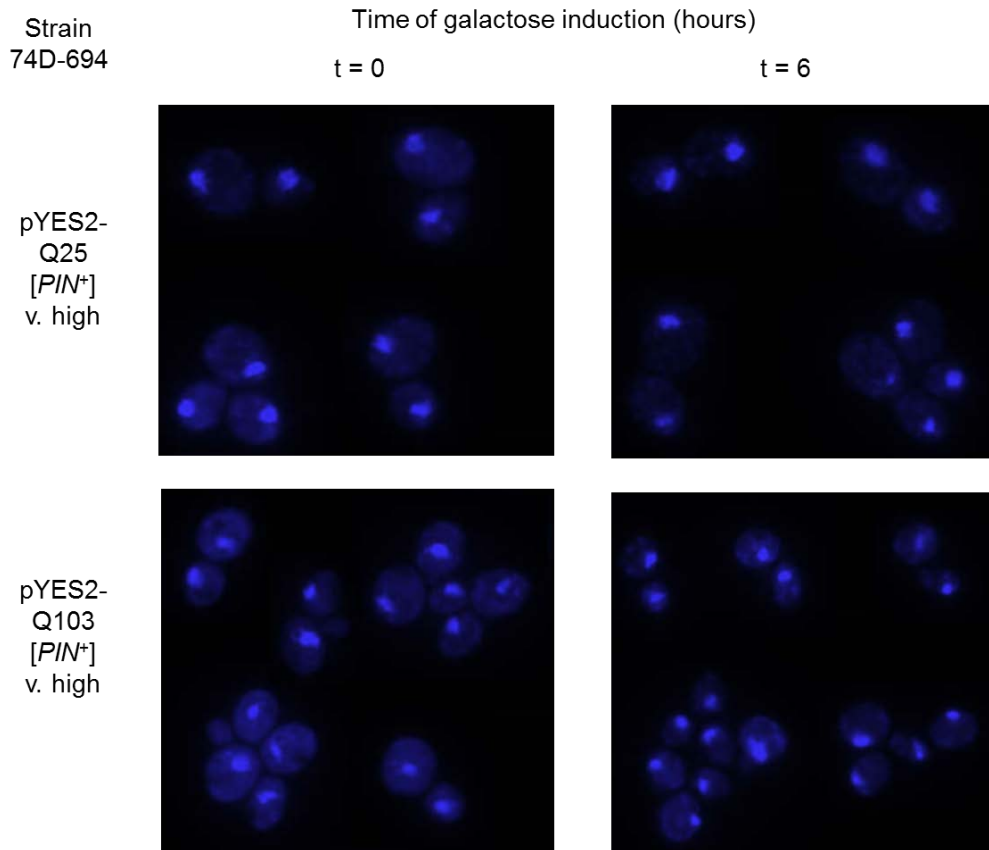


Figure 5.6 Overexpression of Q103 does not cause a nuclear migration defect in 74D-694-based [PIN⁺] cells. Q103 overexpression does not cause nuclear DNA localised to the bud-neck after 6 hours induction in all four [PIN⁺] variants. No nuclear migration defects were detected in strains expressing Q25 (control). Cells were visualised by a blue excitation filter on an Olympus 1X81 fluorescent microscope with Hamamatsu Photonics Orca AG cooled CCD camera. Images were captured analysed by Olympus CellR software.

Likewise, the same phenotype was observed in 74D-694 cells. The [pin⁻] derivative and four different [PIN⁺] variants showed similar localization of nuclear DNA before (t = 0) and after 6 hours induction (t = 6) by the overexpression of Q103. The nuclear DNA did not stack on the bud-neck of the cell. This observation indicated that Q103 overexpression does not lead to a nuclear migration defect in 74D-694 strains (Figure 5.6).

The nuclear migration defect was not observed in either BY4741 or 74D-694 [PIN⁺] strains when Q103 was overexpressed, but overexpression of Q103 is toxic in [PIN⁺] strains of both BY4741 and 74D-694. This finding would suggest that nuclear migration defect is not associated with Q103 mediated cytotoxicity.

Chapter 5

Table 5.3 Quantitative analysis of the nuclear migration defect mediated by overexpression of polyQ103 in different $[PIN^+]$ variants at the 0 and 6 hour time points for each strain of 74D-694 and BY4741

$[PIN^+]$ variant	No. cells analysed	No. cells with nuclear migration defect	No. cells without nuclear migration defect	No. cells with nuclear migration defect	No. cells without nuclear migration defect
		T=0	T=0	T=6	T=6
74D Q25- $[pin^-]$	100	0	100	1	99
74D Q25- $[PIN^+]$ LOW	100	1	99	2	98
74D Q25- $[PIN^+]$ MED	100	1	99	3	97
74D Q25- $[PIN^+]$ HIGH	100	1	99	3	97
74D Q25- $[PIN^+]$ VERY H.	100	3	97	2	98
74D Q25-RNQ1 $[pin^-]$	100	0	100	0	100
74D Q103- $[PIN^+]$ LOW	100	0	100	3	97
74D Q103- $[PIN^+]$ MED	100	0	100	1	99
74D Q103- $[PIN^+]$ HIGH	100	3	97	2	98
74D Q103- $[PIN^+]$ VERY H.	100	1	99	2	98
BY Q103- $[pin^-]$	100	3	97	2	98
BY Q103- $[PIN^+]$	100	1	99	5	95

5.6 Overexpression of Q103 does not lead to mitochondrial dysfunction in a $[PIN^+]$ background

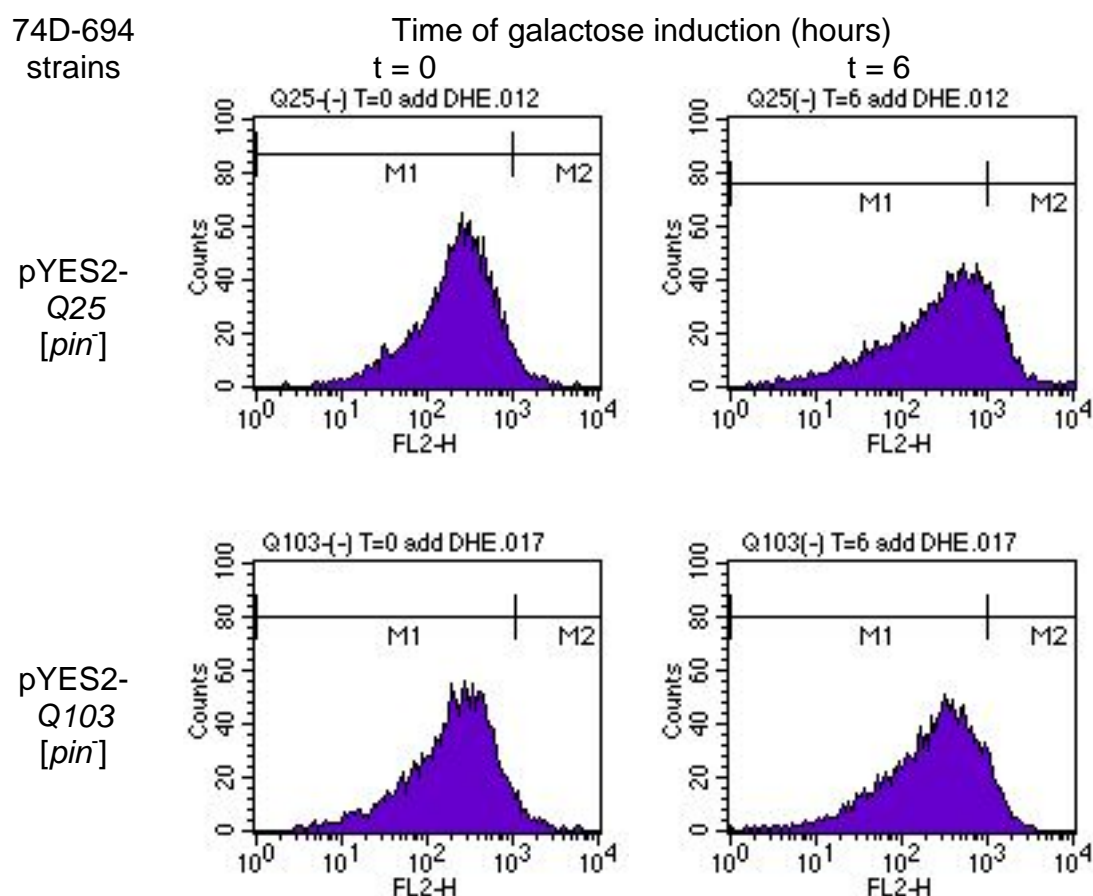
Previous studies revealed that overexpression of polyQ103 resulted in a deficiency in mitochondrial respiratory chain complex II and III that induced a significant increase in the production of reactive oxygen species (ROS) in cells overexpressing polyQ103 (Sloans *et al.*, 2006). It was interesting to further investigate whether polyQ103 overexpression leads to deficiency in mitochondria in different $[PIN^+]$ variants that may contribute to the polyQ103-mediated toxicity.

As described in Section 4.6, ROS assays (see Section 2.9.3) were performed on 74D-694-based $[pin^-]$ and the four $[PIN^+]$ variants before and after induction of overexpression of polyQ103. The reactive oxygen species (ROS) assay used to evaluate mitochondrial dysfunction has been designed to measure the

Chapter 5

level of superoxide in cells with ROS production being estimated by following the oxidation of dihydroethidium (DHE). The level of superoxide in each strain was detected and quantified using a BD FACSCalibur flow cytometer and the results were analysed using BD CellQuest Pro Software. These data (histograms) are shown in Figure 5.7.

In the 74D-694 strains overexpressing polyQ103, the level of superoxide was about 10 times higher after six hours induction than un-induced cells. However, in the control strain (pYES2-Q25), there was also a 6 to 12-fold increase of the superoxide levels in the induced cells overexpressing polyQ25 suggesting that polyQ103 overexpression does not cause a degree of mitochondrial dysfunction in the presence of $[PIN^+]$ (Figure 5.8). In addition, similar result was also found in the $[PIN^+]$ BY4741 strain (Figure 5.9). The opposite finding might be due to inadequate incubation time or effect of GFP tag on the polyQ25 and polyQ103 fragment in detection of ROS.



Chapter 5

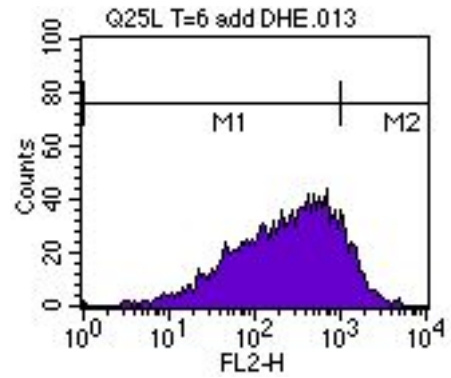
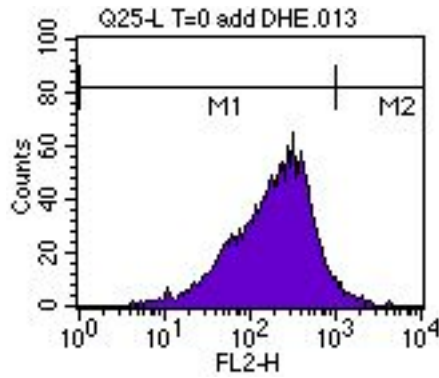
74D-694
strains

Time of galactose induction (hours)

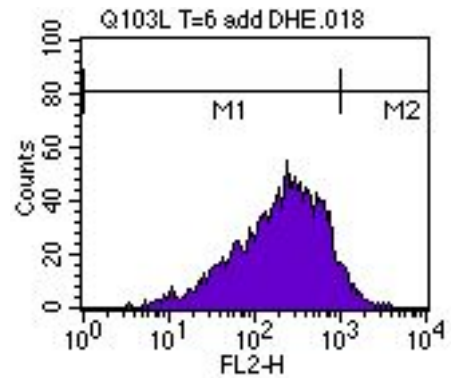
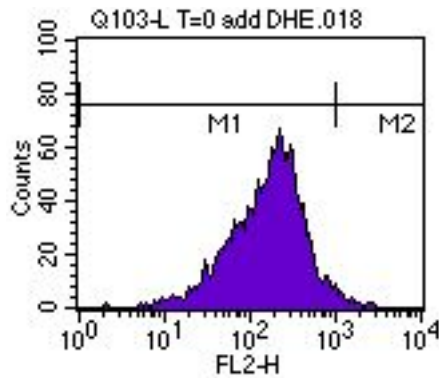
t = 0

t = 6

pYES2-
Q25
[PIN⁺]
low



pYES2-
Q103
[PIN⁺]
low



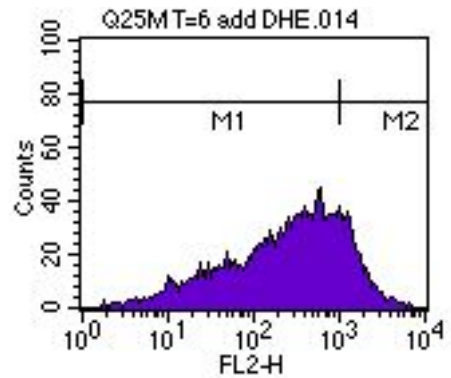
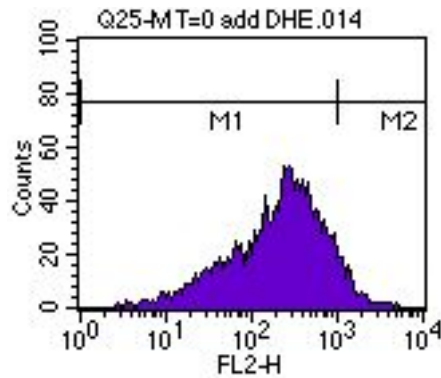
74D-694
strains

Time of galactose induction (hours)

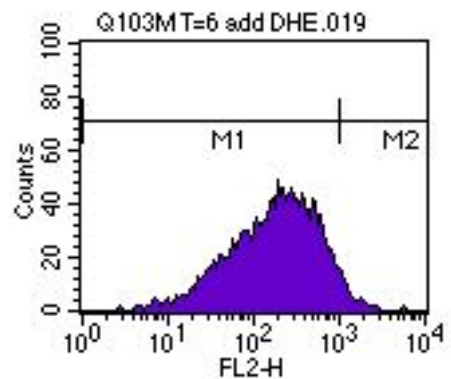
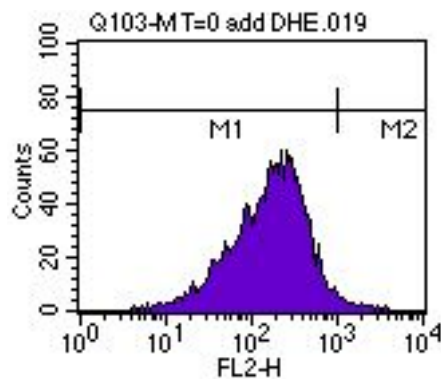
t = 0

t = 6

pYES2-
Q25
[PIN⁺]
medium



pYES2-
Q103
[PIN⁺]
medium



Chapter 5

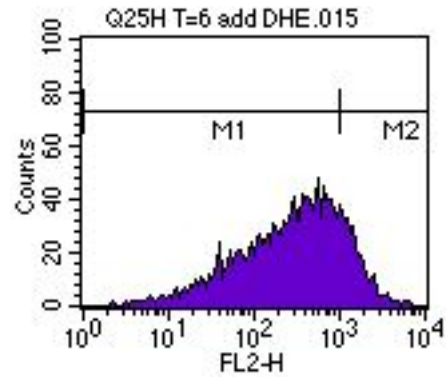
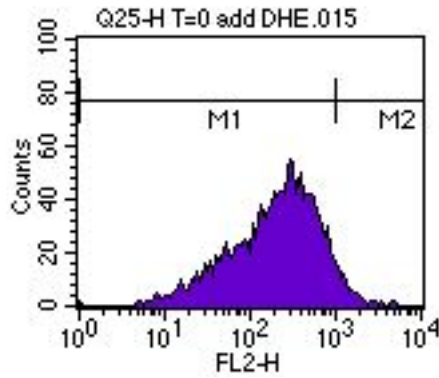
74D-694
strains

Time of galactose induction (hours)

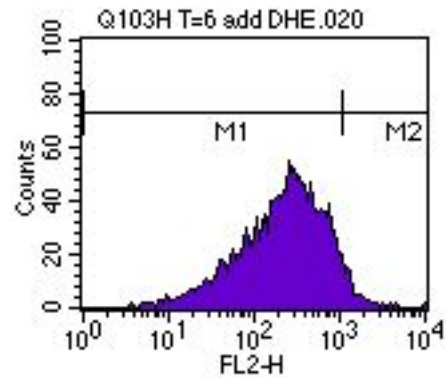
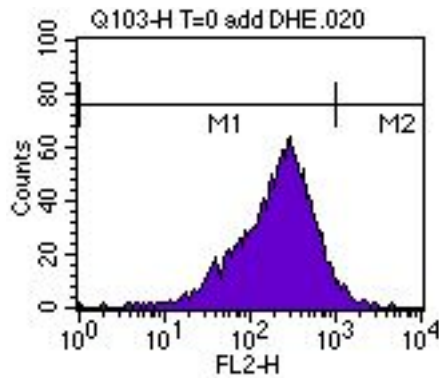
t = 0

t = 6

pYES2-
Q25
[PIN⁺]
high



pYES2-
Q103
[PIN⁺]
high



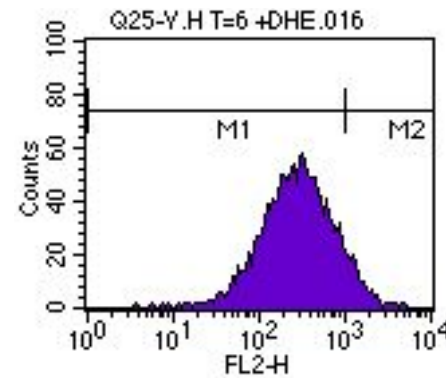
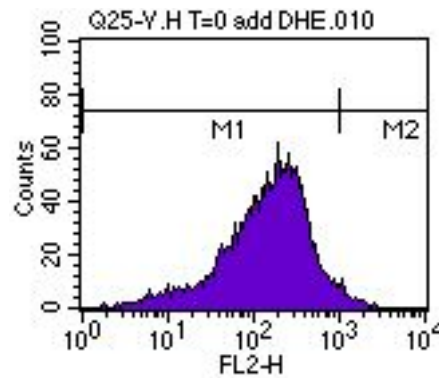
74D-694
strains

Time of galactose induction (hours)

t = 0

t = 6

pYES2-
Q25
[PIN⁺]
v. high



pYES2-
Q103
[PIN⁺]
v. high

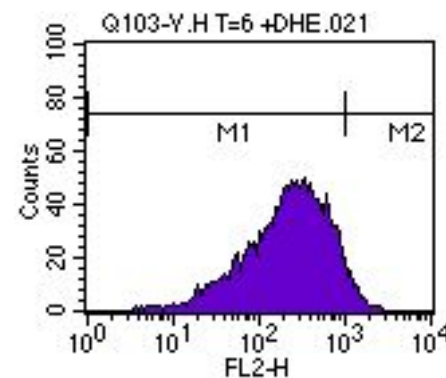
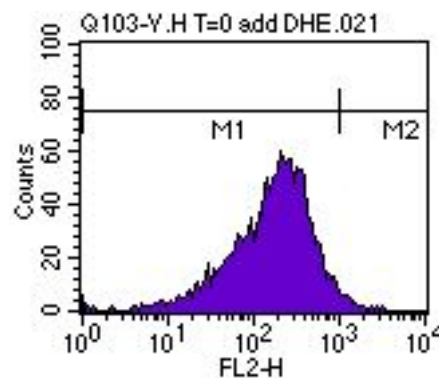


Figure 5.7 The level of superoxide generated by overexpression of polyQ103 as determined by flow cytometry. Marker (M1) represents the control peak which is used to establish the baseline fluorescence intensity. The peak shift to the right, which is the region labelled M2 indicates the amount of cells with mitochondrial defects.

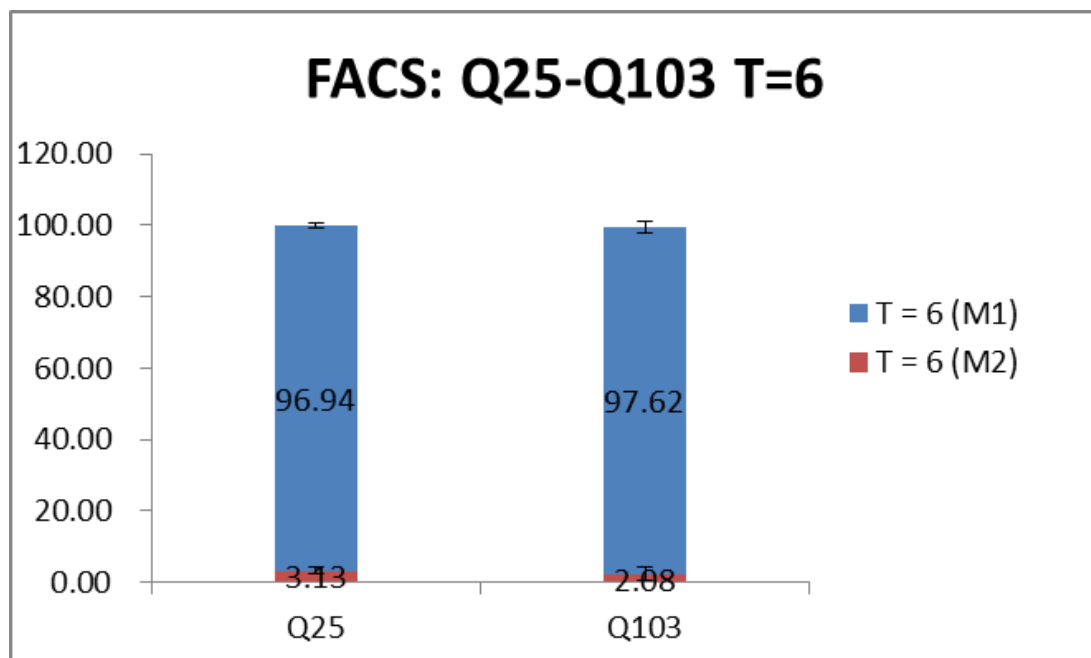
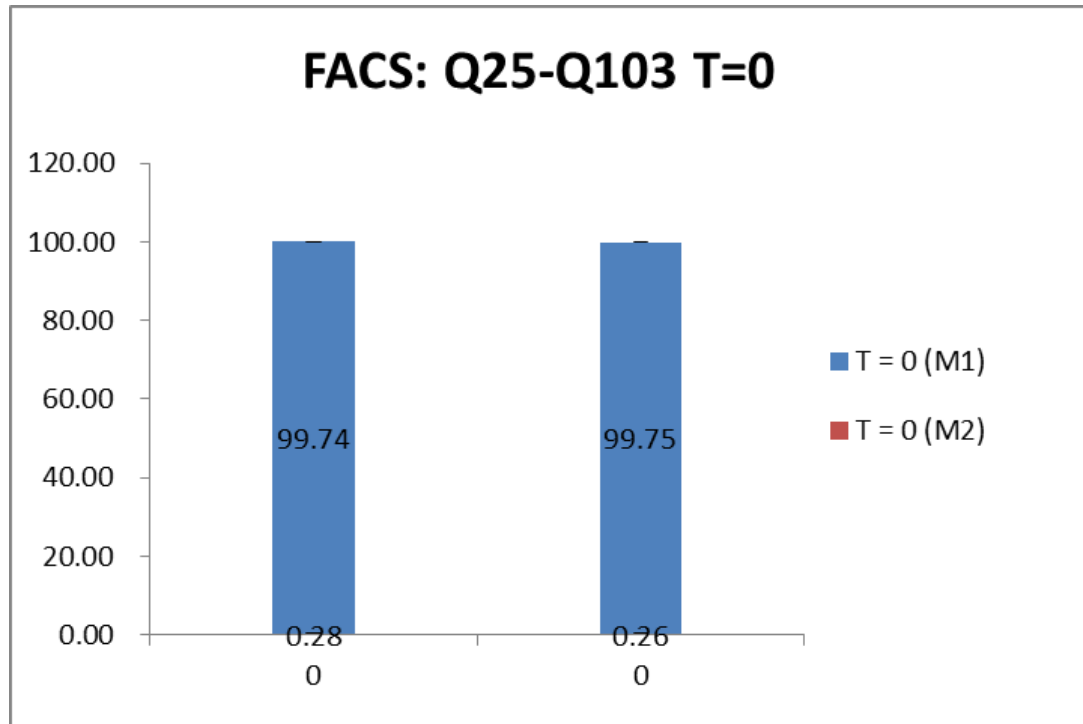
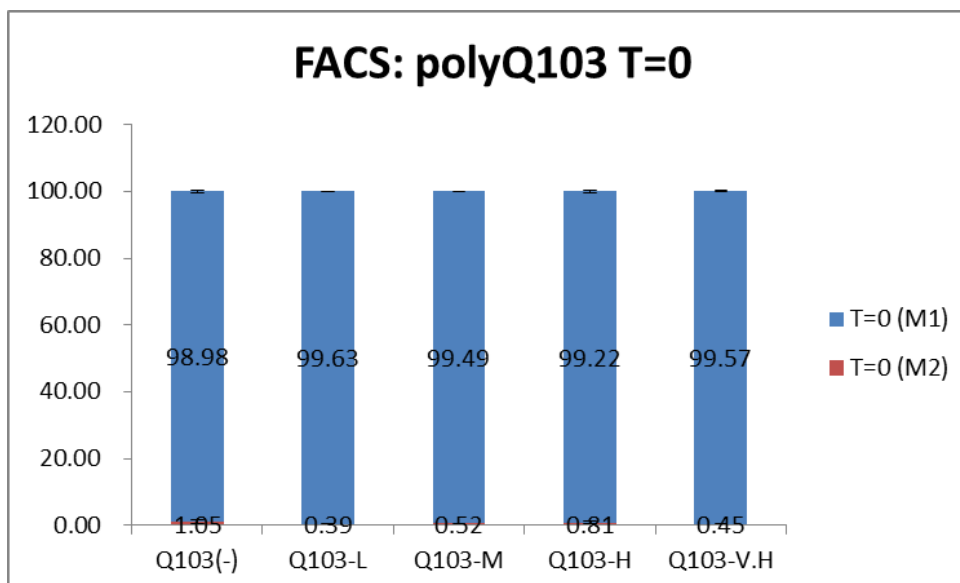
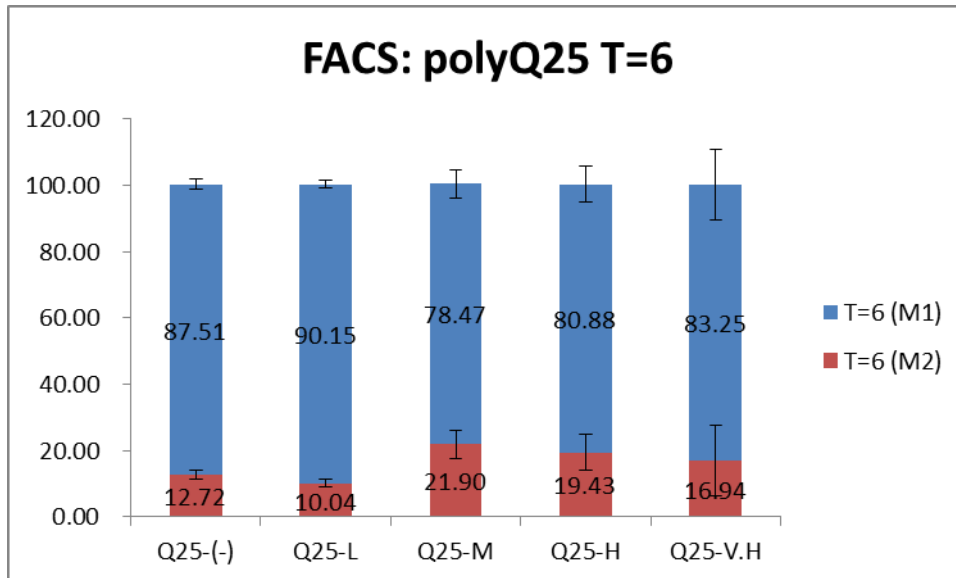
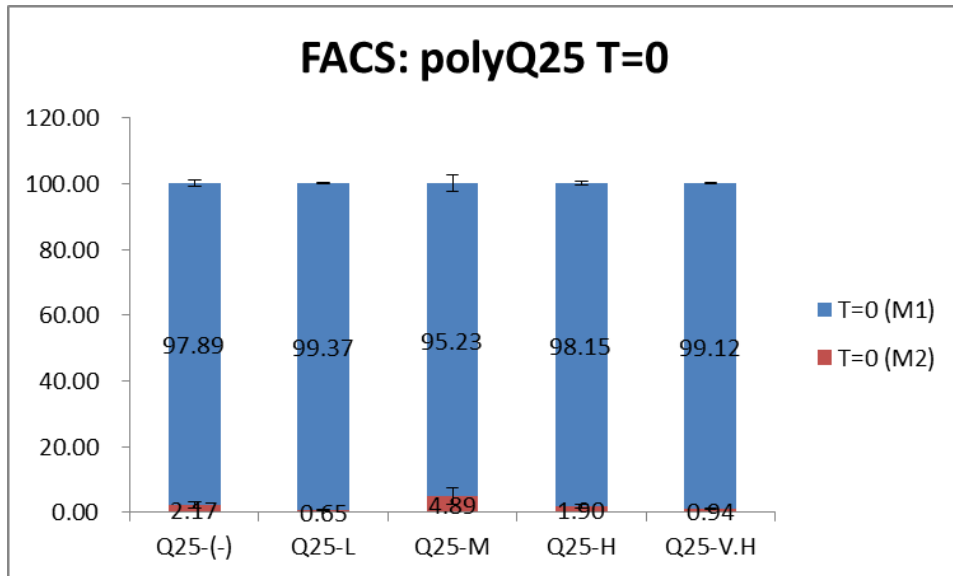


Figure 5.8 Quantitative analysis of ROS production of [*PIN⁺*] variant of BY4741 strains engineered to overexpress polyQ103. The red bars indicate the proportion of cells accumulating high levels of the fluorescence probe (DHE).



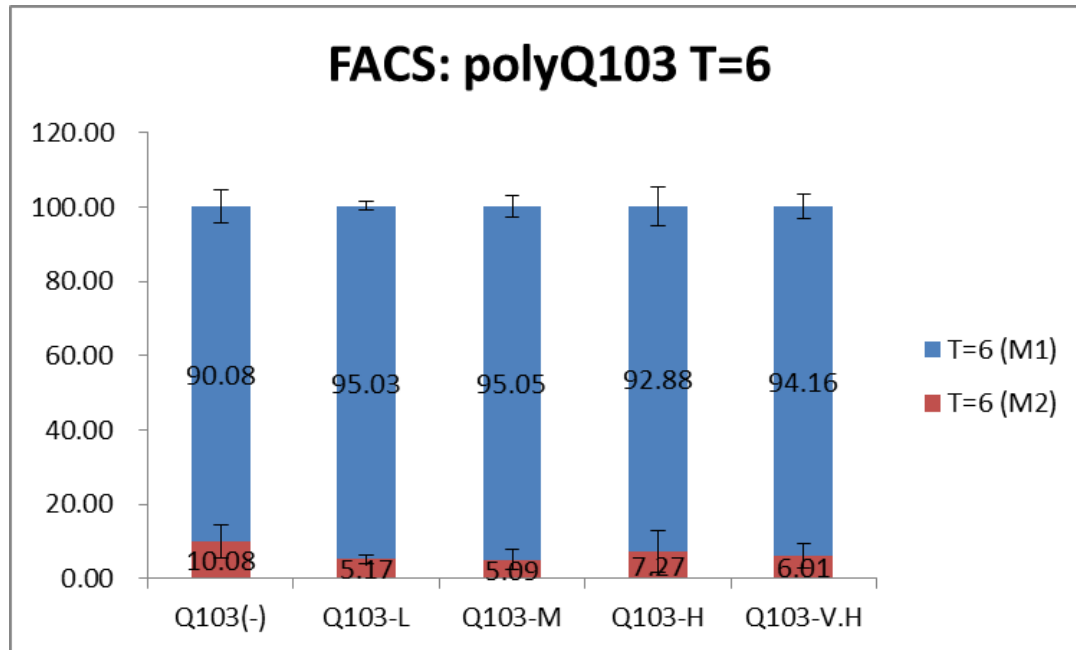


Figure 5.9 Quantitative analysis of ROS production in different $[PIN^+]$ variants of 74D-694 strains engineered to overexpress polyQ103. The red bars indicate the proportion of cells accumulating high levels of the fluorescence probe (DHE).

5.7 Discussion

A number of studies has revealed that defects in mitochondrial function play an essential role in the pathogenic mechanism of Huntington's disease (HD) as well as yeast models of HD. However, the results of the current study show that polyQ103 overexpression does not cause a degree of mitochondrial dysfunction in the presence of $[PIN^+]$. A possible reason for this conflicting result is that experiments were performed under inadequate conditions for this effect to take place.

Firstly, in experiments performed by Solans et al (2006) using yeast models, it was found that the level of ROS was significantly elevated in cells where polyQ103 was overexpressed. Cell respiration was attenuated after 4-6 hours of induction and decreased to 50% of the control after induction for 10 hours. This suggests that the defect in cell respiration may be caused by a change in mitochondrial respiration chain complex II and III (Solans et al., 2006).

Chapter 5

However, in the current study, cells were induced by galactose only for 6 hours thus more incubation time could have been required for the strain used.

Secondly, ROS assays were performed on both [*PIN*⁺] 74D-694 and BY4741 strains which were transformed with plasmid p6431 that had the GFP tag only. There was an 8-10 fold increase of the superoxide levels in both induced and un-induced cells (data not shown). This suggests that the GFP tag on the polyQ25 and polyQ103 fragment has a significant effect in detection of ROS.

Thirdly, it was also established that overexpression of polyQ103 has an impact on mitochondrial morphology and distribution. The polyQ103 aggregates may interact with proteins in the mitochondrial protein network leading to a progressive disruption of the actin cytoskeleton therefore causing an alteration of mitochondrial morphology (Ocampo et al., 2010). However, in this study, the ultrastructure of [*PIN*⁺] variants has not been examined to further evaluate whether polyQ103 overexpression can lead to defects in the mitochondria. In summary, whether overexpression of Q103 leads to mitochondrial dysfunction in a [*PIN*⁺] background cannot be concluded from this study.

Chapter 6

**The role of modifier genes in both Rnq1-
and polyQ- induced toxicity**

6.1 Introduction

Proteins perform their functions in a cell not only depending on their own intrinsic properties but also influenced by physical and/or functional interactions with other proteins. Such protein interactions result in a protein network in the cell that underlies distinct cellular mechanisms. Thus the toxicity induced by a certain protein might be due to interactions between this particular protein and other proteins. It is therefore important to identify genes whose products might enhance or reduce amyloid toxicity in yeast.

As described in Chapter 5, overexpression of polyQ expansion proteins derived from the Htt exon 1 fragment causes cytotoxicity in a [*PIN*⁺] dependent manner in the yeast Huntington's model (Meriin *et al.*, 2002). In 2009, a modulator of polyQ toxicity in *Drosophila*, the upf1 protein, was identified by a high-throughput RNAi screen (Doumanis, 2009). Moreover, preliminary data established by Gemma Staniforth in our laboratory showed that deletion of the *UPF1* gene suppressed both overexpression of Rnq1 and polyQ expansion protein mediated cytotoxicity (Staniforth., 2011). This finding made the upf1 protein a potential candidate to further investigate the mechanism of Rnq1- and polyQ- induced toxicity and the role of other cellular factors.

In *S. cerevisiae*, three proteins namely Upf1, Upf2 and Upf3 (Leeds *et al.*, 1991; Cui *et al.*, 1995; He and Jacobson, 1995) are key components of the nonsense-mediated mRNA decay (NMD) pathway which recognizes and destroys aberrant mRNAs containing premature termination codons (PTCs). The three conserved Upf proteins function as the Upf1–Upf2–Upf3 surveillance complex that is associated with nonsense codon recognition on the ribosome, the mRNA decapping complex and the release factors eRF1 and eRF3 (Swisher and Parker., 2011). Recent studies have revealed that deletion of the *UPF1* or *UPF2* genes results in increased viability of cells containing mutant termination factors as deletion of either *UPF1* or *UPF2* genes increase the viability of Sup45 mutants (Zhuravleva and Gryzina, 2012).

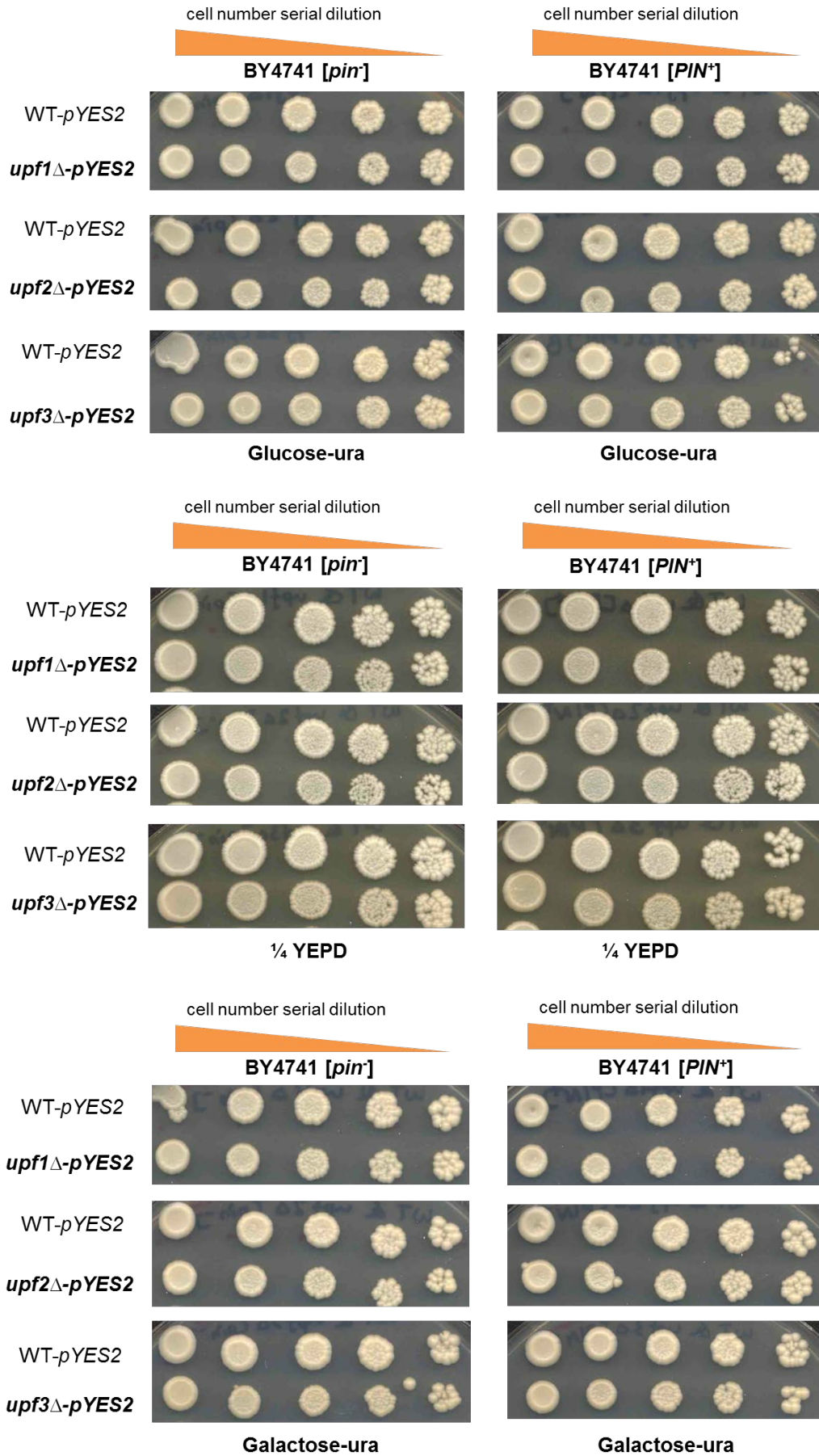
In the Upf complex, the Upf1 protein acts as the essential regulator of NMD while Upf2 works as a scaffolding protein that connects Upf1 and Upf3 (Chamieh *et al.*, 2008). Thus it was interesting to investigate whether the whole Upf complex or the single Upf protein may regulate amyloid toxicity in yeast. In this chapter, a series of cell-based assays coupled with fluorescence microscopy were used to explore the role of the Upf1/2/3 proteins in Rnq1- and polyQ-mediated toxicity.

6.2 Rnq1 and polyQ overexpression-mediated cytotoxicity is suppressed in *upf1* Δ and *upf2* Δ [*PIN*⁺] strains but not in *upf3* Δ [*PIN*⁺] strain

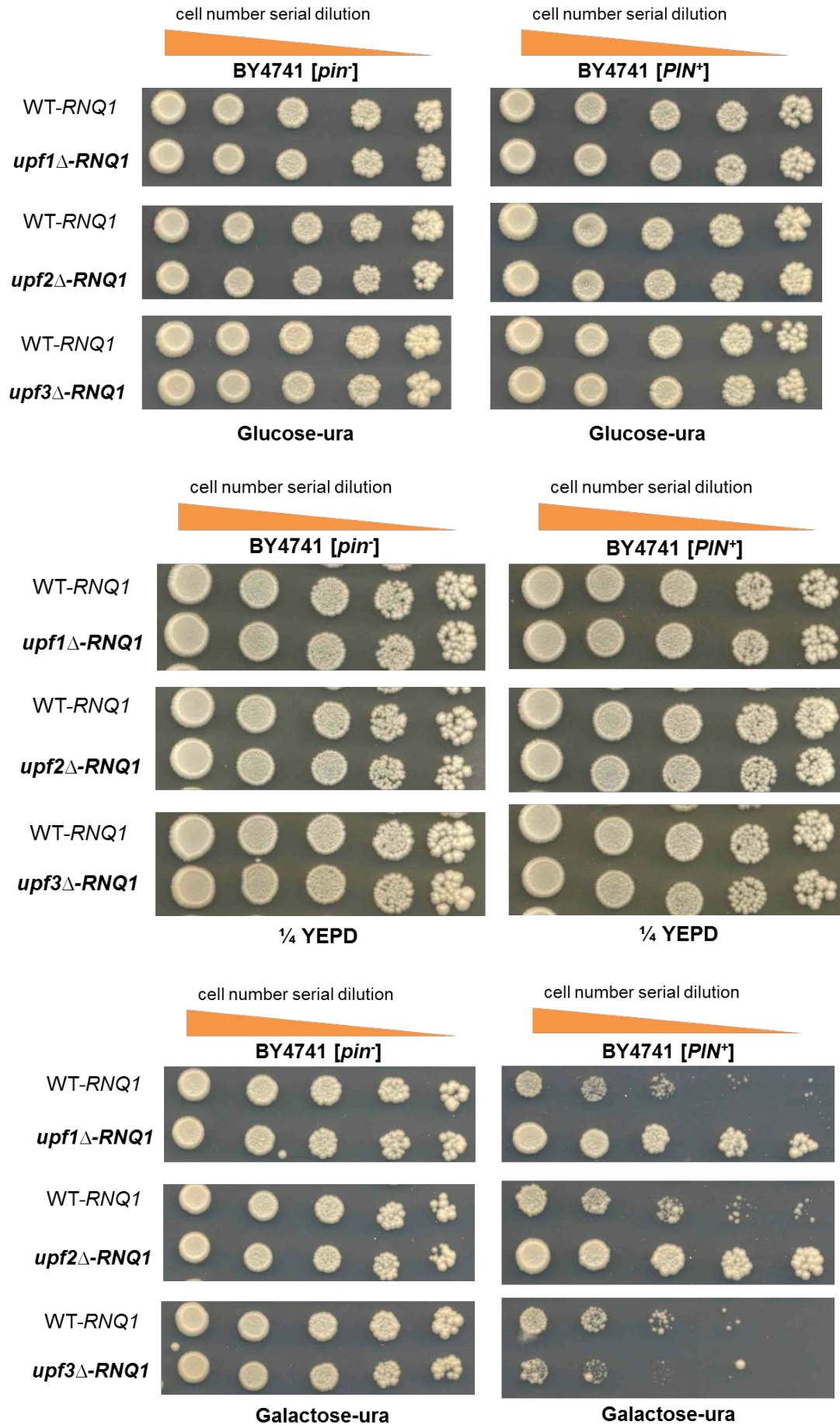
Since the Upf1/2/3 proteins play a very important role in the NMD pathway as a complex (Leeds *et al.*, 1991; Cui *et al.*, 1995; He and Jacobson, 1995) and deletion of the *UPF1* gene suppresses the overexpression of Rnq1- and polyQ-mediated cytotoxicity (Staniforth., 2011), it was interesting to further investigate whether deletion of *UPF2* or *UPF3* can also suppress the Rnq1- and polyQ-induced toxicity.

To test this, [*pin*⁻] and [*PIN*⁺] derivatives of *upf1* Δ or *upf2* Δ or *upf3* Δ deletions in the strain BY4741 were each transformed with either the pYES2 (control) or the pYES2-*RNQ1* plasmids. Toxicity assays (Section 4.1) were then conducted with these deletion strains (Figure 6.1). Similarly, pYES2-Q25 (control) or pYES2-Q103 plasmids were each transformed into these *upf* Δ deletion strains of BY4741 in order to establish if suppression of Rnq1 toxicity by the respective *upf* Δ deletions was specific to the Rnq1 protein or also affected polyglutamine-mediated toxicity (Figure 6.2).

Chapter 6



Chapter 6

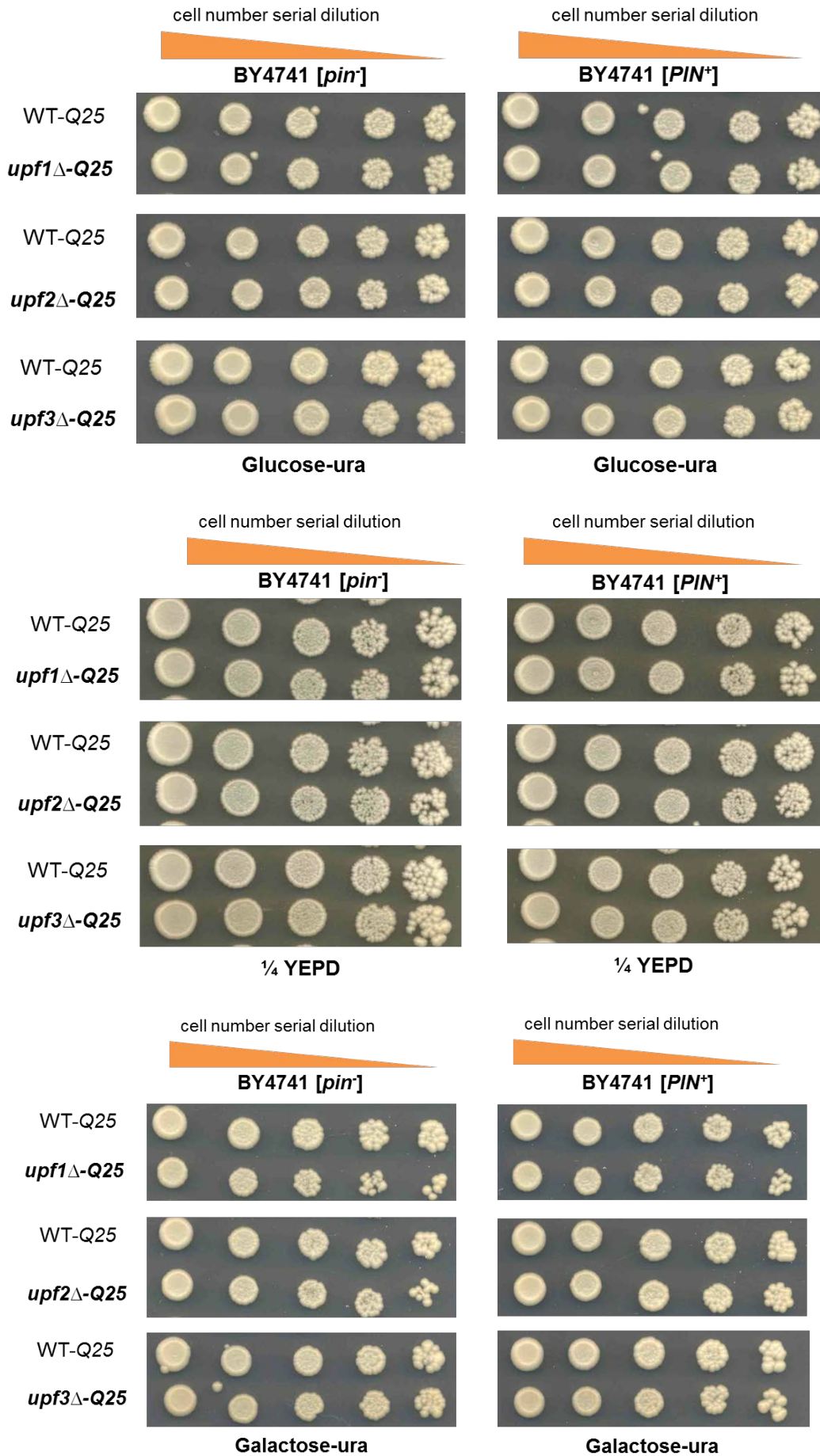


Chapter 6

Figure 6.1 Overexpression of Rnq1-induced toxicity is suppressed in *upf1* Δ and *upf2* Δ strains in a [*PIN*⁺] background. WT is the wild type *UPF*⁺ BY4741 strain. pYES2 is the control plasmid while *RNQ1* is the pYES2 vector with *RNQ1* insert. Rnq1 toxicity was examined on galactose plates since a galactose-inducible promoter *GAL1* was used to overexpress the Rnq1 protein. ¼ YEPD and glucose plates served as controls for any growth defects. Rnq1 toxicity was tested in three deletion strains *upf1* Δ , *upf2* Δ and *upf3* Δ , compared to the wild type *UPF*⁺ BY4741 strains. Three biological replicates were performed for each strain and one representative is shown for each.

Both Rnq1 and polyQ overexpression were found not to be toxic in three deletion strains i.e. *upf1* Δ and *upf2* Δ and *upf3* Δ in a [*pin*] background as is also seen in the *UPF*⁺ [*pin*] control. However, overexpression of Rnq1 and polyQ103 was toxic in wild type *UPF*⁺ and the *upf3* Δ strain in a [*PIN*⁺] dependent manner. Interestingly, both Rnq1 and polyQ103 mediated cytotoxicity is slightly enhanced in the *upf3* Δ strain in a [*PIN*⁺] background. This might be due to the function of Upf3 is distinct and different from Upf1 and Upf2 as Upf3 has been recently identified a novel component in the degradation of mRNA in the nucleus (DNR) (Das et al., 2014). Importantly, Rnq1- and polyQ-mediated cytotoxicity was suppressed in the *upf1* Δ and *upf2* Δ strains in a [*PIN*⁺] background (Figure 6.1/6.2). These findings suggest that the suppression of Rnq1 and polyQ toxicity is not due to the function of the UPF complex *per se* because the Upf3 protein is involved in the core machinery of NMD yet deletion of *UPF3* gene did not suppress the overexpression of Rnq1- and polyQ-mediated toxicity. So this suggests that the NMD pathway does not directly contribute to Rnq1- and polyQ-induced toxicity.

Chapter 6



Chapter 6

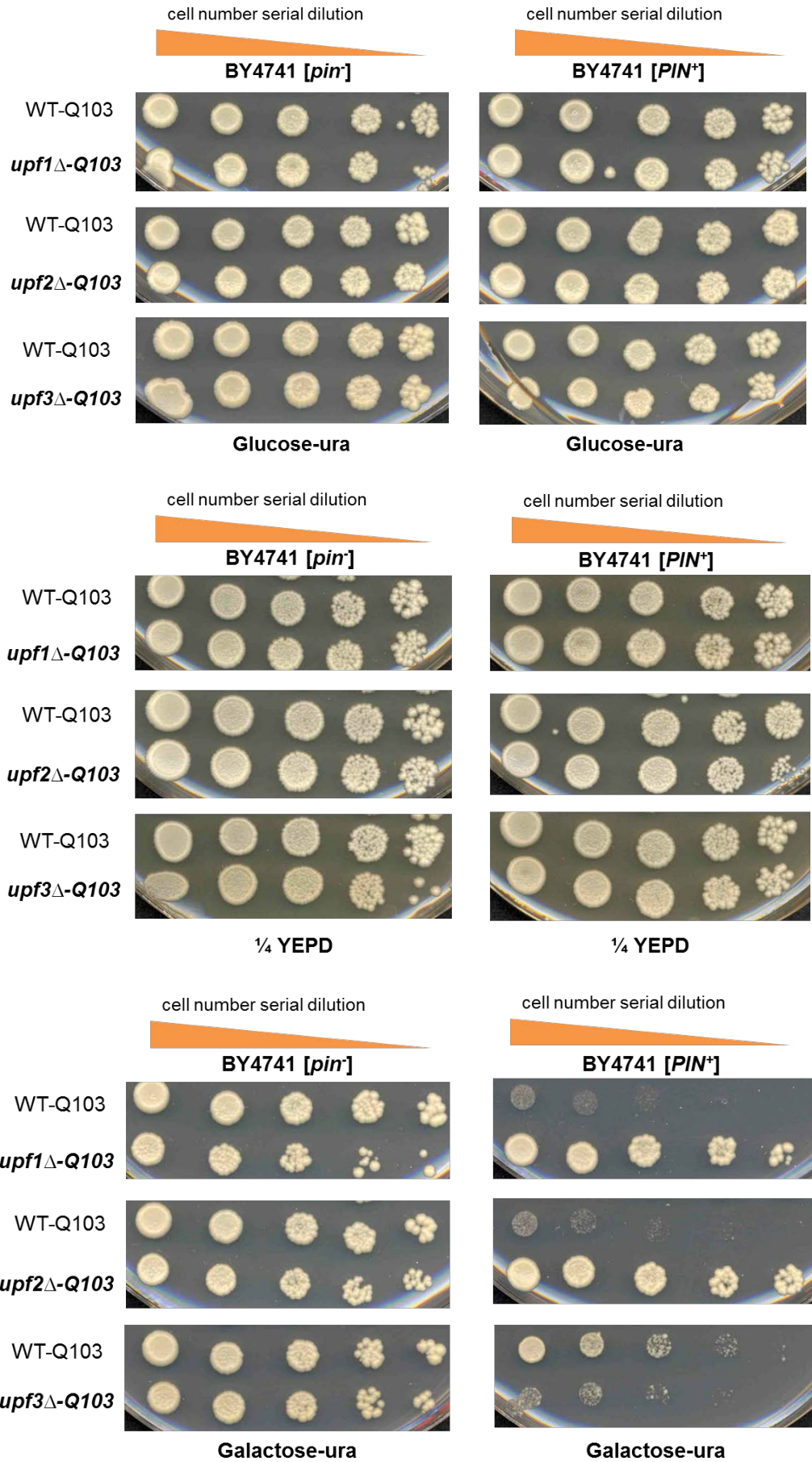


Figure 6.2 PolyQ103-induced toxicity is also suppressed in *upf1* Δ and *upf2* Δ strains in a [*PIN*⁺] background. WT is the wild type *UPF*⁺ BY4741 strain. Q25 is the pYES2 based plasmid with a Q25 insert (control) while Q103 is the pYES2 based vector with a Q103 insert. Polyglutamine toxicity was examined on galactose plates since a galactose-inducible promoter *GAL1* was used to overexpress the polyglutamine protein. ¼ YEPD and glucose plates served as controls for any growth defects. PolyQ toxicity was tested in three deletion strains *upf1* Δ , *upf2* Δ and *upf3* Δ , compared to the wild type *UPF*⁺ BY4741 strains. Three biological replicates were performed for each strain and one representative is shown for each.

6.3 [*PIN*⁺]-dependent growth defect caused by Rnq1 and polyQ103 overexpression is suppressed in *upf1* Δ and *upf2* Δ strains but not in *upf3* Δ strain

In order to further examine the cellular phenotype associated with overexpression of Rnq1 and polyQ, growth analysis was repeated in the *upf1/2/3* Δ deletion [*PIN*⁺] strains of BY4741 to quantify the impact of Rnq1 and polyQ overexpression on the growth rate over a 36 hour period. As described in Chapter 4 (Section 4.3), cells were switched to galactose-containing medium after washing off the remaining glucose-containing medium and then grown for 36 hours at 30°C. Readings of culture density (OD₆₀₀) were recorded every hour using a Fluostar Omega microplate reader (Figure 6.3).

The results obtained showed that overexpression of Rnq1 caused the expected growth defect in the wild type *UPF*⁺ BY4741 and also in the *upf3* Δ strain in a [*PIN*⁺] background. This was not found with the *upf1* Δ and *upf2* Δ strains. In the *upf1* Δ and *upf2* Δ [*PIN*⁺] strains overexpressing Rnq1, the doubling time was about 4 hours compared to 20 hours in BY4741 wild type *UPF*⁺ strain and 27 hours in the *upf3* Δ strain (Table 6.1). The shorter doubling time confirmed that Rnq1 overexpression was less toxic in the *upf1* Δ and *upf2* Δ [*PIN*⁺] strains. By contrast, there was no growth defect observed in BY4741 wild type *UPF*⁺ and all three *upf* deletion strains when the pYES2 plasmid backbone was expressed (Figure 6.3). The doubling time of the corresponding control strain was similar (Table 6.1). These results confirmed that Rnq1 toxicity is suppressed in *upf1* Δ and *upf2* Δ strains in a [*PIN*⁺] dependent manner.

Chapter 6

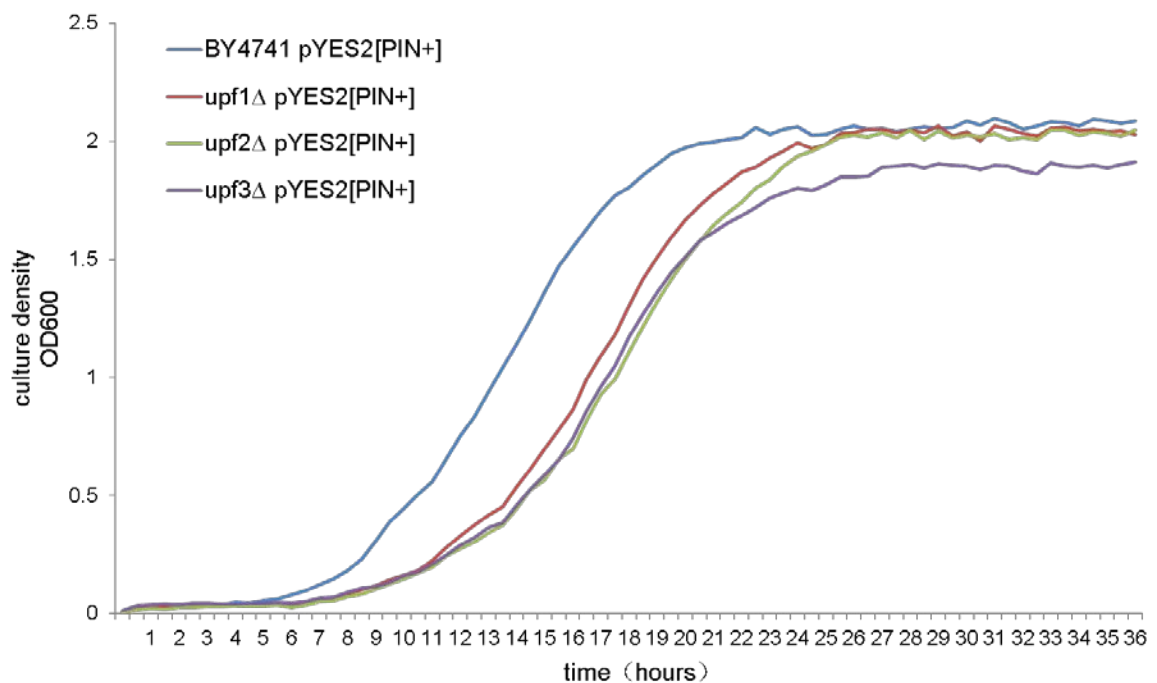
In parallel, no growth defect of overexpression of the Q25 protein in the BY4741 [*PIN*⁺] wild type *UPF*⁺ and the three *upf* deletion strains was observed. The doubling time of each control strain was between 4 and 5 hours (Table 6.1). By contrast, overexpression of polyQ103 led to a growth defect in the BY4741 wild type *UPF*⁺ [*PIN*⁺] strain and the *upf3*Δ [*PIN*⁺] strain while it was slightly recovered in the *upf1*Δ and *upf2*Δ in a [*PIN*⁺]-dependent manner (Figure 6.4). In the *upf1*Δ and *upf2*Δ [*PIN*⁺] strains overexpressing polyQ103, the doubling time was between 5 and 7 hours compared to approximately 16 hours in the BY4741 wild type *UPF*⁺ [*PIN*⁺] strain and the *upf3*Δ [*PIN*⁺] strain (Table 6.1).

Similar to the [*PIN*⁺] strains overexpressing Rnq1, the shorter doubling time obtained in the *upf1*Δ and *upf2*Δ [*PIN*⁺] strains overexpressing polyQ103 also confirmed that polyQ103-mediated toxicity was suppressed in *upf1*Δ and *upf2*Δ strains in a [*PIN*⁺] background. Moreover, according to the estimated doubling time, there is about a 5-fold increase in growth rate in the *upf1*Δ and *upf2*Δ [*PIN*⁺] strains overexpressing Rnq1, while only 2-3-fold increase was observed in the *upf1*Δ and *upf2*Δ [*PIN*⁺] strains overexpressing polyQ103 (Table 6.1). Thus the overall conclusion from these experiments is that suppression of Rnq1-mediated toxicity was greater than the suppression of polyQ103-induced toxicity in the *upf1*Δ and *upf2*Δ strains in a [*PIN*⁺] background.

Chapter 6

Table 6.1 Doubling time in exponential growth and cell density measured by the optical density of 600nm at the 36 hour time point for each strain of BY4741.

Strain	Plasmid	Doubling time (hr)	OD600 t = 36 h
BY4741[<i>PIN</i> ⁺]	pYES2	3.87	2.08
<i>upf1</i> Δ[<i>PIN</i> ⁺]	pYES2	3.77	2.02
<i>upf2</i> Δ[<i>PIN</i> ⁺]	pYES2	4.42	2.04
<i>upf3</i> Δ[<i>PIN</i> ⁺]	pYES2	3.99	1.91
BY4741[<i>PIN</i> ⁺]	pYES2- <i>RNQ1</i>	20.01	1.13
<i>upf1</i> Δ[<i>PIN</i> ⁺]	pYES2- <i>RNQ1</i>	4.98	2.18
<i>upf2</i> Δ[<i>PIN</i> ⁺]	pYES2- <i>RNQ1</i>	4.33	2.27
<i>upf3</i> Δ[<i>PIN</i> ⁺]	pYES2- <i>RNQ1</i>	27.57	0.89
BY4741[<i>PIN</i> ⁺]	pYES2- <i>Q25</i>	4.13	2.08
<i>upf1</i> Δ[<i>PIN</i> ⁺]	pYES2- <i>Q25</i>	5.15	2.04
<i>upf2</i> Δ[<i>PIN</i> ⁺]	pYES2- <i>Q25</i>	4.66	2.25
<i>upf3</i> Δ[<i>PIN</i> ⁺]	pYES2- <i>Q25</i>	4.52	1.95
BY4741[<i>PIN</i> ⁺]	pYES2- <i>Q103</i>	16.27	1.02
<i>upf1</i> Δ[<i>PIN</i> ⁺]	pYES2- <i>Q103</i>	7.83	1.85
<i>upf2</i> Δ[<i>PIN</i> ⁺]	pYES2- <i>Q103</i>	5.14	2.01
<i>upf3</i> Δ[<i>PIN</i> ⁺]	pYES2- <i>Q103</i>	15.58	1.24



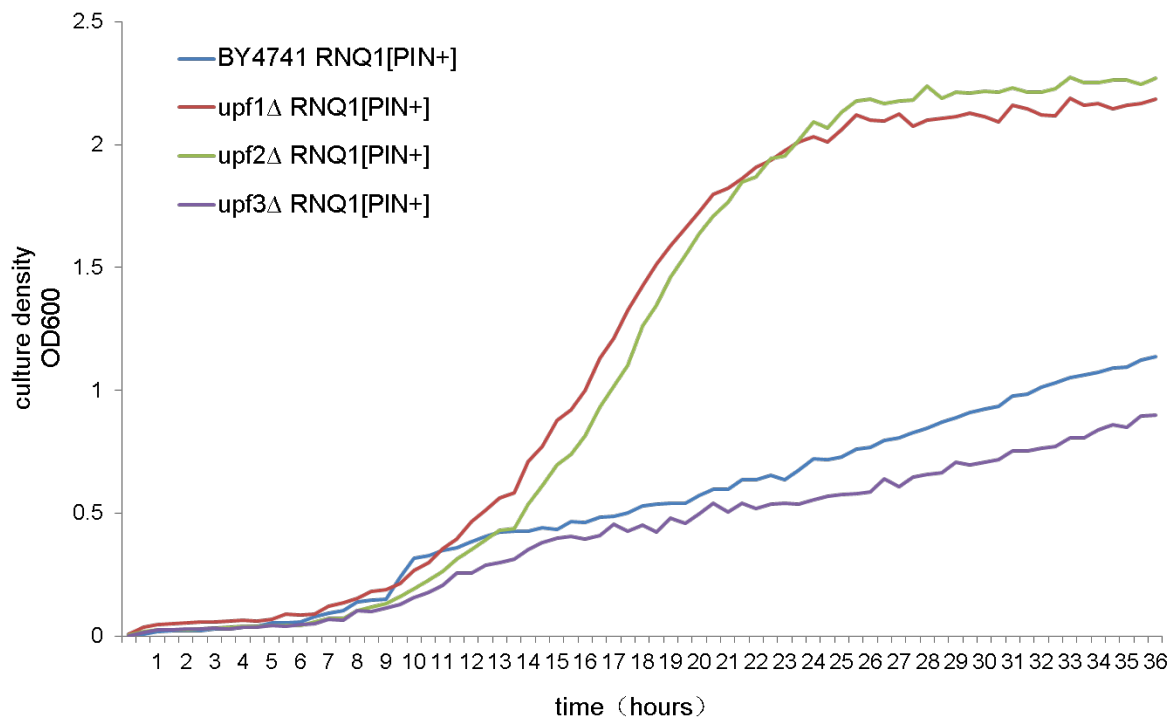
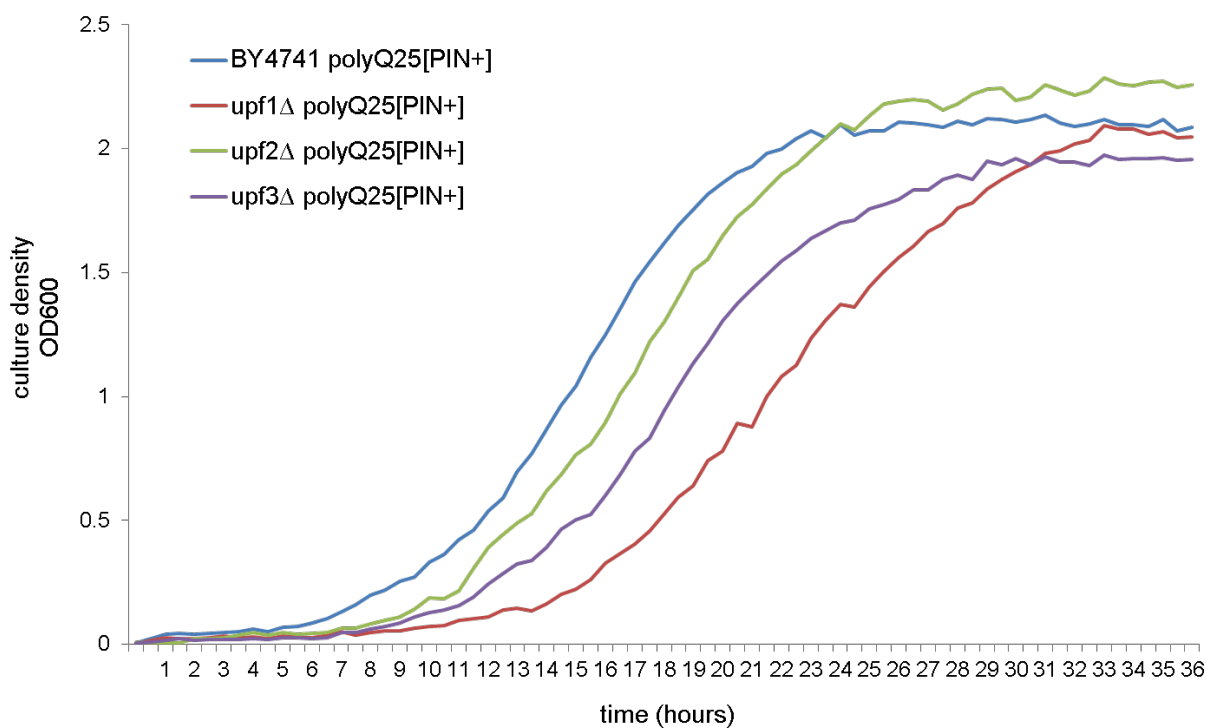


Figure 6.3 Overexpression of Rnq1 does not lead to a growth defect in *upf1*Δ and *upf2*Δ strains in a [PIN⁺] background. Cell density was determined in the inducing medium i.e. SD 2% galactose-ura for 36 hours at 30°C. The effect of Rnq1-mediated toxicity was tested in three deletion strains *upf1*Δ, *upf2*Δ and *upf3*Δ, compared to the wild type *UPF*⁺ BY4741 strains. pYES2 is the control plasmid while *RNQ1* is the pYES2 vector with *RNQ1* insert. Three biological replicates were performed for each strain and average is plotted in the above.



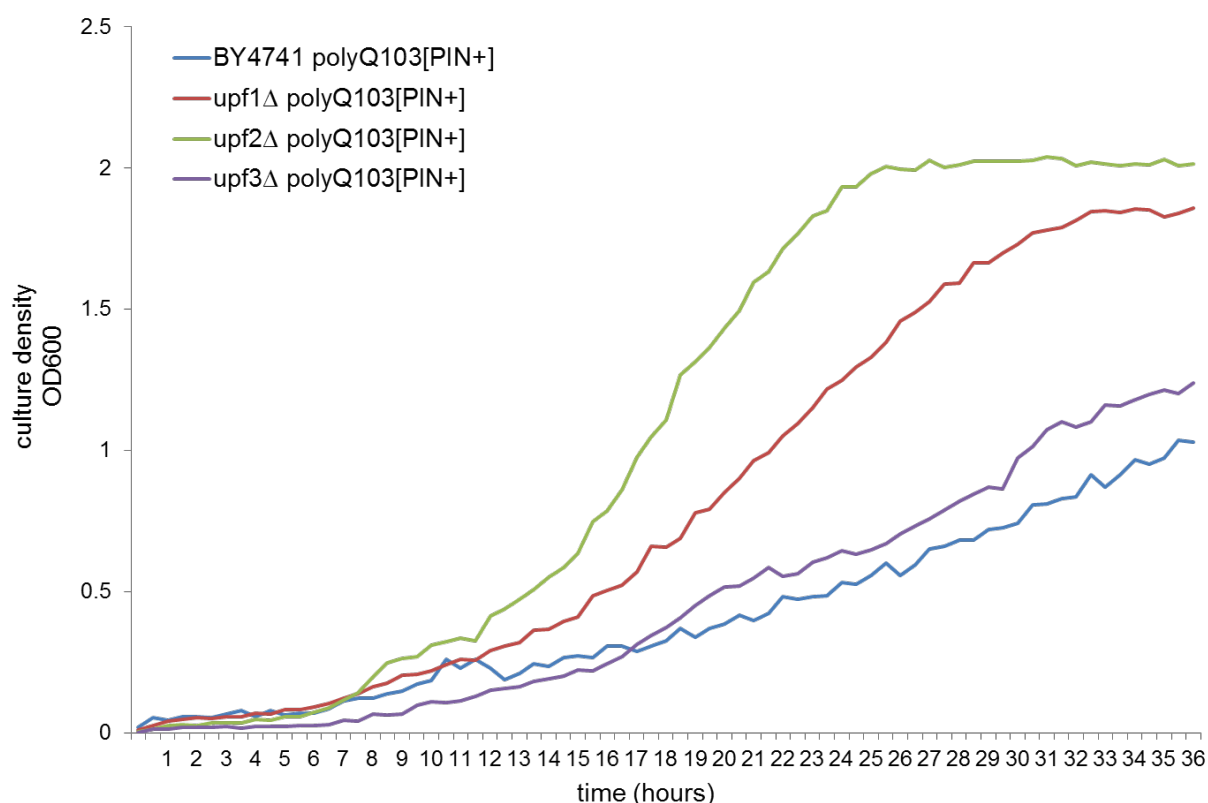


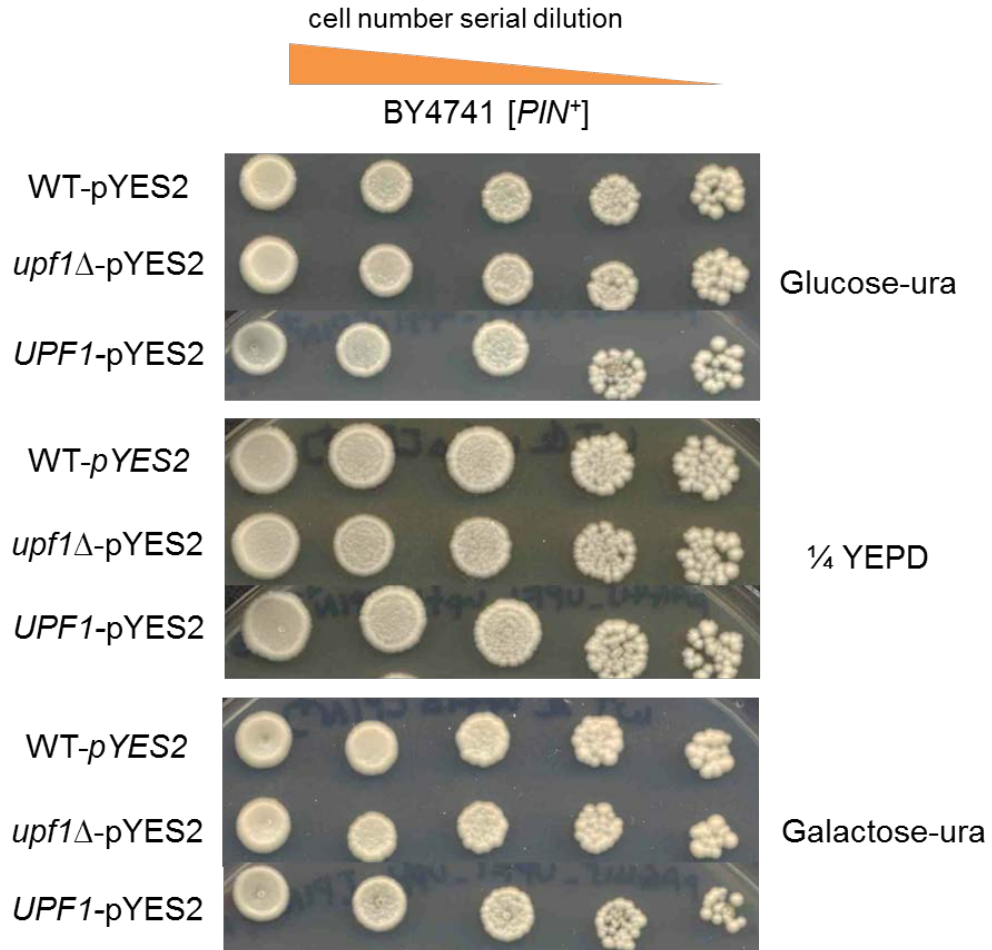
Figure 6.4 Overexpression of polyQ does not lead to a growth defect in *upf1*Δ and *upf2*Δ strains in a [*PIN*⁺] background. Cell density was determined in the inducing medium i.e. SD 2% galactose-ura for 36 hours at 30°C. The effect of polyQ-mediated toxicity was tested in three deletion strains *upf1*Δ, *upf2*Δ and *upf3*Δ, compared to the wild type UPF⁺ BY4741 strains. Q25 is the pYES2 based plasmid with a Q25 insert (control) while Q103 is the pYES2 based vector with a Q103 insert. Three biological replicates were performed for each strain and average is plotted in the above.

6.4 Expression of the wild type *UPF1* gene in the *upf1*Δ strain restores both Rnq1- and polyQ103-induced toxicity

In order to confirm the observed suppression of overexpression of Rnq1-induced toxicity by the *upf1*Δ strain was specific for the *upf1*Δ deletion, the *UPF1* gene with its own promoter was cloned into the pAG415 plasmid (Staniforth, 2011). This was then used to determine whether expression of the wild type Upf1 protein in the *upf1*Δ strain restored the Rnq1- and polyQ103-induced toxicity in a [*PIN*⁺] background. The pYES2 (control) or the pYES2-*RNQ1* plasmids were each co-transformed with the pAG415-*UPF1* plasmid into the *upf1*Δ [*PIN*⁺] strain (Figure 6.5). Similarly, the pYES2-Q25 (control) or

Chapter 6

the pYES2-Q103 plasmids were also co-transformed with the pAG415-UPF1 plasmid for expressing the Upf1 protein in a [*PIN*⁺] background (Figure 6.6).



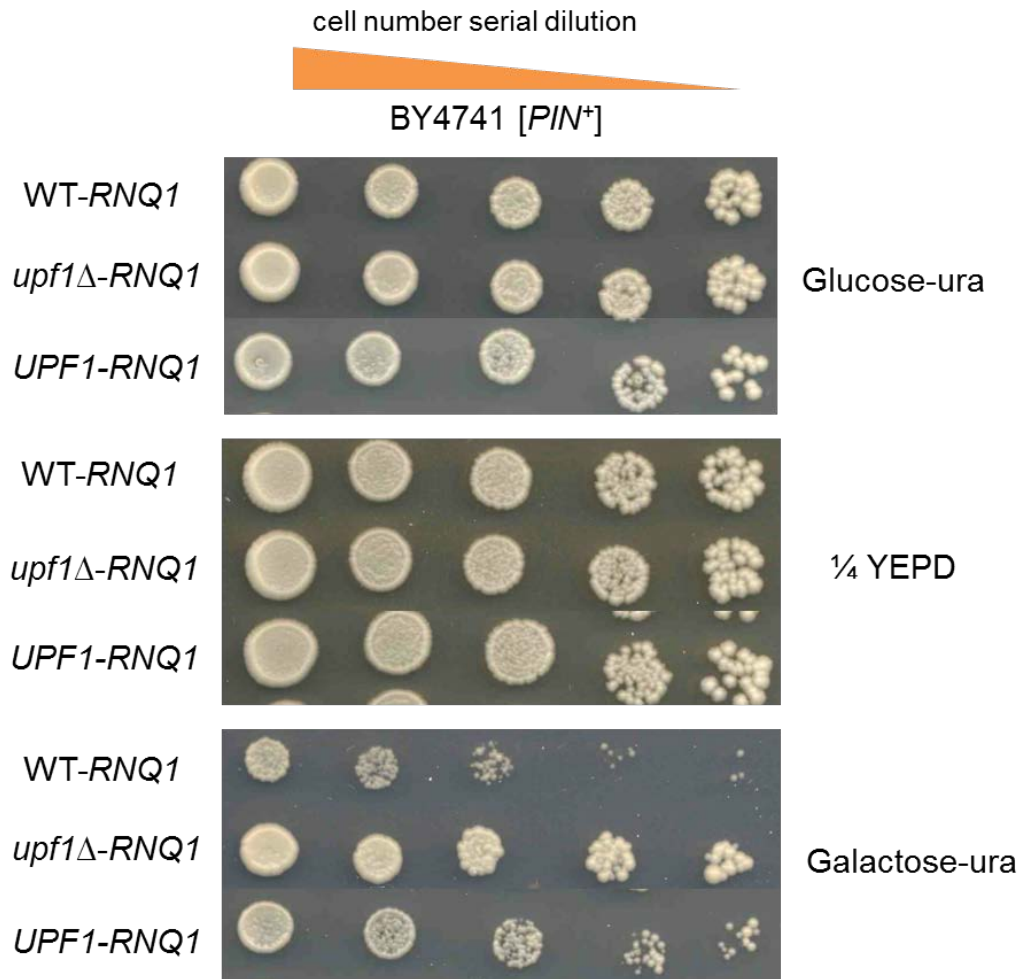
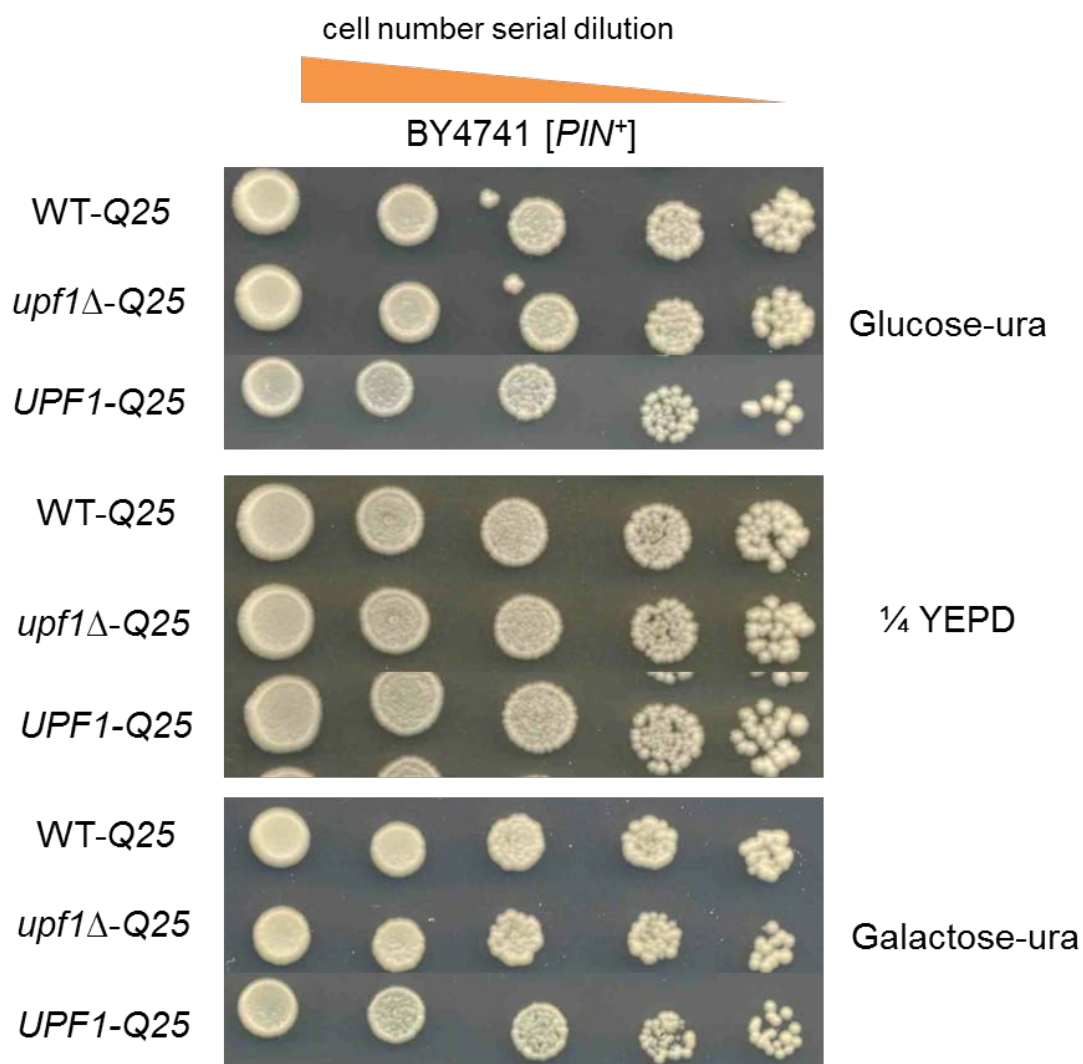


Figure 6.5 Suppression of the Rnq1 overexpression-induced toxicity in a *upf1*Δ strain is restored when the wild type Upf1 protein is expressed in a [*PIN*⁺] background. WT is the wild type *UPF*⁺ BY4741 strain. pYES2 is the control plasmid while *RNQ1* is the pYES2 vector with *RNQ1* gene insert. *UPF1-RNQ1* is the co-transformed strain expressing both Rnq1 and Upf1. Rnq1 toxicity was examined on galactose plates since the galactose-inducible promoter *GAL1* was used to overexpress the Rnq1 protein. 1/4 YEPD and glucose plates served as controls for any growth defects. Rnq1 toxicity was tested in the *upf1*Δ strain that was also expressing the Upf1 protein, compared to the wild type *UPF*⁺ BY4741 strain and the representative *upf1*Δ strain. Three biological replicates were performed for each strain and one representative is shown for each.

Chapter 6

As shown in Figure 6.5 and 6.6, overexpression of Rnq1 and polyQ103 was toxic in a [*PIN*⁺] background but this toxicity was suppressed in a *upf1*Δ [*PIN*⁺] strain. Expression of the wild type Upf1 protein in the *upf1*Δ strain partially restored the overexpression of Rnq1- and polyQ103-induced toxicity. One reason for the toxicity was partially restored rather than fully restored might be due to lower levels of the Upf1 protein. These findings confirmed that the suppression of Rnq1 and polyQ103 overexpression-mediated toxicity in the *upf1*Δ [*PIN*⁺] strains was specific to the deletion of the *UPF1* gene and not due to any secondary mutation that may have been introduced in a second gene during construction of the *upf1*Δ knockout.



Chapter 6

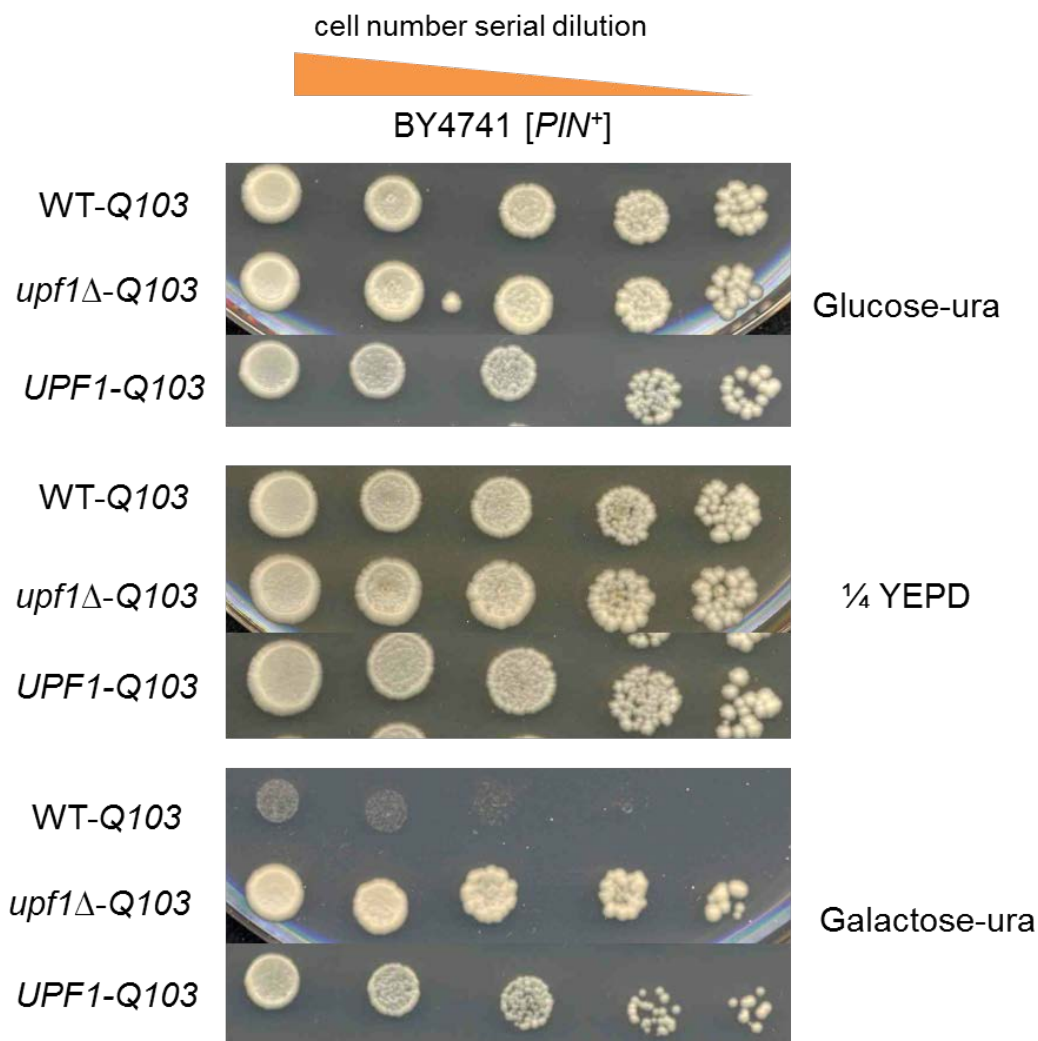


Figure 6.6 Suppression of the polyQ103 overexpression-induced toxicity in a *upf1* Δ strain is partially suppressed when the wild type Upf1 protein is expressed in a [*PIN*⁺] background. WT is the wild type *UPF*⁺ BY4741 strain. Q25 is the pYES2 based plasmid with a Q25 insert (control) while Q103 is the pYES2 based vector with a Q103 insert. *UPF1*-Q103 is the co-transformed strain expressing both polyQ103 and Upf1. Polyglutamine toxicity was examined on galactose plates since the galactose-inducible promoter *GAL1* was used to overexpress the polyglutamine protein. $\frac{1}{4}$ YEPD and glucose plates served as controls for any growth defects. PolyQ toxicity was tested in the *upf1* Δ strain that was also expressing the Upf1 protein, compared to the wild type *UPF*⁺ BY4741 strain and the representative *upf1* Δ strain. Three biological replicates were performed for each strain and one representative is shown for each.

6.5 Expression of the Upf1 protein in the *upf1* Δ strain shows the growth defects caused by Rnq1- and polyQ103 overexpression-mediated toxicity

As described in Section 6.3, quantitative growth analysis was also carried out with the *upf1* Δ strain expressing the wild type Upf1 protein. The impact of overexpression of Rnq1 and polyQ103 on the growth rate in this strain was compared to the control wild type *UPF*⁺ and *upf1* Δ strains of BY4741 (Figure 6.7).

In strains carrying the control plasmid pYES2, the doubling time of the *upf1* Δ strain was similar to the strain expressing the wild type Upf1 protein, and to the wild type *UPF*⁺ strain of BY4741. This indicates that the three tested strains grew normally as expected although the slope of the growth curve of the *upf1* Δ strain expressing the wild type Upf1 protein was lower than the wild type *UPF*⁺ strain and the *upf1* Δ strain (Figure 6.7).

In strains overexpressing the Rnq1 protein, a growth defect was seen in the wild type *UPF*⁺ strain as expected while the *upf1* Δ strain restored growth to that of the control (Figure 6.7). The doubling time of the *upf1* Δ strain expressing the pYES2 plasmid backbone was similar to the *upf1* Δ strain overexpressing the Rnq1 protein which was between 3.8 and 5.5 hours (Table 6.2). Importantly, the *upf1* Δ strain also expressing the wild type Upf1 protein showed a partial growth defect compared to the wild type *UPF*⁺ strain overexpressing Rnq1. The doubling time of the *upf1* Δ strain expressing the wild type Upf1 was 9 hours while the wild type *UPF*⁺ strain showed a doubling time of 20 hours (Table 6.2). This indicates that suppression of Rnq1 toxicity in the *upf1* Δ strain was not fully restored when the wild type Upf1 protein was expressed. This finding is consistent with the result obtained from the toxicity assay described in Section 6.4. One reason for this difference might be due to lower levels of the Upf1 protein.

Chapter 6

Similarly, in strains overexpressing the polyQ103 protein, a growth defect was found in the wild type *UPF*⁺ strain with a doubling time of 16 hours while the *upf1*Δ strain restored this growth to the corresponding control strain (Figure 6.7). The doubling time was 4 hours in the *upf1*Δ strain overexpressing Q25 (control) and 7 hours in the *upf1*Δ strain overexpressing Q103 (Table 6.2). Likewise, the *upf1*Δ strain also expressing the wild type Upf1 protein showed a partial growth defect compared to the wild type *UPF*⁺ strain overexpressing Q103 with a doubling time of 10 hours a value between the wild type *UPF*⁺ strain and the *upf1*Δ strain (Table 6.2). This further suggests that suppression of polyQ103 toxicity in the *upf1*Δ strain was not fully restored when the wild type Upf1 protein was expressed.

Table 6.2 Doubling time in exponential growth and cell density measured by the optical density of 600nm at the 36 hour time point for each strain of BY4741.

Strain	Plasmid	Doubling time	OD600 t = 36 h
BY4741 [<i>PIN</i> ⁺]	pYES2	3.87	2.08
<i>upf1</i> Δ [<i>PIN</i> ⁺]	pYES2	3.77	2.02
<i>upf1</i> Δ [<i>PIN</i> ⁺]	pAG415- <i>UPF1</i> + pYES2	4.81	1.59
BY4741 [<i>PIN</i> ⁺]	pYES2- <i>RNQ1</i>	20.01	1.13
<i>upf1</i> Δ [<i>PIN</i> ⁺]	pYES2- <i>RNQ1</i>	5.49	1.82
<i>upf1</i> Δ [<i>PIN</i> ⁺]	pAG415- <i>UPF1</i> + pYES2- <i>RNQ1</i>	9.09	1.26
BY4741 [<i>PIN</i> ⁺]	pYES2-Q25	4.17	2.08
<i>upf1</i> Δ [<i>PIN</i> ⁺]	pYES2-Q25	4.26	2.37
<i>upf1</i> Δ [<i>PIN</i> ⁺]	pAG415- <i>UPF1</i> + pYES2-Q25	5.56	2.18
BY4741 [<i>PIN</i> ⁺]	pYES2-Q103	16.27	1.02
<i>upf1</i> Δ [<i>PIN</i> ⁺]	pYES2-Q103	7.83	1.85
<i>upf1</i> Δ [<i>PIN</i> ⁺]	pAG415- <i>UPF1</i> + pYES2-Q103	10.91	1.48

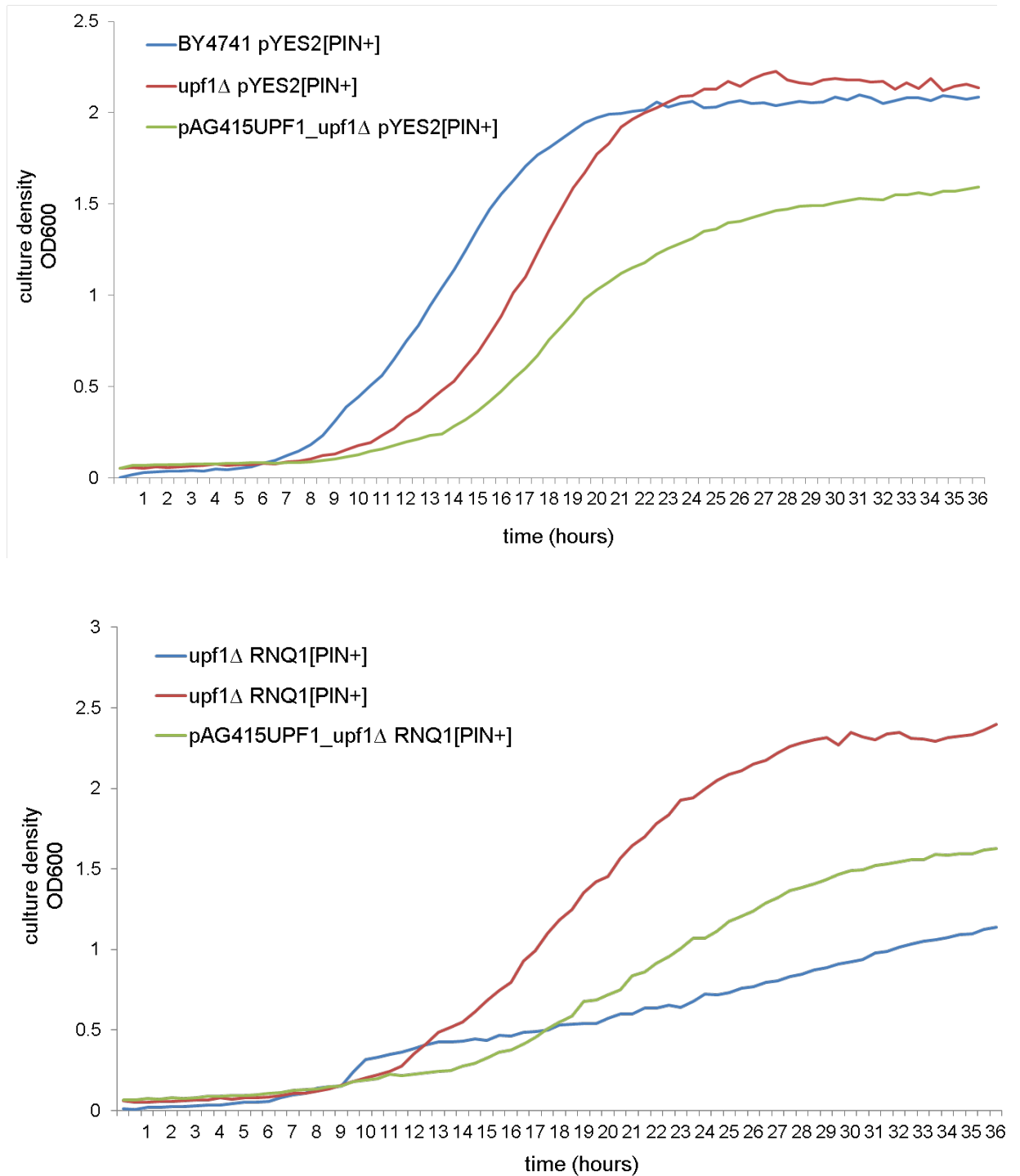


Figure 6.7 Overexpression of Rnq1 leads to a growth defect in the *upf1*Δ strain also expressing the wild type Upf1 protein in a *[PIN⁺]* background. Cell density was determined in the inducing medium i.e. SD 2% galactose-ura for 36 hours at 30°C. The effect of Rnq1 toxicity was tested in the *upf1*Δ strain also expressing the wild type Upf1 protein, compared to the wild type *UPF⁺* BY4741 and the *upf1*Δ strains. pYES2 is the control plasmid while *RNQ1* is the pYES2 vector with *RNQ1* insert. Three biological replicates were performed for each strain and average is plotted in the above.

Chapter 6

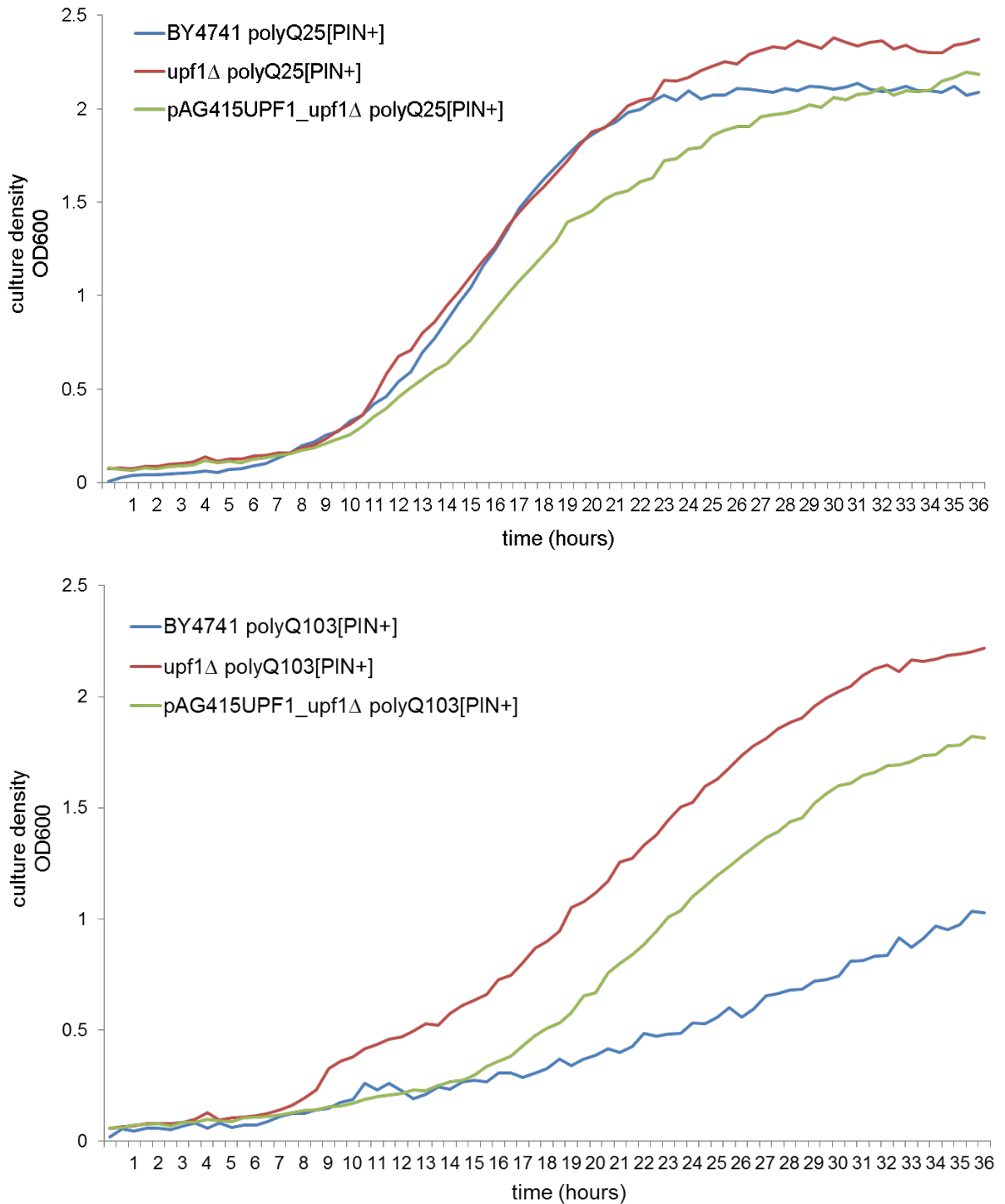


Figure 6.8 Overexpression of polyQ103 causes a detectable growth defect in the *upf1*Δ strain also expressing the wild type Upf1 protein in a [PIN⁺] background. Cell density was determined in the inducing medium i.e. SD 2% galactose-ura for 36 hours at 30°C. The effect of polyQ-mediated toxicity was tested in the *upf1*Δ strain also expressing the wild type Upf1 protein, compared to the wild type *UPF*⁺ BY4741 and the *upf1*Δ strains. Q25 is the pYES2 based plasmid with a Q25 insert (control) while Q103 is the pYES2 based vector with a Q103 insert. Three biological replicates were performed for each strain and average is plotted in the above.

6.6 Rnq1 overexpression does not cause a nuclear migration defect in the *upf1* Δ and *upf2* Δ strains

As described in Section 4.5, overexpression of Rnq1 resulted in a nuclear migration defect in BY4741 [*PIN*⁺] cells. It was therefore interesting to investigate whether the nuclear migration defect was also observed in the *upf1* Δ and *upf2* Δ strains as Rnq1 overexpression-induced toxicity was suppressed in the *upf1* Δ and *upf2* Δ strains.

Log phase *upf1* Δ and *upf2* Δ cells of BY4741 were observed following staining with 4',6-diamidino-2-phenylindole (DAPI) which is widely used to visualise nuclear DNA or mitochondrial DNA (Chazotte., 2011). The [*PIN*⁺] derivatives of the *upf1* Δ and *upf2* Δ deletion strains of BY4741 were each transformed with either the pYES2 (control) or the pYES2-*RNQ1* plasmids. The nuclear DNA was visualized by fluorescence microscopy under ultraviolet light using DAPI to stain the DNA (Figure 6.9).

In the *upf1* Δ and *upf2* Δ strains overexpressing Rnq1, the localization of nuclear DNA was similar to that seen in strains expressing the pYES2 backbone (control) before (t = 0) and after 6 hours induction (t = 6) and also similar with the un-induced cells i.e. (at t = 0). Thus no defect in nuclear migration was detected in the *upf1* Δ and *upf2* Δ [*PIN*⁺] strains (Figure 6.9). Although earlier findings reported in Chapter 4 (Section 4.5) concluded that Rnq1 overexpression-induced cytotoxicity is not associated with the nuclear migration defect (Section 4.5), the data shown in Figure 6.9 suggest that the Upf1 and Upf2 proteins might have a positive effect on nuclear migration and/or cell cycle control independent of Rnq1 overexpression mediated cytotoxicity since the nuclear migration defect would be expected to lead to a cell cycle blockage (Treich and Lindquist, 2012).

Chapter 6

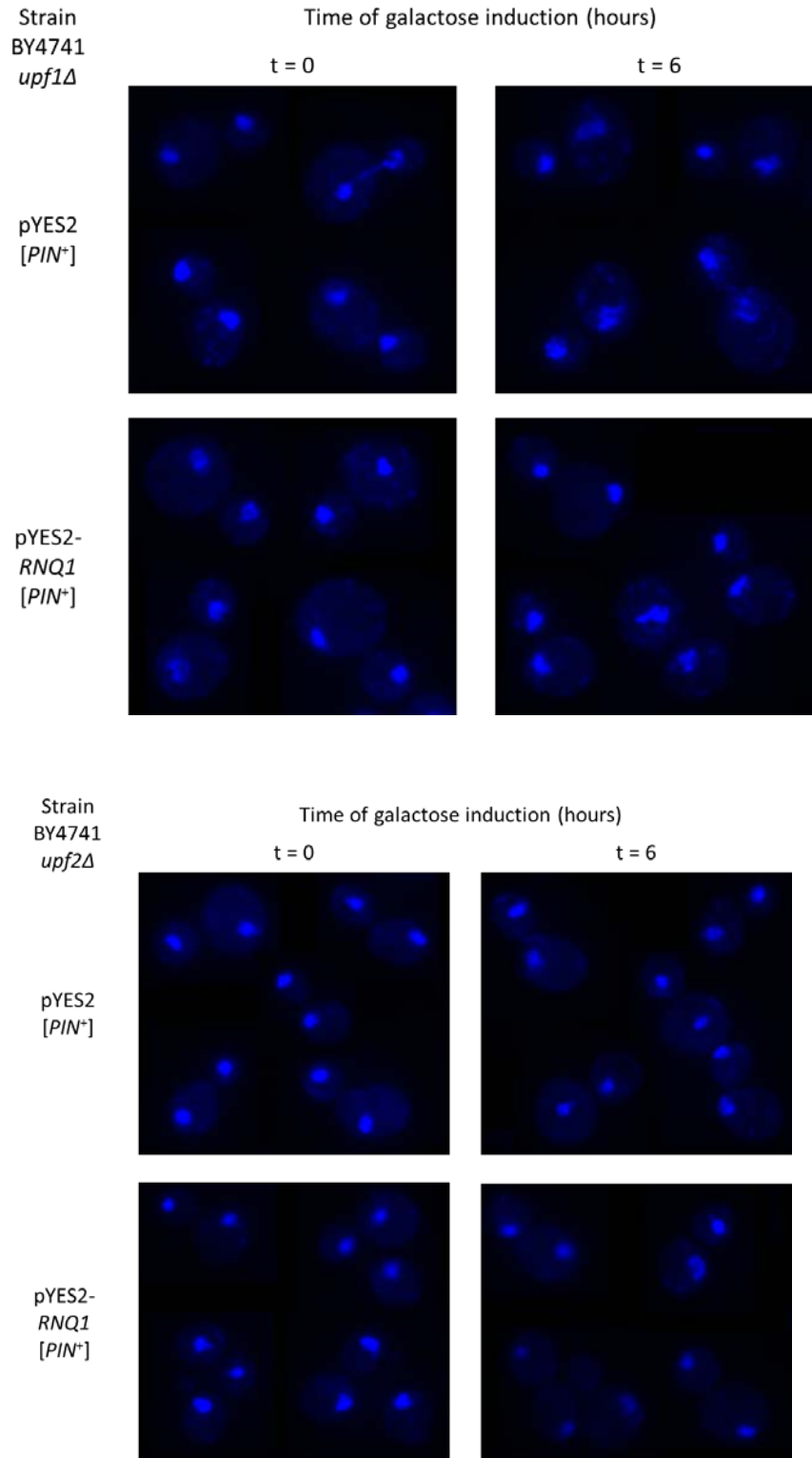


Figure 6.9 Overexpression of Rnq1 does not cause a nuclear migration defect in the *upf1* Δ and *upf2* Δ strains of BY4741 in a [*PIN*⁺] background. Rnq1 overexpression does not cause nuclear DNA localised to the bud-neck after 6 hours induction in the *upf1* Δ and *upf2* Δ strains. No the nuclear migration defects were detected in pYES2 control strains. Cells were visualised by a blue excitation filter on an Olympus 1X81 fluorescent microscope with Hamamatsu Photonics Orca AG cooled CCD camera. Images were captured analysed by Olympus CellIR software

Chapter 6

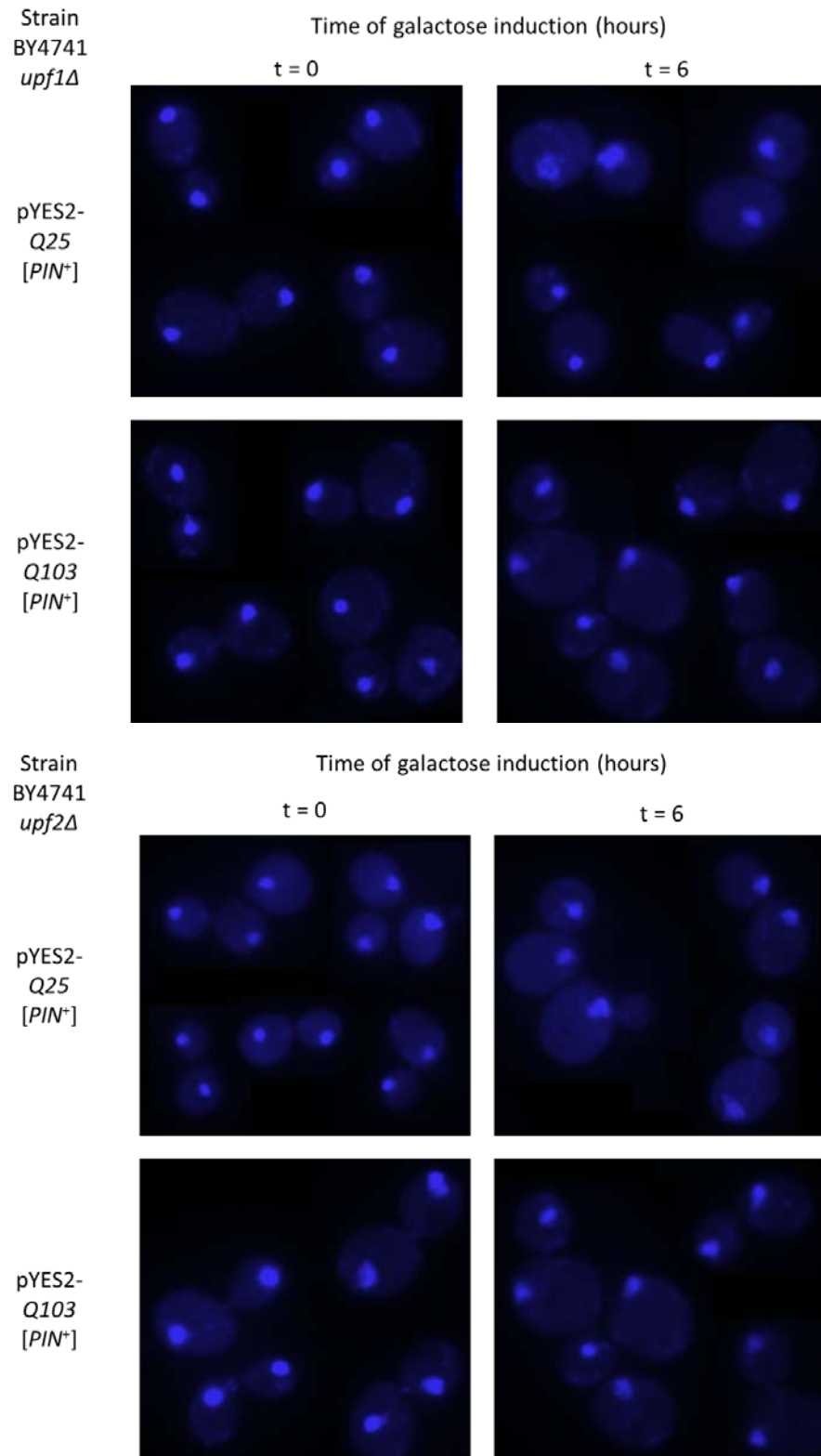


Figure 6.10 Overexpression of polyQ103 does not cause a nuclear migration defect in the *upf1* Δ and *upf2* Δ strains of BY4741 in a [*PIN*⁺] background. Rnq1 overexpression does not cause nuclear DNA localised to the bud-neck after 6 hours induction in the *upf1* Δ and *upf2* Δ strains. No nuclear migration defects were detected in pYES2 control strains. Cells were visualised by a blue excitation filter on an Olympus 1X81 fluorescent microscope with Hamamatsu Photonics Orca AG cooled CCD camera. Images were captured analysed by Olympus CellR software.

Likewise, the same experiments were carried out in parallel in BY4741 [*PIN*⁺] cells overexpressing polyQ103, however, polyQ103 overexpression did not cause a nuclear migration defect (see Chapter 5, Section 5.5). In order to explore whether the Upf1 or Upf2 protein may cause a nuclear migration defect when polyQ103 was overexpressed, pYES2-Q25 (control) or pYES2-Q103 plasmids were each transformed into the *upf1*Δ and *upf2*Δ strains of BY4741. The nuclear DNA was visualized by fluorescence microscopy under ultraviolet light using DAPI to stain the DNA (Figure 6.10).

As in the *upf1*Δ and *upf2*Δ strains overexpressing polyQ103, the localization of nuclear DNA was similar with strains overexpressing polyQ25 (control) before (t = 0) and after 6 hours induction (t = 6) and also similar with the un-induced cells overexpressing polyQ103 (t = 0). Therefore no defect in nuclear migration was detected in the *upf1*Δ and *upf2*Δ [*PIN*⁺] strains (Figure 6.10). This finding argues against the Upf1 or Upf2 proteins being associated with nuclear migration and/or cell cycle control.

6.7 Construction of *UPF1* mutations

The *UPF1* gene and its protein product have been intensively studied. The *UPF1* gene encodes a 109-kDa protein which acts as an ATP-dependent RNA helicase. The Upf1 protein is rich in cysteine and histidine residues at its N-terminus representing the key feature of the RNA/DNA helicase superfamily group I (Koonin., 1992). The Upf2 protein interacts with this CH domain of Upf1 resulting in a conformational change of the CH domain that enhances the ATPase and helicase activity of Upf1 while reducing its ability to bind RNA (Clerici *et al.*, 2009; Chakrabarti *et al.*, 2011).

Previous studies established that the ATPase and helicase activity of Upf1 was affected by mutating the lysine residue in position 436 to any of the five residues which are alanine (A), glutamine (Q), aspartic acid (D), glutamic acid (E), and proline (P) respectively (Weng *et al.*, 1996). This highly conserved lysine (K) residue plays an essential role in ATP binding and hydrolysis in

Chapter 6

other proteins (Fry *et al.*, 1986). Thus the K436 mutations resulted in an impaired NMD pathway by inhibiting the functions of Upf1 in promoting mRNA decay (Weng *et al.*, 1996).

In addition to its role in ATP binding and hydrolysis, the CH domain of Upf1 also act as a catalytic domain of the E3 ubiquitin ligase that in turn interacts with a specific E2 namely Ubc2 in yeast (Takahashi *et al.*, 2008). Mutating the histidine (H) residue in position 94 to an arginine (R) in the CH domain results in an inhibition of the E3 ubiquitin ligase activity upon its interaction with Upf3 (Takahashi *et al.*, 2008).

In order to identify which function of Upf1 is associated with overexpression of Rnq1- and polyQ103-induced toxicity, two mutated variants of Upf1, H94R and K436A, were created respectively using site-directed mutagenesis (See Section 2.X). Mutants were generated in a three step protocol. Firstly, the plasmid DNA pAG415-UPF1 and two oligonucleotide primers each complementary to opposite strands of the vector containing any of the desired mutation, (i.e. H94R or K436A), were used for synthesis of the mutant DNA strand by polymerase chain reaction (PCR). Then the Dpn I endonuclease was used to digest the parental DNA template which is methylated thus only the mutant-containing DNA strand remains after digestion. Finally, the newly synthesised plasmid DNA with the desired mutation was transformed into XL1-Blue supercompetent *E. coli* cells. Four colonies of each putative mutant of Upf1 were purified and sent for sequencing (Section 2.6.6). All four tested DNA samples of each Upf1 mutant contained the desired amino acid residue (Figure 6.11).

```
Position: 94
280-282
H
pAG415-UPF1 AAATGGTTTTGTAACACTAAAAACGGTACAAGCAGCTCCCACATTGTTAATCACTTAGTT 300
mpAG415-UPF1 AAATGGTTTTGTAACACTAAAAACGGTACAAGCAGCTCCCGCATTGTTAATCACTTAGTT 300
R
```

Position: 436
1306-1308

K

pAG415- <i>UPF1</i>	TTACAACGTCCGTTATCTTTAATTCAAGGCCACCAGGCACTGGT AAA ACAGTTACTTCA 1320
mpAG415- <i>UPF1</i>	TTACAACGTCCGTTATCTTTAATTCAAGGCCACCAGGCACTGGT GCA ACAGTTACTTCA 1320

A

Figure 6.11 Construction of *UPF1* mutations using site-directed mutagenesis. A histidine (H) residue in position 94 was mutagenized to an arginine (R) and a lysine residue in position 436 was mutagenized to an alanine (A). Four DNA samples were tested for each mutation and one representative is shown for each.

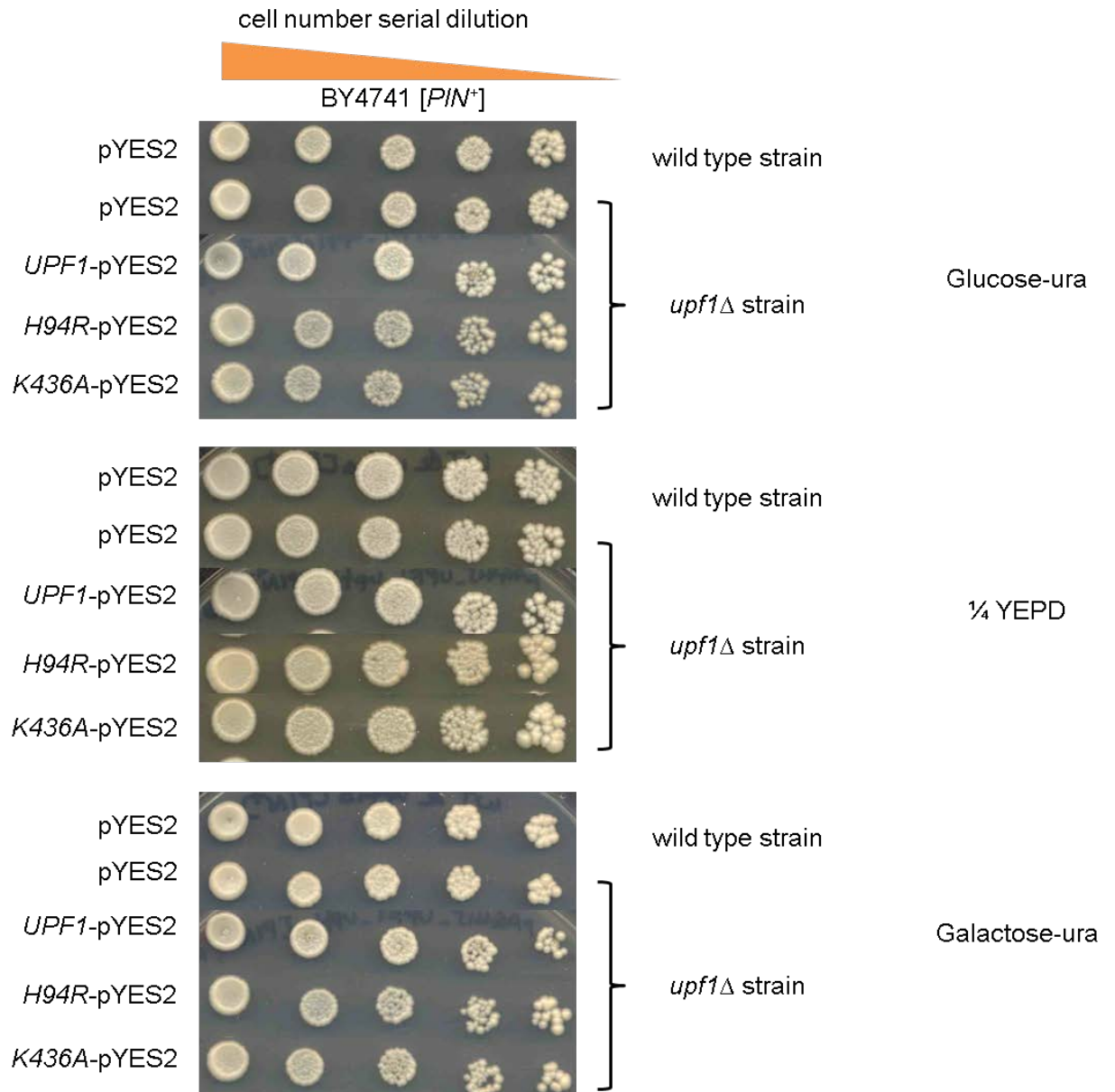
6.8 Expression of *upf1* mutant genes in the *upf1* Δ strain partially suppress Rnq1 and polyQ overexpression-induced toxicity in [*PIN*⁺] cells

As describe in Section 6.7, two single mutations i.e. H94R and K436A were generated respectively in the *UPF1* gene of a pAG415-*UPF1* plasmid. In order to explore either the ATPase and helicase activity or the E3 ubiquitin ligase activity of Upf1 is important for its role in Rnq1- and polyq103-mediated toxicity, the pYES2 (control) or the pYES2-*RNQ1* plasmids were each co-transformed with the pAG415-*UPF1* plasmid containing either H94R or K436A mutation into the *upf1* Δ [*PIN*⁺] strain (Figure 6.12). Similarly, the pYES2-Q25 (control) or the pYES2-Q103 plasmids were also co-transformed into a [*PIN*⁺] *upf1* Δ strain with the pAG415- *upf1* plasmid expressing the desired *upf1* mutant (Figure 6.13). Toxicity assays (Section 4.1) were then performed with these *upf1* mutant strains (Figure 6.12, 6.13).

As shown in Figure 6.12 and 6.13, overexpression of Rnq1 and polyQ103 was toxic in a [*PIN*⁺] background as expected while this toxicity was suppressed in a *upf1* Δ [*PIN*⁺] strain as previously shown in Section 6.2. By comparison, expression of the H94R and K436A variants of the Upf1 protein in the *upf1* Δ strain partially restored the overexpressing of Rnq1- and polyQ103-induced toxicity to a similar seen when the wild type Upf1 protein was expressed in the *upf1* Δ [*PIN*⁺] strain. As described in Section 6.4, the partial restoration of

Chapter 6

Rnq1- and polyQ103-induced toxicity might be due to lower level of the wild type Upf1 expression. This result suggests that neither H94R nor K436A mutant of Upf1 has an impact on the Rnq1- and polyQ103-mediated toxicity indicating neither the ATPase and helicase activity nor the E3 ubiquitin ligase activity of Upf1 is associated with overexpression of Rnq1- and polyQ103-mediated toxicity.



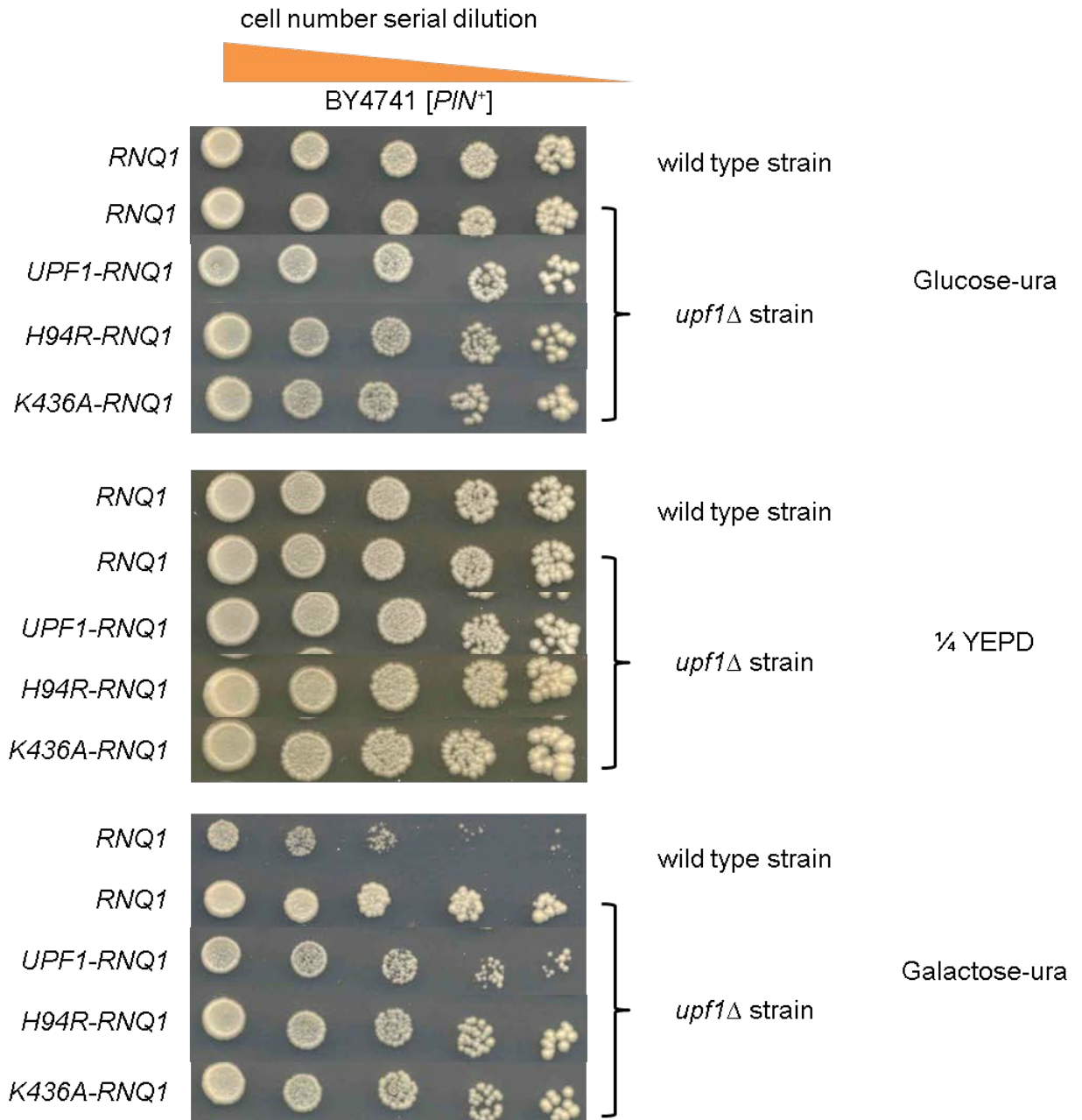
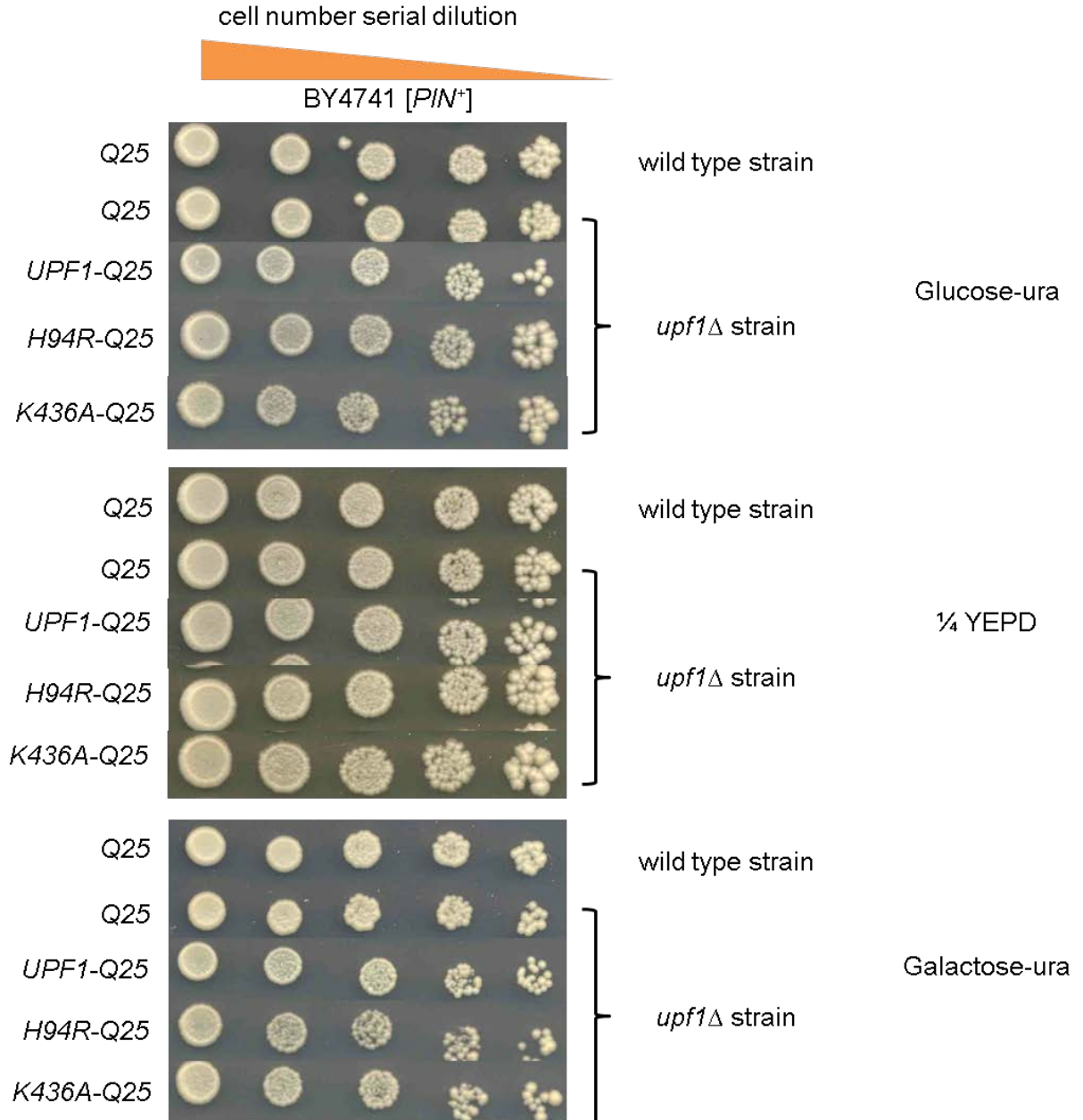


Figure 6.12 Suppression of the Rnq1 overexpression-induced toxicity in a *upf1*Δ strain is partially restored when either the H94R or K436A Upf1 mutant proteins are expressed in a [*PIN*⁺] background. WT is the wild type *UPF*⁺ BY4741 strain. pYES2 is the control plasmid while *RNQ1* is the pYES2 vector with *RNQ1* insert. *UPF1-RNQ1* is the co-transformed strain expressing both Rnq1 and Upf1. *H94R-RNQ1* is the co-transformed strain expressing both Rnq1 and the H94R mutant Upf1. *K436A-RNQ1* is the co-transformed strain expressing both Rnq1 and the K436A mutant Upf1. Rnq1 toxicity was examined on galactose plates since the galactose-inducible promoter *GAL1* was used to overexpress the Rnq1 protein. 1/4 YEPD and glucose plates served as controls for any growth defects. Rnq1 toxicity was tested in the *upf1*Δ strain that was also expressing the wild type and the two mutant Upf1 proteins, compared to the wild type *UPF*⁺ BY4741 strain and the representative *upf1*Δ strain. Three biological replicates were performed for each strain and one representative is shown for each.

Chapter 6



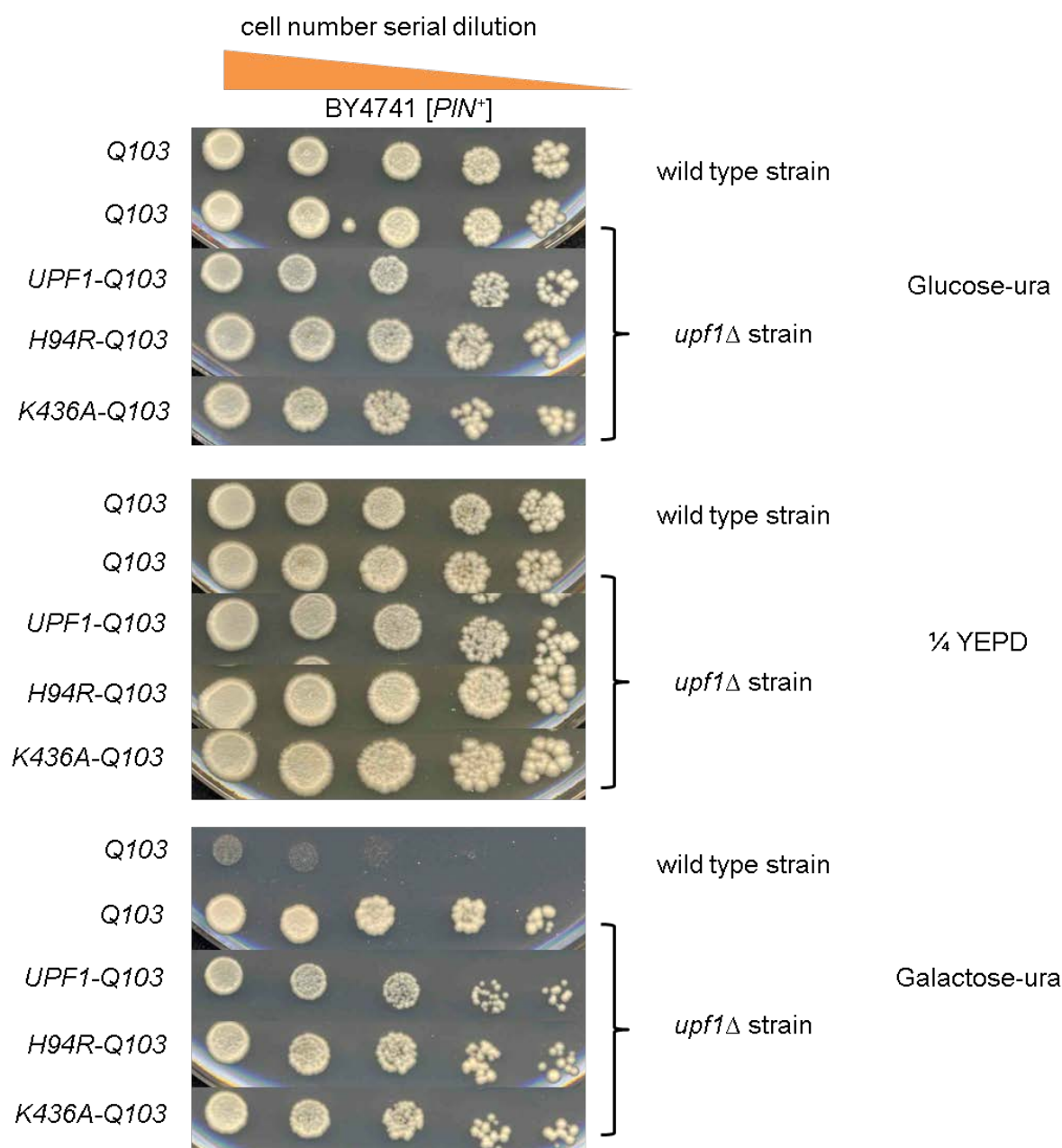


Figure 6.13 Suppression of the polyQ103 overexpression-induced toxicity in a *upf1*Δ strain is partially restored when any of the two mutant forms H94R and K436A of the Upf1 protein is expressed in a [*PIN*⁺] background. WT is the wild type *UPF*⁺ BY4741 strain. Q25 is the pYES2 based plasmid with a Q25 insert (control) while Q103 is the pYES2 based vector with a Q103 insert. *UPF1*-Q103 is the co-transformed strain expressing both polyQ103 and Upf1. *H94R*-Q103 is the co-transformed strain expressing both polyQ103 and the H94R mutant Upf1. *K436A*-Q103 is the co-transformed strain expressing both polyQ103 and the K436A mutant Upf1. Polyglutamine toxicity was examined on galactose plates since the galactose-inducible promoter *GAL1* was used to overexpress the polyglutamine protein. 1/4 YEPD and glucose plates served as controls for any growth defects. PolyQ toxicity was tested in the *upf1*Δ strain that was also expressing the wild type and the two mutant Upf1 protein, compared to the wild type *UPF*⁺ BY4741 strain and the representative *upf1*Δ strain. Three biological replicates were performed for each strain and one representative is shown for each.

6.9 Expression of the mutant Upf1 protein in the *upf1*Δ strain shows the general growth defects

In order to further investigate the cellular phenotype of the Upf1 mutants when Rnq1 or polyQ103 were overexpressed, quantitative growth analysis was repeated in the H94R and K436A mutants of the *upf1*Δ [*PIN*⁺] strain of BY4741 to quantify the impact of Rnq1 and polyQ overexpression on the growth rate. The result of the *upf1*Δ strain expressing the mutant Upf1 was compared with the wild type *UPF*⁺ strain, *upf1*Δ strain and the *upf1*Δ strain also expressing the wild type Upf1 protein (Figure 6.14, 6.15). The growth conditions were as described in Section 4.3.

As expected, in strains carrying the pYES2 and pYES2-Q25 control plasmids, no growth defect was found in the wild type *UPF*⁺ strain, *upf1*Δ strain and the *upf1*Δ strain expressing the wild type Upf1 protein (Figure 6.14, 6.15). The doubling time of these strains was between 3 to 5 hours (Table 6.3). However, a growth defect was seen in strains expressing the H94R and K436A mutant of Upf1 in the *upf1*Δ strain with a doubling time around 10 to 12 hours (Table 6.3).

By contrast, a growth defect was seen in the wild type *UPF*⁺ [*PIN*⁺] strain while the *upf1*Δ [*PIN*⁺] strain restored this growth to that of the control when Rnq1 or polyQ103 was overexpressed. The doubling time showed a 2 to 4-fold increase in the wild type *UPF*⁺ strain overexpressing polyQ103 and Rnq1 respectively when compared with the corresponding *upf1*Δ strain (Table 6.3). As described in Section 6.5, in *upf1*Δ [*PIN*⁺] strains also expressing the wild type Upf1 protein, a partial growth defect was seen when Rnq1 or polyQ103 was overexpressed. Similarly, this partial growth defect was also found in strains expressing the H94R and K436A mutant of Upf1 in the *upf1*Δ [*PIN*⁺] strain (Figure 6.14, 6.15). According to the doubling time (Table 6.3), overexpression of Rnq1 and polyQ103 slightly elevated levels of toxicity in the *upf1*Δ [*PIN*⁺] strains compared to the *upf1*Δ [*PIN*⁺] strains expressing the wild type Upf1. Importantly, the doubling time of the constructs *upf1*Δ [*PIN*⁺] strain expressing the pYES2 and pYES2-Q25 was similar to that of overexpressing

Chapter 6

Rnq1 and polyQ103 (Table 6.3). Since the growth defect in the mutant *upf1Δ* [*PIN⁺*] strains overexpressing Rnq1 and polyQ103 was also found in strains expressing the pYES2 and pYES2-Q25, the overall conclusion is that the H94R and K436A mutants of Upf1 are generally toxic to cells, but not as a consequence of overexpression of Rnq1 or polyQ103. This finding also confirmed that overexpression of Rnq1- and polyQ103-mediated toxicity is not caused by either the ATPase and helicase activity or the E3 ubiquitin ligase activity of Upf1.

Table 6.3 Doubling time in exponential growth and cell density measured by the optical density of 600nm at the 36 hour time point for each strain of BY4741.

Strain	Plasmid	Doubling time	OD600 t = 36 h
BY4741 [<i>PIN⁺</i>]	pYES2	3.87	2.08
<i>upf1Δ</i> [<i>PIN⁺</i>]	pYES2	3.77	2.02
<i>upf1Δ</i> [<i>PIN⁺</i>]	pAG415- <i>UPF1</i> + pYES2	4.81	1.59
<i>upf1Δ</i> [<i>PIN⁺</i>]	pAG415- <i>UPF1</i> _H94R + pYES2	11.28	1.02
<i>upf1Δ</i> [<i>PIN⁺</i>]	pAG415- <i>UPF1</i> _K436A + pYES2	12.65	1.15
BY4741 [<i>PIN⁺</i>]	pYES2- <i>RNQ1</i>	20.01	1.13
<i>upf1Δ</i> [<i>PIN⁺</i>]	pYES2- <i>RNQ1</i>	5.49	1.82
<i>upf1Δ</i> [<i>PIN⁺</i>]	pAG415- <i>UPF1</i> + pYES2- <i>RNQ1</i>	9.09	1.26
<i>upf1Δ</i> [<i>PIN⁺</i>]	pAG415- <i>UPF1</i> _H94R + pYES2- <i>RNQ1</i>	13.25	1.08
<i>upf1Δ</i> [<i>PIN⁺</i>]	pAG415- <i>UPF1</i> _K436A + pYES2- <i>RNQ1</i>	15.35	0.98
BY4741 [<i>PIN⁺</i>]	pYES2-Q25	4.17	2.08
<i>upf1Δ</i> [<i>PIN⁺</i>]	pYES2-Q25	4.26	2.37
<i>upf1Δ</i> [<i>PIN⁺</i>]	pAG415- <i>UPF1</i> + pYES2-Q25	5.56	2.18
<i>upf1Δ</i> [<i>PIN⁺</i>]	pAG415- <i>UPF1</i> _H94R + pYES2-Q25	10.83	1.30
<i>upf1Δ</i> [<i>PIN⁺</i>]	pAG415- <i>UPF1</i> _K436A + pYES2-Q25	11.18	1.13
BY4741 [<i>PIN⁺</i>]	pYES2-Q103	16.27	1.02
<i>upf1Δ</i> [<i>PIN⁺</i>]	pYES2-Q103	7.83	1.85
<i>upf1Δ</i> [<i>PIN⁺</i>]	pAG415- <i>UPF1</i> + pYES2-Q103	10.91	1.48
<i>upf1Δ</i> [<i>PIN⁺</i>]	pAG415- <i>UPF1</i> _H94R + pYES2-Q103	11.66	1.25
<i>upf1Δ</i> [<i>PIN⁺</i>]	pAG415- <i>UPF1</i> _K436A + pYES2-Q103	12.2	1.09

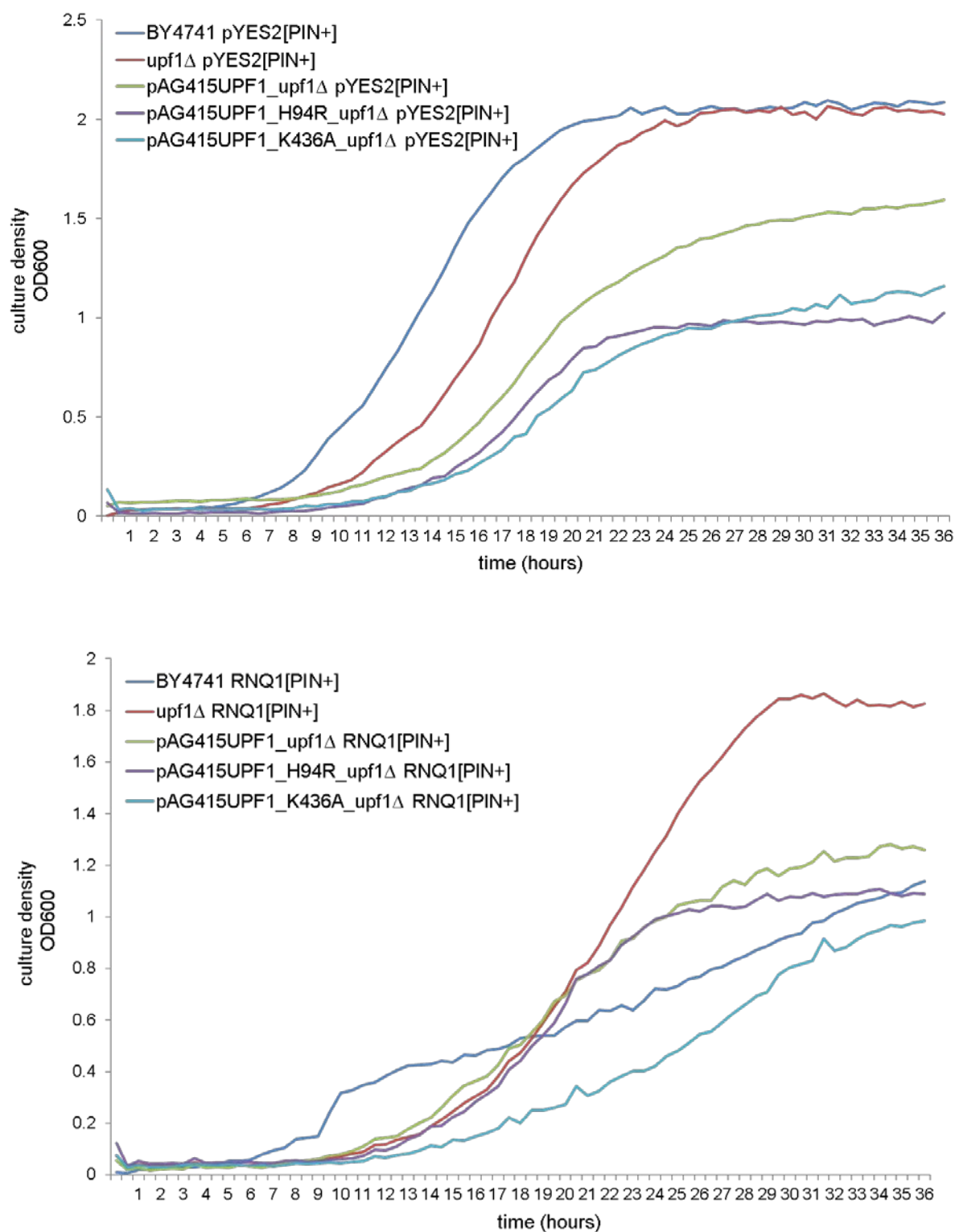


Figure 6.14 Expression of H94R or K436A mutants of Upf1 leads to a growth defect in the *upf1*Δ strain in a [PIN⁺] background independent of overexpression of Rnq1. Cell density was determined in the inducing medium i.e. SD 2% galactose-ura for 36 hours at 30°C. The effect of Rnq1 toxicity was tested in the *upf1*Δ strain expressing the H94R or K436A mutant Upf1, compared to the *upf1*Δ strain also expressing the wild type Upf1 protein, the wild type *UPF*⁺ BY4741 and the *upf1*Δ strains. pYES2 is the control plasmid while *RNQ1* is the pYES2 vector with *RNQ1* insert. Three biological replicates were performed for each strain and average is plotted in the above.

Chapter 6

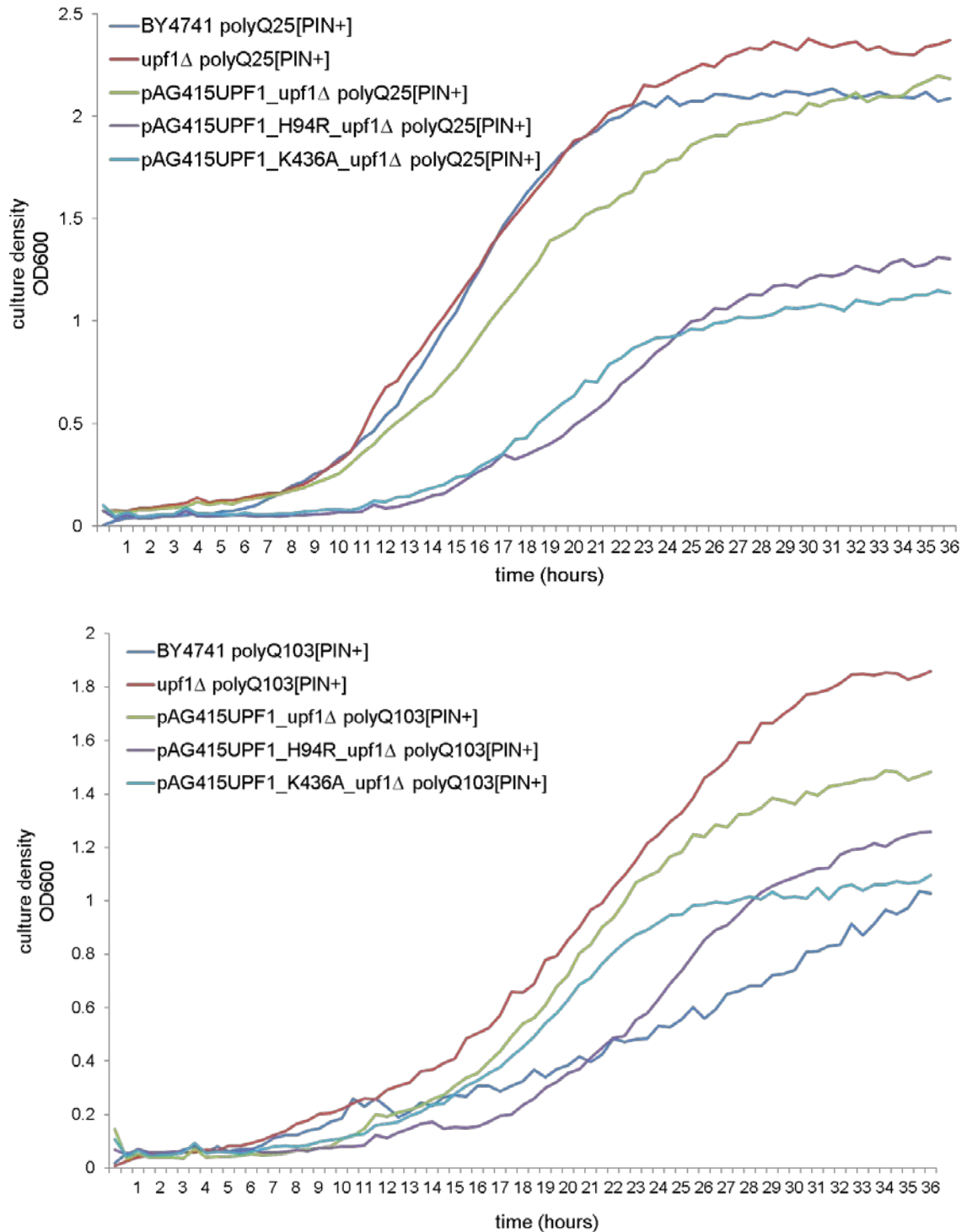


Figure 6.15 Expression of H94R or K436A mutants of Upf1 leads to a growth defect in the *upf1*Δ strain in a [PIN⁺] background independent of overexpression of polyQ103. Cell density was determined in the inducing medium i.e. SD 2% galactose-ura for 36 hours at 30°C. The effect of polyQ toxicity was tested in the *upf1*Δ strain expressing the H94R or K436A mutant Upf1, compared to the *upf1*Δ strain also expressing the wild type Upf1 protein, the wild type *UPF*⁺ BY4741 and the *upf1*Δ strains. Q25 is the pYES2 based plasmid with a Q25 insert (control) while Q103 is the pYES2 based vector with a Q103 insert. Three biological replicates were performed for each strain and average is plotted in the above.

6.10 Rnq1 and polyQ103 overexpression-mediated cytotoxicity is suppressed in a *bna4* Δ [*PIN*⁺] strain

A second deletion strain namely *bna4* Δ was also studied to further investigate the impact of different genetic modifiers on Rnq1- and polyQ103-mediated toxicity. Giorgini et al. (2005) discovered that deletion of the *BNA4* gene strongly suppressed polyQ103-induced toxicity in yeast. *BNA4* encodes an enzyme, kynurenine 3-monooxygenase, which plays an essential role in tryptophan degradation via the mitochondrial kynurenine pathway (KP). Deletion of the *BNA4* gene decreases the production two KP metabolites which are elevated in Huntington disease patients. Studies on the *bna4* Δ strain have provided a direct association between the pathogenesis of Huntington disease and cellular toxicity in the yeast model (Giorgini et al., 2005).

As overexpression of Rnq1- and polyQ103-mediated toxicity is suppressed in *upf1* Δ or *upf2* Δ strains (Section 6.2), it was interesting to examine whether deletion of *BNA4* can also suppress the Rnq1-induced toxicity. To test this, [*pin*⁻] and [*PIN*⁺] derivatives of *bna4* Δ deletion in the strain BY4741 were each transformed with either the pYES2 (control) or the pYES2-*RNQ1* plasmids. Toxicity assays (Section 4.1) were then conducted with this deletion strain (Figure 6.16). In comparison, the pYES2-*Q103* plasmid was also transformed into the *bna4* Δ deletion strain of BY4741. In addition, the pYES2 empty plasmid was used as control strains for both Rnq1- and polyQ103 strains as the pYES2-*Q25* plasmid did not transform successfully into the [*pin*⁻] or [*PIN*⁺] derivatives of the *bna4* Δ deletion strain of BY4741. The reasons for this could not be established.

As expected, overexpression of Rnq1 and polyQ103 was not toxic to the *bna4* Δ [*pin*⁻] strain as is also seen in the *UPF*⁺ [*pin*⁻] control while it was toxic in the *UPF*⁺ [*PIN*⁺] strain (Figure 6.16). Importantly, both Rnq1- and polyQ103-mediated cytotoxicity were suppressed in the *bna4* Δ [*PIN*⁺] strain. This result

was consistent with the previously published results (Giorgini *et al.*, 2005; Staniforth., 2011)

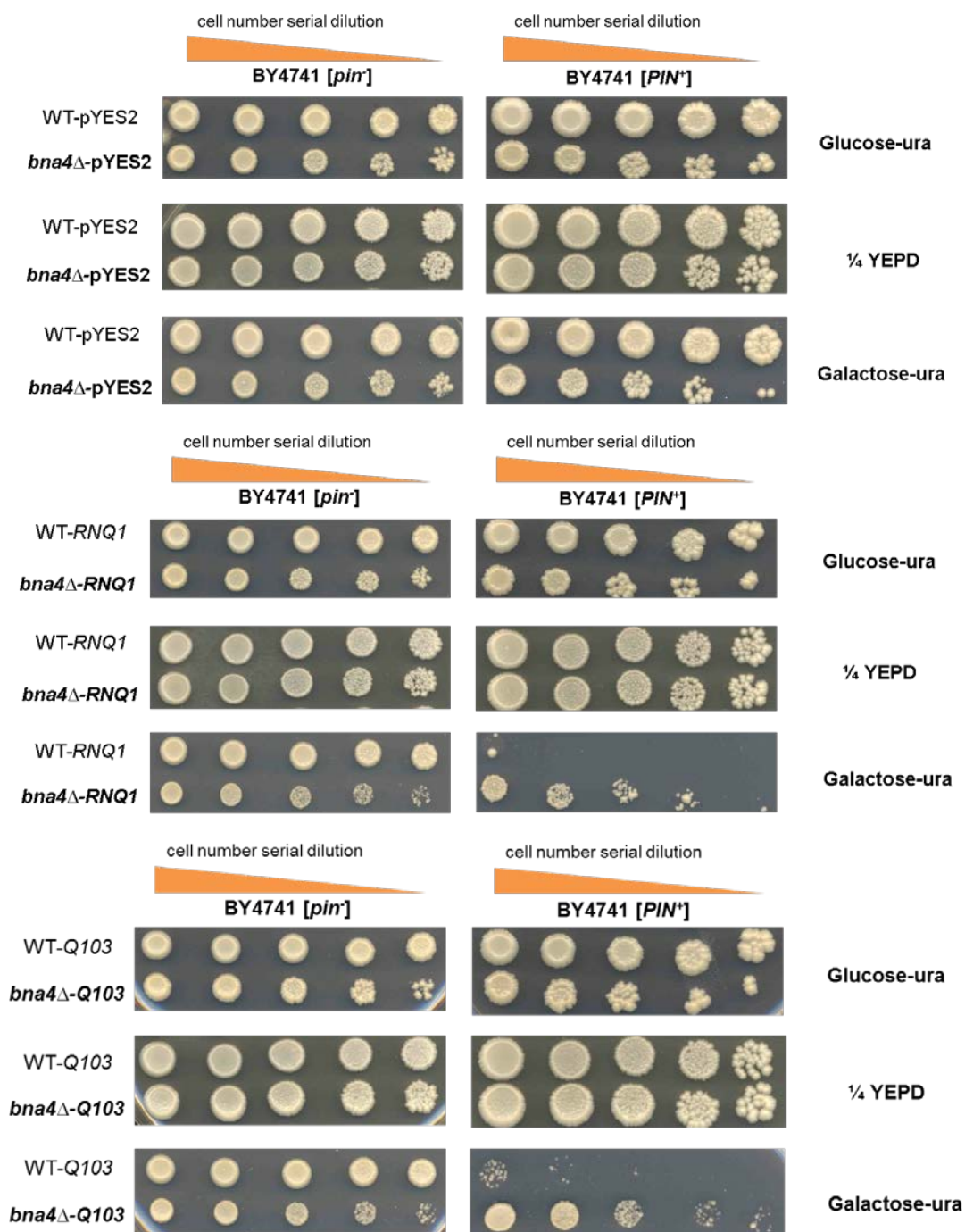
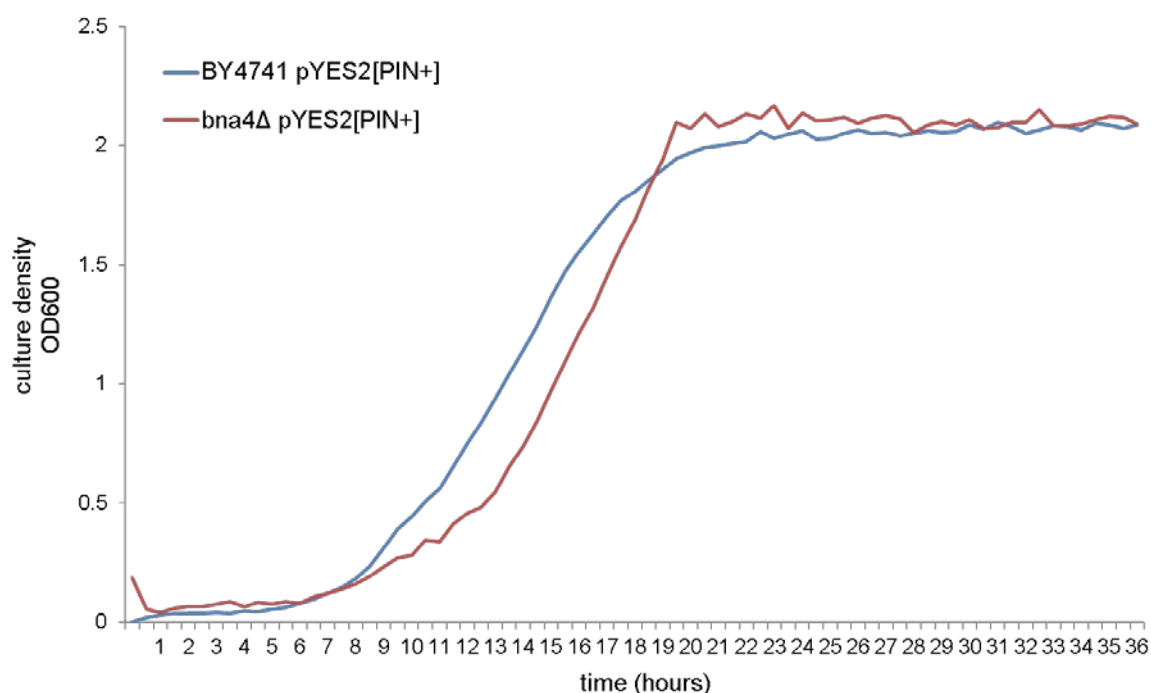


Figure 6.16 Overexpression of Rnq1- and polyQ103-induced toxicity is suppressed in the *bna4*Δ [*PIN*⁺] strain. WT is the wild type *BNA4*⁺ BY4741 strain. pYES2 is the control plasmid while *RNQ1* is the pYES2 vector with *RNQ1* insert. *Q103* is the pYES2 based vector with a *Q103* insert. Rnq1 and polyQ103 toxicity was examined on galactose plates since a galactose-inducible promoter *GAL1* was used to overexpress the Rnq1 protein. 1/4 YEPD and glucose plates served as controls for any growth defects. Rnq1 and polyQ103 toxicity was tested in the deletion strain *bna4*Δ, compared to the wild type *UPF*⁺ BY4741 strains. Three biological replicates were performed for each strain and one representative is shown for each.

6.11 [*PIN*⁺]-dependent growth defect caused by Rnq1 and polyQ103 overexpression is suppressed in the *bna4* Δ strain

As described in Section 6.3, 36 hour growth analysis was repeated in the *bna4* Δ deletion [*PIN*⁺] strains of BY4741 to quantify the impact of Rnq1 and polyQ overexpression on the growth rate.

As previously found, overexpression of Rnq1 and polyQ103 caused a growth defect in the wild type *BNA4*⁺ [*PIN*⁺] strain of BY4741 while normal growth was observed in BY4741 wild type *BNA4*⁺ and the *bna4* Δ deletion strains when the control pYES2 plasmid backbone was expressed (Figure 6.17). In the *bna4* Δ [*PIN*⁺] strain overexpressing Rnq1 and polyQ103, growth was similar to that of expressing the control pYES2 plasmid thus confirming that the growth defect caused by Rnq1 and polyQ103 overexpression was suppressed in the *bna4* Δ [*PIN*⁺] strain. This result confirmed that Rnq1 and polyQ103 toxicity is suppressed in the *bna4* Δ strain in a [*PIN*⁺] dependent manner.



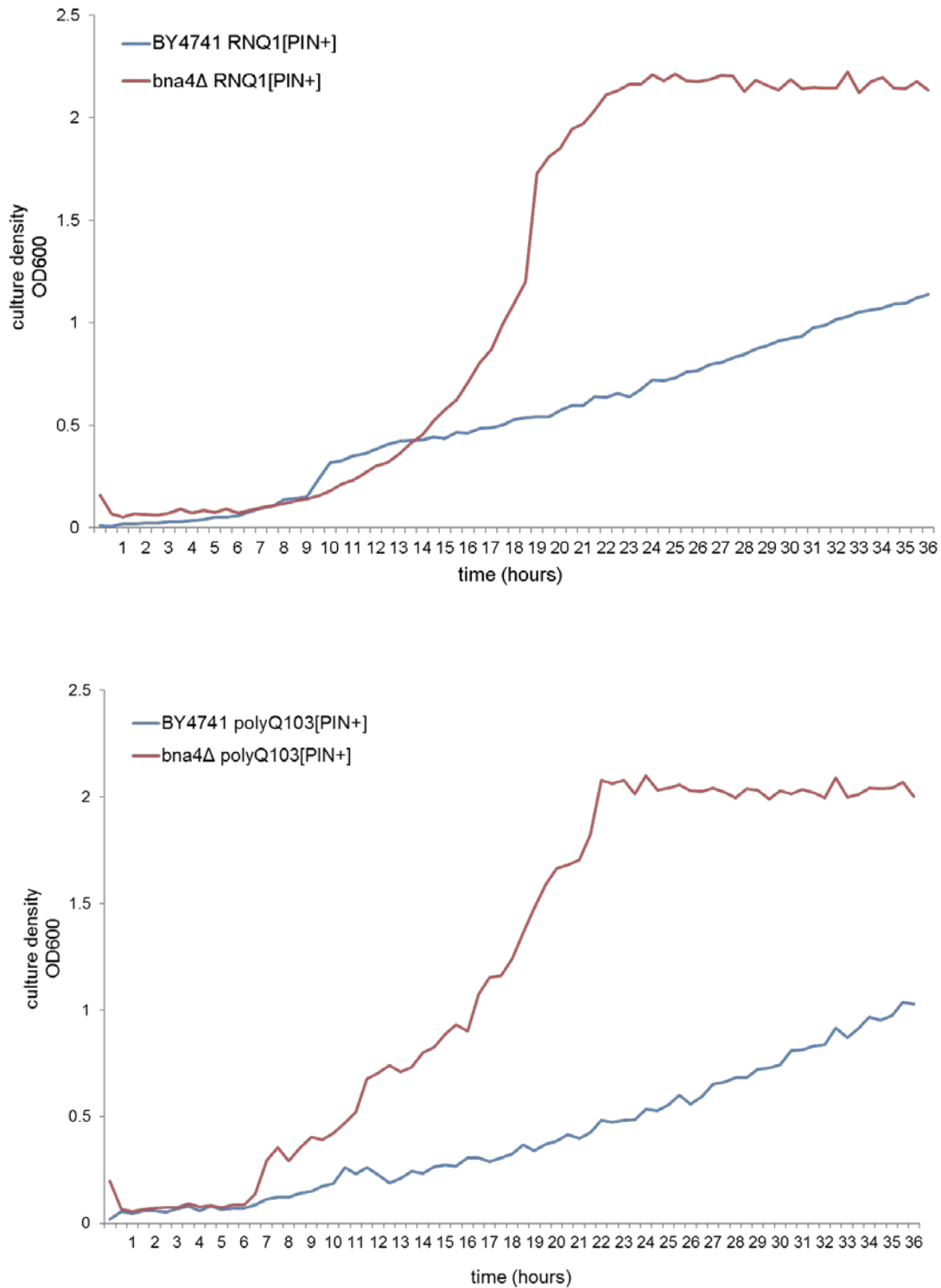


Figure 6.17 Overexpression of Rnq1 and polyQ103 does not lead to a growth defect in the *bna4Δ* [*PIN*⁺] strain. Cell density was determined in the inducing medium i.e. SD 2% galactose-ura for 36 hours at 30°C. The effect of Rnq1 and polyQ toxicity was tested in the [*PIN*⁺] deletion strain *bna4Δ*, compared to the wild type *BNA4*⁺ BY4741 strains. pYES2 is the control plasmid while *RNQ1* is the pYES2 vector with *RNQ1* insert. *Q103* is the pYES2 based vector with a *Q103* insert. Three biological replicates were performed for each strain and average is plotted in the above.

Table 6.4 Doubling time in exponential growth and cell density measured by the optical density of 600nm at the 36 hour time point for each strain of BY4741.

Strain	Plasmid	Doubling time	OD600 t = 36 h
BY4741 [<i>PIN</i> ⁺]	pYES2	3.87	2.08
<i>bna4</i> Δ [<i>PIN</i> ⁺]	pYES2	3.57	2.09
BY4741 [<i>PIN</i> ⁺]	pYES2- <i>RNQ1</i>	20.01	1.13
<i>bna4</i> Δ [<i>PIN</i> ⁺]	pYES2- <i>RNQ1</i>	4.42	2.13
BY4741 [<i>PIN</i> ⁺]	pYES2-Q103	16.27	1.02
<i>bna4</i> Δ [<i>PIN</i> ⁺]	pYES2-Q103	6.9	2.00

6.12 Rnq1 and polyQ103 overexpression does not cause a nuclear migration defect in the *bna4*Δ strain

As described in Section 4.5 and 6.6, overexpression of Rnq1 resulted in a nuclear migration defect in BY4741 [*PIN*⁺] cells but not in the *upf1*Δ and *upf2*Δ [*PIN*⁺] cells. It was therefore interesting to investigate whether the nuclear migration defect was also observed in the *bna4*Δ strains as Rnq1 overexpression-induced toxicity was suppressed in the *bna4*Δ strain in a [*PIN*⁺] background.

Similar to all strains used to observe the nuclear migration defect, log phase *bna4*Δ cells of BY4741 were stained with 4',6-diamidino-2-phenylindole (DAPI) (Chazotte., 2011). The [*pin*⁻] and [*PIN*⁺] derivatives of the *bna4*Δ deletion strain were each transformed with either the pYES2 (control) or the pYES2-*RNQ1* plasmids. The DAPI-stained nuclear DNA was visualized by fluorescence microscopy under ultraviolet light (Figure 6.18).

In the *bna4*Δ [*PIN*⁺] strain overexpressing Rnq1, the localization of nuclear DNA was similar with strains expressing the pYES2 backbone plasmid (control) before (t = 0) and after 6 hours induction (t = 6) and also similar with the un-induced cells overexpressing Rnq1 (t = 0). The same observation was also seen in the *bna4*Δ [*pin*⁻] strains (Figure 6.18). Thus no defect in nuclear migration was detected in the *bna4*Δ [*PIN*⁺] strains when Rnq1 was

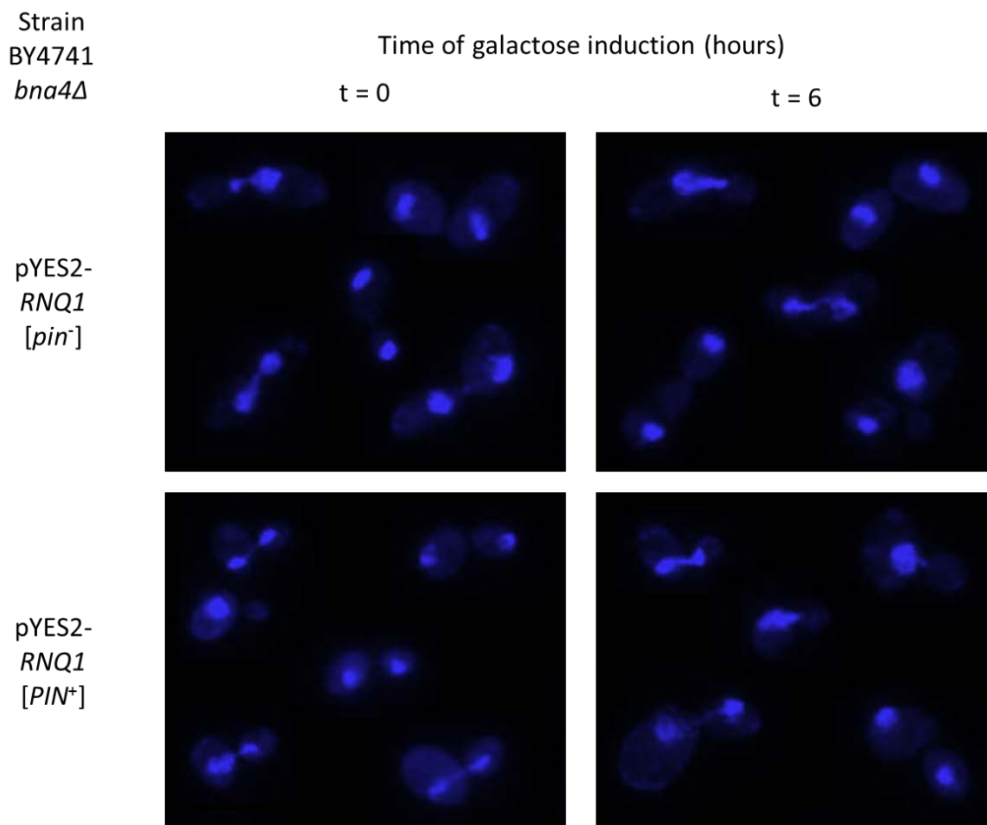
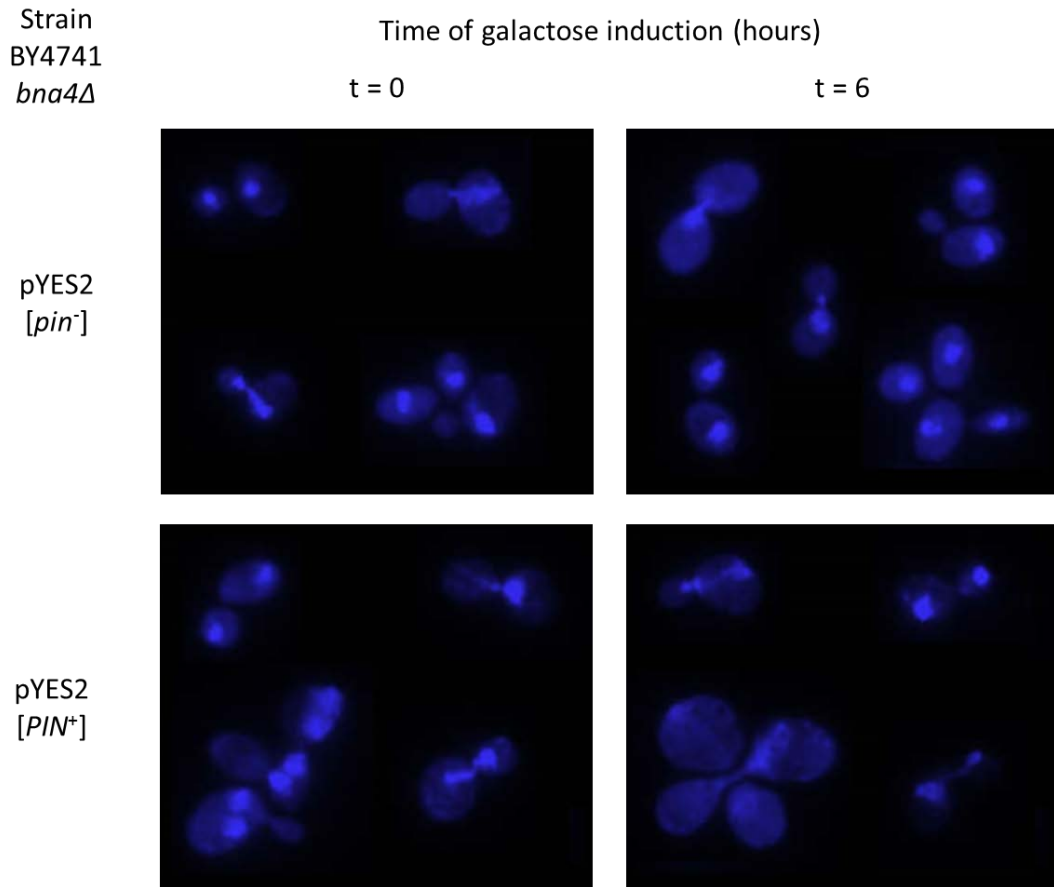
Chapter 6

overexpressed. As it was concluded that Rnq1 overexpression-induced cytotoxicity is not directly associated with a nuclear migration defect (Section 4.5) and there was a nuclear migration defect in the wild type *BNA4⁺ [PIN⁺]* strain suggesting the Bna4 protein might not be related to nuclear migration or cell cycle control.

The same experiments were also carried out in the log-phase BY4741 [*PIN⁺*] cells overexpressing polyQ103. However, polyQ103 overexpression did not cause a nuclear migration defect (see Section 5.5). In order to investigate whether deletion of the Bna4 protein may cause a nuclear migration defect when polyQ103 was overexpressed, pYES2-Q103 plasmid was transformed into both [*pin⁻*] and [*PIN⁺*] derivatives of the *bna4Δ* deletion strain of BY4741. The DAPI-stained nuclear DNA was visualized by fluorescence microscopy under ultraviolet light (Figure 6.18).

In the *bna4Δ* strain overexpressing polyQ103, the localization of nuclear DNA was similar to that seen in strains overexpressing the pYES2 empty plasmid (control) before ($t = 0$) and after 6 hours induction ($t = 6$) and also similar with the un-induced cells overexpressing polyQ103 ($t = 0$). Therefore no defect in nuclear migration was seen in the *bna4Δ* [*PIN⁺*] strain (Figure 6.18). This finding suggests that the Bna4 protein might not be associated with nuclear migration or cell cycle control.

Chapter 6



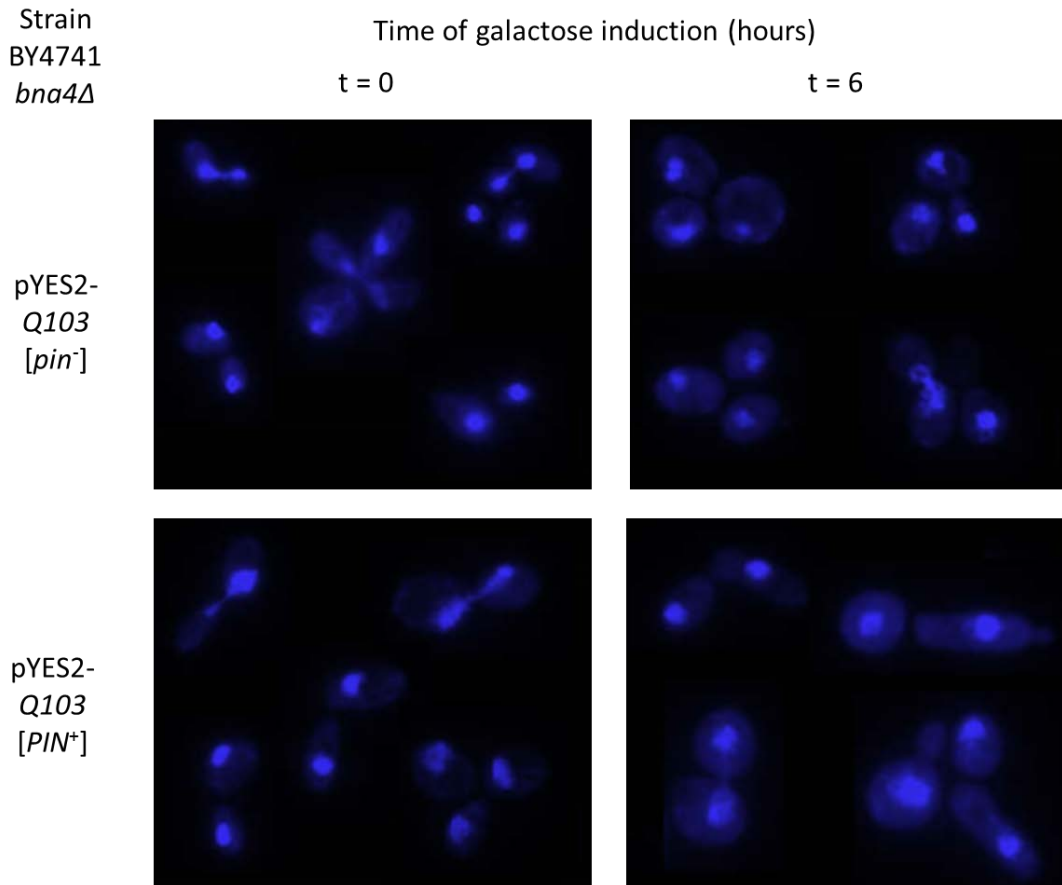


Figure 6.18 Overexpression of Rnq1 and polyQ103 does not cause a nuclear migration defect in the *bna4* Δ strain of BY4741 in a [*PIN*⁺] background. Rnq1 and polyQ103 overexpression do not cause nuclear DNA localised to the bud-neck after 6 hours induction in the *bna4* Δ strain. No the nuclear migration defects were detected in pYES2 control strains and the corresponding [*pin*⁻] strains. Cells were visualised by a blue excitation filter on an Olympus 1X81 fluorescent microscope with Hamamatsu Photonics Orca AG cooled CCD camera. Images were captured analysed by Olympus CellR software.

6.13 Discussion

In the current study, the results show that Rnq1 and polyQ overexpression-mediated cytotoxicity is suppressed in *upf1* Δ and *upf2* Δ [*PIN*⁺] strains but not in *upf3* Δ [*PIN*⁺] strain as well as the [*PIN*⁺]-dependent growth defect caused by Rnq1 and polyQ103 overexpression is suppressed in *upf1* Δ and *upf2* Δ strains but not in *upf3* Δ strain. It has been also noticed that the cytotoxicity

Chapter 6

and growth defect mediated by Rnq1 and polyQ103 is slightly enhanced in the *upf3* Δ strain in a [*PIN*⁺]-dependent manner.

As far as we know, the upf proteins function as a complex which plays an important role in the nonsense-mediated mRNA decay (NMD) pathway. So the question is why the Upf3 protein is distinct from the Upf1 and upf2 proteins in Rnq1 and polyQ103 mediated cytotoxicity and growth defects.

According to the studies based on the degradation of mRNA, four different pathways have been established in *Saccharomyces cerevisiae*: (i) A major pathway degrades normal mature mRNAs through a major 5'-to-3' manner (Decker and Parker, 1993; Tucker et al., 2001). (ii) Deadenylated mRNAs are subjected to 3'→5' degradation by the action of the exosome in the minor pathway (Mitchell et al., 1997). Both of the major and minor pathways take place in the cytoplasm. (iii) A specialized pathway, known as nonsense-mediated mRNA decay (NMD) pathway, is a translation-coupled mechanism that eliminates mRNAs containing premature translation-termination codons (PTCs). The Upf1, Upf2 and Upf3 proteins are the key components of the conserved core of NMD pathway (Lelivelt and Culbertson, 1999). (iv) A novel pathway, named as Degradation of mRNA in the Nucleus (DRN), act on RNAs preferentially retained in the nucleus depending on the nuclear mRNA cap-binding protein, Cbc1p (Das et al., 2003). Recent studies revealed that the Upf3 protein is involved in the DRN pathway by employing a genetic screen (Das et al., 2014). Therefore, the Upf3 protein has been found to be involved in both NMD and DRN pathways indicating that it may possess a unique function which has an impact on Rnq1 and polyQ103 mediated cytotoxicity and growth defects.

Chapter 7

General Discussion

7.1 Overview of the project

Many neurodegenerative diseases are associated with amyloids which are deposited in different tissues. Amyloids are formed by the seeded aggregation of proteins that, in the case of prions, can convert normal folded proteins into different heritable conformers of these proteins. Different prion variants cause different characteristics of the disease i.e. different pathologies. However, the mechanism of amyloid-mediated toxicity associated with these diseases still remains unclear. Moreover, at a molecular level, information about how different prion variants lead to distinct pathologies and how they are generated is still very limited. Considerable insight into amyloid biology and toxicity has come from studies with the yeast *Saccharomyces cerevisiae*.

In this thesis, I describe studies on four different variants of [*PIN*⁺], the prion form of the protein Rnq1. To further investigate Rnq1-mediated amyloid toxicity I compared the findings made with polyQ103-induced toxicity in the four different [*PIN*⁺] variants. The effects of genetic background on Rnq1- and polyQ103-induced toxicity were also investigated by comparing behaviour in two genetically unrelated yeast laboratory strains: BY4741 (a derivative of the standard laboratory strain S288c) and a strain derived from a Russian collection (74D-694). Furthermore, several deletion strains of the BY4741 strain were used to further investigate the mechanism of Rnq1- and polyQ103-mediated toxicity. The findings are summarised in Tables 7.1 to 7.4.

Chapter 7

Table 7.1 *De novo* formation of [PSI⁺] prion detected by different [PIN⁺] variants

74D-694 strains					
	[pin⁻]	Low [PIN⁺]	Medium [PIN⁺]	High [PIN⁺]	very high [PIN⁺]
protein level of Rnq1	NA	low	low	high	high
ability of <i>de novo</i> formation of [PSI ⁺]	No	Yes (lowest efficiency)	Yes	Yes	Yes (highest efficiency)
ability of <i>de novo</i> formation of strong [PSI ⁺]	No	Yes	Yes	Yes	Yes (highest efficiency)
ability of <i>de novo</i> formation of weak [PSI ⁺]	No	Yes (preferable)	Yes (preferable)	Yes (highest efficiency)	Yes

Table 7.2 Overexpression of Rnq1- and polyQ-mediated toxicity in BY4741 [PIN⁺] strains

BY4741[PIN⁺]	Rnq1 overexpression	Q103 overexpression
Cytotoxicity	Yes	Yes
Growth defect	Yes	Yes
Fluorescence foci	multiple dot	multiple dot
Nuclear migration defect	Yes	No
ROS levels	increased	No
<i>UPF1</i> deletion	suppresses toxicity	suppresses toxicity
<i>UPF2</i> deletion	suppresses toxicity	suppresses toxicity
<i>UPF3</i> deletion	toxic	toxic
Re-introducing <i>UPF1</i>	partially restored toxicity	partially restored toxicity
mutation H94R in <i>UPF1</i>	partially restored toxicity	partially restored toxicity
mutation K436A in <i>UPF1</i>	partially restored toxicity	partially restored toxicity

Chapter 7

Table 7.3 Overexpression of Rnq1-mediated toxicity in different [PIN⁺] variants of 74D-694

74D-694 strains	[pin ⁻]	Rnq1 overexpression			
		low [PIN ⁺]	medium [PIN ⁺]	high [PIN ⁺]	very high [PIN ⁺]
Cytotoxicity	not toxic	Toxic	toxic	toxic	toxic
Growth defect	No	Yes	Yes	Yes	Yes
Fluorescence foci	uniform	single dot	single dot	multiple dot	single dot
Nuclear migration defect	No	No	No	No	No
ROS levels	Increased (2-fold)	Increased (4.5-fold)	Increased (4-fold)	Increased (4.5-fold)	Increased (4-fold)
Ultra structure	normal	Nuclear migration defect & aberrant mitochondrial morphology			

Table 7.4 Overexpression of polyQ103-mediated toxicity in different [PIN⁺] variants of 74D-694

74D-694 strains	[pin ⁻]	Q103 overexpression			
		low [PIN ⁺]	medium [PIN ⁺]	high [PIN ⁺]	very high [PIN ⁺]
Cytotoxicity	not toxic	toxic	toxic	toxic	toxic
Growth defect	No	Yes	Yes	Yes	Yes
Fluorescence foci	uniform	Multiple dot	Multiple dot	Multiple dot	Multiple dot
Nuclear migration defect	No	No	No	No	No
ROS levels	No	No	No	No	No

7.2 Is the mechanism of amyloid toxicity the same for Rnq1 and polyQ103?

Several studies have revealed that the Rnq1 and polyglutamine-containing proteins have many features in common that makes Rnq1 acts a powerful model for investigating the mechanism of the pathological amyloids such as polyQ103. For example, the Sis1 and Hsp104 chaperones involved in the propagation and maintenance of the $[PIN^+]$ prion was also established that were able to modulate the aggregation of polyglutamine proteins (Krobitsch and Lindquist, 2000). It has been shown that both Rnq1 and polyQ103 overexpression is toxic in a $[PIN^+]$ background (Meriin et al., 2002, Chapter 4 and 5) however, what types of protein conformation are toxic to cells has remained unclear. Rnq1 forms amyloid with the characteristic parallel in-register cross-beta-sheet structure (Wickner et al., 2008) while the structure of polyQ-based amyloid has yet to fully elucidated. Most researchers thought that polyglutamines adopt an anti-parallel structure (Thakur and Wetzel, 2002, Sharma et al., 2005, Poirier et al., 2005, Zhang et al., 2011, Sivanandam et al., 2011) although for another polyglutamine protein, ataxin-3, a parallel beta-sheet structure was proposed by infrared spectroscopy (Bevivino and Loll, 2001). Since the lengths of polyglutamine tracts vary between individual HD patients, the polyglutamine aggregates may contain both parallel and anti-parallel beta-sheets structures. Moreover, it was established that polyQ fragments form an alpha-helical oligomer early in the aggregation process [Jayaraman et al., 2012]. Accordingly, as a consequence of the uncertainty of the secondary structure of the various polyglutamine proteins, it is conceivable that Rnq1 and polyQ103 may go through different pathways for their associated toxicity. Protein structure has a great influence on protein-protein interactions that in turn might impact on cellular function leading to the toxic phenotype.

In this study, four deletion strains (*upf1* Δ , *upf2* Δ , *upf3* Δ and *bna4* Δ) were investigated with respect to both Rnq1 and polyQ toxicity. The same result has been found in these deletion stains i.e. Rnq1 and polyQ overexpression-mediated cytotoxicity is suppressed in *upf1* Δ , *upf2* Δ and *bna4* Δ $[PIN^+]$ strains

but not in *upf3Δ* [*PIN*⁺] strain. This suggests that one or more aspects of the mechanism of Rnq1 and polyQ103-mediated toxicity overlap, perhaps targeting some fundamental cellular process such as the mitochondrial kynurenine pathway for synthesis NAD⁺.

7.3 Is mitochondrial deficiency a consequence of amyloid toxicity in yeast?

Over the past 30 years, studies have demonstrated that mutant polyglutamine proteins associated with mitochondrial dysfunctions play an essential role in the pathogenesis of Huntington disease. In this study, an increase of ROS levels was not detected in either 74D-694 and BY4741 strains overexpressing polyQ103 by 6 hours post induction. One reason for the unexpected result is that the induction time was not sufficient.

However, the levels of ROS did increase in cells overexpressing Rnq1 in a [*PIN*⁺] manner (Figure 4.11-12) suggesting that Rnq1 overexpression causes a degree of mitochondrial dysfunction. In addition, the observed aberrant morphology of mitochondrial ultrastructure in [*PIN*⁺] cells when Rnq1 was overexpressed (Figure 4.13) is consistent with this conclusion. This might be due to Rnq1 overexpression interfering with the cytoskeleton that would in turn impact on mitochondrial trafficking leading to changes in mitochondrial morphology and eventually mitochondrial dysfunction.

7.4 Is nuclear migration defect a feature of amyloid toxicity?

As summarised in Tables 7.2 - 7.4, a nuclear migration defect was only observed in the [*PIN*⁺] strain of BY4741 when Rnq1 was overexpressed. The fluorescence images obtained using DAPI to stain DNA showed that nuclear DNA localised to the bud-neck 6 hours post induction of Rnq1 overexpression in the [*PIN*⁺] cells of BY4741. This is further supported by the finding that the

mad2 deletion cells were arrested continued to synthesis DNA but not cytokinesis by Rnq1 overexpression indicating that Rnq1 overexpression induces a spindle checkpoint resulting in cell cycle arrest (Treusch and Lindquist, 2012). Moreover, a monopolar spindle was seen by electron microscopy in [*PIN*⁺] cells when Rnq1 was overexpressed suggesting that Rnq1 toxicity triggers a defect in spindle pole body duplication (Treusch and Lindquist, 2012). This would be expected to lead to a nuclear migration defect.

By contrast, the nuclear migration defect was not observed in either BY4741 or 74D-694 [*PIN*⁺] strains when Q103 was overexpressed. Since a nuclear migration defect would be expected to lead to a cell cycle blockage, cells overexpressing polyQ103 may undertake another mechanism that affects cell cycle blockage. For example, recent evidence has demonstrated that there was a defect in spindle extension process when polyQ56 is present. Importantly, the assembly of the septin ring was also interrupted resulting in a production of polyploid cells (Kaiser *et al.*, 2013).

Therefore, the cell cycle blockage triggered by Rnq1 or polyglutamine expansion proteins may do so via different mechanisms. Furthermore, there was an effect on nuclear migration by Rnq1 overexpression that was dependent on the genetic background of the strain in which the studies were carried out. Therefore a nuclear migration defect may not be a common feature of amyloid toxicity, but rather may be a specific event in certain genetic backgrounds.

7.5 Why dose Upf1 and Upf2 proteins suppress amyloid toxicity?

In this study, overexpression of Rnq1 and polyQ mediated cytotoxicity was suppressed in both the *upf1* Δ and *upf2* Δ [*PIN*⁺] strains. The Upf1 protein is a multifunctional protein that acts as an ATPase, an RNA helicase and a ubiquitin ligase (Czaplinski *et al.*, 1995, Chamieh *et al.*, 2008, Takahashi *et al.*, 2008). However, introduction of two point mutations K436A and H94R that

Chapter 7

inhibit the ATPase/helicase activity and the E3 ubiquitin ligase activity of Upf1 respectively (Weng et al., 1996, Takahashi et al., 2008) did not ablate toxicity suggesting that these activities of Upf1 are not associated with overexpression of Rnq1 and polyQ103 mediated cytotoxicity. The Upf2 protein acts as a bridge to connect the Upf1 and Upf3 proteins and the *upf1*, *upf2* and *upf3* function as a complex in the NMD machinery (He et al., 1997). However, overexpression of Rnq1 and polyQ was toxic in the *upf3* Δ [*PIN*⁺] strain suggesting that the NMD pathway has no impact on Rnq1 and polyQ103.

So why is Rnq1 and polyQ103-mediated amyloid toxicity suppressed in the *upf1* and *upf2* deletion strains but not the *upf3* defective strain? One possible reason is that the Upf1 and Upf2 proteins interact with Rnq1 and polyQ103 directly or indirectly thus facilitating the aggregation of Rnq1 and polyQ103 thereby generating toxic aggregates in a [*PIN*⁺] background. However, deletion of either *upf1* or *upf2* may affect the protein-protein interaction and thus Rnq1 and polyQ103 may tend to form inclusion bodies which are not toxic to the cell.

Recent research was established that the Q-rich PrDs (prion forming domains) are able to suppress polyQ toxicity by interaction with the toxic oligomers and facilitates the formation of large non-toxic aggregates (Kayatekin et al., 2014). Another possible reason for why deletion of *UPF1* and *UPF2* genes suppresses amyloid toxicity is that a particular sequence in the Upf1 or Upf2 (but not Upf3) plays a role in the formation of toxic oligomers which do not form in the absence of either protein. This sequence might give rise to a specific structure that inhibit or slow down the process for forming large nontoxic aggregates or degrade into monomeric proteins.

7.6 Why does *bna4* Δ suppress amyloid toxicity?

As described in chapter 6, Rnq1 and polyQ103 toxicity were suppressed in the *bna4* Δ [*PIN*⁺] strain. Ban4 encodes an enzyme that plays a key role in the mitochondrial kynurenine pathway for synthesis of NAD⁺. Overexpression of polyQ103 upregulates the kynurenine pathway thus increasing the production

Chapter 7

of 3-hydroxykynurenine (3-HK) and quinolinic acid which are two neurotoxic intermediates. Deletion of the *BNA4* gene decreases the production of the two intermediate of KP that overcomes the toxicity of mutant polyQ proteins (Giorgini et al., 2005, Giorgini et al., 2008).

References

References

Alberti S., Halfmann R., King O., Kapila A., and Lindquist S. (2009) A systematic survey identifies prions and illuminates sequence features of prionogenic proteins. *Cell* 137: 146-158.

Astbury WT¹, Dickinson S, Bailey K.(1935) The X-ray interpretation of denaturation and the structure of the seed globulins. *Biochem J.* 29(10):2351-2360.1.

Allen, K.D., Wegrzyn, R.D., Chernova, T.A., Muller, S., Newnam, G.P., Winslett, P.A., et al. (2005) Hsp70 chaperones as modulators of prion life cycle: novel effects of Ssa and Ssb on the *Saccharomyces cerevisiae* prion [PSI⁺]. *Genetics* 169: 1227-1242.

Balbirnie M¹, Grothe R, (2001) An amyloid-forming peptide from the yeast prion Sup35 reveals a dehydrated beta-sheet structure for amyloid. *Eisenberg DSProc Natl Acad Sci U S A.*98(5):2375-80.

Bradley M.E., Edskes H.K., Hong J.Y., Wickner R.B., and Liebman S.W. (2002) Interactions among prions and prion "strains" in yeast. *Proc Natl Acad Sci U S A* 99 Suppl 4: 16392-16399.

Chernoff Y.O., Derkach I.L., and Inge-Vechtomov S.G. (1993) Multicopy SUP35 gene induces de-novo appearance of psi-like factors in the yeast *Saccharomyces cerevisiae*. *Curr Genet* 24: 268-270

Chernoff, Y.O., Lindquist, S.L., Ono, B., Inge-Vechtomov, S.G., and Liebman, S.W. (1995) Role of the chaperone protein Hsp104 in propagation of the yeast prion-like factor [PSI⁺]. *Science* 268: 880-884.

Coustou V¹, Deleu C, Saupe S, Begueret JProc (1997) The protein product of the het-s heterokaryon incompatibility gene of the fungus *Podospira anserina* behaves as a prion analog. *Natl Acad Sci U S A.* 2;94(18):9773-8.

Cox, B. S. (1965) [PSI], a cytoplasmic suppressor of super-suppressors in yeast. *Heredity* 20: 505-521.

D'Autréaux B, Toledano MB. (2007) ROS as signalling molecules: mechanisms that generate specificity in ROS homeostasis ; *Nat Rev Mol Cell Biol.*8(10):813-24.

References

DePace, A.H., Santoso, A., Hillner, P., and Weissman, J.S. (1998) A critical role for amino-terminal glutamine/asparagine repeats in the formation and propagation of a yeast prion. *Cell* 93: 1241-1252.

Derkatch IL¹, Chernoff YO, Kushnirov VV, Inge-Vechtomov SG, Liebman SW (1996) Genesis and variability of [PSI] prion factors in *Saccharomyces cerevisiae*. *Genetics*.;144(4):1375-86.

Derkatch IL¹, Bradley ME, Zhou P, Chernoff YO, Liebman SW. (1997) Genetic and environmental factors affecting the de novo appearance of the [PSI⁺] prion in *Saccharomyces cerevisiae*. *Genetics*.;147(2):507-19.

Derkatch I.L., Bradley M.E., Masse S.V., Zadorsky S.P., Polozkov G.V., Inge-Vechtomov S.G., and Liebman S.W. (2000) Dependence and independence of [PSI⁺] and [PIN⁺]: A two-prion system in yeast? *EMBO J* 19: 1942-1952.

Derkatch I.L., Bradley M.E., Hong J.Y., and Liebman S.W. (2001) Prions affect the appearance of other prions: The story of [PIN⁺]. *Cell* 106: 171-182.

Derkatch I.L., Uptain S.M., Outeiro T.F., Krishnan R., Lindquist S.L., and Liebman S.W. (2004) Effects of Q/N-rich, polyQ, and non-polyQ amyloids on the de novo formation of the [PSI⁺] prion in yeast and aggregation of Sup35 in vitro. *Proc Natl Acad Sci U S A* 101: 12934-12939

Derkatch IL1, Uptain SM, Outeiro TF, Krishnan R, Lindquist SL, Liebman SW. (2004) Effects of Q/N-rich, polyQ, and non-polyQ amyloids on the de novo formation of the [PSI⁺] prion in yeast and aggregation of Sup35 in vitro. *Proc Natl Acad Sci U S A*. 101(35):12934-9. Epub 2004 Aug 23.

Douglas P.M., Treusch S., Ren H.Y., Halfmann R., Duennwald M.L., Lindquist S., and Cyr D.M. (2008a) Chaperone-dependent amyloid assembly protects cells from prion toxicity. *Proc Natl Acad Sci U S A* 105: 7206-7211

Du Z., Park K.W., Yu H., Fan Q., and Li L. (2008) Newly identified prion linked to the chromatin-remodeling factor Swi1 in *Saccharomyces cerevisiae*. *Nat Genet* 40: 460-465.

Eaglestone, S. S., B. S. Cox, and M. F. Tuite. (1999) Translation termination efficiency can be regulated in *Saccharomyces cerevisiae* by environmental stress through a prion-mediated mechanism. *EMBO J* 18: 1974-81.

References

Eaglestone SS1, Ruddock LW, Cox BS, Tuite MF. (2000) Guanidine hydrochloride blocks a critical step in the propagation of the prion-like determinant [PSI(+)] of *Saccharomyces cerevisiae*. *Proc Natl Acad Sci U S A*;97(1):240-4.

Ferreira P.C., Ness F., Edwards S.R., Cox B.S., and Tuite M.F. (2001) The elimination of the yeast [PSI⁺] prion by guanidine hydrochloride is the result of Hsp104 inactivation. *Mol Microbiol* 40: 1357-1369

Glover, J.R. and Lindquist, S. (1998) Hsp104, Hsp70, and Hsp40: a novel chaperone system that rescues previously aggregated proteins. *Cell* 94: 73-82.

Gordon WS. Advances in veterinary research. *Vet Rec.* 1946. 58:518-525.

Giorgini F., Guidetti P., Nguyen Q., Bennett S.C., and Muchowski P.J. (2005) A genomic screen in yeast implicates kynurenine 3-monooxygenase as a therapeutic target for huntington disease. *Nat Genet* 37: 526-531

Giorgini F., Moller T., Kwan W., Zwilling D., Wacker J.L., Hong S., *et al.* (2008) Histone deacetylase inhibition modulates kynurenine pathway activation in yeast, microglia, and mice expressing a mutant huntingtin fragment. *J Biol Chem* 283: 7390-7400.

Goldfarb L.G., Brown P., McCombie W.R., Goldgaber D., Swergold G.D., Wills P.R., *et al.* (1991) Transmissible familial creutzfeldt-jakob disease associated with five, seven, and eight extra octapeptide coding repeats in the PRNP gene. *Proc Natl Acad Sci U S A* 88: 10926-10930.

Griffith, J.S. (1967) Self-replication and scrapie. *Nature* 215: 1043-1044.

He F., Brown A.H., and Jacobson A. (1997) Upf1p, Nmd2p, and Upf3p are interacting components of the yeast nonsense-mediated mRNA decay pathway. *Mol Cell Biol* 17: 1580-1594.

Leeds P., Peltz S.W., Jacobson A., and Culbertson M.R. (1991) The product of the yeast UPF1 gene is required for rapid turnover of mRNAs containing a premature translational termination codon. *Genes Dev* 5: 2303-2314

Schwimmer C¹, Masison DC. (2002) Antagonistic interactions between yeast [PSI(+)] and [URE3] prions and curing of [URE3] by Hsp70 protein chaperone Ssa1p but not by Ssa2p. *Mol Cell Biol.* ;22(11):3590-8.

References

- Meriin A.B., Zhang X, He X, Newnam GP, Chernoff YO, Sherman MY. (2002) Huntington toxicity in yeast model depends on polyglutamine aggregation mediated by a prion-like protein Rnq1. *J Cell Biol.* ;157(6):997-1004.
- Meriin A.B, Zhang X, He X, Newnam GP, Chernoff YO, Sherman MY. (2002) Huntington toxicity in yeast model depends on polyglutamine aggregation mediated by a prion-like protein Rnq1. *J Cell Biol*;157(6):997-1004.
- Morley JF, Brignull HR, Weyers JJ, Morimoto RI. (2002) The threshold for polyglutamine-expansion protein aggregation and cellular toxicity is dynamic and influenced by aging in *Caenorhabditis elegans*. *Proc Natl Acad Sci USA*. 99:10417-22.
- Nelson R., Sawaya M.R., Balbirnie M., Madsen A. Ø., Riek C., Grothe R., Eisenberg D. (2005) Structure of the cross-beta spine of amyloid-like fibrils. *Nature* 435: 773–778.
- Osherovich L.Z., and Weissman J.S. (2001) Multiple Gln/Asn-rich prion domains confer susceptibility to induction of the yeast [PSI⁺] prion. *Cell* 106: 183-194.
- Pan, K.M., Baldwin, M., Nguyen, J., Gasset, M., Serban, A., Groth, D., et al. (1993) Conversion of alpha-helices into beta-sheets features in the formation of the scrapie prion proteins. *Proc Natl Acad Sci. USA* 90: 10962-10966.
- Patel B.K., Gavin-Smyth J., and Liebman S.W. (2009) The yeast global transcriptional co-repressor protein Cyc8 can propagate as a prion. *Nat Cell Biol* 11: 344-349.
- Pawar, A. P., K. F. Dubay, et al. (2005). "Prediction of "Aggregation-prone" and "Aggregation-susceptible" Regions in Proteins Associated with Neurodegenerative Diseases." *J Mol Biol* 350: 379-92.
- Prusiner S.B. (1982) Novel proteinaceous infectious particles cause scrapie *Science* 216: 136-144.
- Prusiner, S.B. (1991) Molecular biology of prion diseases. *Science* 252: 1515-1522.
- Rogoza T., Goginashvili A., Rodionova S., Ivanov M., Viktorovskaya O., Rubel A., et al. (2010) Non-mendelian determinant [I^{SP+}] in yeast is a nuclear-residing prion form of the global transcriptional regulator Sfp1. *Proc Natl Acad Sci U S A* 107: 10573-10577.
- Stolz M¹, Stoffler D, Aebi U, Goldsbury C. (2000) Monitoring biomolecular interactions by time-lapse atomic force microscopy. *J Struct Biol.* ;131(3):171-80.

References

Sondheimer, N. and Lindquist, S. (2000) Rnq1: an epigenetic modifier of protein function in yeast. *Molecular Cell* 5: 163-172.

Sondheimer N., Lopez N., Craig E.A., and Lindquist S. (2001) The role of Sis1 in the maintenance of the [RNQ⁺] prion. *EMBO J* 20: 2435-2442

Scherzinger, E., R. Lurz, M. Turmaine, L. Mangiarini, B. Hollenbach, R. Hasenbank, G.P. Bates, S.W. Davies, H. Lehrach, and E.E. Wanker. (1997) Huntingtin-encoded polyglutamine expansions form amyloid-like protein aggregates in vitro and in vivo. *Cell* 90:549–558.

Stansfield I., Jones K.M., Kushnirov V.V., Dagkesamanskaya A.R., Poznyakovski A.I., Paushkin S.V., *et al.* (1995) The products of the SUP45 (eRF1) and SUP35 genes interact to mediate translation termination in *Saccharomyces cerevisiae*. *EMBO J* 14: 4365-4373

Swisher KD1, Parker R. (2011) Interactions between Upf1 and the decapping factors Edc3 and Pat1 in *Saccharomyces cerevisiae*. *PLoS One*.;6(10):e26547. doi: 10.1371/journal.pone.0026547.

Tuite, M.F., Mundy, C.R., and Cox, B.S. (1981) Agents that cause a high frequency of genetic change from [PSI⁺] to [psi⁻] in *Saccharomyces cerevisiae*. *Genetics* 98: 691-711.

Tuite MF1, Serio TR. (2010) The prion hypothesis: from biological anomaly to basic regulatory mechanism. *Nat Rev Mol Cell Biol*.11(12):823-33.

Ter-Avanesyan MD1, Kushnirov VV, Dagkesamanskaya AR, Didichenko SA, Chernoff YO, Inge-Vechtomov SG, Smirnov VN. (1993) Deletion analysis of the SUP35 gene of the yeast *Saccharomyces cerevisiae* reveals two non-overlapping functional regions in the encoded protein. *Mol Microbiol*;7(5):683-92.

Treusch S1, Lindquist S. (2012) An intrinsically disordered yeast prion arrests the cell cycle by sequestering a spindle pole body component. *J Cell Biol*.;197(3):369-79

True H.L., and Lindquist S.L. (2000) A yeast prion provides a mechanism for genetic variation and phenotypic diversity. *Nature* 407: 477-483.

Volkov K.V., Aksenova A.Y., Soom M.J., Osipov K.V., Svitin A.V., Kurischko C., *et al.* (2002) Novel non-mendelian determinant involved in the control of translation accuracy in *Saccharomyces cerevisiae*. *Genetics* 160: 25-36

Wickner R.B. (1994) URE3] as an altered URE2 protein: Evidence for a prion analog in *Saccharomyces cerevisiae* *Science* 264: 566-569.

References

Zhuravleva GA, Gryzina VA. (2012) [The influence of UPF genes on the severity of SUP45 mutations]. *Mol Biol (Mosk)*;46(2):285-97.

Zhou P., Derkatch I.L., Uptain S.M., Patino M.M., Lindquist S., and Liebman S.W. (1999) The yeast non-mendelian factor [ETA+] is a variant of [PSI+], a prion-like form of release factor eRF3. *EMBO J* 18: 1182-1191

Zünd D1, Gruber AR, Zavolan M, Mühlemann O. (2013) Translation-dependent displacement of UPF1 from coding sequences causes its enrichment in 3' UTRs. *Nat Struct Mol Biol*;20(8):936-43.